Report from Task 6 of MEWS Project: experimental assessment of water penetration and entry into wood-frame wall specimens: final report

Lacasse, M. A.; O'Connor, T.; Nunes, S. C.; Beaulieu, P.

Research Report (National Research Council of Canada. Institute for Research in Construction); no. RR-133, 2003-02-01

National Research Council Canada | Conseil national de recherches Canada

NRC · CNRC

Report from Task 6 of MEWS Project
Experimental Assessment of Water Penetration and Entry into Wood-Frame Wall Specimens – Final Report

Lacasse, M.A.; O'Connor, T.J.; Nunes, S.; Beaulieu, P.

IRC-RR-133

February 2003

http://irc.nrc-cnrc.gc.ca/ircpubs

Institute for Research in Construction | Institut de recherche en construction | IRC

IMPORTANT NOTICE TO READERS

The main emphasis of the MEWS project was to predict the hygrothermal responses of several wall assemblies that are exposed to North American climate loads, and a range of water leakage loads. Researchers used a method based on both laboratory experimentation and 2-D modeling with IRC's benchmarked model, hygIRC. This method introduced built-in detailing deficiencies that allowed water leakage into the stud cavity - both in the laboratory test specimens and in the virtual (modeling) "specimens"- for the purpose of investigating water entry rates into the stud cavity and the drying potential of the wall assemblies under different climate loads. Since the project was a first step in investigating a range of wall hygrothermal responses in a parametric analysis, no field study of building characteristics was performed to confirm inputs such as water entry rates and outputs such as wall response in a given climate. Rather, ranges from 'no water entry and no response' to 'too much water entry and too wet for too long' were investigated.

Also, for the sake of convenience, the project used the generic cladding systems (e.g., stucco, masonry, EIFS, and wood and vinyl siding) for labeling and reporting the results on all wall assemblies examined in the study. However, when reading the MEWS publications, the reader must bear in mind that the reported results are more closely related to the nature of the deliberately introduced deficiencies (allowing wetting of the stud cavity) and the construction details of the wall systems investigated (allowing wetting/drying of the assembly) than to the generic cladding systems themselves. As a general rule, the reader must assume, unless told otherwise, that the nature of the deficiencies and the water entry rates into the stud cavity were different for each of the seventeen wall specimens tested as well as for each of the four types of wall assemblies investigated in the modeling study. For this reason, simply comparing the order of magnitude of results between different cladding systems would take the results out of context and likely lead to erroneous conclusions.

Chapter 1

Overview of Experimental work

TABLE OF CONTENTS

— CHAPTER 1 —

OVERVIEW OF EXPERIMENTAL WORK

LIST OF FIGURES

LIST OF TABLES

1.1 Introduction

i. Objectives

The objective of this task was to measure the moisture control performance of wall systems and subsystems and to determine the quantity of water entry in relation to climate loads.

ii. Approach

The requirements, as set out for the MEWS project, for understanding and assessing the moisture management potential of different wall assembly types when subjected to North American climate loads necessitated developing a flexible approach that would permit obtaining on the one hand, qualitative information on watertightness performance and on the other, quantitative information for the purposes of providing the simulation model data in a form useful for carrying out the parametric studies.

QUALITATIVE ASSESSMENT

In terms of qualitative information, the intent was to subject the different types of walls to simulated wind-driven rain at loads and for time periods in keeping with current industrial standards. Typically in industrial performance tests, wind-driven rain is simulated by the simultaneous application of water spray, per unit time and specimen surface area, and pressure difference across the specimen. Evidently the spray is intended to emulate the deposition of water on the facade due to rainfall whereas pressure difference mimics the action of wind. Standard performance assessment tests, such as the ASTM standard, require the wall specimens be subjected to a specific spray rate and pressure differential for a given amount of time. The assessment is based on whether penetration was observed over the course of the specified test period under the designated test conditions. Given this situation, it was felt that additional information could be gained from applying test pressures in increasing steps of pressure differential at a given spray rate. It was surmised that a water penetration ‘event’, indicative of when penetration of the assembly was first observed and conditions under which it occurred, could be established over the course of the tests. This ‘staged’ approach thus permitted assessing the pressure level at which penetration events occurred offering a rough estimate of the degree to which resistance to penetration might be achieved for a given wall specimen. Additionally, such type of tests could provide information on the most vulnerable parts of the assembly given that observation of an ‘event’ would also include where penetration was observed to occur.

In addition to the above water penetration assessments, information was sought on the air tightness of the assemblies as well as pressure response, in both the static and dynamic mode, as this might offer indications of a propensity for water entry. Obtaining pressure differentials across as well as from various points within the assembly would provide a measure of the potential for driving water across openings in the interstitial layers of the assembly. Characterising the air leakage of specimens was sought to provide a means of assessing whether the degree of air leakage could be readily related to a propensity for water penetration; e.g. is water penetration more or less likely to occur in walls that have a high degree of air leakage?

Given that at least in some specimens water penetration was likely to occur, information was also sought on the likelihood of moisture penetration to the wood-based and other moisture sensitive materials in the assembly, in particular oriented strand board (OSB). Electric sensors were used to indicate the presence of moisture and taking into consideration the limited number of sensors available, these were located in proximity to areas where water was likely to penetrate or migrate to. The activation of sensors over the test period provided a ready assessment of the degree of penetration to specific elements and hence the extent to which moisture might migrate in a given time under the specified conditions. In essence, it offered a qualitative measure of the resistance to entry of different assemblies based on the total number of sensors activated over the course of a test. As well, it helped identify the moisture sensitive locations of a specimen. In combining information obtained from moisture sensors and penetration 'events', a qualitative assessment of the watertightness of the specimen was completed.

It is to be noted that the specimens in this sequence of performance tests were prepared without any specified deficiencies in the cladding proper, although the specimens did include deficiencies in the second line of defence as described in MEWS Report T2-02[1]. The basis for choosing the various deficiencies is provided in Appendix – A[2] whereas MEWS Report T2-02, provides details on how the specimens were built and what deficiencies were introduced in the several layers of components making up the specimens. The generic deficiencies for a typical wall assembly, as provided in Appendix – A, in the first and second lines of defense, are given in Figures 1.1 and 1.2 respectively.

---

[1] Bomberg et al. (2002), "Description of 17 large-scale wall specimens built for water entry investigation in IRC dynamic wall testing facility: Summary Report from MEWS Task 2", MEWS Project Report T2-02, Institute for Research in Construction, May 2002, 134p.

[2] MEWS Task Group 2 (1999), "Recommendation for the selection of deficiencies for the 17 wall specimens to be investigated for water ingress using the dynamic wall testing facility", MEWS Report T2-02, 15 p.

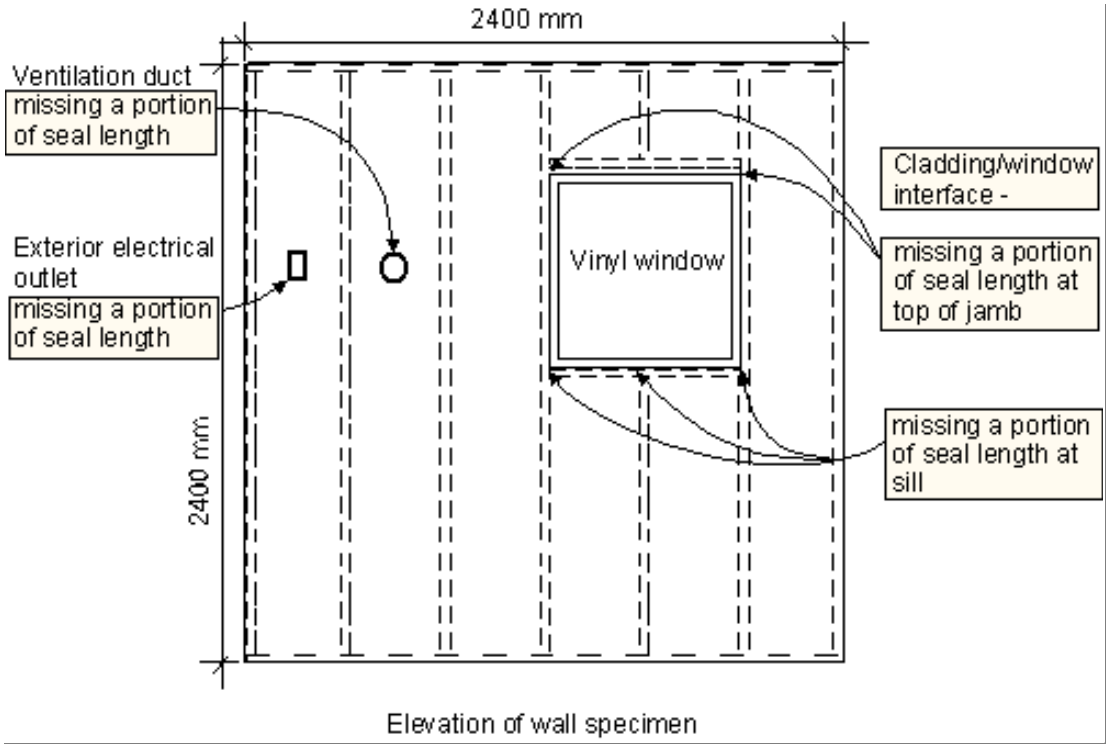

Figure 1.1 Generic deficiencies in the first line of defense of a typical wall specimen

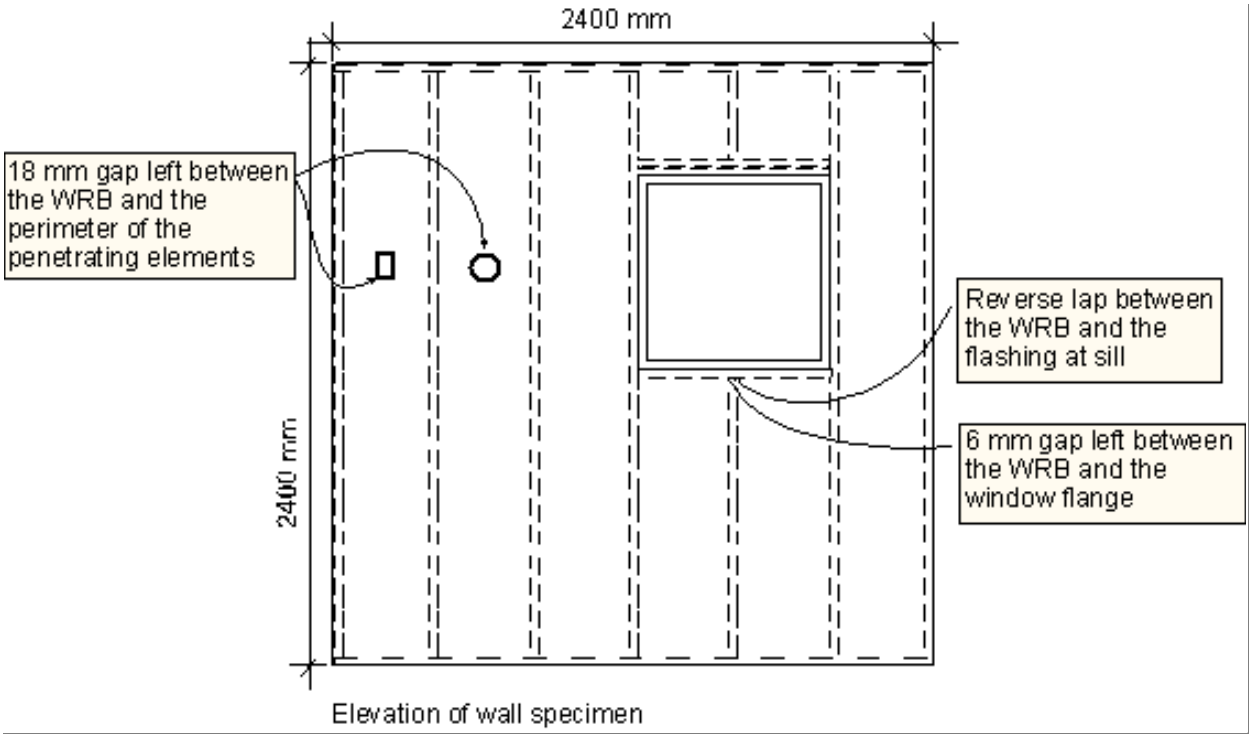

Figure 1.2 Generic deficiencies in the second line of defense of a typical wall specimen

Additional information concerning the configuration of the test specimens and details regarding deficiencies is provided in §1.2 of this chapter.

It is also worthwhile noting that given the specimens were fabricated in a laboratory setting, considerable care went into insuring that common elements among the different specimens were fabricated as specified.

QUANTITATIVE TRIALS

In regard to obtaining quantitative information for the purposes of providing the simulation model useful input for parametric studies, this portion of the test sequence was carried out on specimens that included specified cladding deficiencies. Cladding deficiencies represented openings of known type, size and location that were incorporated in the cladding such that water passing over these deficiencies might enter within the wall assembly proper. These, as mentioned previously, are provided in Appendix – A.

The simulation program required information on hourly rates of water entry at a given location in the wall assembly for specified climatic conditions. In essence, a relation was needed that linked climate variables, such as wind speed and rainfall rate, to water entry. Hence the test sequence required some measure of water entry rates at specified locations under simulated wind-driven rain conditions. This was achieved by the collection of water in troughs at specified locations over a known period when the specimen was subjected to a series of simulated wind-driven rain conditions. The simulated wind-driven rain conditions were implemented by applying increasing levels of pressure difference across the specimen at given water spray rates. Using this approach, rates of entry at specified locations in the specimen were obtained for each combination of pressure differential and spray rate. This provided a basis for generalising water entry for specific types of wall assemblies in relation to climate variables such as wind speed and rainfall intensity. Each generic type of specimen (i.e. Base-case, stucco, EIFS, brick masonry, siding) had water entry functions developed that were used as a basis for admitting water into the wall assembly for use in the simulation program.

This experimental program was hence comprised of two test sequences: water penetration performance assessments and water entry trials. These formed the basis for the results provided in the subsequent chapters of this report.

iii. **Overview of report**

The following provides an overview of the work reported in the accompanying chapters.

- Chapter 1 - Introductory chapter providing the objectives, approach and description of test facility, test protocol and test parameters used in the experimental work.
- Chapter 2 - Results from water entry experiments carried out on the acrylic sheathing wall assembly (base-case) and subsequently used in the development of water entry functions for the wall assemblies.
- Chapter 3 - Summary report on results from water penetration trials and entry assessments on stucco wall assemblies. Selected air leakage, static and dynamic pressure response characteristics of the stucco wall assemblies are provided in Appendix - B.
- Chapter 4 – Summary report on results from EIFS wall assemblies; selected air leakage and pressure response information provided in the Appendix B.
- Chapter 5 – Summary report on brick masonry clad wall assemblies; additional information on air leakage and pressure response given in the Appendix B
- Chapter 6 – Summary report on siding wall assemblies; selected information on air leakage and pressure response provided in the Appendix B
- Chapter 7 – Overview of results from the 17 wall assemblies, including a review of water penetration, water entry and the derivation of water entry functions. Details of experiments carried out on the deposition of water in the stud cavity are provided in Appendix B.
- Appendix – A: provides information on the basis for the selection of deficiencies in the cladding and within the wall assembly.
- Appendix – B: offering selected air leakage, static and dynamic pressure response information.

Each of the Summary reports on water penetration trials and water entry assessments are essentially self-contained and include an overview of the type of wall construction and the key components of the wall assembly as well as a summary of the test protocol described in this chapter. As well, the overview chapter (Chapter 7) provides additional information regarding the comportment of the different wall assemblies in relation to one another not provided in the other chapters.

The following sections provide information on the test facility, details regarding the test specimens, common to all wall assemblies, and the test protocol.

1.2 Description of Test Facility

The facility used to conduct the tests was the Dynamic Wind and Wall test Facility (DWTF). This facility, shown in Figure 1.3 to 1.4, is capable of subjecting full-scale test specimens (nominal size 2.44 by 2.44-m) to static or dynamic pressure fluctuations of over 2 KPa and spray rates of up to 8 L/min.-m^2 (Figure 1.3 and Figure 1.6). Dynamic pressure fluctuations are obtained by the displacement of a sealed 2.4-m diameter piston, which forms part of the back of the apparatus (Figure 1.5). The displacement of the piston (up to 75 mm) causes the volume of the space between it and the test specimen assembly to increase or decrease, thus varying the air pressure difference across the specimen. The movement of the piston can be programmed to produce sinusoidal, triangular or square waveforms of air pressure at frequencies ranging from 0.1 to 10Hz and amplitudes up to or exceeding 2KPa. A secondary blower generates the steady-state (static) component of air pressure. This blower provided the means to assess the air leakage characteristics of the specimens.

The apparatus also contains a pressure regulated water spray system (Figure 1.4) that simulates the action of rain deposition on the cladding surface. Different water deposition rates (hereafter referred to as spray rates) are achieved by regulating the pressure level along specific arrays of spray nozzles.

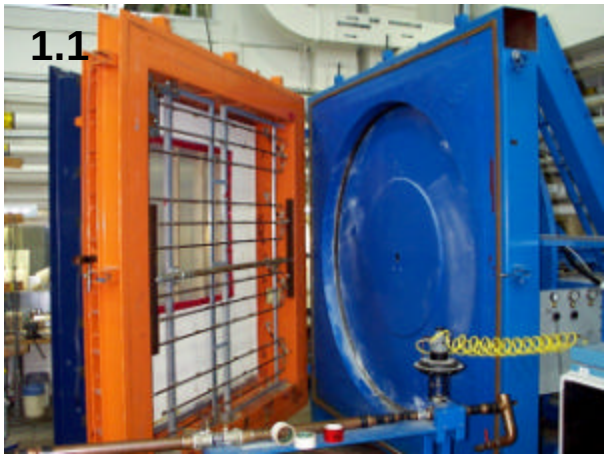

Figure 1.3 - **Inside view of apparatus** showing test specimen (sizes up to 2.44 by 2.44-m). The exterior cladding faces the inside of the apparatus.
Figure 1.4 **- Inside view of apparatus** showing piston and water spray racks.
Figure 1.5 - Rear view of apparatus showing piston and hydraulic gear.
Figure 1.6 **- Front view of apparatus** - The wall specimen is installed integrally to the metal test frame (in blue). The specimen test frame is in turn mounted and sealed to the facility test frame (in orange). The facility test frame supports the water spray racks and is the operable door to the apparatus.

1.3 Description of Test specimens

i. Introduction

The basis for development of the final configuration of the test specimens is provided in Appendix – A[3]. The approach and most of the deficiencies proposed in Appendix – A have been adopted for implementation in the experimental work described in this Chapter. During the course of the project, TG 6 and TG 2 further revised the selection of the deficiencies in consultation with the industry partners representing each of the four generic cladding system (e.g. Masonry Canada and Canada Brick for the four masonry specimens) in the months that preceded the construction and testing of those specimens. Given these activities some of the deficiencies proposed by the working group were not implemented for the following reasons:

- Some deficiencies would have been difficult to reproduce in a consistent manner from specimen to specimen (e.g. poor bond between masonry units, or blocked drainage holes);
- The number of test parameters was limited in any given specimen so that the analysis and interpretation of the experimental results would meet the objectives.

Finally, report TG2-02 entitled "Description of 17 large-scale wall specimens built for water entry investigation in IRC Dynamic Wall Testing facility" provides details on how the specimens were built and what deficiencies were introduced in the several layers of components making up the specimens.

The final test configuration showing the location of pressure taps, moisture sensors and water entry points are provided in Figures 1 to 3 respectively.

ii. Sensors

A photograph depicting the specimen is provided in Figure 1.7 and shows the stud cavity side of the specimen in which the various pressure and moisture sensors are identified.

PRESSURE TAPS

Pressure taps are located in six wall portions (Figure 1.8), with the first portion located at the left extremity of the wall (facing the weather-side). Typically in each portion, taps are located both in the wall cavity between the cladding and the sheathing board and in the stud space.

[3] MEWS Task Group 2 (1999), “Recommendation for the selection of deficiencies for the 17 wall specimens to be investigated for water ingress using the dynamic wall testing facility”, MEWS Report T2-02, 15 p.

Additionally, taps have been added to obtain measurements of pressure differential at points of water entry.

AIR BARRIER SYSTEM LEAKAGE

Air barrier system (ABS) leakage was regulated by introducing a series of ca. 6-mm diameter holes in the ABS (Figure 1.8), a series of seven (one in each stud cavity) representing an equivalent leakage area (ELA) of 169-mm^2, provided a nominal ABS leakage of 0.2 L/s-m^2. An ABS leakage of 0.5 L/s-m^2 (ELA 508-mm^2) was achieved using twenty-one holes of the same diameter, three in each stud cavity. The desired nominal leakage through the ABS was achieved by "opening" or "closing" the appropriate number of holes in the ABS.

MOISTURE SENSORS IN OSB

Photographs of typical moisture sensors are provided in Figure 1.9 and their location in the wall specimen is shown in Figure 1.10. Sixteen (16) moisture pin pairs (imbedded to either ¼ or ¾ sheathing thickness; e.g. see schematic) were placed in the OSB sheathing at locations where either water might first accumulate or at the base of the wall.

Moisture pin pairs imbedded at ¾ thickness provided moisture contents in proximity to the front of the sheathing; those at ¼ thickness (#4 & #12) were intended to offer information of the moisture profile across the sheathing. The sensors had been previously calibrated such that a light diode, located between the pairs of pins, activated if the moisture content reached or exceeded ca. 14%. The calibration curve used for relating electrical resistance to moisture content of the sheathing board is provided in Appendix B, §4. Over a test period, note was taken of the time and conditions under which the light was first activated

WATER ENTRY POINTS

The location of specified water entry points, provided in Figure 1.11, were deemed representative of typical deficiencies located at the interface between the cladding and penetrations, and include the following entry points:

- Above the electrical outlet – a 50-mm length of sealant is missing between the outlet cover and the wall (approximate size: 1-mm by 50-mm)
- Above the duct – a 50-mm length of sealant is missing between the duct and the wall (approximate size: 1-mm by 50-mm)
- Below the windowsill and between finishing strips – a 90-mm length of sealant is missing between the ending strips (approximate size: 10-mm by 90-mm).

.

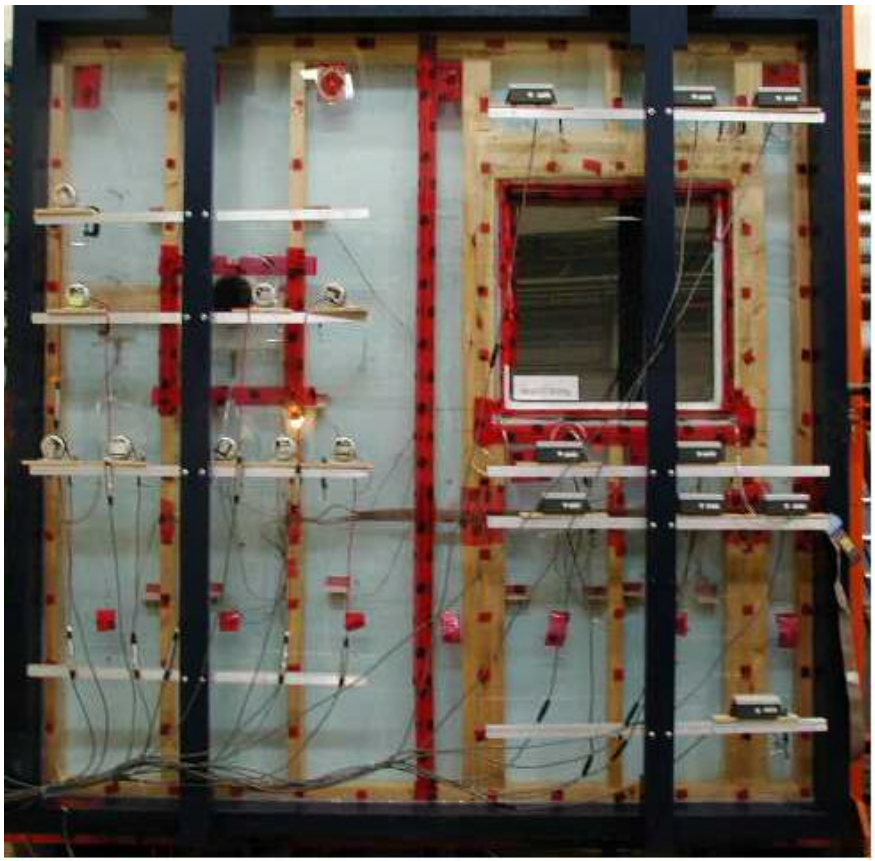

Figure 1.7 : View of 'stud-cavity' side of specimen WA-17 (Brick masonry veneer)

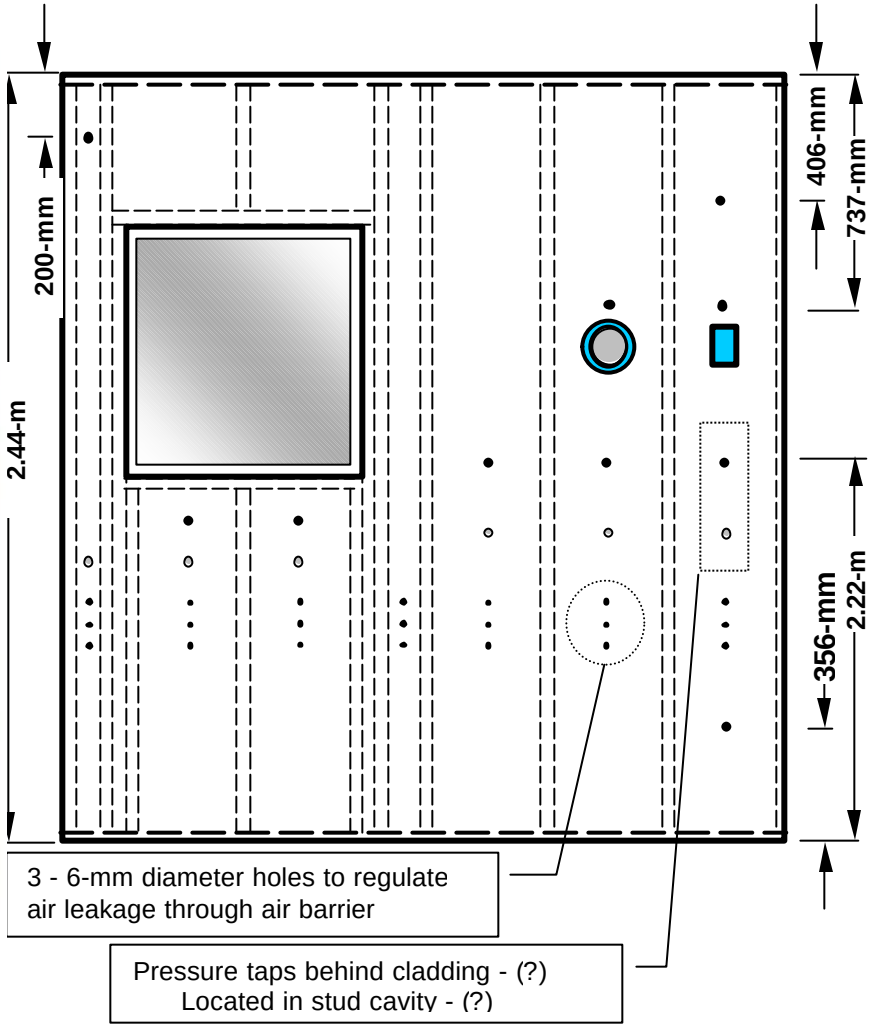

Figure 1.8 : Location of pressure taps and air leakage openings

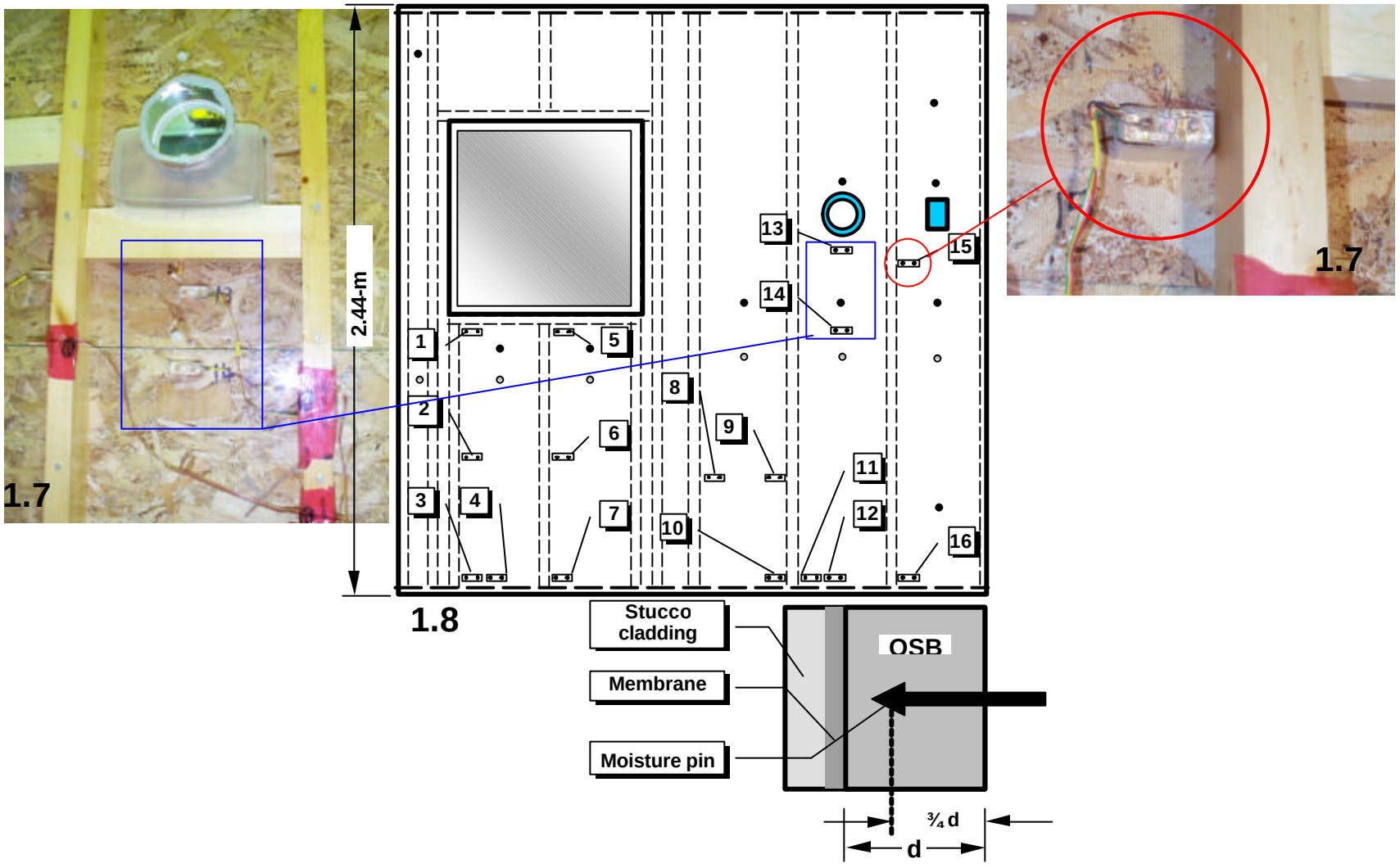

Figure 1.9: View of moisture sensors in stucco wall specimen (WA-2A)

Figure 1.10: Location of moisture sensors in a stucco-clad specimen

1.4 Description of Test protocol – summary

The protocol was established to determine the air leakage, pressure equalisation response and water penetration and entry characteristics of different wall assemblies when subjected to simulated driving rain using the DWTF. The approach adopted for the protocol consisted of conducting the tests in a series of stages, each of which is described below.

1. Characterisation of air leakage and pressure equalisation potential of the wall assembly.
2. Water penetration trials in both static and dynamic mode at a nominal spray rate of 3.4 L/s-m^2 (no planned deficiencies incorporated in cladding)
3. Subjecting specimen to 16 hours continuous water spray of 0.4 L/s-m^2 at a nominal pressure difference of 20 Pa to simulate effects of exposure to a long-term rain event.
4. Characterisation of water entry through specified deficiencies in the wall assembly using both static and dynamic pressure differentials and varying spray rates.

A description of each stage is provided below, complete with test condition inputs and expected outputs. Where possible, water entering cavities and interstitial spaces through specified deficiencies was collected such that the rate of water entry at these locations could be estimated.

Cavity and driving pressures were measured using differential pressure transducers such that the driving potentials for each water entry point could be estimated. Pressure data was collected on a continual basis over the duration of a test at specified locations shown in Figure 1.8. The location, configuration and size of specified deficiencies are identified in Figure 1.11.

Air leakage characteristics for the entire wall (perimeter leakage; window leakage, etc.) as well as for each of the specified deficiencies (i.e. water entry points) were determined using no less than five pressure data points and including a pressure point at 75Pa. Nominal air barrier leakage was set a 0.2 L/s-m^2.

Water entry data was collected at each entry point having a collection trough and rates of water entry were calculated for both static and dynamic conditions for each of the pressure steps. Data on water entry under the influence of gravity alone (i.e. no pressure differential across assembly) was also obtained.

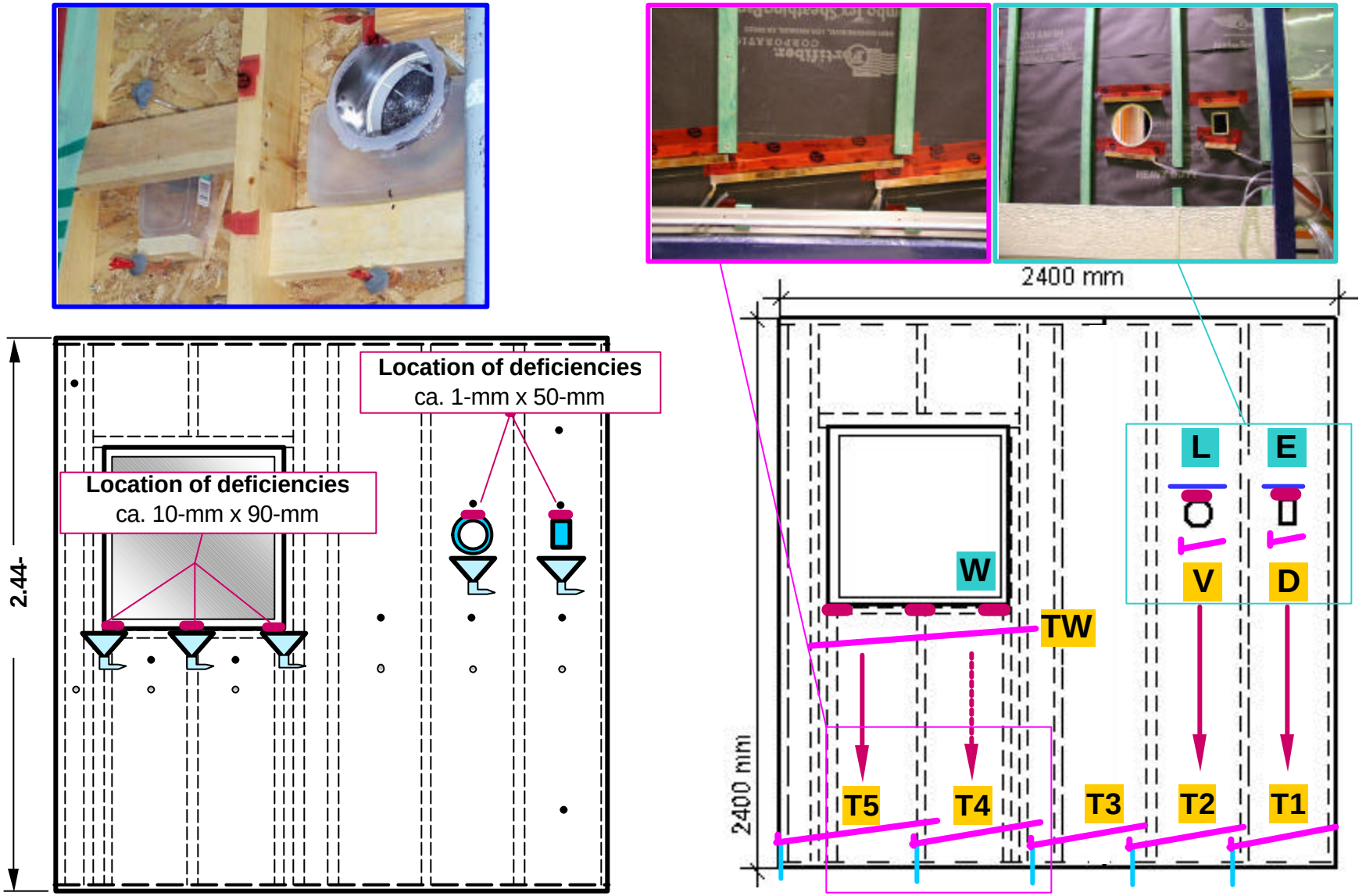

Figure 1.11 : Location of water collection points and troughs

i. *STAGE 1 - AIR LEAKAGE AND PRESSURE EQUALISATION CHARACTERISTICS*

AIR LEAKAGE:

Air leakage is to be measured using laminar flow elements (MIRIAM) from which pressure readings are taken using a micromanometer (Air Limited) capable of assessing pressures to an accuracy of ± 0.5 Pa. For each test sequence, laboratory temperature and atmospheric pressure are measured to apply corrections to the results obtained using the micromanometer.

The system leakage, Q_s is given by: $Q_s = Q_{tl} – (Q_{bl} + Q_{pl})$

Where:

- Q_{tl}: Total system leakage derived from leakage tests at different pressures.
- Q_{bl}: Base leakage (Leakage around DWTF door and piston) – Polyethylene is tightly sealed to the steel frame on the laboratory side of the DWTF covering the specimen and its seal to the frame such that the only leakage is through the seals around the door and piston.
- Q_{pl}: Specimen perimeter leakage – All leakage holes in the air barrier system are closed such that leakage occurs through the specimen perimeter seal.

Air barrier system leakage – The air leakage across a series of holes in the air barrier was evaluated such that the chosen combination of holes provides the nominal requirement of 0.6 L/s or less (i.e. 0.1 L/s-m^2 for a specimen having an area of 5.95m^2) at a pressure difference of 75 Pa. Air leakage through the system was measured as a function of static pressure difference across the assembly.

The characteristic leakage rate (L/s) of airflow through leakage holes was fitted to the pressure difference across the air barrier system by a least squares fit to the following equation:

$$Q = C \bullet ?P^n$$

Leakage tests were conducted at the static pressure differentials provided in Table 1.1:

Table 1.1 – Static test pressures

Step	Static pressure, Pa
1	50
2	75
3	150
4	300
5	500
6	1000

PRESSURE EQUALISATION POTENTIAL

Dynamic tests were conducted to evaluate the pressure equalisation potential of the wall assemblies. Dynamic tests were conducted under a sinusoidal varying pressure with mean and amplitude given in Table 1.2 below. Two (2) test frequencies were used to assess the pressure equalisation response of the wall assemblies: 0.5 Hz and 2 Hz.

Table 1.2 – Dynamic pressure fluctuations

Step	Dynamic pressure, Pa
1	75 + 40•sin(*2pft*)
2	150 + 60•sin(*2pft*)
3	300 + 125•sin(*2pft*)
4	700 + 300•sin(*2pft*)

The driving pressure and pressure differences at each of the pressure taps were recorded and fitted to sine/cosine functions using a least squares fit. For the analysis of the data, amplitude and phase angle were determined and pressure equalisation response calculated.

ii. *STAGE 2 - WATER PENETRATION TRIALS*

WATER PENETRATION UNDER STATIC CONDITIONS – NO SPECIFIED DEFICIENCES

Water penetration trials of Stage 2 were conducted on wall assemblies having no specified deficiencies. Wall assemblies were subjected to both static and dynamic pressure differentials and water entry was monitored through the use of moisture resistance sensors and by visual inspection. Water entry assessment through specified deficiencies is described in Stage 4 of the protocol.

The water penetration trials under static conditions consisted of 6 steps of increasing static pressure differential (Table 1.3) subjected to a nominal water spray rate of 3.4 L/s-m^2. Each pressure “step” was conducted over either a 10 or 20-minute period such that water entry through the assembly can be determined either through the use of moisture resistance sensors or by visual inspection of the second line of defence.

Table 1.3 – Static test pressures at nominal spray rate of 3.4 L/s-m^2

Step	Static pressure, Pa	Dwell time, min.
1	0	20
2	75	20
3	150	20
4	300	20
5	500	20
6	1000	20 Total = 120

WATER PENETRATION UNDER DYNAMIC CONDITIONS – NO SPECIFIED DEFICIENCES

Water penetration trials under dynamic conditions consisted of 5 steps of increasing dynamic pressure differential at 0.5 Hz (Table 1.4) and simultaneous application of a nominal water spray rate of 3.4 L/s-m^2. Each pressure "step" was conducted over a 20-minute period such that water entry through the assembly could be determined either through the use of moisture resistance sensors (if these have not been activated in the previous trial) or by visual inspection of the second line of defence.

Table 1.4 – Dynamic pressure loads at nominal spray rate of 3.4 L/s-m^2

Step	**Dynamic pressure, Pa**	**Dwell time, min.**
1	75 + 40•sin(*2pft*)	20
2	150 + 60•sin(*2pft*)	20
3	300 + 125•sin(*2pft*)	20
4	700 + 300•sin(*2pft*)	20 Total = 80

iii. *STAGE 3 – EFFECT OF CONTINUOUS WATER SPRAY*

Immediately following Stage 2, water was applied to the surface of the wall specimen over a 16-hour period at a rate of 0.4 L/s-m^2 and a pressure differential of 50 Pa. The intent was to observe evidence of water penetration through unidentified deficiencies in the wall proper when subjecting the wall to a simulated extended "rain event".

iv. *STAGE 4 - WATER ENTRY ASSESSMENTS*

Water entry through specified deficiencies in the wall assembly was characterised using both static and dynamic pressure differentials and varying spray rates. Rates of water entry through specified deficiencies in the wall assembly were determined from the collection of water in troughs over a given time period. The troughs were fitted to the backside of the second line of defence as shown in Figure 1.11 or in the ventilation-drainage (hereafter referred to as drainage space) for specimens incorporating such a space.

WATER ENTRY THROUGH SPECIFIED DEFICIENCIES UNDER STATIC CONDITIONS

The water entry assessments under static conditions consisted of 3 steps of increasing static pressure differential (Table 1.5) with simultaneous application of nominal rates of spray of 1.7 L/s-m^2 and 3.4 L/s-m^2. Each pressure "step" was conducted over either a 10 or 20-minute period such that water entry through the assembly could be determined from collection in specified gauges located behind second line of defence.

Table 1.5 – Static test conditions

Step	Nominal spray rate L/s-m^2	Static pressure, Pa	Dwell time, min.
1	1.7	0*	20
2		300	20
3		150	20
4		75	20
5	3.4	75	20
6		150	20
7		300	20

*preconditioning of simulated defects

WATER ENTRY THROUGH SPECIFIED DEFECIENCIES UNDER DYNAMIC CONDITIONS

Water entry trials under dynamic conditions consisted of 3 steps of increasing dynamic pressure differential at 0.5 Hz (Table 1.6) with simultaneous application of nominal rates of spray of 1.7 L/s-m^2 and 3.4 L/s-m^2. Each pressure "step" was conducted over a 20-minute period such that water entry through the assembly could be determined from collection in specified gauges located behind second line of defence.

Table 1.6 –Dynamic test conditions

Step	Nominal spray rate L/s-m^2	Dynamic pressure, Pa	Dwell time, min.
1	1.7	0	5
2		75 + 40•sin(*2pft*)	20
3		150 + 60•sin(*2pft*)	20
4		300 + 125•sin(*2pft*)	20
5	3.4	75 + 40•sin(*2pft*)	20
6		150 + 60•sin(*2pft*)	20
7		300 + 125•sin(*2pft*)	20

Chapter 2

RESULTS ON BASE-CASE WALL ASSEMBLY

TABLE OF CONTENTS

— Chapter 2 —

Results on Base-Case Wall Assembly

LIST OF TABLES

LIST OF FIGURES

2.1 Introduction

Information to help establish the performance characteristics of a “Base-case” wall assembly (initial acrylic wall) provided both qualitative as well as quantitative information on water entry and this would subsequently be used for assessing the water entry performance of generic wall types. Water entry through specified deficiencies located on the rainscreen of known size and location, was quantified in terms of simulated precipitation rate and pressure difference across the wall. Results indicated the quantity of water entering a specific deficiency could be evaluated as a function of the pressure differential across the deficiency. For a given pressure differential, quantities of water entering a deficiency varied in accordance with precipitation rates and the size and nature of the opening.

In this Chapter, observations are provided from data collected on the water entry through a deficiency located in Base case (acrylic) wall assembly No. 2, specifically, an entry point located above a ventilation duct that penetrates the wall assembly proper. This assembly has the same through-wall penetrations (i.e. window, ventilation duct and electrical duplex) incorporated in it as those found in the generic wall assemblies (i.e. stucco, EIFS, masonry, siding).

The prototype wood-frame cavity wall sheathed in clear acrylic was designed and fabricated such that it included a rainscreen, a barrier acting as second line of defence, and an air barrier. Nominally, this permits qualitative information to be derived given that one can see through the clear acrylic sheathing during water entry tests. The use of an impermeable and clear material helped focus the investigation on water entry, exclusive of the effects due to water absorption by the cladding material. Here it is assumed that water will penetrate the first line of defence, and the qualitative information derived from identifying the path the water follows is of importance as is information on the possibility it comes into contact with the second line of defence or inner barrier.

The work focused on quantifying the amount of water entering deficiencies of known size at specific locations on a wall assembly given simulated precipitation rates (water spray rates), wind pressure differentials and air leakage characteristics of the assembly. Based on this information, the likelihood of water reaching the second line of defence for a given simulated wind driven rain condition and known deficiencies on the weather screen, will be a function of the assembly specific conditions, in particular: the dimensions and size of the venting cavity, the vent sizes, and the overall air leakage characteristics of the assembly.

2.2 Experimental approach

The experiment consisted of subjecting an acrylic sheathed wall assembly, in which deficiencies of known type, size and location were introduced, to various levels of simulated precipitation and pressure difference such that the rate of water entry through these deficiencies could be determined.

A diagram depicting the general configuration of the wall in elevation view is given in Figure **2.1**. A description of the types of deficiencies is provided in §2.1. The test procedure is described in §2.2, and includes calibration of simulated precipitation rates in proximity to the deficiencies and system air leakage.

The rainscreen was constructed such that a 19-mm cavity was formed between it and the second line of defence. The air barrier had an effective leakage area (ELA) of 120 $mm^{2,}$ assuming a rigid rainscreen.

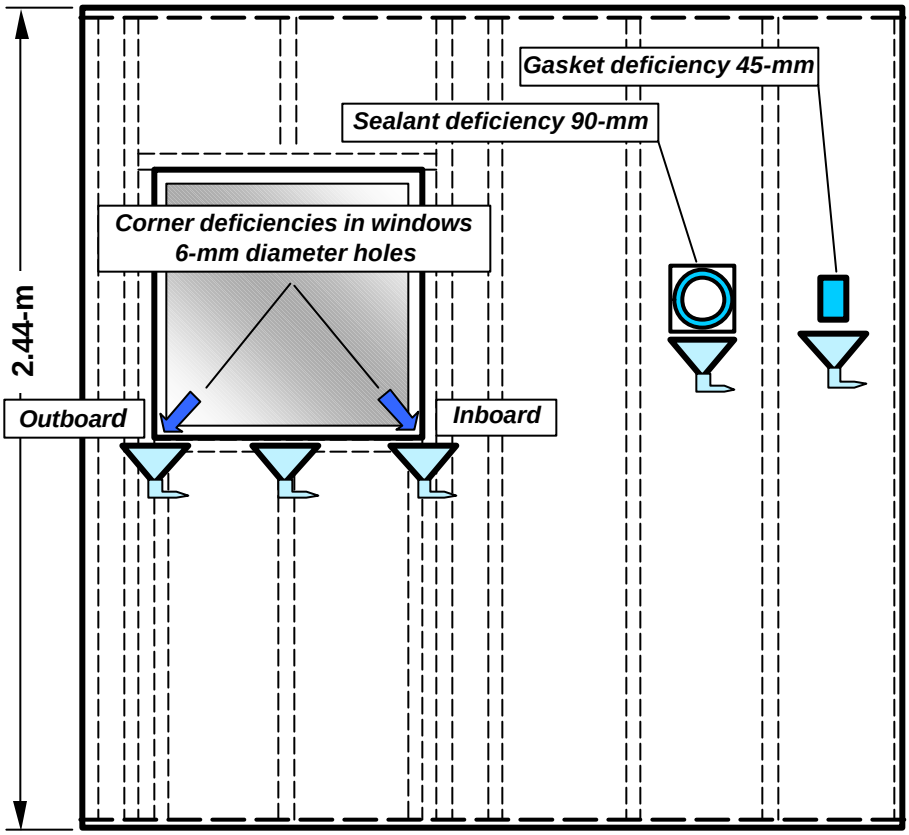

Figure 2.1 - General configuration of the Base-Case wall assembly showing location of nominal deficiencies in wall assembly and water collection troughs

2.2.1 SPECIFIED RAINSCREEN DEFICIENCIES

Details regarding specified deficiencies introduced onto the rainscreen cladding are provided below. Note that when reference is made in this chapter to "deficiencies", in all instances this is referring to specified deficiencies.

2.2.1.1 SPECIFIED ANCILLARY FIXTURE DEFICIENCIES:

(1) Horizontal sealant deficiency: A dryer ventilation duct set into a 175 mm circular opening in the wall at a height of 1590 mm from the bottom of the frame was sealed around its outer flange (flange-wall interface) with the exception of 90 mm of the interface located at the top horizontal edge. The deficiency was 90 mm long by 1.0 mm wide providing a cross sectional area of ca. 90 mm^2

(2) Horizontal sealant deficiency: An exterior electrical outlet with a 45 mm wide deficiency cut into the cover plate neoprene gasket on the top horizontal edge.

2.2.1.2 SPECIFIED WINDOW-WALL INTERFACE DEFICIENCIES:

(3) Horizontal sill deficiency: A 90-mm portion of sealant missing between the windowsill and the wall sill interface (above the backing rod). 3/8" backing rod stuffed into the interface acts as a seal from the weather side elements.

(4) "L" shaped edge deficiency: A 180-mm portion of sealant missing between the window and wall interface at the lower left corner. The deficiency is a combination of a 90-mm horizontal and a 90-mm vertical deficiency. Backing rod (3/8" diameter) is placed in the space between adjacent the interface acts as a seal from the weather side elements.

2.2.1.3 SPECIFIED WINDOW DEFICIENCIES:

(5) Circular hole (6-mm) bored through the weather side of the lower left corner of the vinyl window frame, outboard toward the sill edge. This is to simulate a weather side mitred corner deficiency in the window itself more exposed to the weather side elements than the inboard corner

(6) Circular hole (6-mm) bored through the lower right corner of the vinyl window frame, inboard toward the room side. This is to simulate a weather side mitred corner deficiency in the window less exposed to the weather side elements than the outboard deficiency.

2.2.2 TEST PROCEDURE

2.2.2.1 PRECIPITATION RATES

In order to determine the actual rate of cascading water down the rainscreen surface it was determined that baseline calibration testing should be carried out on the assembly. A 59 cm Plexiglas trough was built, fitted and sealed against the weather-side of the rain screen at each area of the respective deficiency to be evaluated (ventilation duct, electrical outlet and window deficiencies). The trough was graded in ten 1-litre increments. At various pressure and nozzle settings (nozzles at 12-in. centres, at 24-in. centres and at 12/24-in. combination centres) the time for ten litres of water to be collected was recorded to the nearest second and the rate of water spray at a given location calculated in terms of l/min-m^2 based on the gross area extending directly above the width of the trough.

Current standard specifications for water penetration testing are given in Table 2.1. Water spray rates at given test pressures are only measured in terms of initial impinging water on the rainscreen, not impinging and collected run off water.

Table 2.1: Water Penetration Testing Standards

Standard	Test Pressure (Pa)	Water Spray (L/min-m^2)
AAMA 501	575	3.4
ASTM E547	137	3.4
CAN-A440-M	700	3.4
European	500	1.0
JSI-A-1517	490	4.0

Baseline precipitation results are shown in Table 2.2. For the cases of the ventilation duct deficiency and the electrical outlet deficiency the collection area (impinging and runoff) totalled 0.686 m^2 (0.59 m wide X 1.16 m high). The amount of time required for the collection trough to collect 10 litres of run off water was recorded. In order to approximate the current standard specifications for water penetration testing (see Table 2.1) a combination of half the 12" centred nozzles and half the 24" centred nozzles was used. The precipitation calibration procedure does not account for water that bounces off the wall after initial contact.

Table 2.2: Spray (Run Off) Rates in the Proximity of the Ventilation duct and Electrical Outlet Rainscreen Deficiencies for the Base Case Wall as tested in the DWTF

24 " Center Nozzles		12 " Center Nozzles		12/24 " Center Nozzles *	
Regulator Pressure (psi)	Spray Rate (L/min- m^2)	Regulator Pressure (psi)	Spray Rate (L/min- m^2)	Regulator Pressure (psi)	Spray Rate (L/min- m^2)
10	0.85	10	2.99	10	3.90
15	1.02	15	4.17	15	4.28
20	1.15	20	5.21	20	4.56
25	1.24	25	5.91	25	4.73
30	1.25	30	6.38	30	5.57
35	1.31	35	6.63	35	5.83
40	1.35	40	7.00	40	6.07

2.2.2.2 DWTF SYSTEM AIR LEAKAGE

In order to provide accurate air leakage profiles of all specimens, it was necessary to establish baseline air leakage results for the DWTF system as a whole using and air-tight specimen (metal enclosure). The piston, door and specimen seals as well as pipe, wire and instrumentation joint, hatches are not completely air-tight. By isolating certain components of the system with polyethylene sheathing then gathering air leakage data, baseline air leakage results were obtained. Table 2.3 provides results obtained for the DWTF system leakage that have been subsequently plotted in Figure 2.2. Any subsequent specimen results would have this system leakage result deducted from the collected specimen data. Figure 2.2 shows pressure difference as a function of air leakage plotted with logarithmic scales.

Table 2.3: DWTF System Air Leakage Results

Chamber Pressure (Pa)	**Air leakage (l/s)**	**Chamber Pressure (Pa)**	**Air leakage (l/s)**
30	0.0074	400	0.0540
40	0.0082	500	0.0644
50	0.0082	600	0.0788
60	0.0090	700	0.0980
75	**0.0130**	800	0.1251
100	0.0130	900	0.1592
200	0.0203	1000	0.1837
300	0.0404		

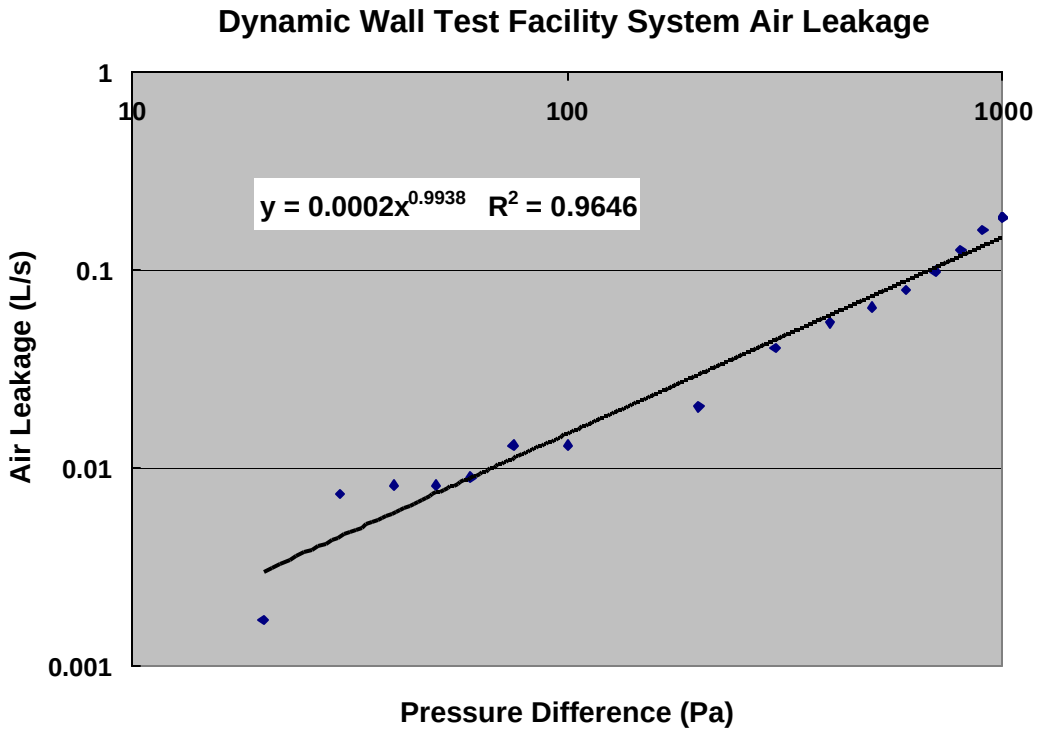

Figure 2.2 - DWTF System Air Leakage, Pressure Difference vs. Air Leakage

2.3 Results

In this Chapter results are provided from water entry through deficiencies located at the top of a ventilation duct (VL), an electrical outlet (E) and at adjacent lower corners of a vinyl window (W). The deficiencies were subjected to simulated precipitation (water spray) concurrent with either static or dynamic pressure differentials across the assembly.

Rates of water collection were recorded for water entry through horizontal sealant deficiencies located on the rainscreen of the wall assembly for the simulated precipitation rates (spray rate) and under both static and dynamic pressure modes (air pressure mode). The degree of venting of the rainscreen was varied between none and fully open. In the case of fully open, the rainscreen had a series of openings at the base of wall assembly that collectively offered approximately 5400-mm^2 of venting area to the rainscreen. Tests were also carried out such that the second line of defence at the periphery of the joint between the ventilation duct and the sheathing board was either sealed or not (i.e. open). An overview of the results is provided in Table 2.4 in which a dot (•) indicates instances where observations have been made, the data from these tests being provided in Table 2.5 to

Table **2.18**.

Table 2.4: Index of Tables for deficiency at the ventilation duct

Table	Spray Rate	Air Pressure mode					Rainscreen Venting		2nd Line of Defence…		*
	3.90-6.07 (l/min m^2)	0-1000 (Pa)	75 ± 40 (Pa)	150 ± 60 (Pa)	300 ± 125 (Pa)	700 ± 300 (Pa)	None (0 mm^2)	Full (5400 mm^2)	Sealed	Open	Deficiency type
6	•	•					•		•		VL
7	•	•						•	•		VL
8	•	•					•			•	VL
9	•	•						•		•	VL
10	•		•	•	•	•	•		•		VL
11	•		•	•	•	•		•	•		VL
12	•		•	•	•	•	•			•	VL
13	•		•	•	•	•		•		•	VL
14	•	•	•	•	•	•	•		•		E
15	•	•	•	•	•	•		•	•		E
16	•	•	•	•	•	•	•		•		W-O
17	•	•	•	•	•	•		•	•		W-O
18	•	•	•	•	•	•	•		•		W-I
19	•	•	•	•	•	•		•	•		W-I

* VL: ventilation duct; E: electrical outlet; W-O: window corner- outboard;

W-I: window corner- inboard

2.3.1 STATIC RESULTS: DEFICIENCY AT VENTILATION DUCT

2.3.1.1 RAINSCREEN NOT VENTED / SECOND LINE OF DEFENCE SEALED

Data is provided in Table 2.5 on water entry rates through a 90-mm horizontal deficiency of ca. 1-mm height located in the top portion of the ventilation duct that penetrates the rainscreen. These trials were conducted for a rainscreen that was not vented and in which the second line of defence around the ventilation duct is sealed.

Table 2.5: Water entry rates through deficiency atop ventilation duct for spray rates of 3.9 to 6.07 L/min.-m^2 at given chamber pressures

Chamber Pressure (Pa)	Water entry through deficiency (L/min.)				Air Leakage Through Deficiency (L/s)
	Nominal Water Spray rate (L/min-m^2)				
	3.90	*4.56*	*5.57*	*6.07*	
0	0.14	0.24	0.36	0.44	0.00
75	0.17	0.29	0.48	0.56	0.42
150	0.18	0.30	0.49	0.59	1.36
300	0.27	0.32	0.54	0.63	2.99
600	0.24	0.32	0.57	0.62	4.33
1000	0.25	0.34	0.58	0.64	5.94

The water entry varies as a function of both the spray rate and differential chamber pressure as shown in Figure 2.3 and Figure 2.4 below. The dependency of water entry on changes in the differential pressure is not as evident as is water entry in relation to the spray rate. As can be seen in Figure 2.4, water entry rates vary linearly as a function of the simulated rate of precipitation up to rates upwards of 6 L/min.-m^2.

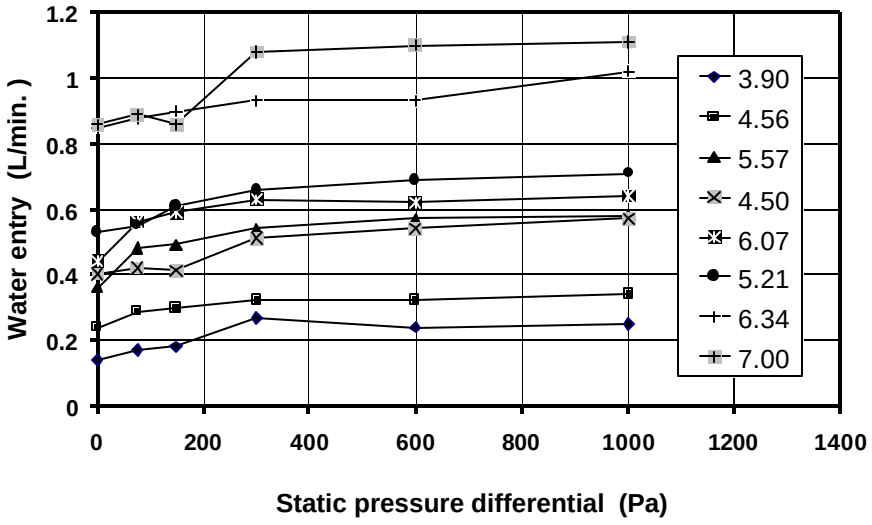

Figure 2.3 - Water entry through deficiency as a function of differential chamber pressure – 90-mm^2 Ventilation duct deficiency through a non-vented rainscreen having a sealed second line of defence

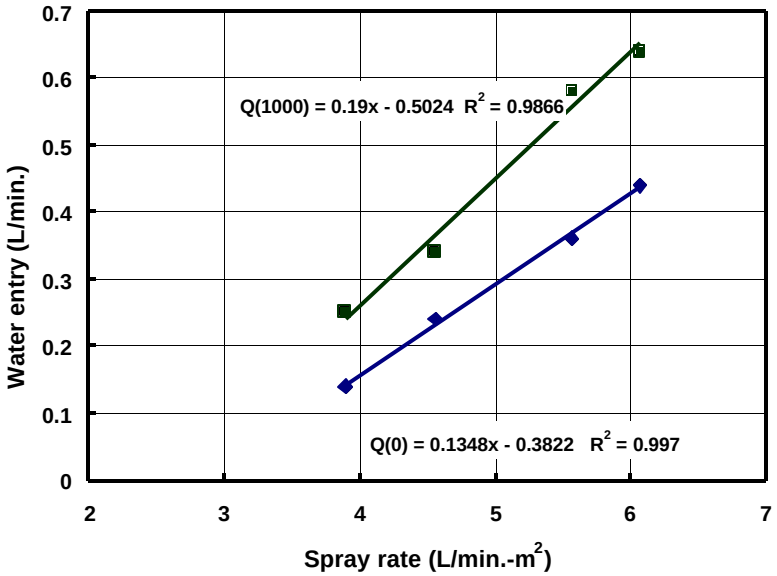

Values in the legend relate to spray rate (L/min-m^2)

Figure 2.4 – Water entry through deficiency as a function of simulated precipitation rate – 90-mm^2 Ventilation duct deficiency through a non-vented rainscreen having a sealed second line of defence

2.3.1.2 RAINSCREEN FULLY VENTED / SECOND LINE OF DEFENCE SEALED

Data is provided in Table 2.6 on water entry rates through a 90-mm horizontal deficiency of ca. 1-mm height located in the top portion of the ventilation duct that penetrates the rainscreen. These trials were conducted for a rainscreen that was fully vented and in which the second line of defence around the ventilation duct is sealed.

Table 2.6: Water entry rates through deficiency atop ventilation duct for spray rates of 3.9 to 6.07 L/min.-m^2 at given chamber pressures
Rainscreen fully vented / second line of defence sealed

Chamber Pressure (Pa)	**Water entry through deficiency (L/min.)**				Air Leakage Through Deficiency (L/s)
	Nominal Water Spray rate (L/min-m^2)				
	3.90	*4.56*	*5.57*	*6.07*	
0	0.14	0.24	0.36	0.44	0.00
75	0.14	0.24	0.39	0.44	0.76
150	0.14	0.24	0.42	0.53	1.76
300	0.16	0.25	0.50	0.54	2.15
600	0.18	0.26	0.53	0.57	4.76
1000	0.20	0.27	0.54	0.60	6.71

The water entry varies as a function of both the spray rate and differential chamber pressure as shown in Figure 2.5 and Figure 2.6 below. As in the previous instance, the dependency of water entry on the spray rate is more significant than for changes in the differential pressure. Water entry rates are shown to vary linearly with precipitation rate (Figure 2.6).

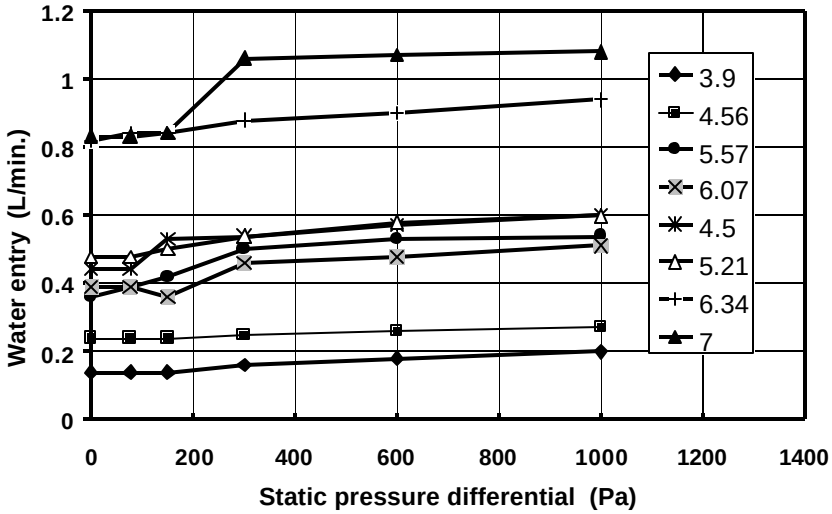

Figure 2.5 – Water entry through deficiency as a function of differential chamber pressure – 90-mm^2 Ventilation duct deficiency through a fully vented rainscreen having a sealed second line of defence Values in the legend relate to spray rate (L/min-m^2)

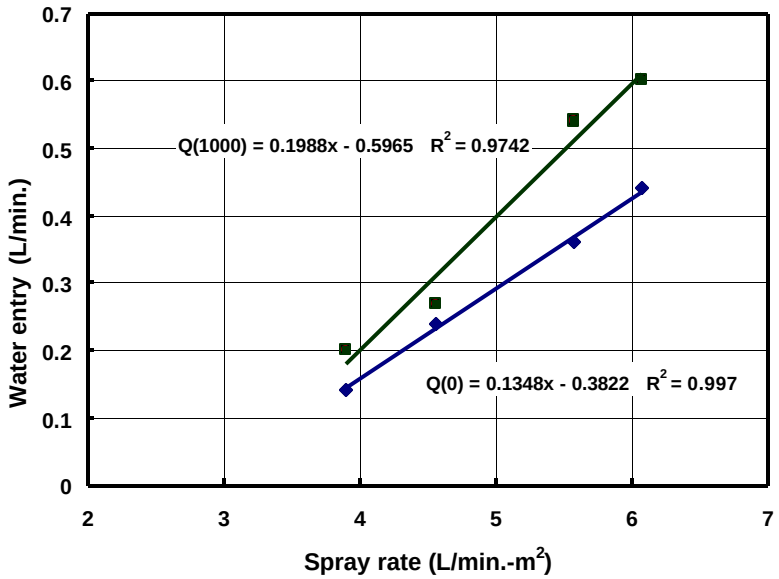

Figure 2.6 – Water entry through deficiency as a function of differential chamber pressure – 90-mm^2 Ventilation duct deficiency through a fully vented rainscreen having a sealed second line of defence

2.3.1.3 RAINSCREEN NOT VENTED / SECOND LINE OF DEFENCE NOT SEALED

Data is provided in Table 2.7 on water entry rates through a 90-mm horizontal deficiency of ca. 1-mm height located in the top portion of the ventilation duct that penetrates the rainscreen. These trials were conducted for a rainscreen that was not vented and in which the second line of defence around the ventilation duct is not sealed.

Table 2.7: Water entry rates through deficiency atop ventilation duct for spray rates of 3.9 to 6.07 L/min.-m^2 at given chamber pressures - Rainscreen not vented / second line of defence not sealed

Chamber Pressure (Pa)	**Water entry through deficiency (L/min.)**				Air Leakage Through Deficiency (L/s)
	Nominal Water Spray rate (L/min-m^2)				
	3.90	*4.56*	*5.57*	*6.07*	
0	0.14	0.24	0.36	0.44	0.00
75	0.16	0.28	0.40	0.50	0.05
150	0.14	0.31	0.41	0.49	0.16
300	0.20	0.32	0.46	0.51	0.56
600	0.21	0.36	0.48	0.52	1.33
1000	0.24	0.41	0.49	0.57	2.02

Water entry varies as a function of both the spray rate and differential chamber pressure and the dependency of water entry on changes in the differential pressure is not as evident as is the water entry in relation to the simulated precipitation rate (Figure 2.7 and Figure 2.8).

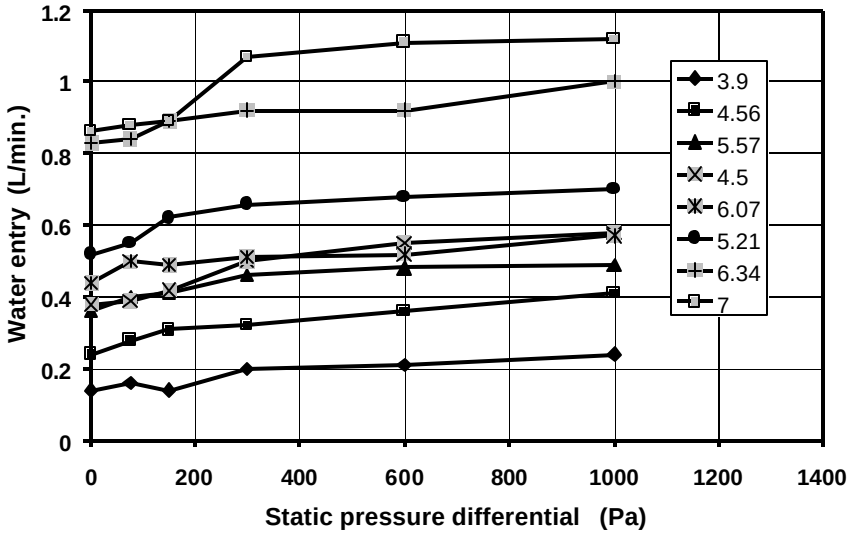

Figure 2.7 – Water entry through deficiency as a function of differential chamber pressure – 90-mm^2 ventilation duct deficiency on non-vented rainscreen having the second line of defence not sealed Values in the legend relate to spray rate (L/min-m^2)

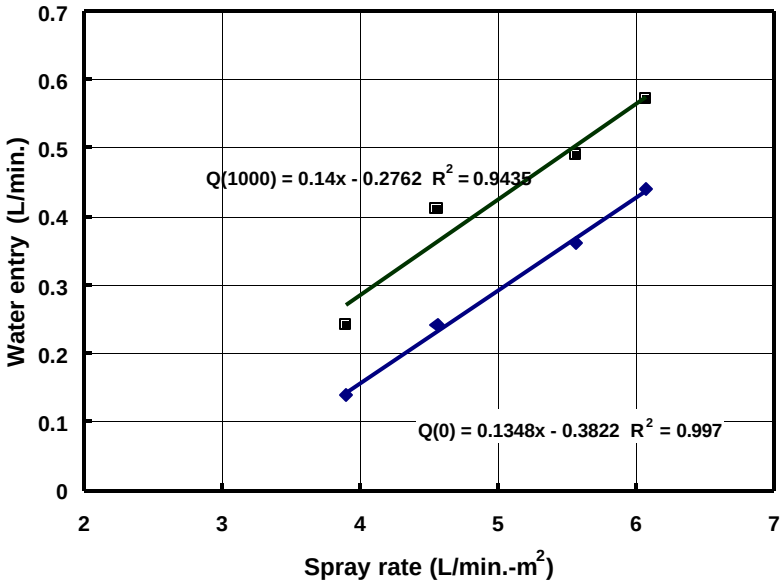

Figure 2.8 – Water entry through deficiency as a function of differential chamber pressure – 90-mm^2 ventilation duct deficiency on non-vented rainscreen having second line of defence not sealed

2.3.1.4 RAINSCREEN FULLY VENTED / SECOND LINE OF DEFENCE NOT SEALED

Data is provided in Table 2.8 on water entry rates through a 90-mm horizontal deficiency of ca. 1-mm height located in the top portion of the ventilation duct that penetrates the rainscreen. These trials were conducted for a rainscreen that was fully vented and in which the second line of defence around the ventilation duct is not sealed.

Table 2.8: Water entry rates through deficiency atop ventilation duct for spray rates of 3.9 to 6.07 L/min.-m^2 at given chamber pressures
Rainscreen fully vented / second line of defence not sealed

Chamber Pressure (Pa)	Water entry through deficiency (L/min.)				Air Leakage Through Deficiency (L/s)
	Nominal Water Spray rate (L/min-m^2)				
	3.90	*4.56*	*5.57*	*6.07*	
0	0.12	0.23	0.35	0.44	0.00
75	0.12	0.22	0.38	0.44	0.99
150	0.13	0.23	0.39	0.50	1.85
300	0.14	0.24	0.44	0.50	2.29
600	0.16	0.25	0.47	0.53	4.79
1000	0.17	0.26	0.52	0.56	6.69

Results plotted in these figures also follow the same pattern reported earlier: water entry varies as a function of both the simulated precipitation rate and differential chamber pressure and the dependency of water entry on changes in the differential pressure are not as evident as is water entry to the spray rate (Figures 2.9 and 2.10)

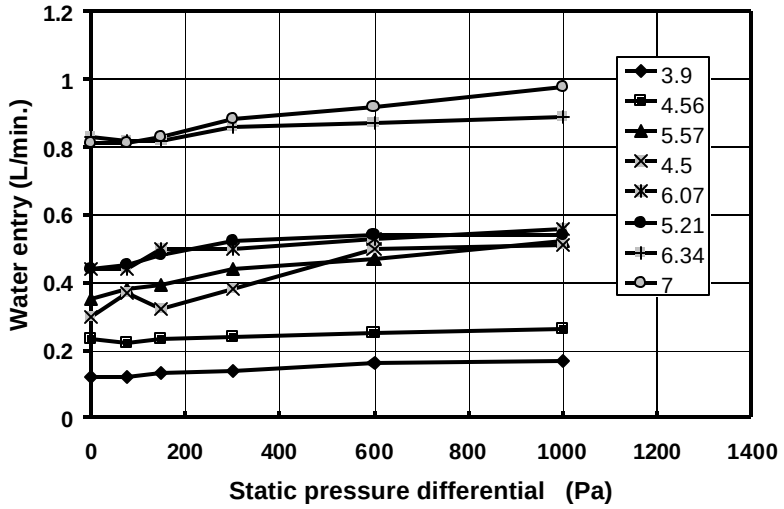

Figure 2.9 – Water entry through deficiency as a function of differential chamber pressure – 90-mm^2 Ventilation duct deficiency; fully vented rainscreen; second line of defence not sealed
Values in the legend relate to spray rate (L/min-m^2)

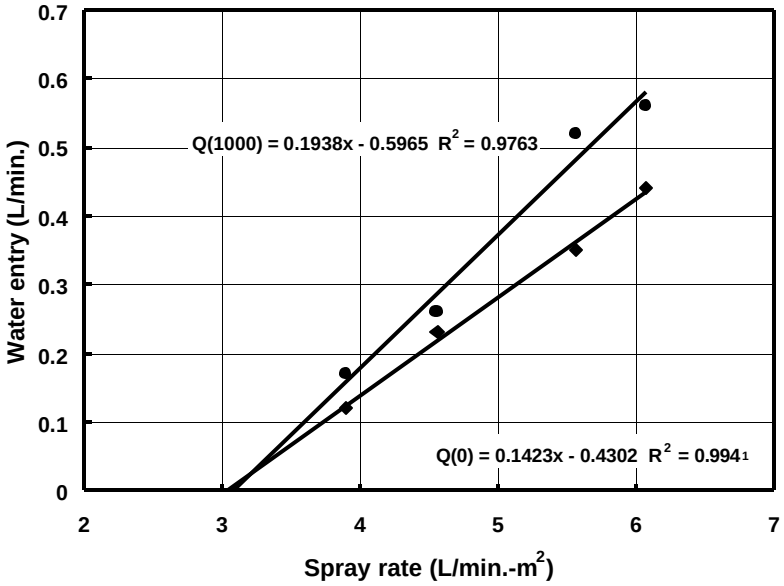

Figure 2.10 – Water entry through deficiency as a function of differential chamber pressure – 90-mm^2 Ventilation duct deficiency on fully vented rainscreen having second line of defence not sealed

2.3.2 DYNAMIC RESULTS : VENTILATION DUCT DEFICIENCY

Results from water entry tests through a deficiency in a ventilation duct and conducted under dynamic pressure conditions (0.5 Hz) are provided in Table 2.9 to 2.21 and Figure 2.11 to 2.15. Details on the type of data specific to a given test condition are provided in the respective sub-sections.

2.3.2.1 RAINSCREEN NOT VENTED / SECOND LINE OF DEFENCE SEALED

Data is provided in Table 2.9 on water entry rates through a 90-mm horizontal deficiency of ca. 1-mm height located in the top portion of the ventilation duct that penetrates the rainscreen. These trials were conducted under dynamic pressure fluctuations for a rainscreen that was not vented and in which the second line of defence around the ventilation duct is sealed.

Table 2.9: Water entry rates through deficiency atop ventilation duct for spray rates of 3.9 to 6.07 L/min.-m^2 at given chamber pressures
Rainscreen not vented / second line of defence sealed

Chamber Dynamic Pressure @ 5 Hz. (Pa)	**Water entry through deficiency (L/min.)**						
	Nominal Water Spray rate (L/min-m^2)						
	3.90	*4.28*	*4.56*	*5.06*	*5.57*	*5.83*	*6.07*
75 ± 50	0.14	0.22	0.34	0.38	0.38	0.42	0.46
150 ± 60	0.16	0.25	0.36	0.38	0.44	0.48	0.53
300 ± 125	0.20	0.24	0.33	0.40	0.46	0.48	0.55
700 ± 300	0.18	0.26	0.38	0.39	0.47	0.52	0.57

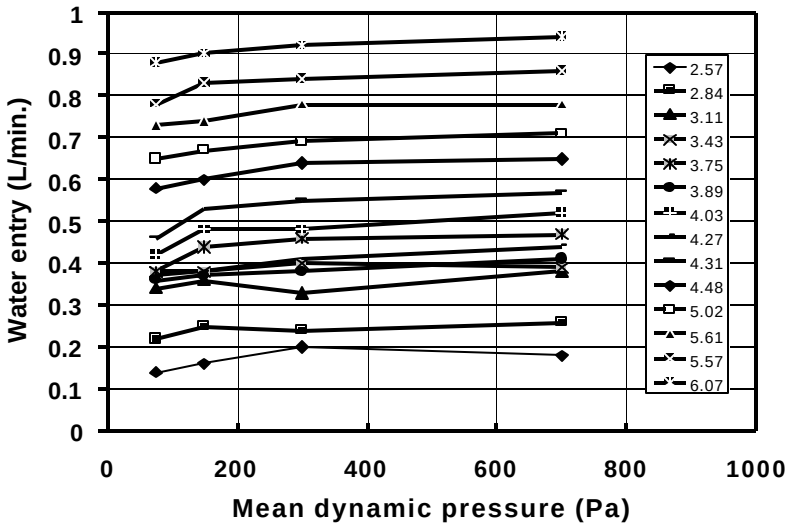

Figure 2.11 - Water entry through deficiency as a function of differential dynamic pressure – 90-mm^2 Ventilation duct deficiency; rainscreen not vented; second line of defence sealed
Values in the legend relate to spray rate (L/min-m^2)

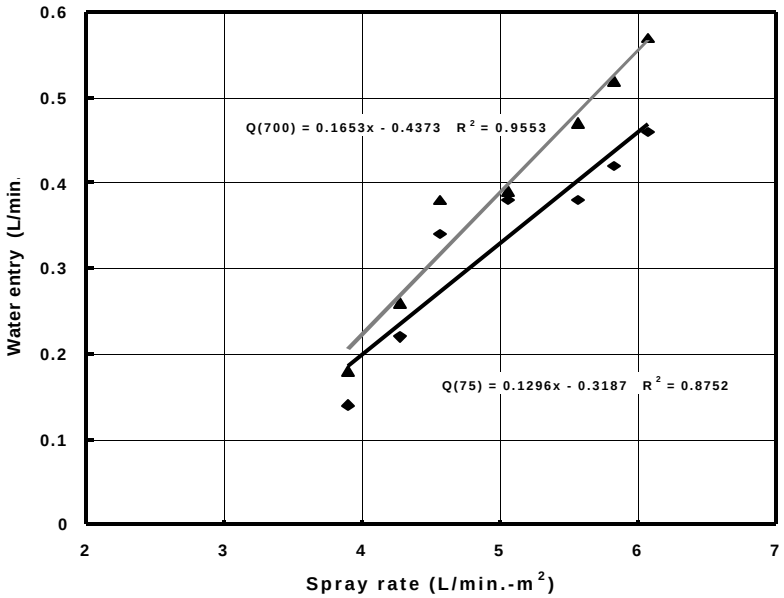

Figure 2.12 - Water entry through deficiency as a function of differential dynamic pressure – 90-mm^2 Ventilation duct deficiency on fully vented rainscreen having the second line of defence sealed

2.3.2.2 RAINSCREEN FULLY VENTED / SECOND LINE OF DEFENCE SEALED

Data is provided in Table 2.10 on water entry rates through a 90-mm horizontal deficiency of ca. 1-mm height located in the top portion of the ventilation duct that penetrates the rainscreen. These trials were conducted under dynamic pressure fluctuations for a rainscreen that was fully vented and in which the second line of defence around the ventilation duct is sealed.

Table 2.10: Water entry rates through deficiency atop ventilation duct for spray rates of 3.9 to 6.07 L/min.-m^2 at given chamber pressures
Rainscreen fully vented / second line of defence sealed

Chamber Dynamic Pressure @ 5 Hz. (Pa)	Volume through deficiency (L/min.)			
	Nominal Water Spray rate (L/min-m^2)			
	3.90	*4.56*	*5.57*	*6.07*
75 ± 50	0.16	0.37	0.45	0.51
150 ± 60	0.20	0.35	0.38	0.49
300 ± 125	0.22	0.34	0.38	0.47
700 ± 300	0.20	0.32	0.37	0.49

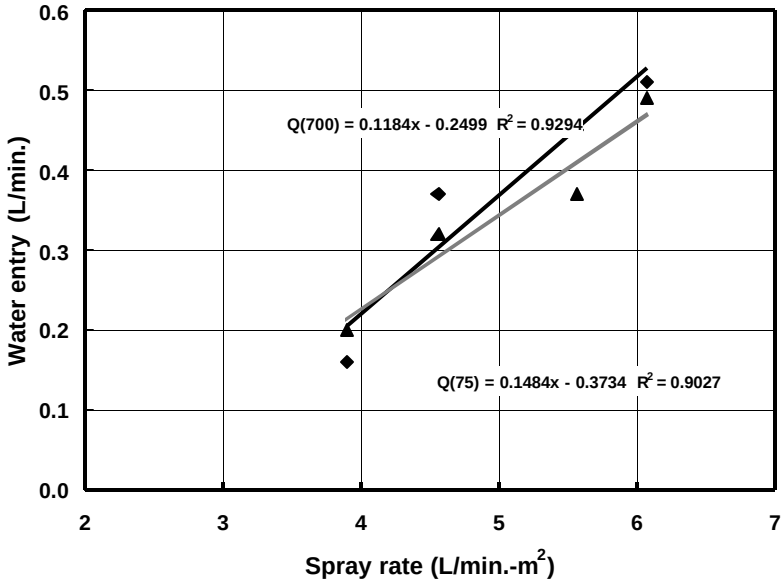

Figure 2.13 - Water entry through deficiency as a function of differential dynamic pressure – 90-mm^2 Ventilation duct deficiency on fully vented rainscreen having the second line of defence sealed

2.3.2.3 RAINSCREEN NOT VENTED / SECOND LINE OF DEFENCE NOT SEALED

Data is provided in Table 2.11 on water entry rates through a 90-mm horizontal deficiency of ca. 1-mm height located in the top portion of the ventilation duct that penetrates the rainscreen. These trials were conducted under dynamic pressure fluctuations for a rainscreen that was not vented and in which the second line of defence around the ventilation duct is not sealed.

Table 2.11: Water entry rates through deficiency atop ventilation duct for spray rates of 3.9 to 6.07 L/min.-m^2 at given chamber pressures
Rainscreen not vented / second line of defence not sealed

Chamber Dynamic Pressure @ 5 Hz. (Pa)	Volume through deficiency (L/min.)			
	Nominal Water Spray rate (L/min-m^2)			
	3.90	*4.56*	*5.57*	*6.07*
75 ± 50	0.23	0.29	0.38	0.57
150 ± 60	0.26	0.34	0.41	0.38
300 ± 125	0.26	0.34	0.42	0.29
700 ± 300	0.27	0.38	0.44	0.23

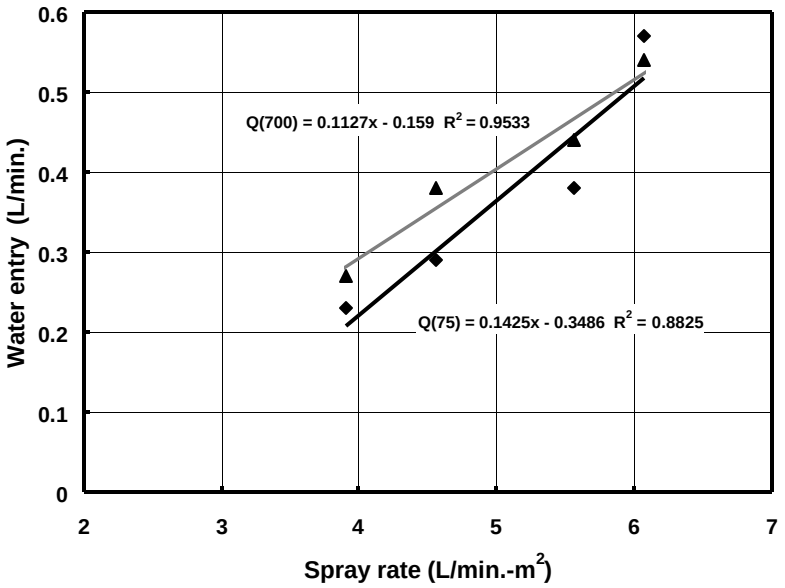

Figure 2.14 - Water entry through deficiency as a function of differential dynamic pressure – 90-mm^2 Ventilation duct deficiency on not vented rainscreen having the second line of defence not sealed

2.3.2.4 RAINSCREEN FULLY VENTED / SECOND LINE OF DEFENCE NOT SEALED

Data is provided in Table 2.12 on water entry rates through a 90-mm horizontal deficiency of ca. 1-mm height located in the top portion of the ventilation duct that penetrates the rainscreen. These trials were conducted under dynamic pressure fluctuations for a rainscreen that was fully vented and in which the second line of defence around the ventilation duct is not sealed.

Table 2.12: Water entry rates through deficiency atop ventilation duct for spray rates of 3.9 to 6.07 L/min.-m^2 at given chamber pressures
Rainscreen fully vented / second line of defence not sealed

Chamber Dynamic Pressure @ 5 Hz. (Pa)	**Volume through deficiency (L/min.)**			
	Nominal Water Spray rate (L/min-m^2)			
	3.90	*4.56*	*5.57*	*6.07*
75 ± 50	0.14	0.38	0.42	0.45
150 ± 60	0.16	0.38	0.43	0.45
300 ± 125	0.17	0.39	0.43	0.46
700 ± 300	0.22	0.40	0.46	0.50

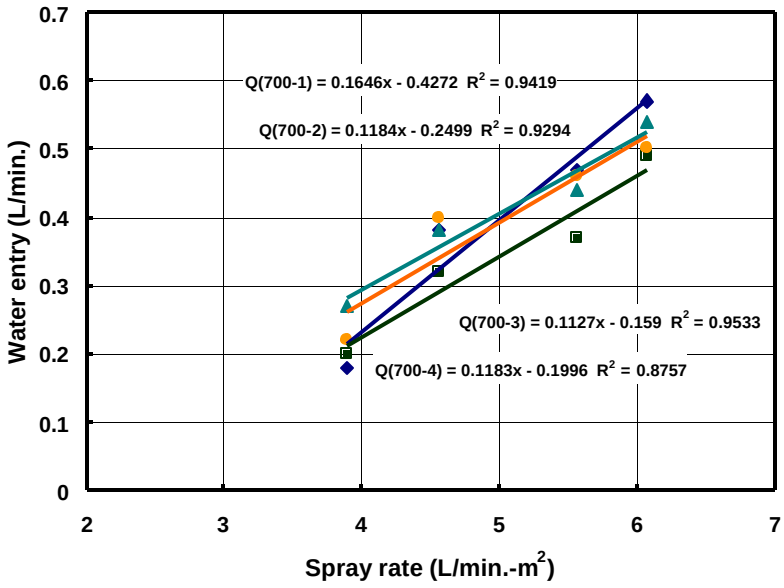

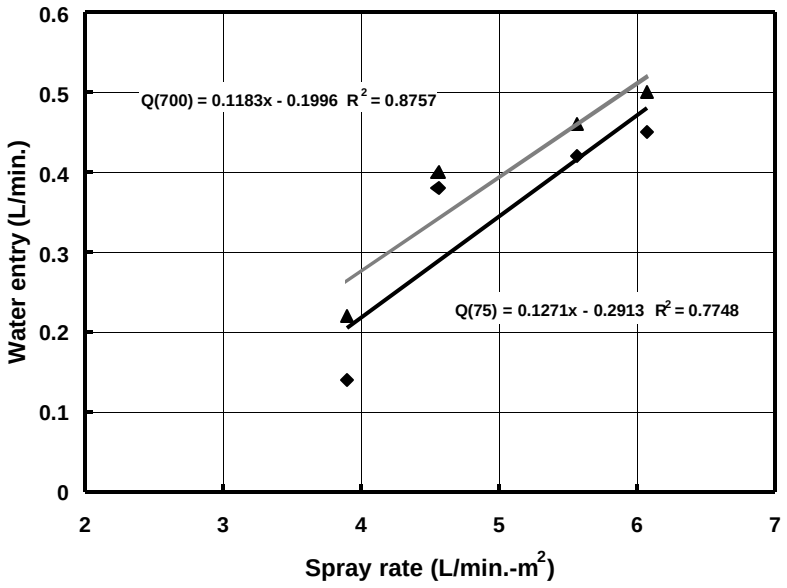

Figure 2.15 - Water entry through deficiency as a function of differential dynamic pressure – 90-mm^2 Ventilation duct deficiency on fully vented rainscreen having the second line of defence not sealed

Figure 2.16 - Water entry through deficiency as a function of spray rate at a mean dynamic pressure differential of 700 Pa for 4 conditions investigated: (1) No rainscreen venting – sealed second line; (2) full rainscreen venting - sealed second line; (3) No rainscreen venting –second line not sealed; and, (4) full rainscreen venting - second line not sealed.

2.3.3 ELECTRICAL OUTLET DEFICIENCY

Results of water entry through a 45-mm deficiency above the gasket of an electrical outlet are presented in Table 2.13 and Table 2.14, and Figure 2.17 and Figure 2.18. Results provided in Table 2.13 are for a non-vented rainscreen whereas those in Table 2.14 are for a fully vented rainscreen. Volumes of water entry in L/min. are presented as a function of either static or dynamic differential chamber pressure for simulated spray rates ranging from 3.9 to 7 L/min-m^2.

Table 2.13: Water collection rates through deficiency above electrical outlet for various water flow rates and chamber pressures - *rainscreen not vented

Chamber Pressure (Pa)	Water entry through deficiency (L/min.)							
	Nominal Water Spray rate (L/min-m^2)							
	3.90	*4.56*	*5.57*	*6.07*	*4.50*	*5.21*	*6.34*	*7.00*
0	0.06	0.07	0.07	0.07	0.05	0.06	0.06	0.06
75	0.08	0.16	0.17	0.18	0.09	0.20	0.22	0.24
150	0.11	0.14	0.19	0.21	0.09	0.24	0.24	0.26
300	0.14	0.22	0.25	0.26	0.15	0.32	0.29	0.30
600	0.16	0.19	0.18	0.27	0.30	0.30	0.31	0.32
1000	0.2	0.22	0.27	0.29	0.21	0.25	0.33	0.32
~75±40	0.08	0.10	0.11	0.12	0.11	0.12	0.14	0.15
~150± 60	0.09	0.09	0.10	0.14	0.14	0.14	0.15	0.17
~300± 125	0.17	0.22	0.24	0.25	0.24	0.26	0.26	0.28
~700± 300	0.21	0.25	0.26	0.31	0.27	0.28	0.29	0.32

Table 2.14: Water collection rates through deficiency above electrical outlet for various water flow rates and chamber pressures - *rainscreen fully vented (5400 mm2)

Chamber Pressure (Pa)	Water entry through deficiency (L/min.)							
	Nominal Water Spray rate (L/min-m^2)							
	3.90	*4.56*	*5.57*	*6.07*	*4.50*	*5.21*	*6.34*	*7.00*
0	0.10	0.08	0.09	0.09	0.07	0.09	0.09	0.08
75	0.08	0.09	0.08	0.10	0.04	0.10	0.12	0.13
150	0.10	0.10	0.09	0.10	0.06	0.09	0.10	0.11
300	0.11	0.11	0.09	0.11	0.08	0.10	0.10	0.10
600	0.12	0.11	0.09	0.10	0.10	0.11	0.11	0.12
1000	0.14	0.12	0.12	0.11	0.10	0.12	0.12	0.14
~75±40	0.03	0.04	0.04	0.05	0.04	0.05	0.05	0.05
~150± 60	0.05	0.06	0.06	0.06	0.06	0.06	0.07	0.07
~300± 125	0.06	0.06	0.07	0.09	0.08	0.08	0.08	0.09
~700± 300	0.08	0.10	0.09	0.10	0.08	0.08	0.10	0.11

Results shown in Figure 2.17 indicate that rates of water entry increase in proportion to the static pressure difference across the assembly and this dependence is shown to occur for each of the precipitation rates (3.9 to 7 L/min.-m^2) to which the deficiency was subjected. The dependency of water entry on precipitation rate is not as significant in these tests as in was for water entry through the larger deficiency above the ventilation duct.

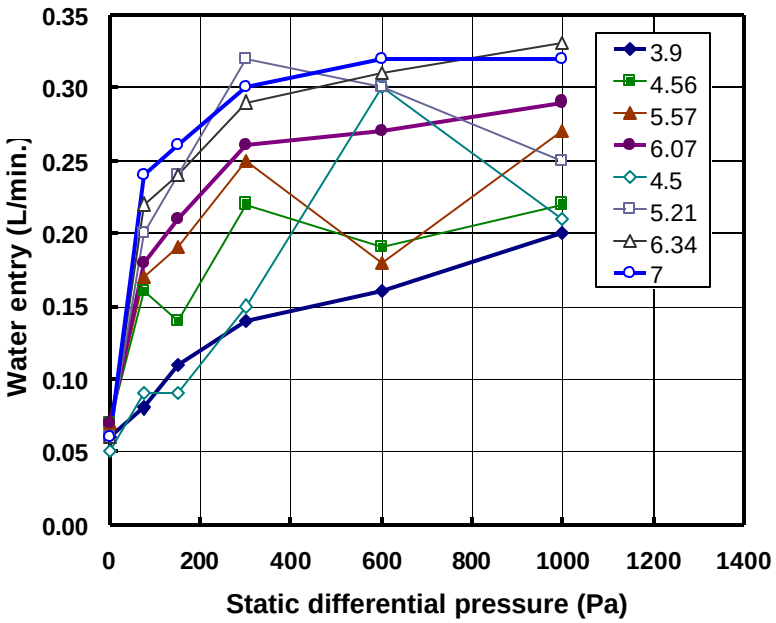

Figure 2.17 – Water entry (L/min.) through deficiency as a function of static differential pressure – 45-mm^2 deficiency above electrical outlet ; non-vented rainscreen; second line of defence not sealed. Values in the legend relate to spray rate (L/min-m^2)

Shown in Figure 2.18 are results from water entry tests under dynamic pressure at mean pressures of 75 and 700 Pa for fully vented and non-vented rainscreens. In can be seen that water entry through a vented rainscreen is markedly less than that for the non-vented rainscreen at both pressure extremities.

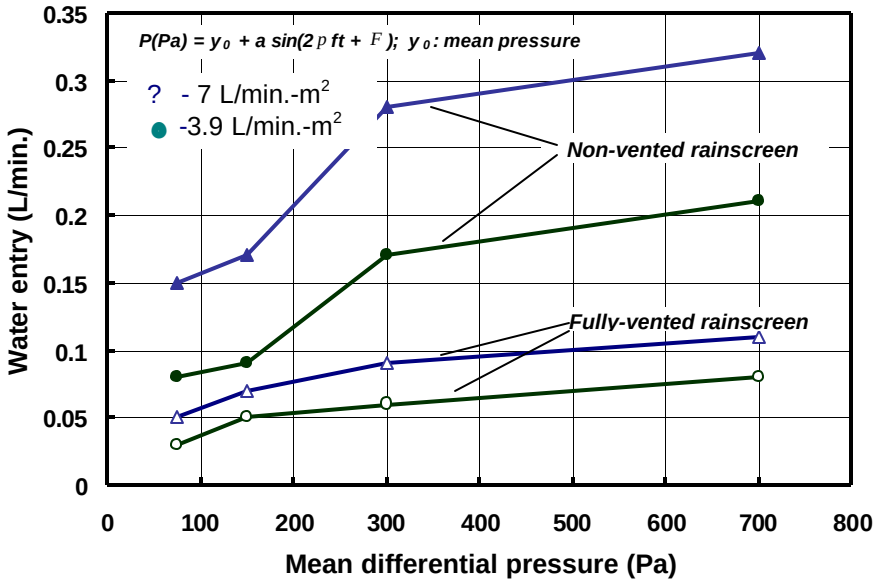

Figure 2.18 – Water entry (L/min.) through a 45-mm^2 deficiency above electrical outlet as a function of mean dynamic differential pressure. Comparison of results derived from a non-vented rainscreen and fully vented rainscreen having the second line of defence not sealed

2.3.4 WINDOW CORNER DEFICIENCIES:

Results of water entry through corner deficiencies in windows are presented in Table 2.15 to Table 2.18 and Figure 2.19 to Figure 2.22.

Water entry through a 6-mm diameter deficiency located in that corner of the window closest to the edge of the test frame (OUTBOARD) for spray rates ranging from 3.9 to 7 L/min.-m^2 and for conditions in which the rainscreen was either not vented or fully vented are provided in Table 2.15 and Table 2.16. Volumes of water entry in L/min. are presented as a function of either static or dynamic differential chamber pressure. It was noted that for all such tests, regardless of whether water penetrated the 6-mm diameter openings, window leaks were observed above 600 Pa pressure in both static and dynamic test modes.

An overview of the results indicates that the volume of water entry increases in relation to the static pressure different across the wall assembly as shown in Figure 2.19. Similar results in regards to the dependence of water entry on the mean dynamic pressure differential were obtained for water entering the outboard deficiency as shown in Figure 2.21.

Figure 2.20 provides results of water entry through the outboard deficiency of a fully vented rainscreen in comparison to that of a non-vented rainscreen. These results suggest that there is little difference in water entry between either condition.

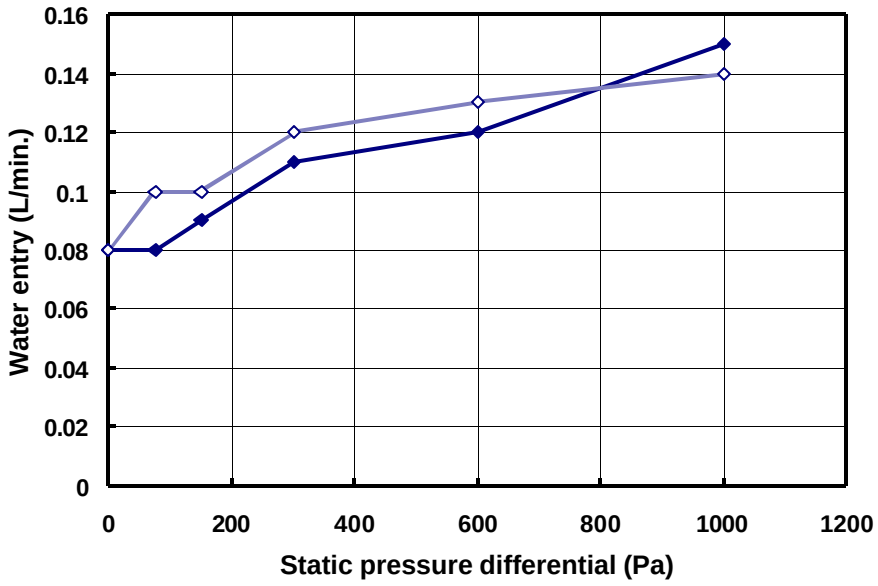

Figure 2.19 – Water entry (L/min.) through a 6-mm diameter deficiency in OUTBOARD corner of window as a function of static pressure differential. Results derived from a non-vented rainscreen having the second line of defence not sealed

Table 2.15: Water entry rates through a 6-mm diameter deficiency in OUTBOARD window corner for spray rates of 3.9 to 7 L/min-m^2 at given chamber pressures
Non- vented rainscreen

Chamber Pressure (Pa)	Water entry through deficiency (L/min.)							
	Nominal Water Spray rate (L/min-m^2)							
	3.90	*4.56*	*5.57*	*6.07*	*4.50*	*5.21*	*6.34*	*7.00*
0	0.08	0.08	0.09	0.10	0.08	0.10	0.09	0.08
75	0.08	0.09	0.10	0.10	0.10	0.12	0.12	0.12
150	0.09	0.09	0.09	0.10	0.08	0.11	0.10	0.12
300	0.11	0.11	0.12	0.12	0.09	0.11	0.11	0.12
600	0.12	0.12	0.12	0.13	0.10	0.12	0.12	0.12
1000	0.15	0.14	0.15	0.15	0.10	0.10	0.10	0.14
~75±40	0.06	0.08	0.09	0.10	0.09	0.11	0.12	0.13
~150± 60	0.07	0.09	0.10	0.11	0.10	0.12	0.13	0.16
~300± 125	0.07	0.08	0.10	0.12	0.11	0.12	0.14	0.14
~700± 300	0.08	0.10	0.11	0.13	0.10	0.13	0.15	0.16

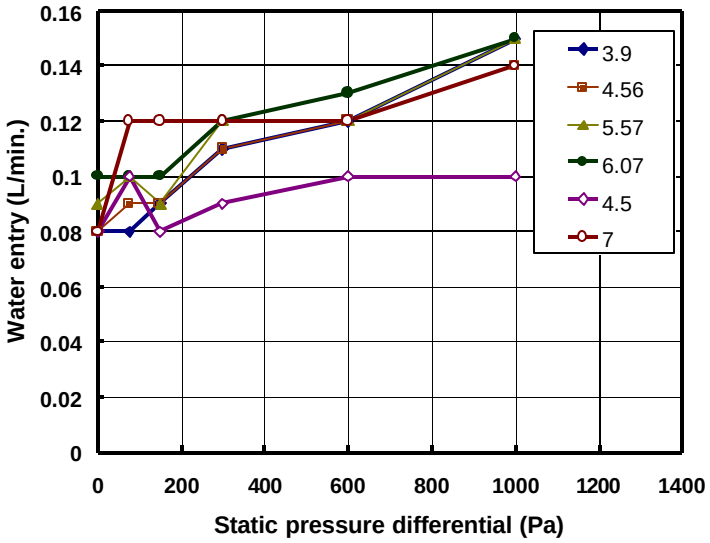

Figure 2.20 – Water entry (L/min.) through a 6-mm diam. deficiency in OUTBOARD corner of window as a function of static pressure differential. Results from vented and non-vented rainscreens; second line of

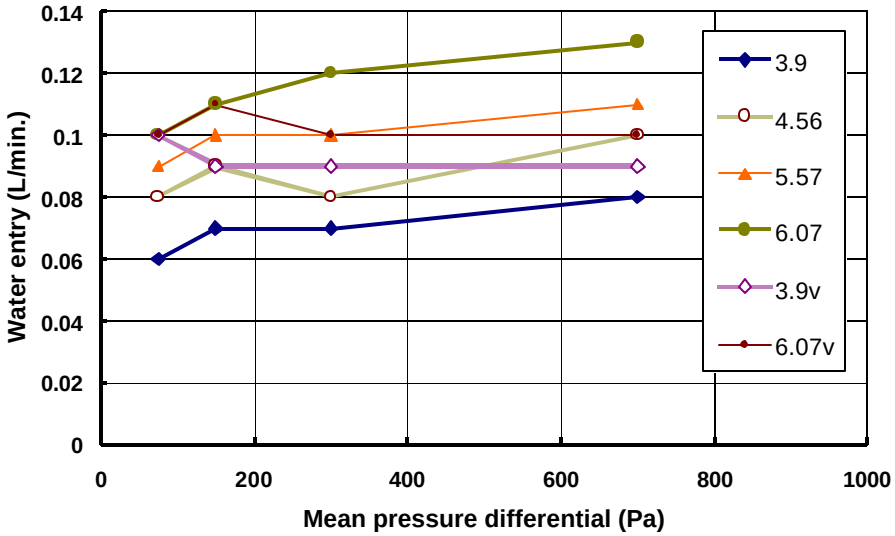

defence not sealed; Values in the legend relate to spray rate (L/min-m^2)

Figure 2.21 – Water entry (L/min.) through a 6-mm diameter deficiency in OUTBOARD corner of window as a function of mean dynamic pressure differential for non-vented rainscreen; second line of defence not sealed; Values in the legend relate to spray rate (L/min-m^2)

Table 2.16: Water entry rates through a 6-mm diameter deficiency in OUTBOARD Window Corner for spray rates of 3.9 to 7 L/min-m^2 at given chamber pressures
Fully vented rainscreen

Chamber Pressure (Pa)	Water entry through deficiency (L/min.)							
	Nominal Water Spray rate (L/min-m^2)							
	3.90	*4.56*	*5.57*	*6.07*	*4.50*	*5.21*	*6.34*	*7.00*
0	0.08	0.08	0.09	0.10	0.09	0.11	0.13	0.12
75	0.10	0.10	0.10	0.10	0.09	0.11	0.13	0.13
150	0.10	0.10	0.10	0.11	0.10	0.11	0.12	0.12
300	0.12	0.12	0.11	0.13	0.07	0.11	0.13	0.13
600	0.13	0.13	0.13	0.14	0.08	0.12	0.13	0.14
1000	0.14	0.14	0.14	0.14	0.12	0.12	0.15	0.17
~75±40	0.10	0.10	0.10	0.10	0.08	0.09	0.11	0.16
~150± 60	0.09	0.10	0.11	0.11	0.07	0.09	0.11	0.15
~300± 125	0.09	0.10	0.10	0.10	0.08	0.09	0.10	0.14
~700± 300	0.09	0.08	0.09	0.10	0.09	0.10	0.12	0.12

Water entry through the a 6-mm diameter deficiency located in that corner of the window furthest from the edge of the test frame (INBOARD) for spray rates ranging from 3.9 to 7 L/min.-m^2 and for conditions in which the rainscreen was either not vented or fully vented are provided in Table 2.17 and

Table **2.18**.

Table 2.17: Water entry rates through a 6 mm diameter deficiency at INBOARD window corner for spray rates of 3.9 to 7 l/min-m^2 at given chamber pressures
Non-vented rainscreen

Chamber Pressure (Pa)	Water entry through deficiency (L/min.)							
	Nominal Water Spray rate (L/min-m^2)							
	3.90	*4.56*	*5.57*	*6.07*	*4.50*	*5.21*	*6.34*	*7.00*
0 75 150 300 600	NIL				NIL			
1000					0.00	0.00	0.02	0.03
~75±40	0.00	0.01	0.01	0.01	0.00	0.02	0.02	0.02
~150± 60	0.01	0.02	0.02	0.01	0.01	0.02	0.02	0.03

~300± 125	0.02	0.02	0.02	0.01	0.01	0.02	0.02	0.04
~700± 300	0.03	0.03	0.02	0.02	0.02	0.02	0.02	0.08

Table 2.18: Water entry rates through a 6 mm diameter deficiency at INBOARD window corner for spray rates of 3.9 to 7 l/min-m^2 at given chamber pressures
Fully vented rainscreen

Chamber Pressure (Pa)	Water entry through deficiency (L/min.)							
	Nominal Water Spray rate (L/min-m^2)							
	3.90	*4.56*	*5.57*	*6.07*	*4.50*	*5.21*	*6.34*	*7.00*
0 75 150 300 600	NIL				NIL			
1000	0.00	0.00	0.02	0.00	0.02	0.04	0.04	0.06
~75 ± 40	0.00	0.00	0.00	0.00	0.00	0.00	0.01	0.03
~150 ± 60	0.00	0.00	0.04	0.00	0.04	0.00	0.03	0.04
~300 ± 125	0.00	0.00	0.05	0.00	0.07	0.03	0.05	0.05
~700 ± 300	0.00	0.00	0.06	0.04	0.08	0.05	0.08	0.10

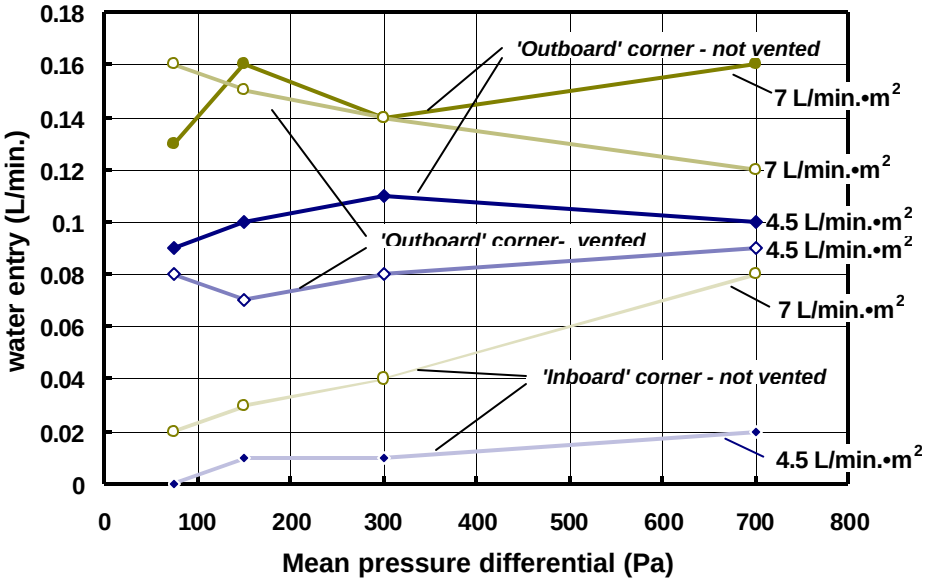

Figure 2.22 – Water entry (L/min.) through 6-mm diameter deficiencies in corner of window as a function of mean dynamic pressure differential for both non-vented and vented rainscreens having the second line of defence not sealed

2.4 Summary

A prototype wood-frame cavity wall, sheathed in clear acrylic, was designed and fabricated such that it included a rainscreen, a barrier acting as second line of defence, and an air barrier. The use of an impermeable and clear material helped focus the investigation on water entry, exclusive of the effects due to water absorption by the cladding material. Results are provided from water entry through deficiencies located in the cladding of Base case wall assembly No. 2 that included deficiencies located:

- Above a ventilation duct (VL); the ventilation duct penetrates the wall assembly proper.
- Above an electrical outlet (E), and
- At adjacent lower corners of a vinyl window (W).

This assembly has the same through-wall penetrations (i.e. window, ventilation duct and electrical duplex) incorporated in it as those in the generic wall assemblies (i.e. stucco, EIFS, siding, masonry). The deficiencies were subjected to simulated precipitation (water spray) concurrent with either static or dynamic pressure differentials across the assembly.

Results indicate that:

For a deficiency located above the ventilation duct –

- When subjected to static pressure differentials, water entry rates vary as a function of both the spray rate and differential chamber pressure; the dependency of rates of water entry on changes in differential pressure across the specimen assembly is not as evident as is rates of entry in relation to the spray rate;
- Water entry rates vary linearly as a function of the simulated rate of precipitation
- No difference is apparent in results for water entry through the deficiency at the ventilation duct when the rainscreen is vented as compared to not vented or when the second line of defence is sealed as compared to not being sealed.
- Tests conducted under dynamic pressure fluctuations provide nominally the same results as those obtained under static pressure conditions; i.e. entry rates vary as a function of both the spray rate and differential chamber pressure; the dependency of rates of water entry on changes in differential pressure across the specimen assembly is not as evident as is rates of entry in relation to the spray rate.

For a deficiency located above the electrical outlet -

- Rates of entry when no pressure is applied across the specimen assembly are significant in relation to those obtained when a pressure differential exists across the assembly;
- Rates of water entry increase in proportion to the static pressure difference across the assembly;
- Water entry through a vented rainscreen is markedly less than that for the non-vented rainscreen at both pressure extremities used in this test sequence.

For deficiencies located at the lower window corners -

- Increases in pressure differential generally bring about an increase in water entry rates;
- Non-vented cavity provides slightly higher rates of water entry as compared to a vented cavity;
- Rates of entry for the inboard window corner deficiency are lower that those for the outboard deficiency; this is likely due to the increased accumulation of water spray towards the center of the specimen as compared to the edge of the specimen.

Chapter 3

Results from Stucco Wall Assemblies

TABLE OF CONTENTS

? Chapter 3 ?

Results from Stucco Wall Assemblies

LIST OF TABLES

LIST OF FIGURES

CHAPTER OVERVIEW

MEWS methodology incorporates the performance testing and characterisation of full-scale wall assemblies to determine air leakage, dynamic response, water-tightness performance and water entry characteristics for each of the wall cladding types being evaluated in this study.

Performance tests were used to qualify the degree to which wall assemblies were able to maintain their watertight integrity when being subjected to static or dynamic pressure differentials concurrent with water spray using the dynamic wall test facility (DWTF). This series of tests were similar to those currently used in industry to assess the likelihood of water penetration under extreme simulated climatic conditions and were conducted at levels comparable to, or in excess of, current industry standards.

Water entry assessments were used to determine the quantities and rates of water that might enter deficiencies of known type, size and location on the cladding when subjected to simulated climatic extremes, likewise using the DWTF. Levels of water spray and pressure differential were consistent with related climatic data of rainfall and wind speed that might occur in an extreme climatic event within a 10 year period in North America. This information provided a basis for a systematic and consistent means of transferring input to hygIRC, the model used in the MEWS parametric analysis.

In this initial test series of wall assemblies, five (5) different types of stucco-clad wall assemblies (6 specimens total) were subjected to performance and water entry assessment tests that included testing under different pressure differentials across the assembly and varying rates of water sprayed onto the cladding surface. Tests were completed in conformance with a protocol derived explicitly for this study and reported earlier (Chap. 1; T6-02-R8).

This report provides results of water penetration trials and water entry assessments for all stucco walls evaluated in this first series of experiments, and air leakage characterisation and dynamic responses of wall assembly, 2A, the first wall evaluated in this test series.

Results for water penetration trials show that all of the wall assemblies exhibited some water entry when subjected to spray rates and pressure differentials used in the test. The points of entry were primarily at wall penetrations; only WA-2B (barrier wall assembly with self-furring woven metal lath and 60-min. rate building paper) showed signs of through-wall penetration. In this instance, water droplets were observed on the inside face of the sheathing board entering along a path made by a staple that had perforated the board. Notably, WA-5, the assembly having a drainage cavity, showed the least evidence of water penetration in all test sequences.

Results for water entry assessments reveal that when subjected to the spray rates in these tests, significant amounts of water can enter under gravity alone. The tests showed that up to 0.05 L/min. could enter certain deficiencies when no pressure is applied across the assembly. Increasing amounts of water entered deficiencies about electrical outlets, ventilation ducts or at wall-window interfaces, when more water is sprayed onto the wall, or when static or dynamic pressure across the assembly is increased. These increases are more important in respect to changes in spray rate than to changes in differential pressure. Rates of entry vary from 0.05 to 0.56 L/min. with the exception of wall assembly WA-5, where little or no water was observed to enter deficiencies in most of the tests conducted.

3.1 Introduction

A series of six stucco walls (Nos. 1, 2A, 2B, 3, 4, 5) were constructed and subsequently tested for water penetration trials and entry assessments using the dynamic wall test facility. Details regarding the fabrication of the specimens, material specifications and proposed deficiencies are provided in report T2-13.

This report provides results of water penetration (Stages 2 and 3) and water entry (Stage 4) tests on stucco wall assemblies according to the test protocol described in report T6-02-R8. A summary of the test protocol is provided below as well as a description of the test specimen, parameters and set-up used in the test. Specifically, details regarding the location of pressure taps, of moisture sensors, of water entry points and means of water collection are outlined in the section on test specimens.

Results from air leakage and dynamic response (Stage 1) of wall assemblies will be provided in a subsequent report.

3.1.1 TEST SPECIMENS

The test configuration showing the location of pressure taps, moisture sensors, and water entry points are provided below in Figures 3.1 to 3.3 respectively.

3.1.1.1 PRESSURE TAPS

Pressure taps are located in six wall portions (Figure 3.1), with the first portion located at the left extremity of the wall (facing the weather-side). Typically in each portion, taps are located both in the wall cavity between the stucco and the OSB sheathing and in the stud space. Additionally, taps have been added to obtain measurements of pressure differential at points of water entry.

3.1.1.2 AIR BARRIER SYSTEM LEAKAGE

Air barrier system (ABS) leakage was regulated by introducing a series of 7-mm diameter holes in the ABS (Figure 3.1), a series of seven (one in each stud cavity) representing an equivalent leakage area (ELA) of 269-mm^2, provided a nominal wall assembly leakage of 0.2 L/s-m^2. A wall assembly leakage of 0.5 L/s-m^2 (ELA 808-mm^2) was achieved using twenty-one holes of the same diameter, three in each stud cavity. The desired nominal leakage through the wall assembly was achieved by “opening” or “closing” the appropriate number of holes in the ABS.

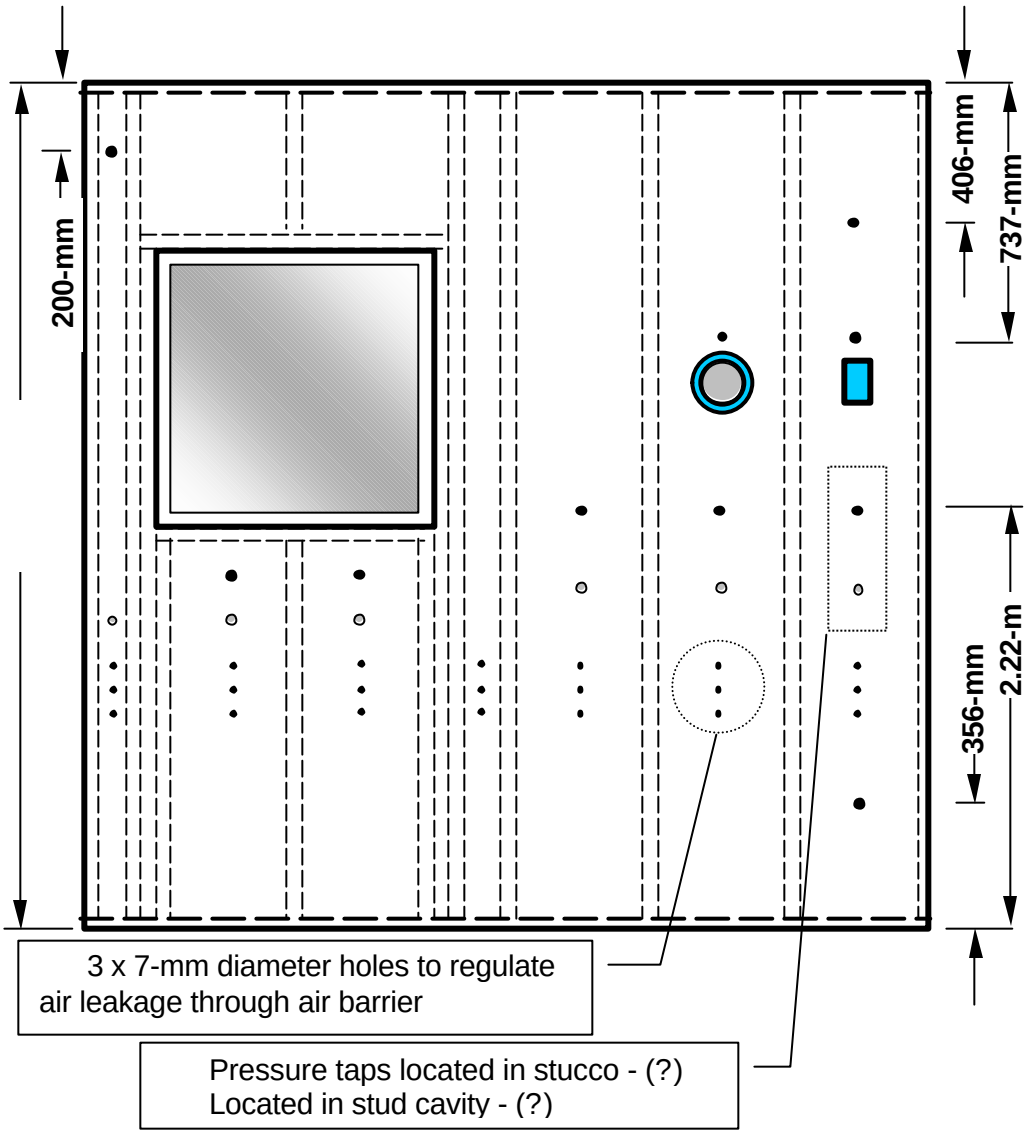

Figure 3.1 - Location of pressure taps and air leakage openings

3.1.1.3 MOISTURE SENSORS IN SHEATHING BOARD

The location of moisture sensors is shown in Figure 3.2 below. Sixteen (16) moisture pin pairs (imbedded to either ¼ or ¾ sheathing thickness; e.g. see schematic, Fig. 3.2) have been placed in the sheathing board (OSB) at locations where either water might first accumulate or at the base of the wall. Moisture pin pairs imbedded at ¾ thickness provide specific moisture contents in proximity to the front of the sheathing; those at ¼ thickness (#4 & #12) were intended to offer information of the moisture profile across the sheathing.

The sensors are calibrated such that a light diode, located between the pairs of pins, is activated if the moisture content reaches or exceeds ca. 14%. Over a test period, note is taken of the time and conditions under which the light is first activated.

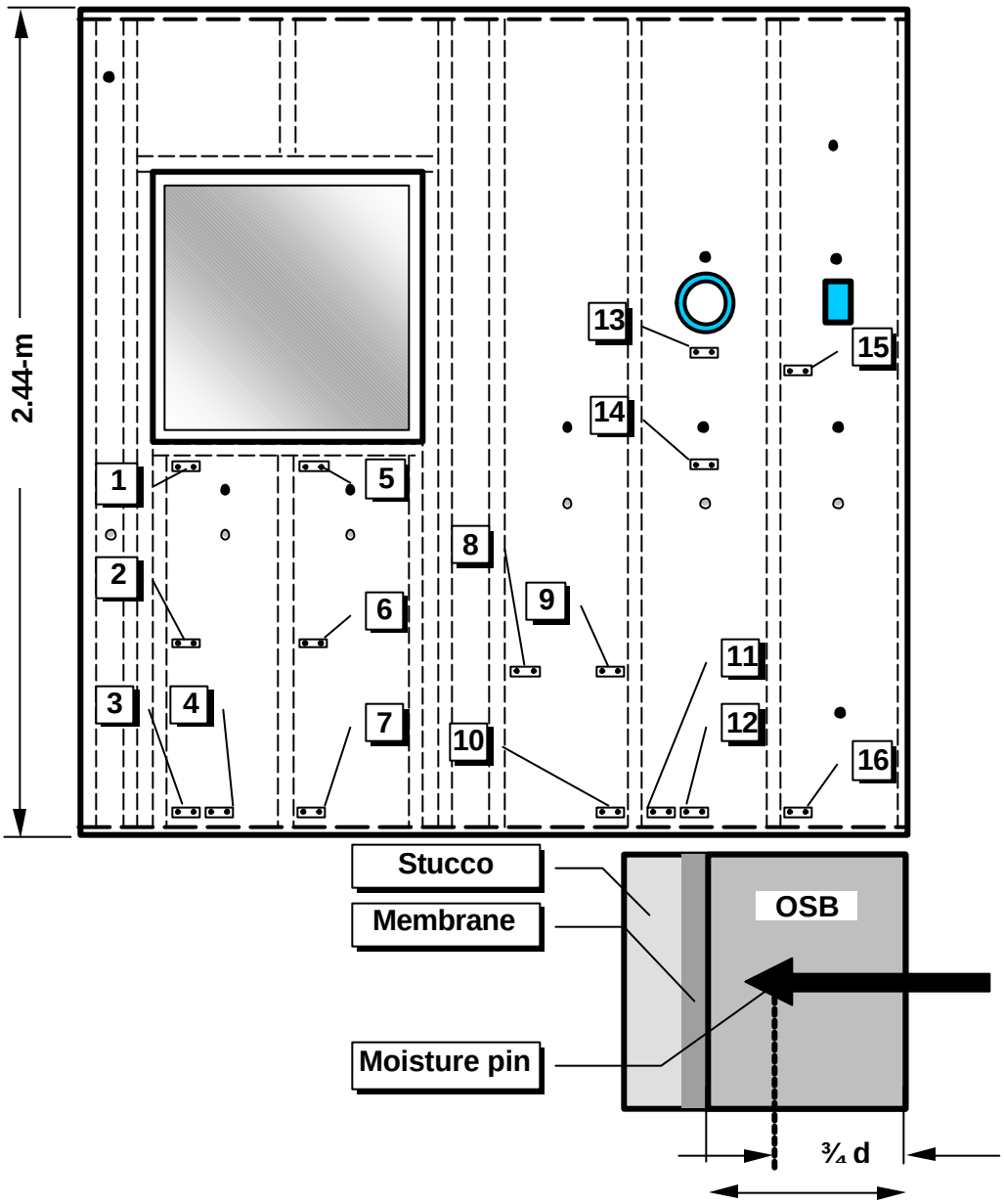

Figure 3.2 - Location of moisture sensors

3.1.1.4 WATER ENTRY POINTS

Water entry points (Figure 3.3), representative of deficiencies in sealing the interfaces between wall components, are located in the following areas:

- Above the electrical outlet – a nominal 50-mm length of sealant is missing between the outlet cover and the wall.
- Above the duct – a nominal 50-mm length of sealant is missing between the duct and the wall.
- Below the window sill and between finishing strips – a 90-mm length of sealant is missing between the ending strips.

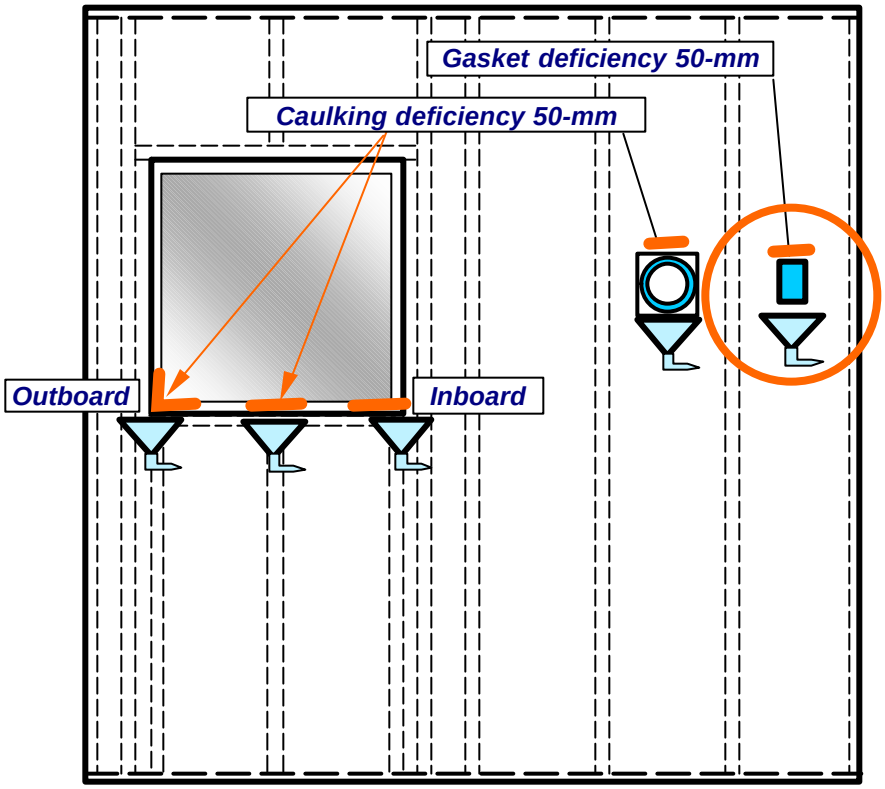

Figure 3.3 - Location of water collection points and troughs

3.1.1.5 CONDITION OF SPECIMENS PRIOR TO TESTING

Prior to being moved to the test laboratory, where the DWTF is located, a visual inspection of the wall surface was made to identify any visible cracks; the specimen was likewise inspected after the move and any additional cracks were noted. A schematic showing visible cracks on the surface of stucco specimen 2A prior to being moved is shown in Figure 3.4; results from inspection of the specimen following the move is given in Figure 3.5. Figure 3.5 represents the nature of the specimen prior to being placed in the DWTF test apparatus. Close observation of the wall after the move indicated no changes to existing cracks. It is unlikely that any of the observed cracks would appear as through-wall defects. Presumably, these are simply surface cracks through which water can enter. All stucco specimens were likewise inspected prior to being placed in the test apparatus.

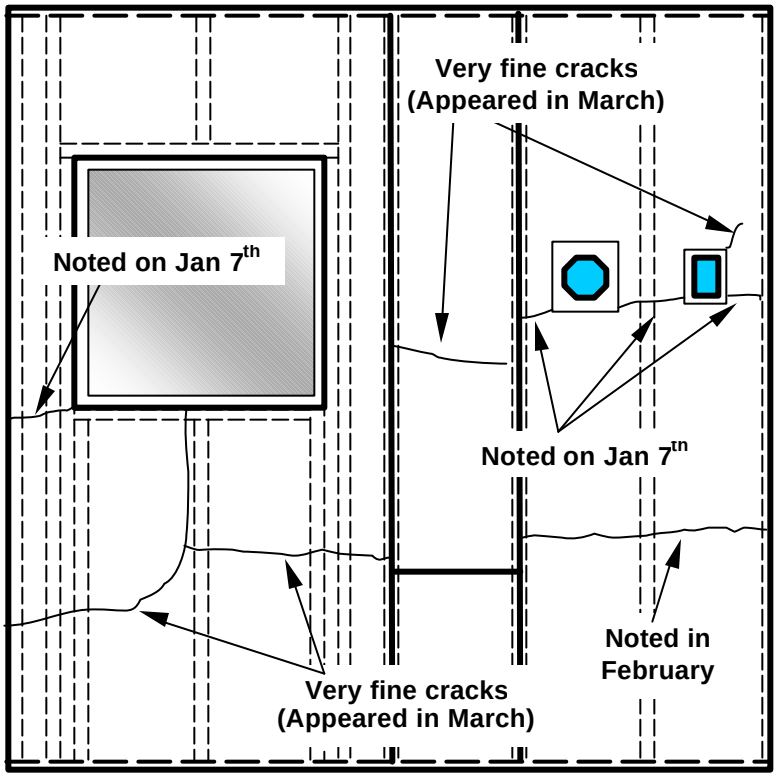

Figure 3.4 – Wall Assembly 2A before transport

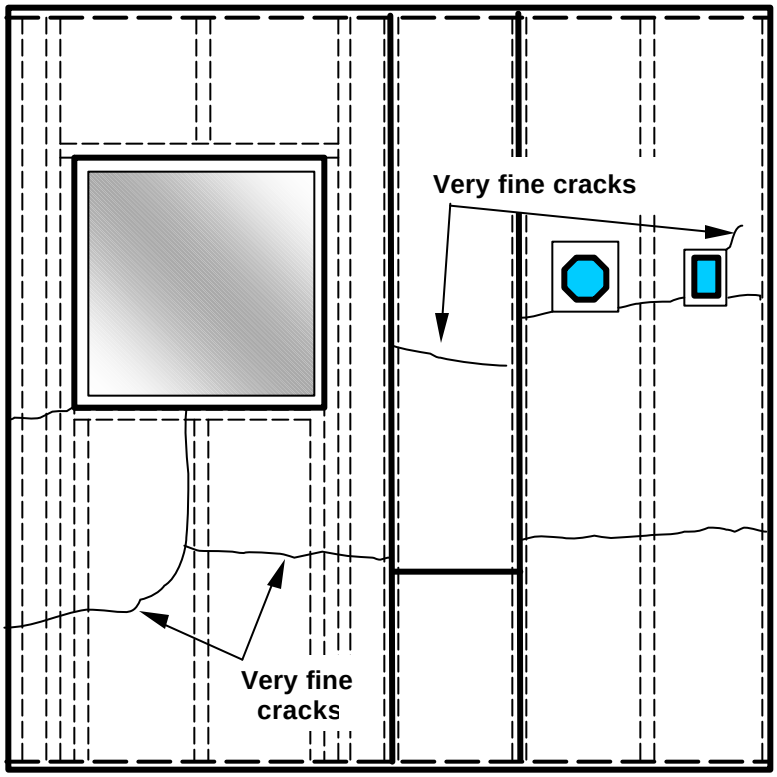

Figure 3.5- Wall Assembly 2A after transport – visual inspection of the surface did not reveal any additional cracks due to transport (6 April 02) – hence figures depict the same series of cracks

3.2 Results

Results from water penetration (Stages 2 and 3) are presented in section 3.1 and water entry (Stage 4) in section 3.2. Results for air leakage and dynamic response for WA-2A (Stage1) are provided in sections 3.3 and 3.4 respectively.

3.2.1 Water Penetration Tests on Stucco-Clad Walls – Stage 2

3.2.1.1 Introduction

Performance tests were used to qualify the degree to which wall assemblies were able to maintain their watertight integrity when being subjected to static or dynamic pressure differentials concurrent with water spray using the dynamic wall test facility (DWTF). This series of tests were similar to those currently used in industry to assess the likelihood of water penetration under extreme simulated climatic conditions and were conducted at levels comparable to, or in excess of, current industry requirements and standards.

Water penetration tests were conducted on all six (6) stucco wall assemblies (WA-1, WA-2A, -2B, -3, -4, and WA-5). A summary of the results from tests on all wall assemblies is provided in Figures 3.6 to 3.15. Each pair of figures provides water penetration results derived from static and dynamic test trials respectively; they follow the test sequence carried out in the protocol given in Chapter 1 (T6-02-R8). Results for WA-5 are also provided in this manner, irrespective of the fact that no water penetration was observed apart from leakage detected about the window during the dynamic trial – these results are however referred to when comparisons are made with those obtained for the other walls.

The results obtained during water penetration trials (Stage 2) are essentially qualitative in nature. Observations were made as to where penetration occurs on the inside of the assembly (e.g. around windows, electrical outlet, and ventilation duct or through the sheathing board) and when it occurs over the course of the test sequence. Test conditions (static or mean dynamic pressure differential) when penetration occurs were noted and these provided a benchmark from which comparisons could then be made. Moisture sensors (MS) placed in the sheathing board at specific locations of the wall assembly indicated whether moisture had penetrated beyond the second line of defence. Activated moisture sensors registered lit if the presence of moisture was detected in the close proximity to the sensor.

Results on each page are presented with four different pieces of information:

1. The configuration of the wall assembly showing the cross-section of the wall and identification of the significant components of the assembly - this provides a point of

reference when comparing results from the different wall assemblies (lower left corner of Fig.).

2. The location of the MS in the wall assembly - Sensors clearly activated from apparent increase in moisture content of the board are marked with light numerals on a dark background. Certain sensors, over the course of the test sequence, were prematurely activated by water cascading from above – these are marked with dark numerals on a dark background (upper left corner of Fig.).
3. The test progression showing the elapsed time and pressure differential (static or dynamic) at each sequence and to which the occurrence of different events can be identified. The sequence of activation of the different moisture sensors is provided - the time at which activation occurred is given and this information is related to the test condition. Note that for the test trials under dynamic pressure fluctuations the test sequence is different than that of the static trials. Static water penetration trials have six (6) sequences of 20 minutes each starting from a low of 0 static pressure differential to a high of 1000 Pa. Dynamic trials have nominally seven (7) sequences, the first four (4) of which are carried out with air barrier leakage set at a nominal value of 0.2 L/s-m^2 and range from 75 to 700 Pa. The values provide in the chart refer to the mean dynamic pressure differential at which the test was carried out (see Table 3.5 for actual pressure functions). The last three (3) sequences drop from 700 to 150 Pa but were carried out at 0.5 L/s-m^2 (upper right corner of Figure)
4. Other notable observations regarding water penetration through the sheathing board leakage around the window, electrical outlet or the ventilation duct are presented in the lower right hand corner of each figure. The time at which the event was observed is given or the test trial (20 minute sequence) in which the event occurred is indicated. In either case, the information is linked to the test trial to identify the test conditions in which these events occurred.

3.2.1.2 WATER PENETRATION ABOUT THROUGH-WALL PENETRATIONS

3.2.1.2 - ii *WINDOWS*

Leakage about windows occurred in all wall assemblies without exception. In instances where water leakage was detected in static tests, leakage was likewise detected in the sequence of tests conducted under dynamic loading. Leakage about windows most likely occurred in dynamic tests given that leakage was detected in the static test series.

Where leakage occurred in static tests, the threshold pressure differential at which water penetration was observed was 300 Pa for WA-2A and –5 and 500 Pa for WA-3 and -4. For the dynamic test sequence, 4 of 5 walls (WA-1, -2B, -3 & -5) had water leakage occur at 700 Pa mean dynamic pressure differential. Leakage was primarily detected in the corners of the windows, weak points in their fabrication.

3.2.1.2 - iii *ELECTRICAL BOX AND VENTILATION DUCT*

No water penetrated at or around the electrical outlet or ventilation duct of WA-3, -4 or WA-5. Penetration was however observed under static conditions for the ventilation duct of WA-1 (at 75 Pa) and under both static and dynamic conditions for both the electrical outlets and ventilation ducts of WA-2A and -2B. In the case of WA-2A, rates of water entry through the deficiency above the ventilation duct at each static or dynamic pressure level are provided in Figures 3.8 and 3.9 respectively. There is an evident increase in water entry rate with a corresponding increase in the pressure differential for both test series.

For WA-2B, penetration was observed to occur at a threshold level of 500 Pa in the static tests and 700 ± 300 Pa in the dynamic test series.

Water entry at these locations is purely indicative of the extent to which care was taken to seal these items from the elements prior to the start of the test and attests to the expected range of performances of similar building components when sealed in field conditions. Specifically, an extremely attentive job at sealing around penetrations is highly unlikely to permit water entry, even in extreme conditions (i.e. high wind and rainfall rate); a perfunctory application may at times allow some water entry in extreme conditions.

3.2.1.2 - iv *EVIDENCE OF WATER PENETRATION OF SHEATHING BOARD*

Water penetration through the wall proper, i.e. beyond the second line of defence was only evident in WA-2B (no penetration of the sheathing board was evident in any of the other walls tested) and was observed only during the dynamic test trials.

Examination of the surface of the sheathing board of WA-2B during dynamic test trials revealed that water penetration occurred in two locations: the first was situated at a staple that had perforated the surface of the OSB in proximity to MS-9. Water droplets were observed seeping from the surface at a mean dynamic pressure differential of 300 Pa and the flow was sustained throughout the remaining test trials (i.e. 80 minutes). The second observed instance of water entry through the sheathing board was in cavity No. 1 at mid-height of the wall assembly; penetration occurred at a mean dynamic pressure differential of 700 Pa and was sustained for the duration of the trial.

The nature of the penetrations is in keeping with that observed from water penetration tests on WA-2A in which it was observed that a similar instance of water penetration into the wall cavity was evident at locations where staples protruded the sheathing board (Figures 3.8 & 3.9). It appears that these are preferential areas where water can readily penetrate at higher differential pressures provided water is present at the interface. It is useful to recall that the location where water penetration occurred is one that is adjacent to a vertical joint between the stucco panels. As well, these joints had been fabricated to reduce the degree of adhesion of the stucco to the vertical metal strip thus permitting water to collect in the interface between these two components.

That water penetration both occurred in WA-2A and -2B under essentially the same transport mechanism suggests that this wall assembly type is potentially susceptible to water penetration under particular conditions. Specifically, two conditions must prevail: water must be present at the interface between the stucco and the sheathing membrane at a staple location, and; sufficient pressure differential must be present to drive the water through the board along the path produced by the staple.

For water to be present at the interface under in-service conditions would require climatic conditions that would bring about the saturation of the stucco layer. Essentially, conditions where continuous and intense rainfall combined with severe winds exist for sufficiently long as to drive water into the stucco and through to the interface. It is expected that such climatic events would occur infrequently in climates having a low moisture index and more often in those having a higher moisture index (e.g. Wilmington). Hence in sheltered climates, it is unlikely that any significant amounts of water would enter the wall cavity in the early term of the life of the assembly.

However, in locations where extreme climatic events occur more frequently, there is an increased likelihood that water may indeed be present at the interface as a consequence of such an event. Hence in these instances, locations where staples perforate both the sheathing membrane and board necessarily offer sites for water intrusion into the board proper. Depending on the degree to which water penetrates along the path of intrusion, the staple withdrawal resistance may, in time, be reduced, potentially causing local failure of the fastener. If this effect is generalised about a group of staples, the integrity of the wall assembly can be compromised. Additional work would be needed to further substantiate this expectation.

3.2.1.3 RESULTS FROM CONTINUOUS WATER SPRAY OVER 16 HR PERIOD - STAGE 3 OF TEST PROTOCOL

The intent of this stage of the test was to determine if, following ca. 4-5 hours of combined static and dynamic water penetration tests, the wall assembly would show signs of water penetration where none was detected in the previous sequence of testing (i.e. from Stage 2 of test protocol). In the case where penetration had been observed in Stage 2 tests, this subsequent test stage would be useful to observe either continued or increased water penetration.

For WA-2A all moisture sensor lights were active after 16 hours of water spray. This indicated that in locations where the sensors had not been prematurely activated by incident wetting on their contact points, the sheathing board had passed the threshold moisture content of ca. 12%.

Results from the succeeding walls in this series were not definite – WA-1 and –5 did not show any change from the water penetration tests (Stage 2); changes were however observed in the remaining wall assemblies.

Specifically for WA-2B, MS-5, -6 and -11 were activated over the 16-hour test indicating that additional water penetration appeared to occur in the sheathing board beneath the window assembly.

For WA-4, MS-2, -3, and -11 were activated over the test period. Moisture sensors -2 and -3 are located beneath the window assembly, MS-11 at the base of the wall in the cavity containing the horizontal joint. However for WA-3, certain sensors that had previously been activated from tests in Stage 2, were no longer indicating the presence of moisture.

That sensors were activated in WA-2B and -4 suggests that these wall assemblies are vulnerable to continued penetration given that water apparently is still present at the interface between stucco and the sheathing membrane following the initial water penetration test series of Stage 2. Although these walls are constructed with self-furring lath and that the self-furring feature is believed to provide some measure of separation between the stucco and the sheathing membrane, certainly these systems do not impart as adequate a protection as a drainage cavity.

Results from tests on full-scale wall assemblies do not correspond with those of small-scale screening assessments of the drainage ability of stucco systems that had previously been completed internally in Task 2 as a screening exercise in the selection of specimen components. This suggests that there are additional factors beyond intuitive concepts of the drainage ability of sheathing membrane that affect moisture management in stucco wall systems. The small-scale screening tests suggested that improved performance with respect to

drainage behind the stucco should be achieved in the case of WA-1 and -2B, in comparison to that of WA-3 or –4. These tests also indicated that the type of sheathing membrane has a greater effect on drainage than the metal lath. That the results from these full-scale tests do not correspond with these interim findings does not imply that the drainage tests in themselves are inconclusive, but rather that other factors more significantly affect drainage capability in these full-scale tests. Factors that immediately come to mind are those related to fabrication of the assembly such as application of the mesh, the placing of fasteners, application of the stucco in layers and method of cure. Other differences between small and full-scale tests on wall assemblies may include the influence of edge effects and differences in overall moisture saturation levels in wall components, as well as differences in the mechanisms of water entry and transport.

3.2.1.4 Summary of results – Water penetration tests

- WA-5 provides the greatest resistance to water penetration beyond the second line of defence. This can be attributed to the lack of evidence of water penetration primarily due to the presence of a drainage cavity between the stucco and sheathing membrane.
- Of the walls tested, only WA-2B had evidence of through-wall penetration – this is in keeping with that observed in work on WA-2A, a wall assembly having similar construction details.
- Water penetration through the sheathing board occurred exclusively at locations where staple fasteners had perforated the surface of the board.
- It is surmised that for specimens such as WA-2B, localised failure of fasteners may occur at locations where groups of staples perforate the sheathing board should the such specimens be subjected to climates having frequent extreme rainfall events – further testing would be needed to substantiate this expectation.
- Leakage about windows and other through-wall penetrations occurred primarily at high pressure differentials, typically in excess of 300 Pa.
- No observable difference was noted for the incidence of water penetration of wall assemblies tested with air barrier systems having different levels of leakage under dynamic loads (i.e. incidence of water penetration was the same for walls configured with system leakage of either 0.2 or 0.5 L/s-m^2)
- No definite inferences can be made in regard to the drainage ability of different combinations of sheathing membrane and metal lath based on these full-scale performance tests.

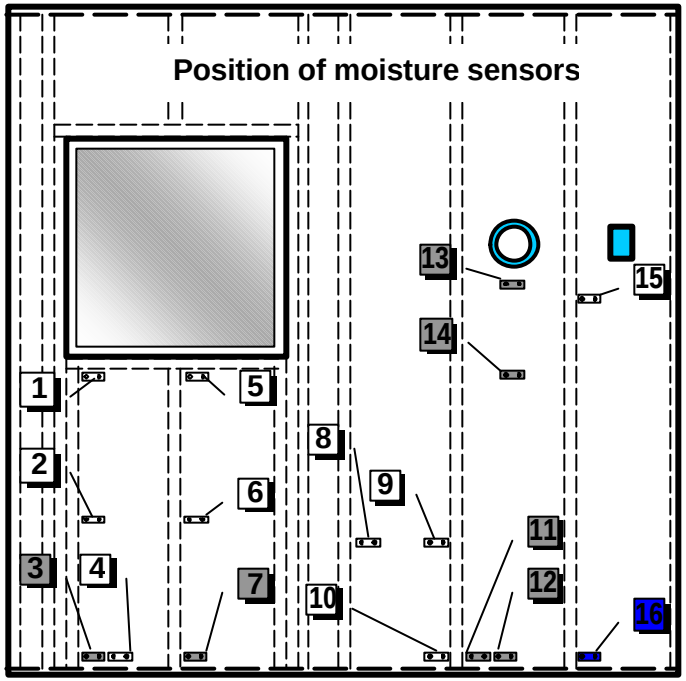

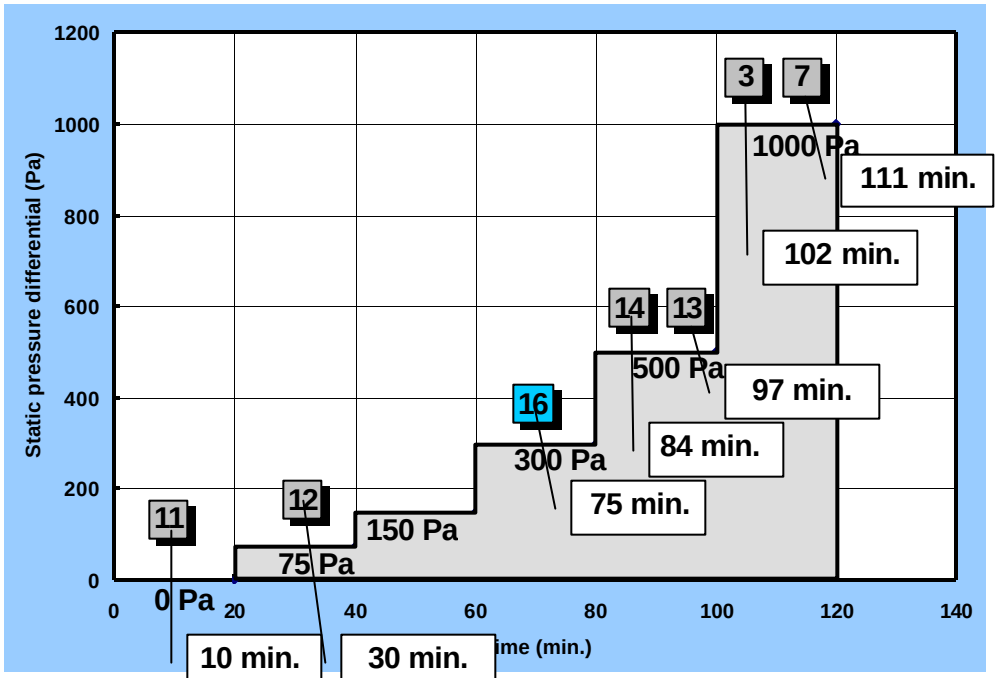

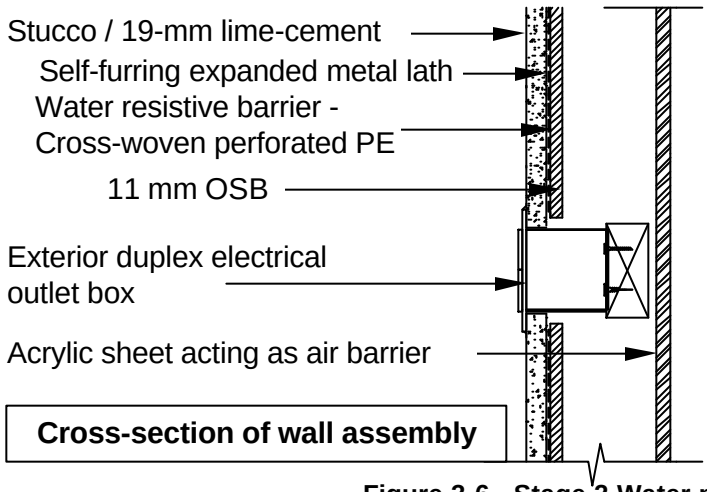

Cross-section of wall assembly

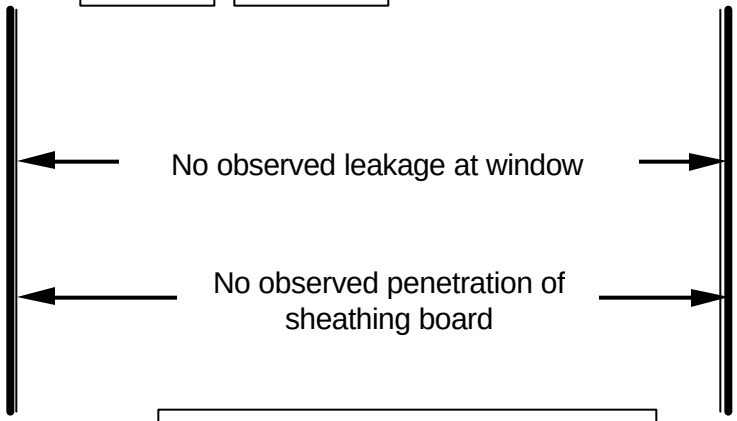

Observations during TEST

Figure 3.6 - Stage 2 Water penetration of WA-1 - Static test on Stucco-clad walls

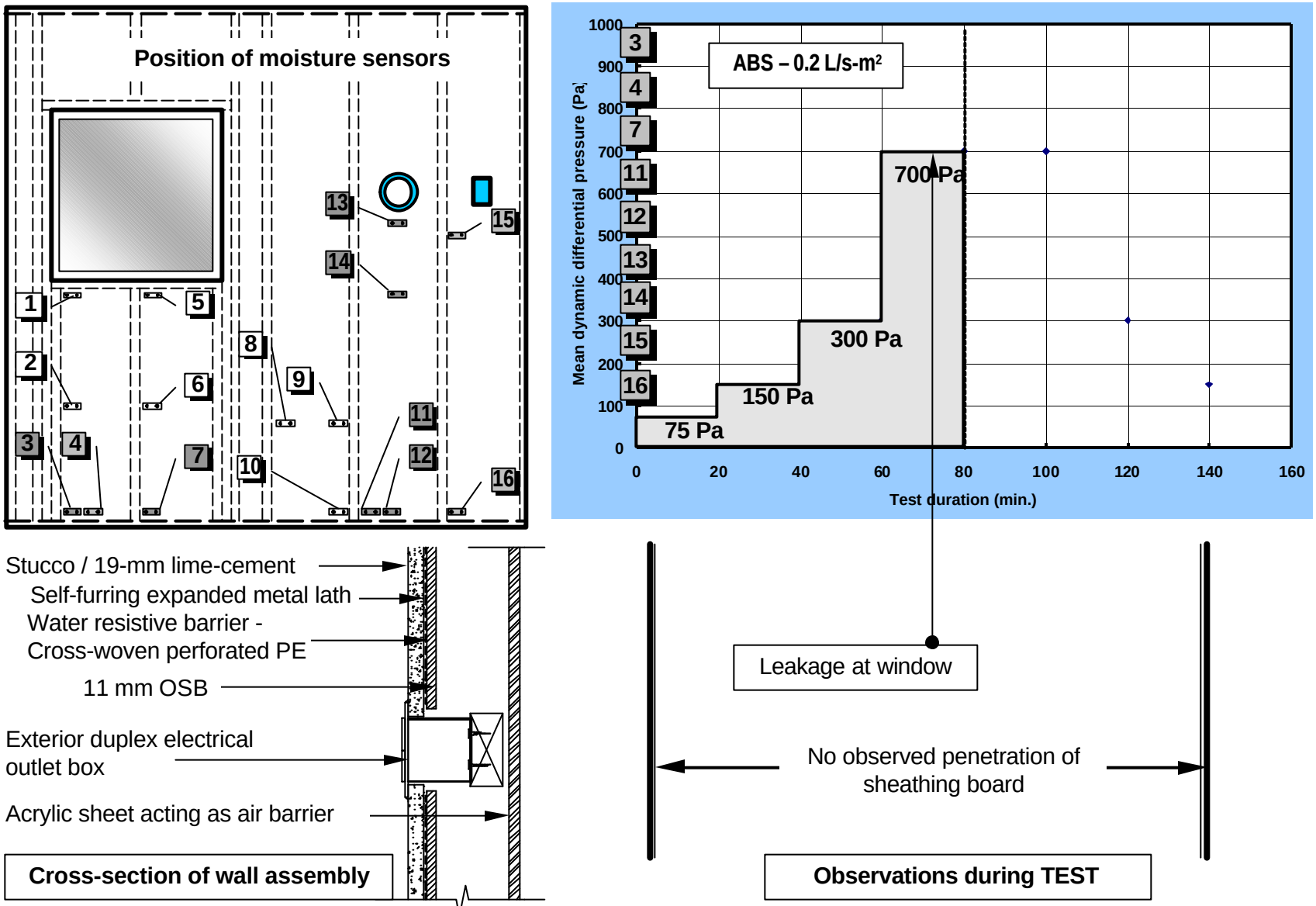

Figure 3.7- Stage 2 Water penetration of WA-1 - Dynamic test on Stucco-clad walls

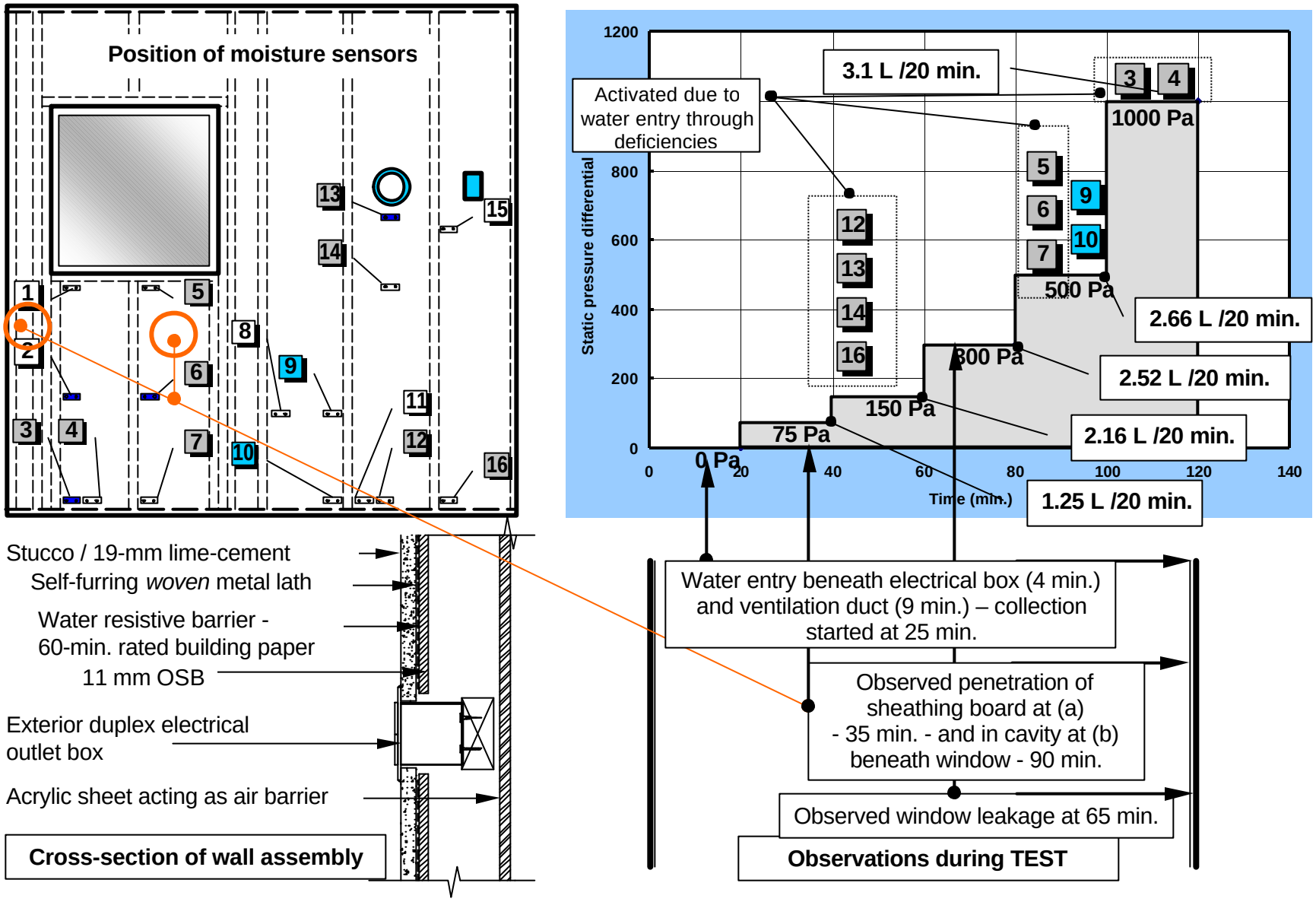

Figure 3.8. Stage 2 Water penetration of WA-2A - Static test on Stucco-clad walls

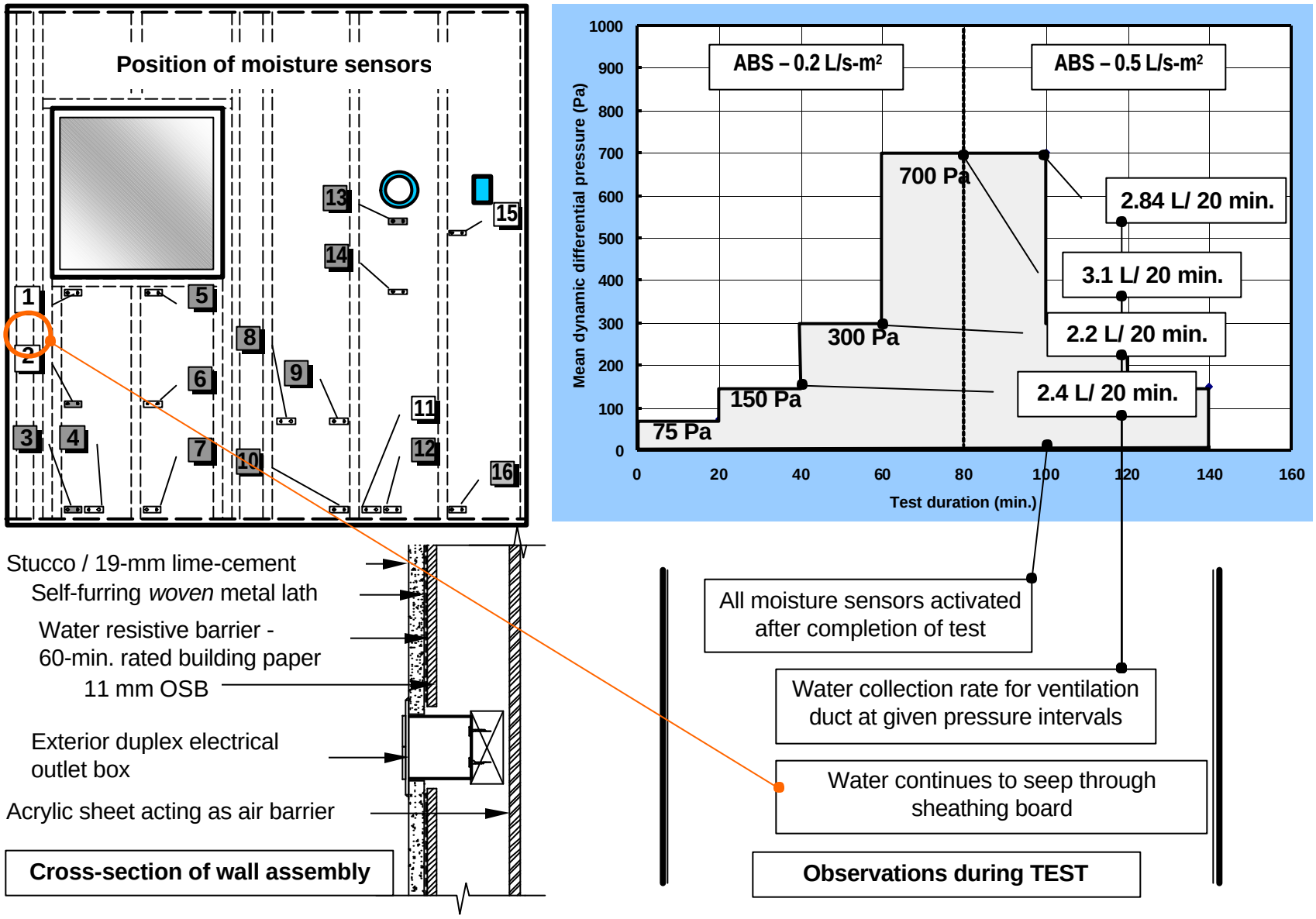

Figure 3.9- Stage 2 Water penetration of WA-2A - Dynamic test on Stucco-clad walls

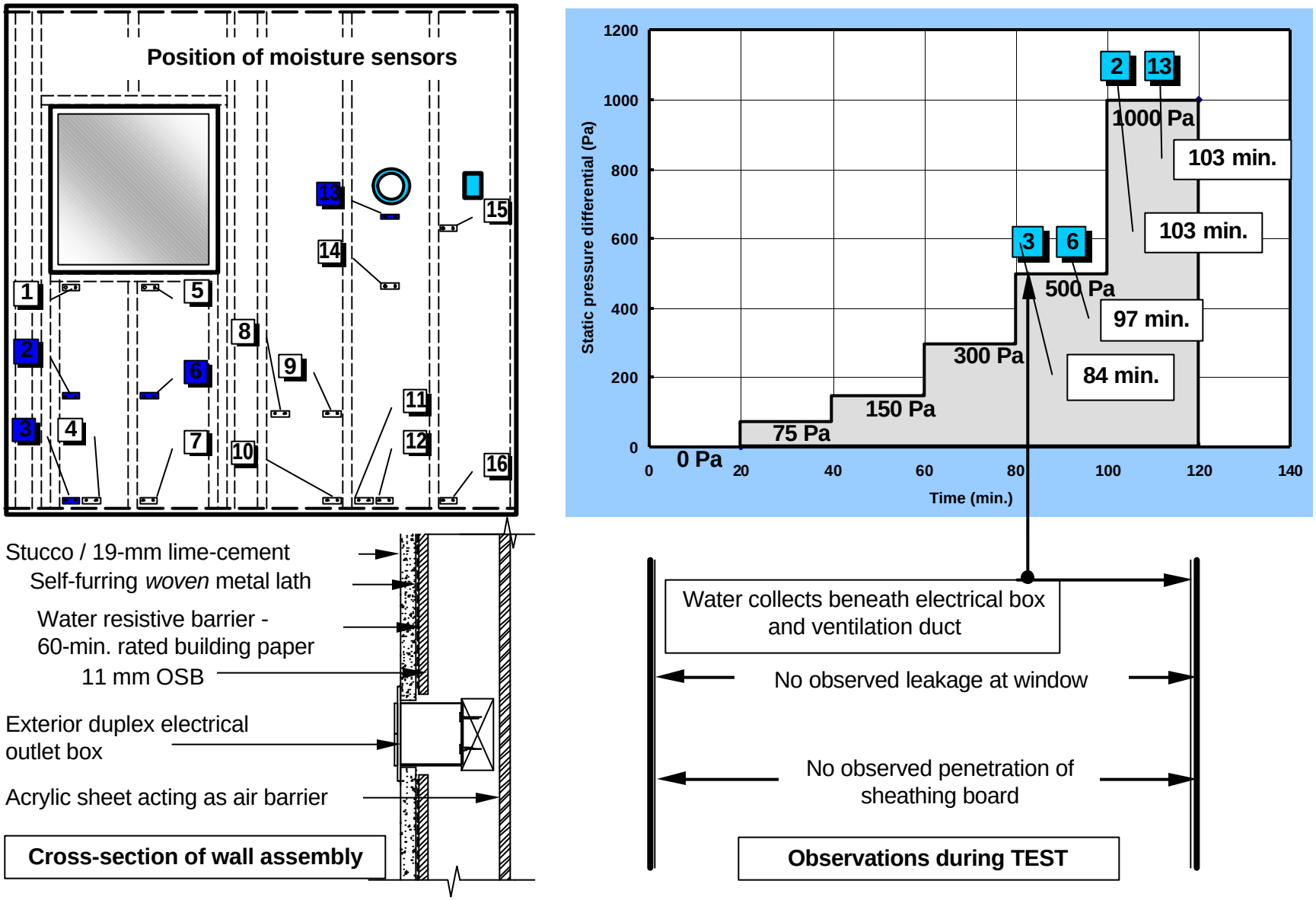

Figure 3.10 Stage 2 Water penetration of WA-2B - Static test on Stucco-clad walls

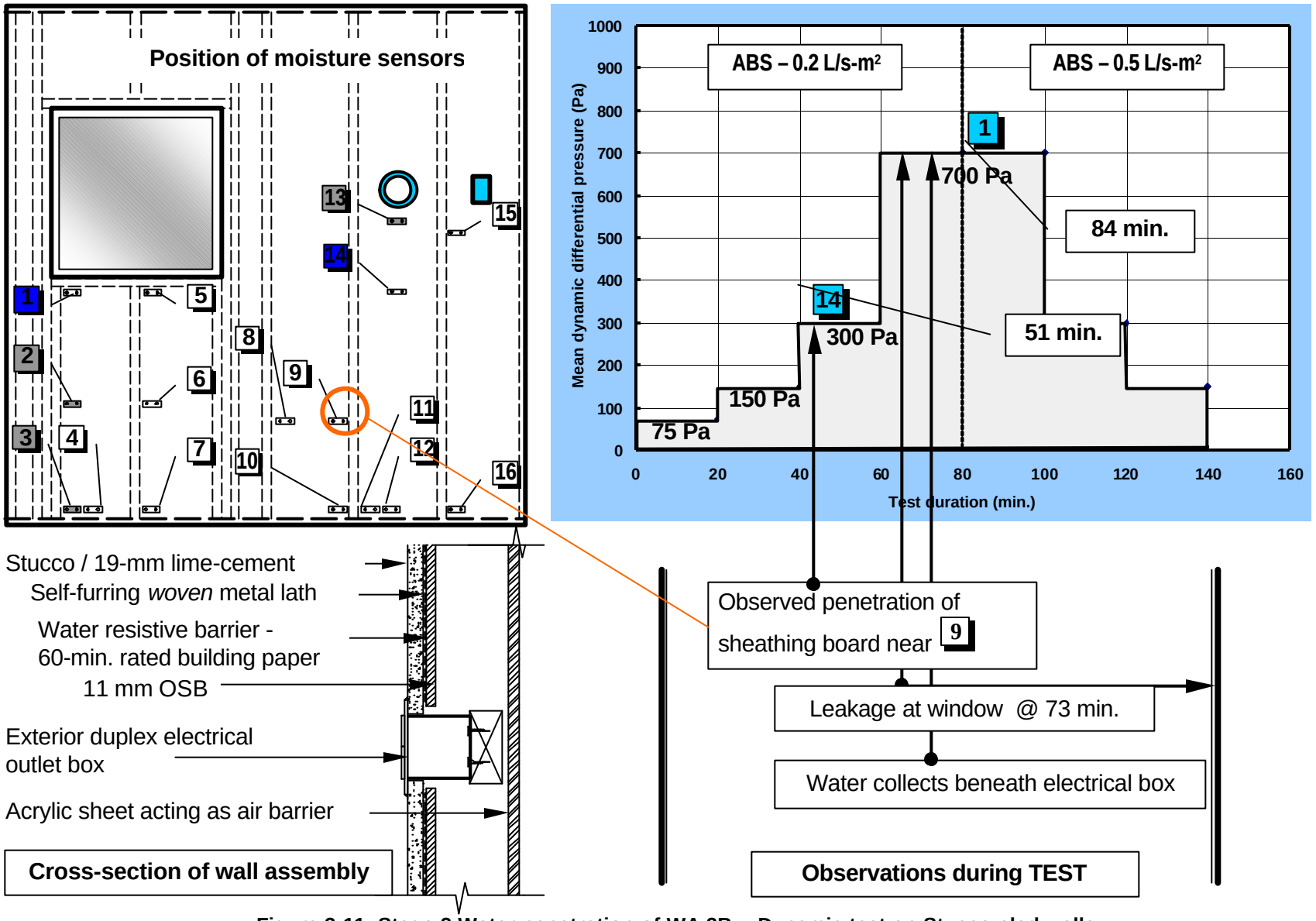

Figure 3.11- Stage 2 Water penetration of WA-2B - Dynamic test on Stucco-clad walls

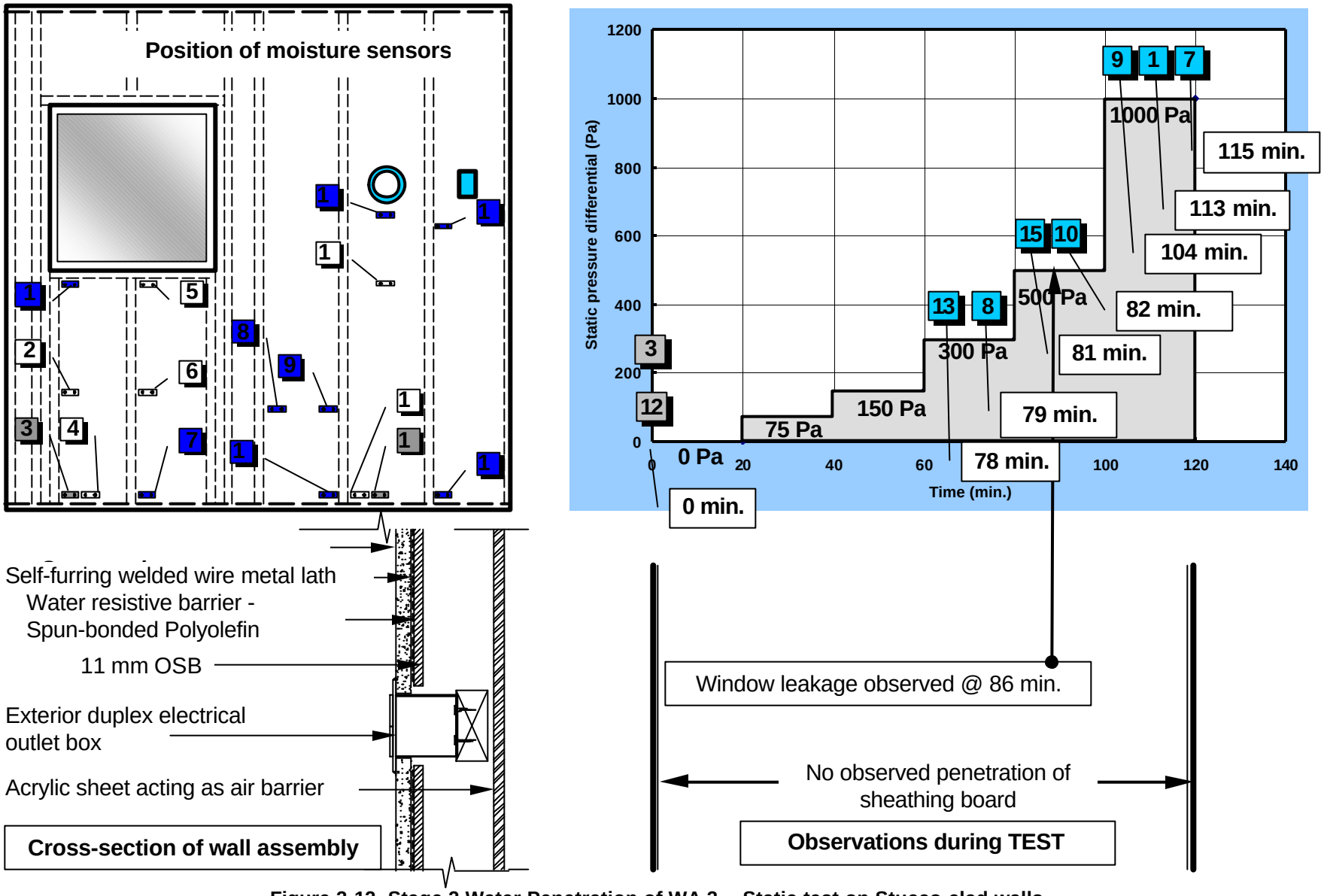

Figure 3.12- Stage 2 Water Penetration of WA-3 - Static test on Stucco-clad walls

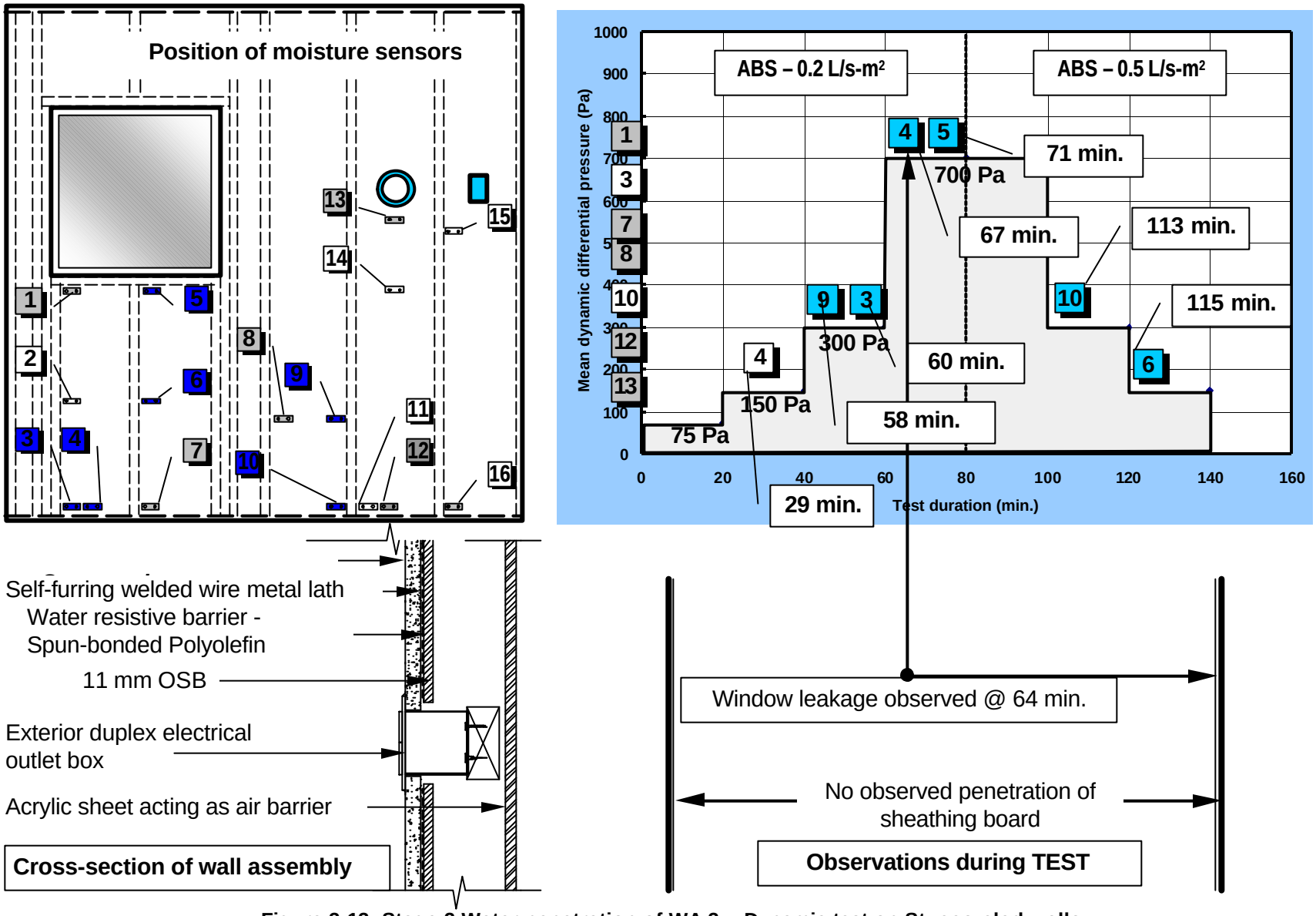

Figure 3.13- Stage 2 Water penetration of WA-3 - Dynamic test on Stucco-clad walls

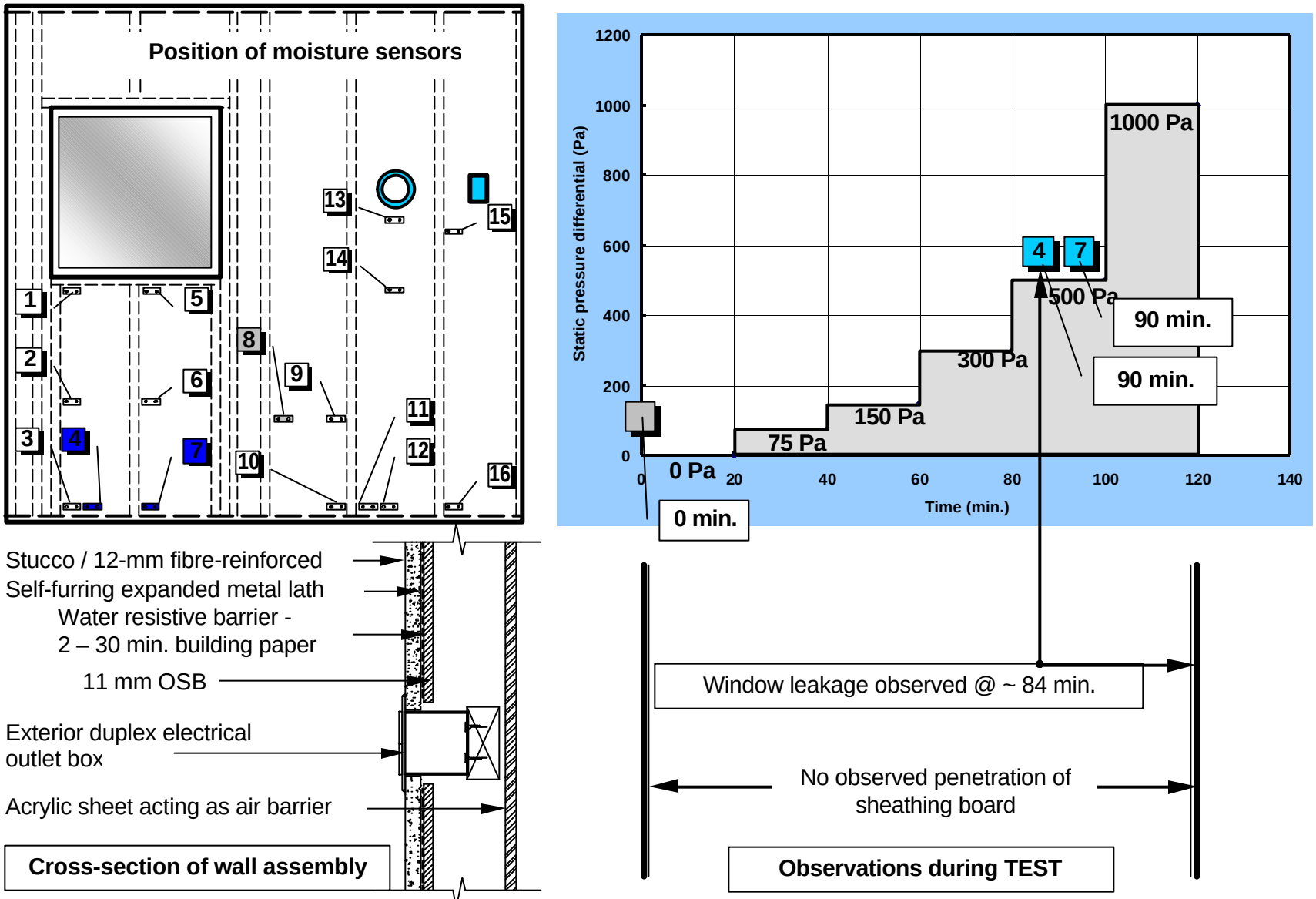

Figure 3.14- Stage 2 Water Penetration of WA-4 Static test on Stucco-clad walls

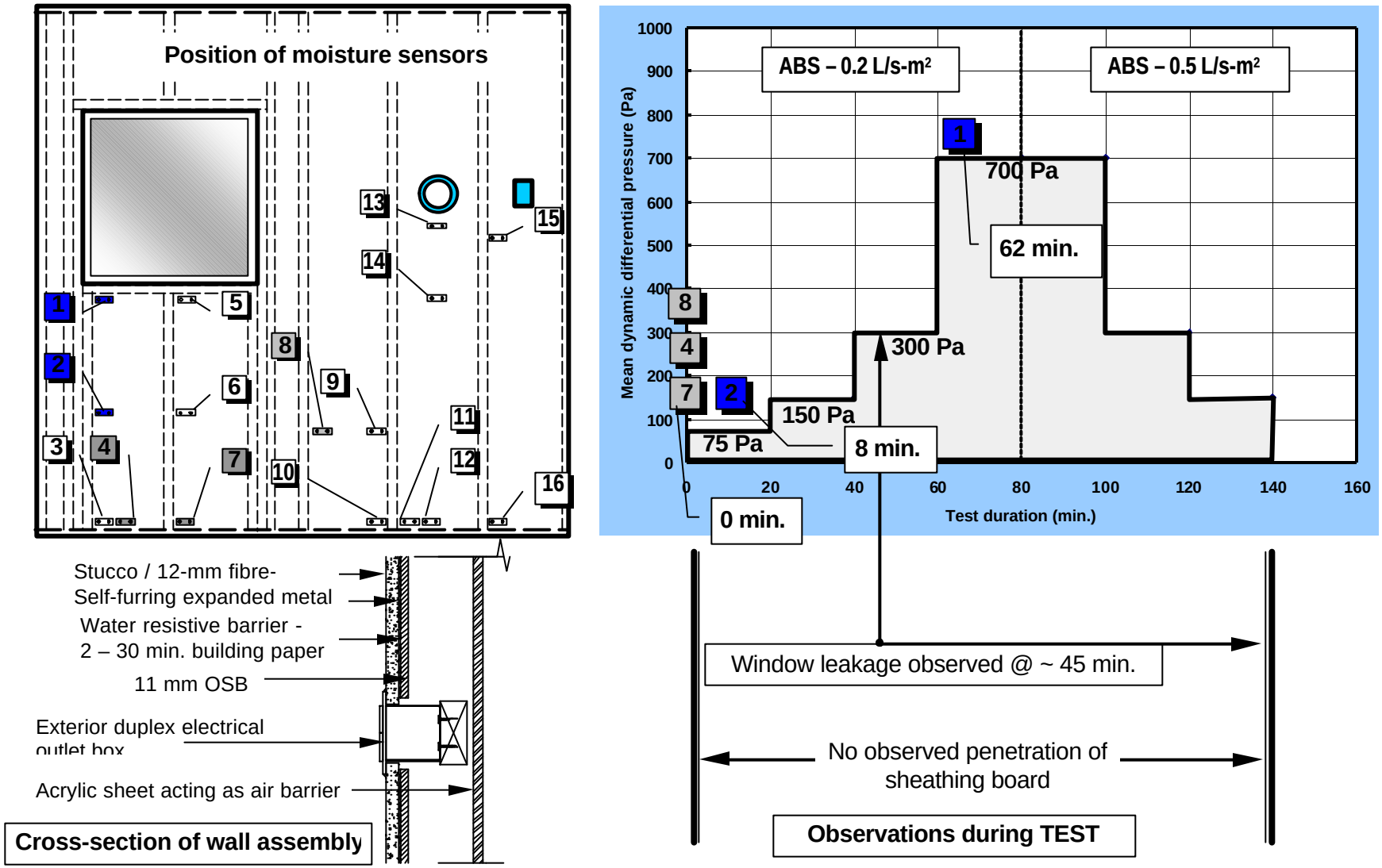

Figure 3.15 - Stage 2 Water penetration of WA-4 - Dynamic test on Stucco-clad walls

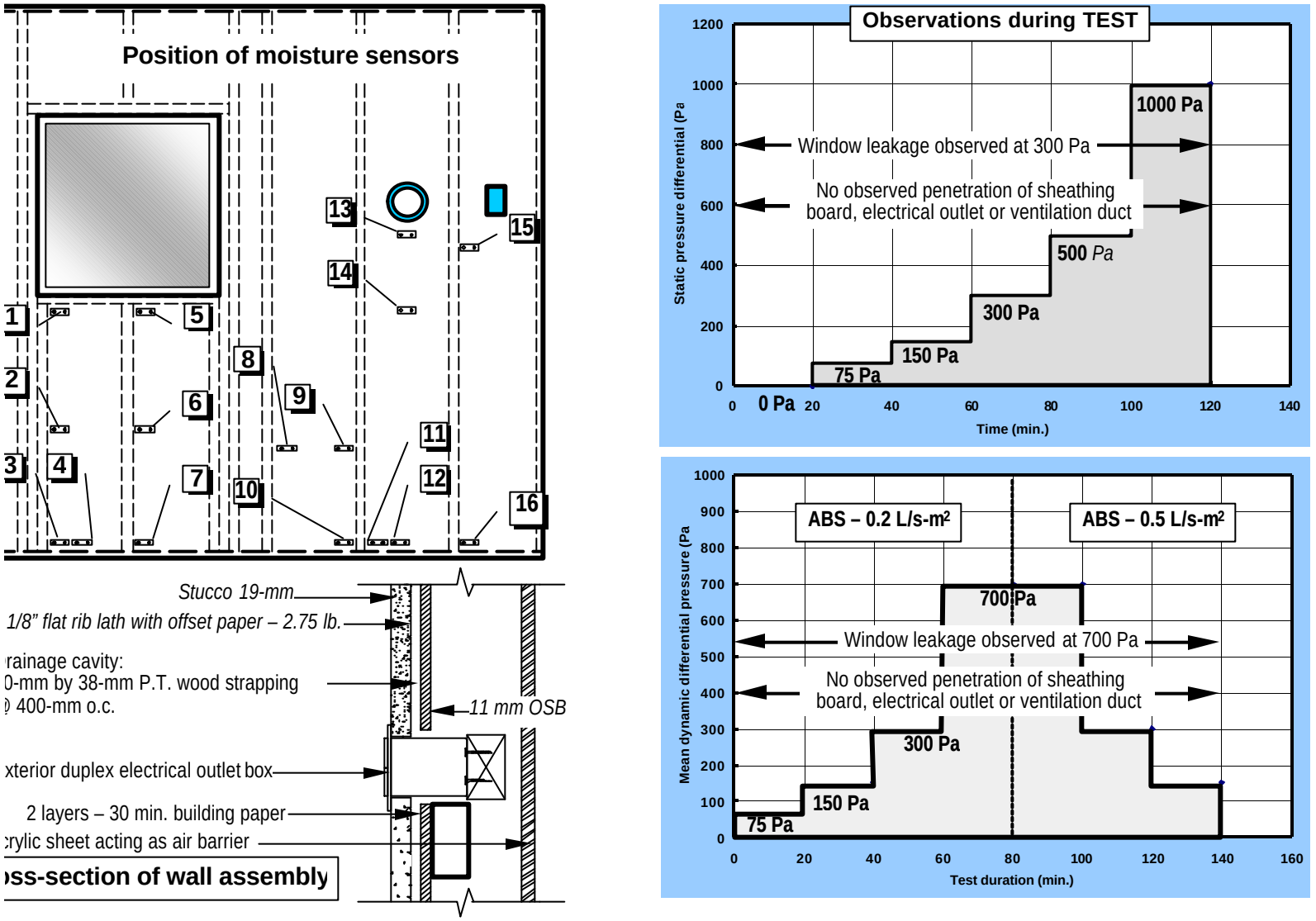

Figure 3.16 - Stage 2 Water penetration of WA-5 - Dynamic test on Stucco-clad walls

3.2.2 WATER ENTRY ASSESSMENTS THROUGH SPECIFIED DEFICIENCIES– STAGE 4 (STAGES 5,6 AND 7)

3.2.2.1 INTRODUCTION

Water entry assessments were used to determine the quantities and rates of water that might enter specified deficiencies of known type, size and location on the cladding when subjected to simulated climatic extremes, likewise using the DWTF. Levels of water spray and pressure differential were consistent with related climatic data of rainfall and wind speed that might occur in an extreme climatic event within a 10 year period in North America. This information provided a basis for a systematic and consistent means of transferring input to hygIRC, the hygrothermal model used in the MEWS analytical studies. Note that when reference is made in this chapter to "deficiencies", in all instances this is referring to specified deficiencies.

Results for water entry through deficiencies in stucco walls subjected to static pressure differentials are provided in Figures 3.16 to 3.25 and under dynamic pressure fluctuations in Figures 3.26 to 3.29. Each trial lasted up to 20 minutes and was carried out at spray rates of both 1.7 and 3.4 L/min.-m^2, with a system air leakage of 0.2 or 0.5 L/s-m^2 as required by the test protocol. Water was collected in troughs beneath water entry points at the electrical outlet and the ventilation duct, as well as through conduits flowing from either window edge and through its center section.

Information related to water entry through deficiencies above the electrical outlet are first discussed (Figures 3.16 and 3.17) followed by results obtained from entry through deficiencies located above the ventilation duct (Figures 3.19 and 3.20), and thereafter, for entry about windows (Figures 3.21 and 3.25). Water entry under dynamic pressure is then addressed in the same order as presented for the results from static pressure tests, i.e., results from the electrical outlet are followed by those obtained from the ventilation duct.

Comparisons are made with respect to:

- The relative rates of water entry obtained among the different types of deficiency
- The range and maximum values obtained at given spray rates;

General trends as to the changes in rate of entry in relation to increases in spray rate or static differential pressure (ΔP_s) are also noted. For the purposes of this work, it was deemed acceptable to generate what trends could be discerned on the basis of these results given the time and resources available to carry out the work.

A summary of the salient points regarding results of these test trials follows the discussion of the results.

3.2.2.2 WATER ENTRY ABOVE ELECTRICAL OUTLET

Results for water entry through a deficiency above an electrical outlet are given in Figures 3.16 and 3.17, a summary of which is provided in Table 6 below. The values in Table 3.6 relate to all walls in the test series.

Table 3.1– Water entry rates through deficiency above electrical outlet at given spray rates

***Spray** Rate L/min.-m^2*	**Rate of water entry, L/min.**			
	Maximum	*Avg. at 0 Pa*	*Avg. at 300 Pa*	*Range*
1.7	0.086	0.054	0.069	0.015
3.4	0.33	0.05	0.20	0.15

The following was noted:

- A maximum rate of water entry at a ΔP_s of 300 Pa of 0.069 L/min. was achieved for WA-2A, representing a significant amount of water entry if averaged over an hourly period (i.e. 4.2 L/hr.).
- Water entry due to gravity effects when no pressure difference is applied to the wall (i.e. $\Delta P_s = 0$) was also observed in most walls (i.e. WA-2A, -2B, -3 and WA–4). The average value of water entry in such conditions was 0.054 L/min. (ca. 3.2 L/hr.) representing, nonetheless, a singular quantity of average water entry. Given that WA-1 to -4 (5 walls) are essentially barrier wall assemblies that rely on the integrity of the seal at joints located at the outermost face to insure water-tightness of the assembly, the importance of maintaining these interfaces is emphasised in consideration of these results. That is, water entry through gross deficiencies located on the outside of walls is immanent when rainfall wets the surface of the wall at rates comparable to those used in the test series. This brings to mind the consequences of improper detailing and perfunctory installation methods typically found in field conditions
- WA-5, an assembly incorporating a drainage cavity, did not exhibit any water entry at any of the pressure differentials.
- The values of water entry rate between 0 and 300 Pa ΔP_s ranged from 0.054 to 0.069 L/min.; this value is less than the range obtained at the higher spray rate.
- Repeatability of results of subsequent test trials is demonstrated by comparing results from WA-2A at a ΔP_s of 150 and 300 Pa. The coefficient of variation of two consecutive trials at either 150 Pa or 300 Pa was less than 5% in both cases.

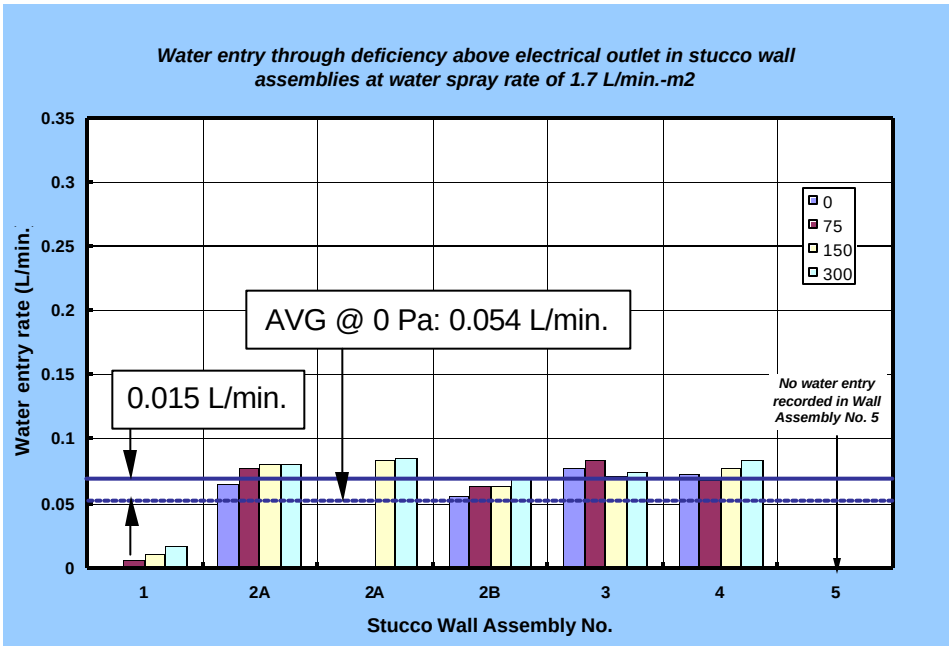

Figure 3.17 – Water entry under static pressure differential through deficiency above electrical outlet for stucco wall assemblies at a spray rate of 1.7 L/min.-m^2

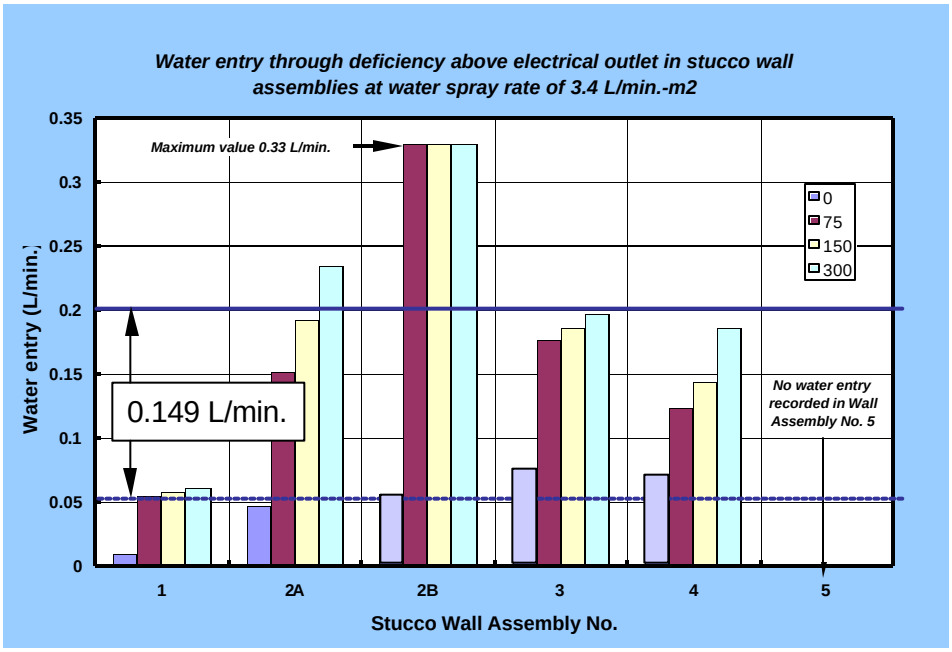

Figure 3.18– Water entry under static pressure differential through deficiency above electrical outlet for stucco wall assemblies at a spray rate of 3.4 L/min.-m^2

- For walls having water entry, the degree of response of the rate of entry to changes in ΔP_s is small relative to the changes brought about by different spray rates. For example, water entry rates varied on average 0.0155 L/min. between ΔP_s ranging from 0 to 300 Pa. This suggest that the degree of response for all barrier walls is essentially the same; differences among these walls are evidently due to the amounts of water entry when $\Delta P_s = 0$ as can be seen when comparing results from WA-1 to those of WA-2A to -4.
- No water entry is observed in WA-1 at a ΔP_s of 0. This is not believed to be a result of the inherent nature of the assembly, but more likely, due to the manner in which the receptacle cover and adjacent gasket was attached to the wall. Such types of details appear to greatly affect water entry rates irrespective of the care and attention used to prepare the specimens.

Figure 3.17 provides results from water entry at a spray rate of 3.4 L/min.-m^2 – the following was observed:

- The maximum rate of entry was 0.33 L/min. (WA-2B at 300 Pa ΔP_s) with the average rate of entry at 300 Pa ΔP_s of 0.2 L/min.
- Results at $\Delta P_s = 0$ were only obtained for WA-1 and 2A. No values were obtained for WA-2B, -3 or WA-4. With the two values recorded at no pressure differential (0.0095 and 0.047 L/min.) it can be stated that comparable amounts of water entered at a spray rate of 3.4 L/min.-m^2 as that obtained at 1.7 L/min.-m^2, the lower rate of spray.
- No water entry was observed for WA-5 – this is the same result as that obtained at 1.7 L/min.-m^2, the lower spray rate.
- For wall assemblies having water entry, the response of rates of entry to increases in ΔP_s is more significant at 3.4 L/min.-m^2, the higher spray rate.
- Comparing the relative change in rates of water entry between 75 and 300 Pa ΔP_s (3 trials), the average change over this range is 0.0342 L/min. (barrier walls). Water entry through deficiencies above the electrical outlet appears to be more greatly affected by changes in spray rate than changes in pressure difference. E.g. at a ΔP_s of 300 Pa, increases in spray rate from 1.7 to 3.4 L/min. bring about a 3-fold increase in rate of water entry. This is illustrated in Figure 3.18 below, showing water entry rates through the deficiency above the electrical outlet at the two spray rates. It is seen that the primary trend affecting rates of water entry for this deficiency in stucco wall assemblies is the spray rate impinging on the wall surface.

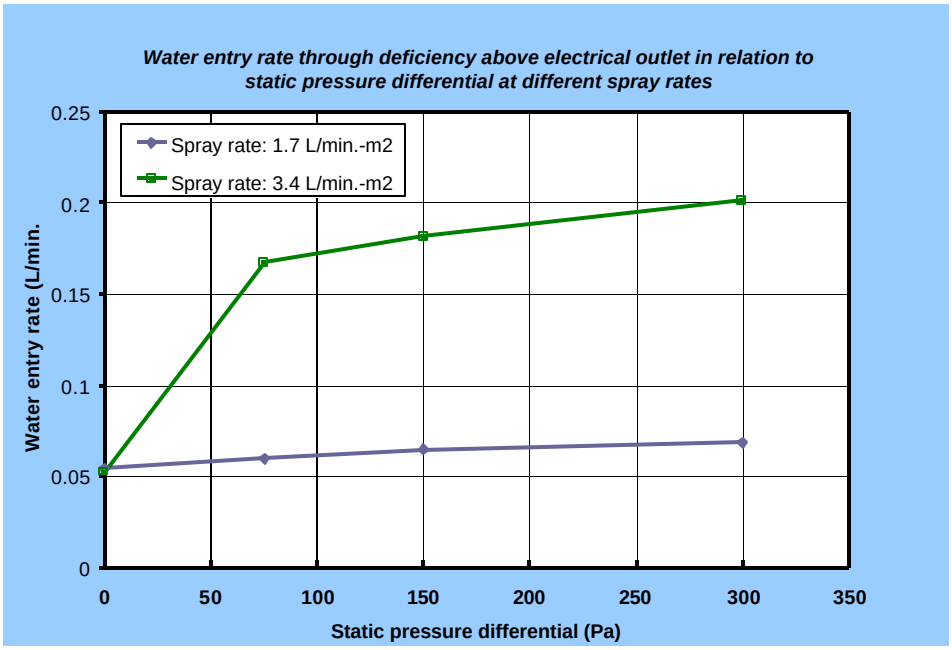

Figure 3.19 – Water entry through the deficiency above the electrical outlet in relation to static pressure differential at different spray rates

3.2.2.3 WATER ENTRY ABOVE VENTILATION DUCT

Figures 3.19 and 3.20 offer results for rates of water entry through deficiencies above a ventilation duct – an overview is provided below in Table 3.7:

Table 3.2– Water entry rates through the deficiency above the ventilation duct at given spray rates

Spray Rates *L/min.-m²*	Rate of water entry, L/min.			
	Maximum	*Avg. at 0 Pa*	*Avg. at 300 Pa*	*Range*
1.7	0.51	0.10	0.11	0.01
3.4	0.56	0.11	0.31	0.2

The following was noted:

- A the lower spray rate (1.7 L/min.-m^2 – Figure 3.19) values for water entry are in the same order of magnitude as those obtained for the deficiency above the electrical outlet with the exception of those values for WA-4. Results for WA-4 are appear to be anomalous when compared to the rates of entry obtained for the other wall types and is most likely due to a breach of the seal that prevents water from entering the duct itself.
- The remaining wall assemblies (WA-1, 2A, -2B and WA-3) had rates of water entry ranging from 0.006 (WA-2B; $\Delta P_s = 0$) to 0.049 L/min. (WA-3, $\Delta P_s = 300$ Pa).
- Within this same group (i.e. WA-1 to -3) there was an evident dependency of water entry rates on pressure differential across the assembly.
- No water entry was observed for WA-5 at this spray rate.
- At the higher spray rate, (3.4 L/min.-m^2 – Figure 3.20) significant increases in rates of water entry were recorded for all assemblies, with the exception of WA-4.
- For the other wall assemblies there was a ca. 10-fold increase in rates of water entry at a ΔP_s of 300 Pa when comparing changes in the average rates for WA-1, WA-2A, -2B and WA-3.
- Comparing results to those obtained for the electrical outlet at a ΔP_s of 300 Pa indicates that values of the higher spray rate (3.4 L/min.-m^2) are in the same order of magnitude with the average for all walls, excluding WA-5. WA-5 is the wall assembly that contains a cavity. Water entry in this instance is believed to be due to water entering through the duct itself as opposed to water that has entered from around the duct.

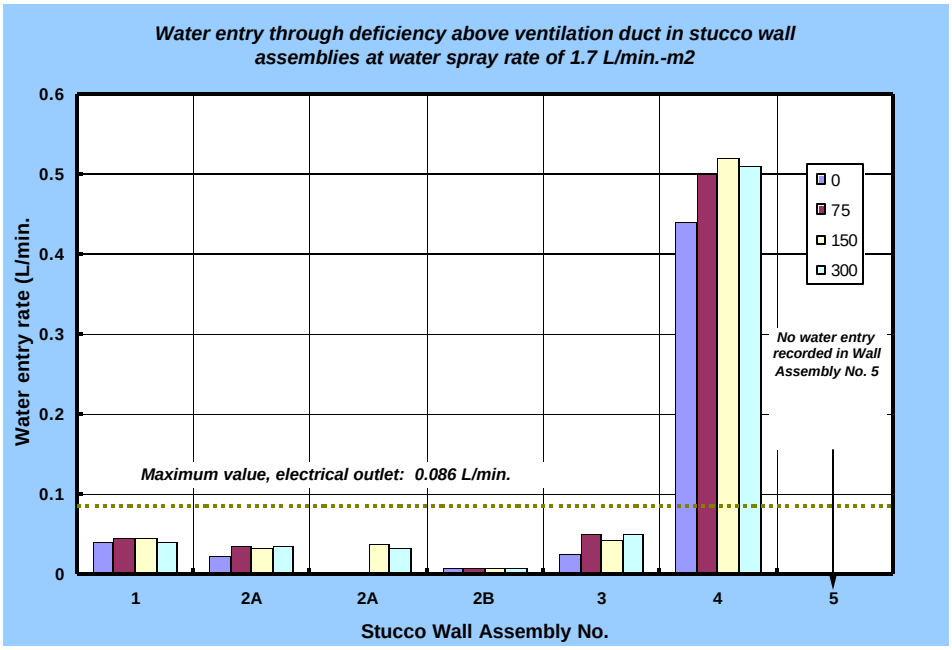

Figure 3.20 – Water entry under static pressure differential through deficiency above ventilation duct for stucco wall assemblies at a spray rate of 1.7 L/min.-m^2

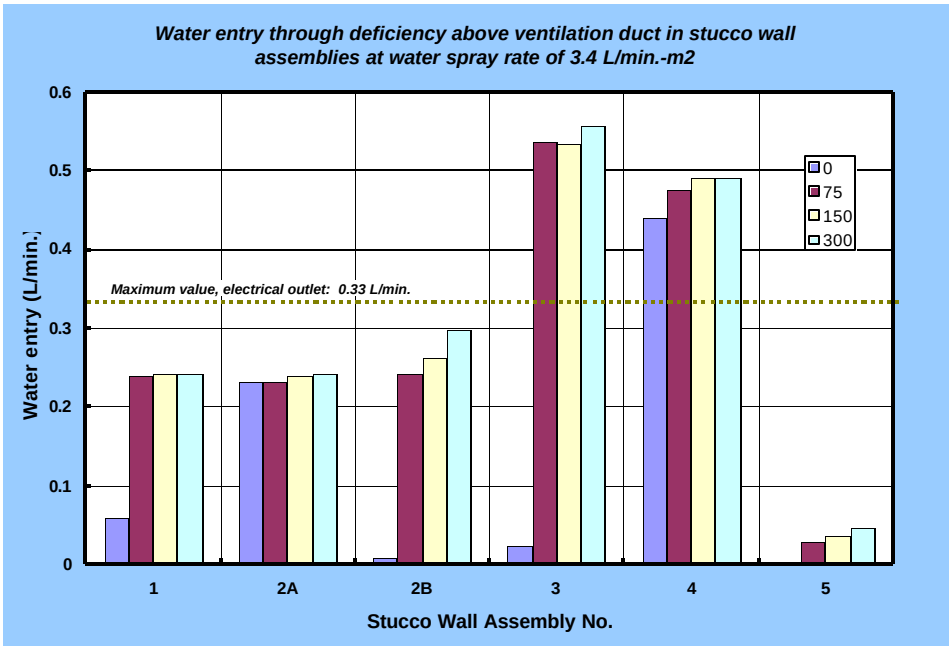

Figure 3.21– Water entry under static pressure differential through deficiency above ventilation duct for stucco wall assemblies at a spray rate of 3.4 L/min.-m^2

3.2.2.4 WATER ENTRY ABOUT WINDOWS

Results regarding water entry through deficiencies located at the window interface are presented in Figures 3.21 and 3.2, as relates to water collected at the window edge, and Figures 3.22 and 3.23 from that collected in the trough at the base of the window beneath the window center.

3.2.2.4 -i *COLLECTION AT WINDOW EDGE*

As before, results are grouped in relation to spray rate; information on rates of water entry at 1.7 L/min.-m^2 are given in Figure 3.21. Of those walls from which water was collected (i.e. WA-2A, -2B and –3) water entry was strongly dependent on test pressure. E.g. for WA-1, there was an increase of 0.08L/min. over a pressure range between 0 and 300 Pa, representing a ca. 12-fold increase in entry rate between extremes in pressure difference.

Maximum values for water entry rate were 0.087 L/min. (WA-2A); these are in the same order of magnitude as those obtained for either the electrical outlet or ventilation duct.

On average there is an increase in rate of water entry of 0.05 L/min. due to changes in pressure difference (for WA-2A, -2B, and –3). Such values can not be directly attributable to the edge deficiency at the interface between the window and the cladding given the apparently convoluted path for water to reach the collection trough (see e.g. Figure 23). Collection at this point is believed to be representative of water entry through deficiencies in the window frame. That certain windows did not exhibit failure is symptomatic of the random nature of failure of these components.

At higher spray rates (3.4 L/min.-m^2 - Figure 3.22) similar results were obtained as compared to those at the lower spray rate: i.e.

- No water entry at the window in WA-1, -4 and WA-5)
- Values in the same order of magnitude for the respective wall assemblies
- Maximum values are similar to those obtained at the lower spray rate.

However, the dependency of entry rates on the pressure differential is neither as pronounced nor as even as that obtained at the lower spray rate. Only in certain cases were entry rates increasing with corresponding increase in pressure differential.

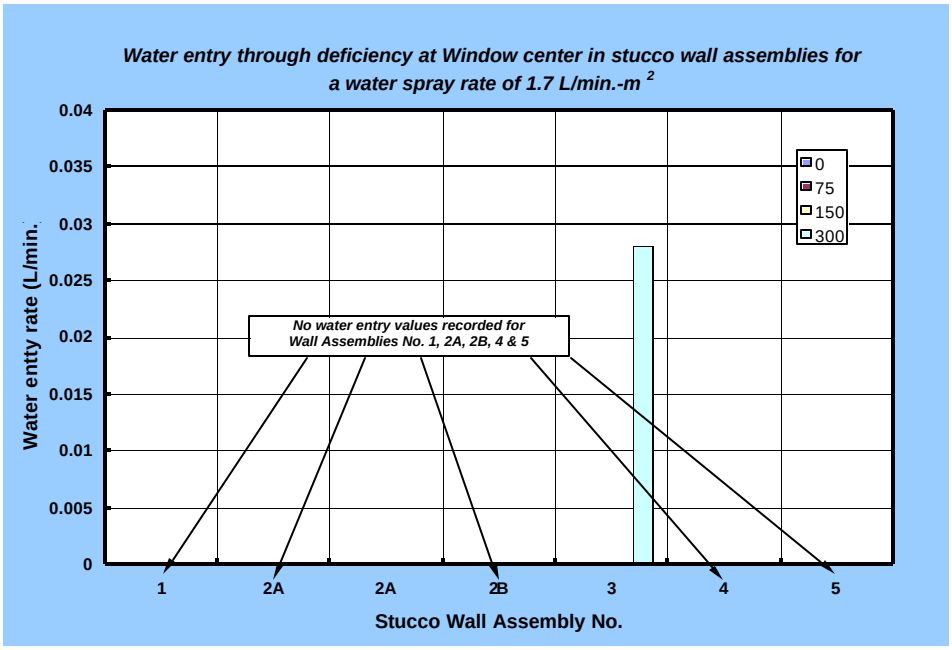

Figure 3.22– Water entry under static pressure differential through deficiency at window centre for stucco wall assemblies at a spray rate of 1.7 L/min.-m^2.

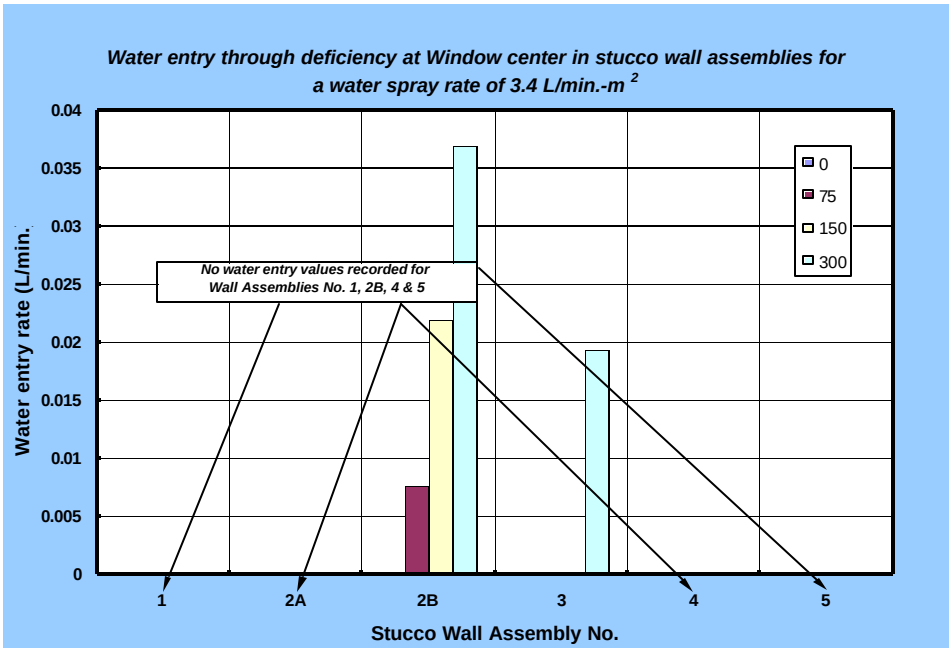

Figure 3.23– Water entry under static pressure differential through deficiency at window centre for stucco wall assemblies at a spray rate of 3.4 L/min.-m^2.

3.2.2.4 - ii *COLLECTION AT BASE OF WINDOW*

The following was observed from results for water entry of deficiencies at the base of the window in troughs located beneath the window centre (Figures 3.24 and 3.25):

- Collection at the base of the window in the centre collection trough did not provide any results with the exception of WA-3;
- No water was observed to enter WA-1, 2A, 2B, -4 and –5 at the lower spray rate;
- WA-3 was the only assembly having water entry occur at both the window edge and centre at both levels of water spray.
- Water entry was only observed at the highest pressure differential (300 Pa) and at a rate comparable to that obtained for the ventilation duct (0.028 L/min.).

These results do not suggest any specific pattern for water entry due to the deficiency at the centre of the window. Results appear to reflect entry based on the integrity of the window frame as opposed to the lack of soundness of the joint seal at the wall-window interface as suggested in Figure 3.23 below.

Rates of water entry are below those obtained for water entry at comparable spray rates and pressure differentials; at least a 2-fold decrease ranging from at least 2 to ca. 10-time less water entry at this joint.

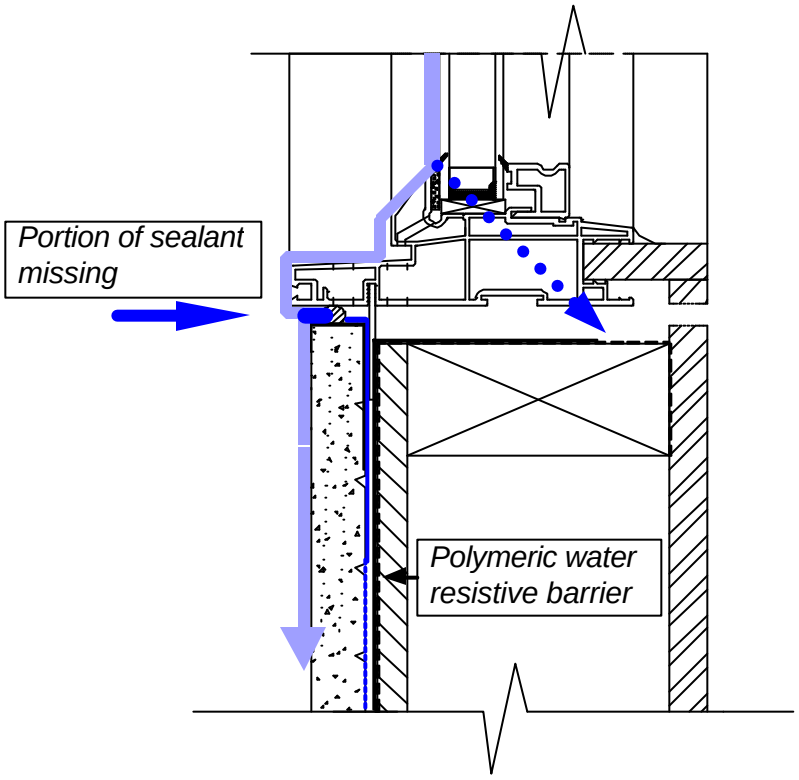

Figure 3.24 – Notional path of water entry at wall-window interface about deficiency

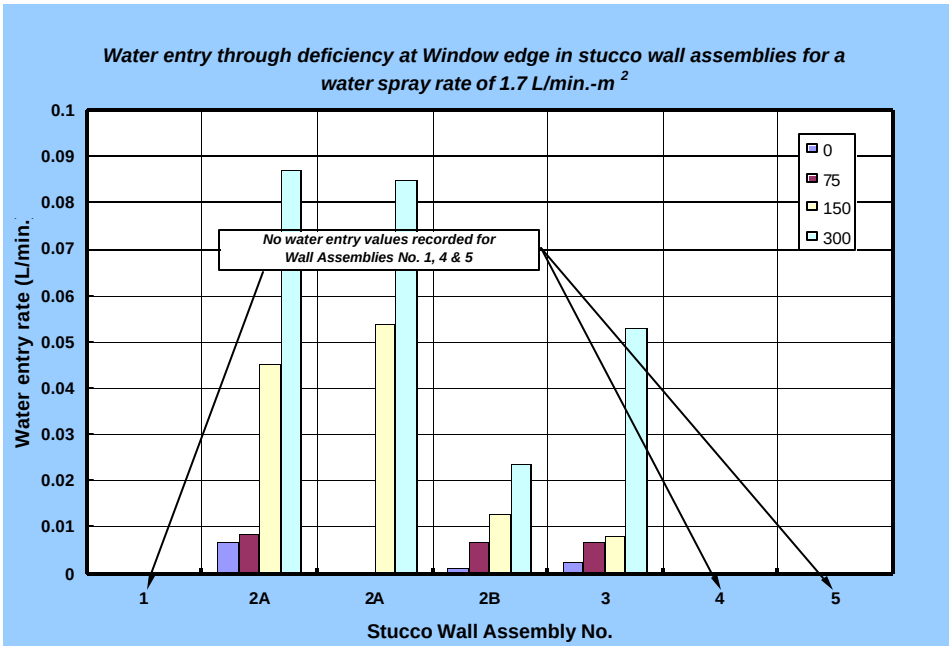

Figure 3.25– Water entry under static pressure differential through deficiency at window edge for stucco wall assemblies at a spray rate of 1.7 L/min.-m^2.

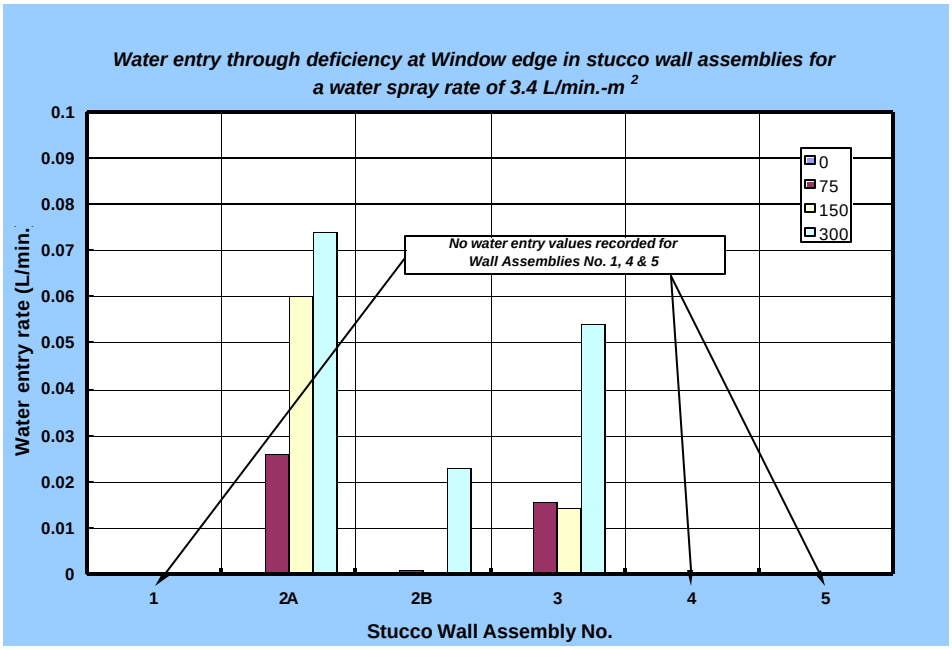

Figure 3.26– Water entry under static pressure differential through deficiency at window edge for stucco wall assemblies at a spray rate of 3.4 L/min.-m^2.

3.2.2.5 *WATER ENTRY UNDER DYNAMIC PRESSURE FLUCTUATIONS*

Results for water entry through deficiencies under dynamic pressure fluctuations are provided in Figures 3.26 to 3.29.

General observations made in regard to results obtained under static pressure differential can apply for these results:

- Water enters when no pressure is present;
- Increasing amounts of water enters as pressure fluctuations increase;
- The variation in water entry rates is small in comparison to that which characterises rates of entry for a given combination of wall assembly type and related deficiency.

A comparison is made of results obtained for the deficiency above the electrical outlet at both spray rates is summarised in Table 3.8 below. For dynamic tests at the lower spray rate (1.7 L/min.-m^2):

- Maximum value was 0.086 L/min. (at 300 Pa ΔP_s);
- Average value at 300 Pa was 0.066 L/min.

These results are essentially the same result as that obtained under static testing.
At the higher spray rate (3.4 L/min.-m^2):

- Maximum value was 0.33 L/min.; this is comparable to that of the static tests.
- The average rate at 300 Pa ΔP_s was 0.20 L/min. with a range of 0.09 L/min.

All of these values are essentially comparable to those obtained in static tests.

Results of water entry through the deficiency above the ventilation duct provide a similar comparison between dynamic and static test - values are essentially the same irrespective of the test mode.

Table 3.3 – Comparison of water entry rates obtained under static and dynamic tests

Test Mode	Water entry rate (L/min.)					
	Spray rate - 1.7 (L/min.-m^2)			*Spray rate – 3.4 (L/min.-m^2)*		
	Maximum value	Avg. value at 300 Pa*	Range from 0-300 Pa	Maximum value	Avg. value at 300 Pa*	Range from 0-300 Pa
Static	0.086	0.069	0.015	0.33	0.20	0.15
Dynamic	0.086	0.066	0.014	0.34	0.20	0.09

* under dynamic testing, the values were obtained under a fluctuating pressure differential of 300 ± 125•sin ($2\pi ft$) Pa, with nominal mean pressure of 300 Pa.

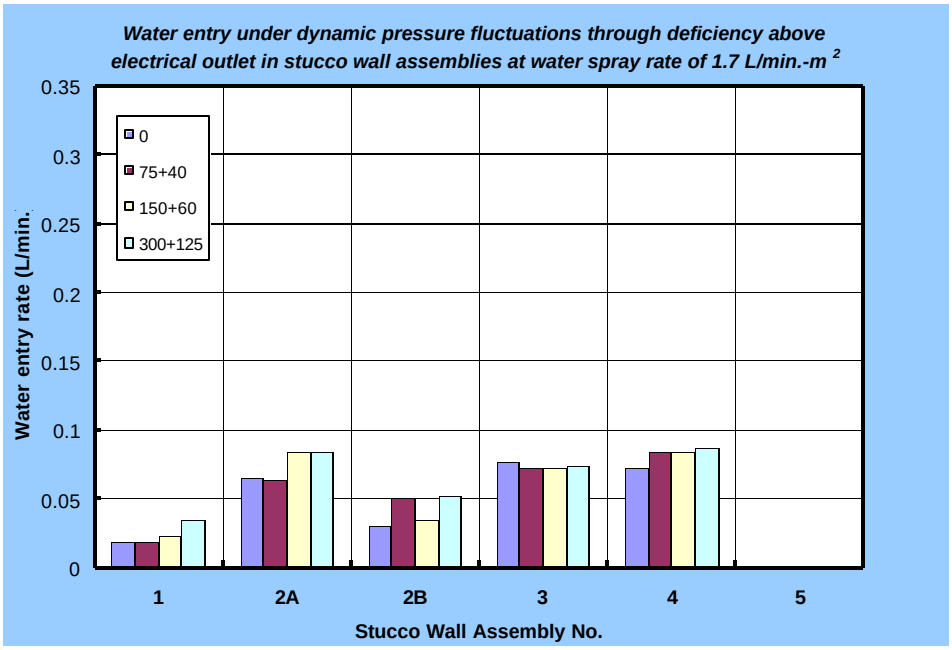

Figure 3.27– Water entry under dynamic pressure fluctuations through deficiency above electrical outlet of stucco wall assemblies at a spray rate of 1.7 L/min.-m^2

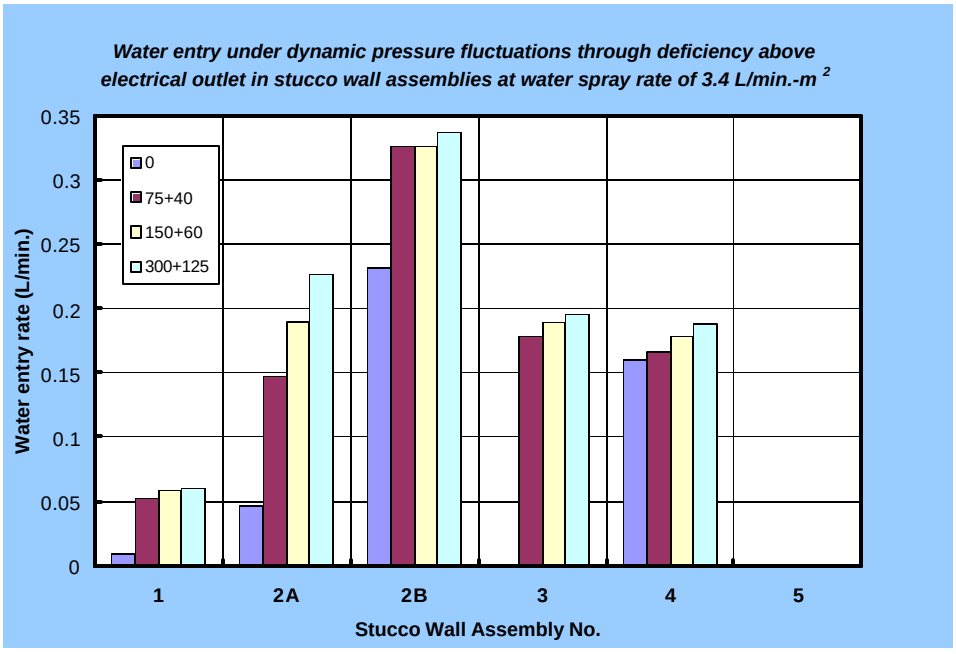

Figure 3.28– Water entry under dynamic pressure fluctuations through deficiency above electrical outlet of stucco wall assemblies at a spray rate of 3.4 L/min.-m^2

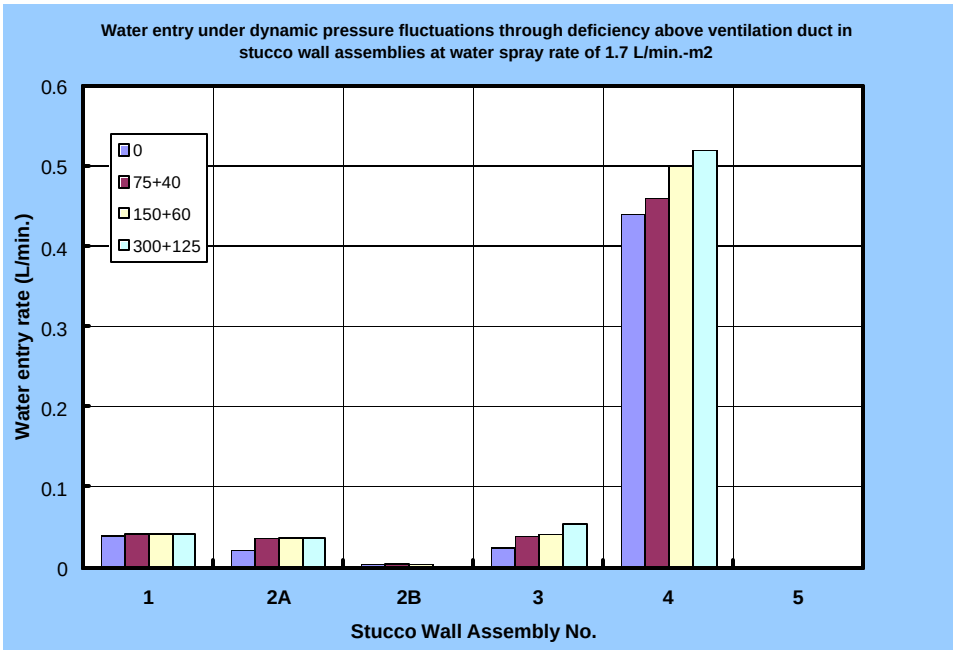

Figure 3.29– Water entry under dynamic pressure fluctuations through deficiency above ventilation duct of stucco wall assemblies at a spray rate of 1.7 L/min.-m^2

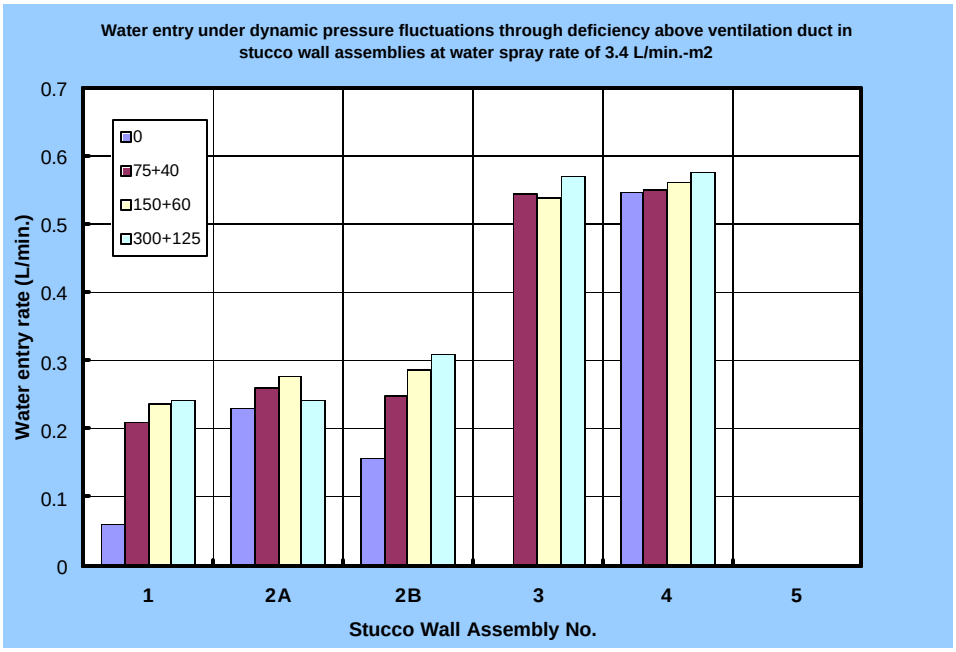

Figure 3.30– Water entry under dynamic pressure fluctuations through deficiency above ventilation duct of stucco wall assemblies at a spray rate of 3.4 L/min.-m^2

3.2.2.6 *SUMMARY*

Results indicate that:

- Substantial amounts of water can enter defects under gravity alone (e.g. WA-2A: 1.3-L/20min. through the deficiency in the electrical outlet).
- An increase in pressure does, in general increase the amount of water entry, but not in a consistent and proportional manner. This suggests that the quantities of water flowing through deficiencies are below the flow capacity of the deficiency.
- Rates of water entry through the electrical outlet vary, for both spray rates, according to the static pressure difference across the wall assembly; as well, at a given pressure greater rates of water entry are achieved at the higher precipitation rate.
- Equivalent amounts of water pass through the deficiency in the ventilation duct in comparison to that of the electrical outlet.
- Water entry is dependent on the nature of water deposition at the deficiency proper, further suggesting that the deficiency above the electrical outlet has a greater direct water deposition than that of the deficiency at the ventilation duct.
- Values for water entry rate at the window are in the same order of magnitude as those obtained for either the electrical outlet or ventilation duct.
- For either type of deficiency, the dependence of water entry over a change in pressure differential is not as significant as that for variations in spray rate.
- Water entry through deficiencies in WA-5 is dissimilar to other walls because this wall has a 10-mm cavity between the cladding and the inner wall sheathing. Consequently, water passing the cladding has a greater chance of collecting in this cavity and being drained from the assembly through openings at its' base than it has of crossing the gap and entering openings in the 2nd line of defence.

This last statement is demonstrated in Figure 3.30 that shows sectional views at the height of the electrical outlet of WA-5 (a) and a generic wall assembly (b) representative of the remaining walls. In the case of WA-5, and consistent with test results, the notional path for water entry is shown to primarily collect in the drainage cavity, with little or no water passing the opening in the sheathing board. This suggests that only in extreme events would water likely cross the opening.

The other wall assemblies have no such cavity into which water may drain, nor a gap over which water must pass to enter the stud cavity. Consequently in extreme rainfall events, most, if not all, of the water entering the deficiency will likely find its way into the cavity.

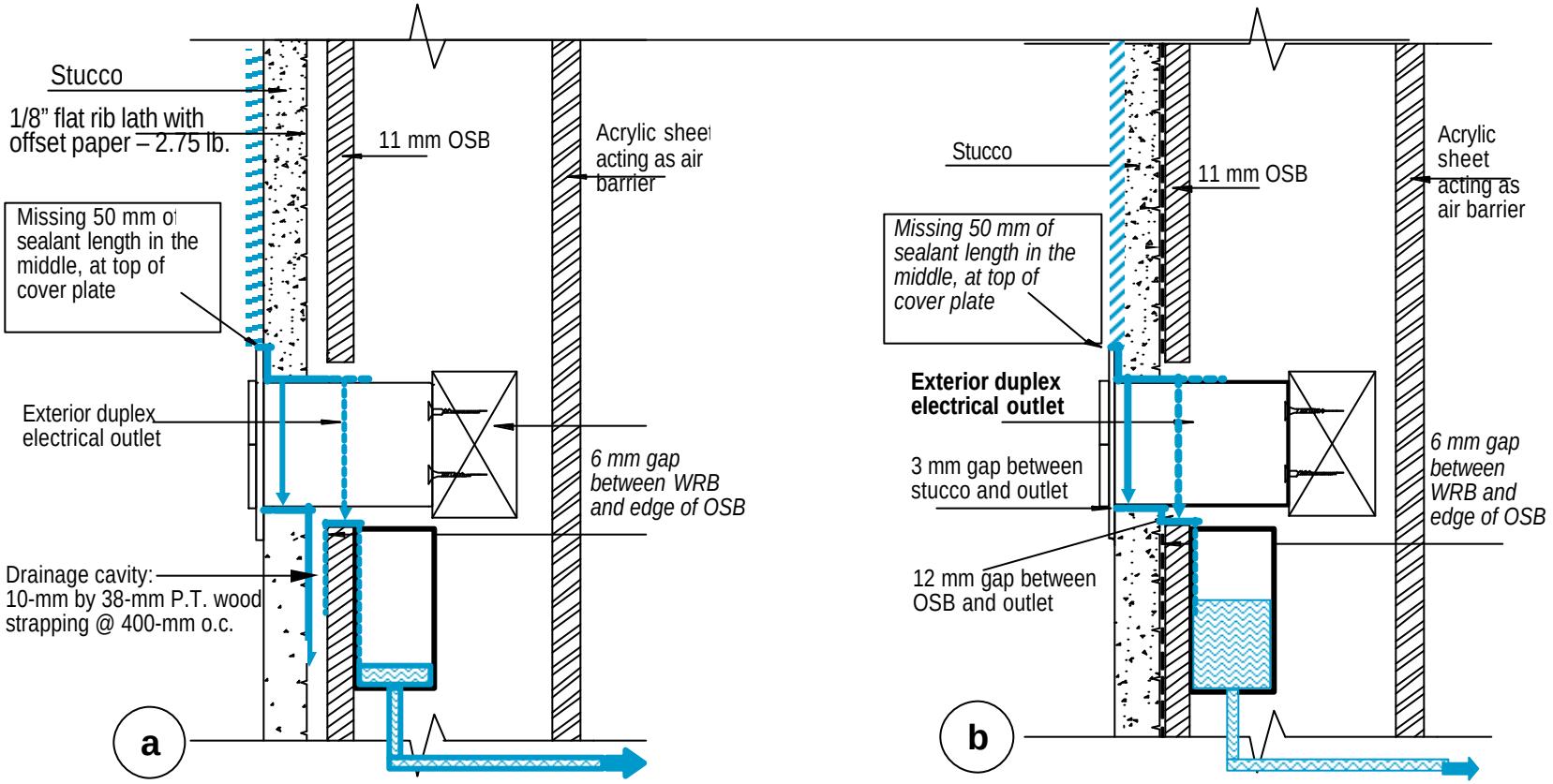

Figure 3.31– Sectional views representative of (a) WA-5, having a 10-mm drainage cavity, and (b) the other stucco wall assembly types showing the notional path of water entry through a deficiency above the electrical outlet.

Chapter 4

Results from EIFS Wall Assemblies

TABLE OF CONTENTS

— Chapter 4 —

Results from EIFS Wall Assemblies

LIST OF FIGURES

LIST OF TABLES

CHAPTER OVERVIEW

MEWS methodology incorporates the performance testing and characterisation of full-scale wall assemblies to determine air leakage, dynamic response, water-tightness performance and water entry characteristics for each of the wall cladding types being evaluated in this study.

Performance tests were used to qualify the degree to which wall assemblies were able to maintain their watertight integrity when being subjected to static or dynamic pressure differentials concurrent with water spray using the dynamic wall test facility (DWTF). This series of tests were similar those currently used in industry to assess the likelihood of water penetration under extreme simulated climatic conditions and were conducted at levels comparable to, or in excess of, current industry standards.

Water entry assessments were used to determine the quantities and rates of water that might enter deficiencies of known type, size and location on the cladding when subjected to simulated climatic extremes, likewise using the DWTF. Levels of water spray and pressure differential were consistent with related climatic data of rainfall and wind speed that might occur in an extreme climatic event within a 10 year period in North America. This information provided a basis for a systematic and consistent means of transferring input to hygIRC, the model used in the MEWS parametric studies.

In this test series, five (5) different types of EIFS-clad wall assemblies were subjected to performance and water entry assessments tests that included testing under different pressure differentials across the assembly and varying rates of water sprayed onto the cladding surface. Tests were completed in conformance with a protocol derived explicitly for this study and provided in Chapter 1 (T6-02-R8).

Results for water penetration trials show that:

- Water entry about inherent (non-specified) deficiencies in the cladding at the electrical outlet and window penetration; no penetration was observed at the ventilation duct.
- Certain walls did not exhibit any signs of water penetration into the stud cavity (WA-8 and WA-9); WA-8 is a dual barrier wall using vertical grooves in the adhesive layer to aid the drainage process; WA-9 uses grooves in the EPS to help achieve the same result.
- Water entry about the window penetration occurred in three of the five wall assemblies and at pressure levels well in excess (i.e. 500 and 1000 Pa) of the rated window performance (300 Pa).
- Water penetration was observed between sheathing boards of WA-6, in the stud cavity beneath the ventilation duct; the duct is the likely source of water entry.
- Irrespective of whether water was observed to enter the stud cavity at through-wall penetrations (i.e. window, ventilation duct and electrical outlet) on the basis of results obtained from the moisture sensors, water was present in the EPS and in the sheathing board.
- Most of the activity occurred in sensors located beneath the windows; this is consistent with water penetration at the window corners in three of five wall assemblies.
- WA-7 appeared to be most affected by water penetration in the bulk of the wall cladding; 29 of 40 sensors lit over the course of the test and the conditions in which they were activated suggests that this wall assembly is most susceptible to water penetration under these test conditions.

- WA-8 also had a number of sensors activated (19/40) over the course of the test although most of these occurred in the final performance test in which the specimen is subjected to a continuous water spray under pressure differential for 16 hours; this suggests that the process of water penetration and migration continues even under less severe conditions.
- WA-10 had a limited number of sensors activated (6) in particular sensors located beneath the window; results are consistent with that observed from water entry about the window.
- WA-6 had the least number of sensors activated; the activation of these sensors is consistent with that observed from water entry points between sheathing boards, about the ventilation duct and window penetrations.
- WA-9 did not have any sensors activated; this suggests that this wall assembly as compared to the other EIFS wall assemblies is the least susceptible to water penetration under these specific test conditions. Furthermore, the results appear to suggest that for this drained screen wall assembly the vertical grooves in the EPS insulation provided some drainage from the sheathing membrane when subjected to these test conditions.

Results for assessments of water entry through specified deficiencies reveal that:

- Water entry through specified deficiencies about the electrical outlet was evident for all Stages in WA-7 and -9 and in Stage 5 for WA-10; no water entry was recorded for WA-6 and WA-8.
- The range of values obtained for rates of water entry related to the electrical outlet in the EIFS-clad assemblies are in the same order as those obtained for stucco walls. The range of values is comparable; ca. 0.1 L/min. for EIFS walls assemblies exhibiting water entry as compared to ca. 0.12 L/min. for stucco-clad wall assemblies. Values range between 0.075 L/min. to 0.167 L/min. for EIFS whereas for stucco wall assemblies values ranged between 0.053 L/min. and 0.17 L/min.
- As was found in the case of stucco-clad walls, water entered through specified deficiencies under gravity alone, i.e. instances when there was no driving pressure across the assembly
- Rates of entry for the electrical outlet are primarily dependent on the amount of water deposited on the wall; increased rates of entry were evident for corresponding increases in rates of water sprayed onto the cladding surface.
- In the case of WA-8, for which water entering through the specified deficiency about the electrical outlet did not collect in the stud cavity, the likely path of water subsequent to entry was drainage between the adhesive layer and water-resistant barrier (polymer cement coating) down through vertical channels located in the adhesive.
- No water entry was observed through the specified deficiency about the ventilation duct for WA–8, in Stage 5 (sealant and backer rod in place) of WA-9 and in Stages 5 and 7 (no sealant or backer rod in place) of WA-10.
- Rates of entry for the specified deficiency about the ventilation duct are primarily dependent on the amount of water deposited on the wall; increased rates of entry were evident for corresponding increases in rates of water sprayed onto the cladding surface.
- Similar rates of water entry at the specified deficiency about the ventilation duct were found for EIFS walls as compared to results derived from tests on stucco walls.
- For water entry thought the specified deficiency about the vertical joint, none entered the joint in WA–6 or –8; water entry results were obtained for all other wall assemblies.
- For assemblies having water entry about the specified deficiency at the vertical joint, rates of entry were dependent on pressure differences across the assembly
- With the exception of WA–6, no water was collected about windows for any of the other wall assemblies.

4.1 Introduction

A series of five EIFS walls (Nos. 6, 7, 8, 9 & 10) were constructed and subsequently tested for water penetration trials and entry assessments using the dynamic wall test facility. Details regarding the fabrication of the specimens, material specifications and specified deficiencies are provided in Appendix A. An overview of the different specimens showing the key components of the wall assemblies is provided in Table 4.1 below.

This report provides results of water penetration (Stages 2 and 3) and water entry (Stages 5, 6 and Stage 7 – previously 4) tests on EIFS wall assemblies according to the test protocol described in Chapter 1. A summary of the test protocol is provided below as well as a description of the test specimen, parameters and set-up used in the test. Specifically, details regarding the location of pressure taps, of moisture sensors, of water entry points at specified deficiencies and means of water collection are outlined in the section on test specimens.

4.1.1 TEST SPECIMENS

The test configuration showing the location of pressure taps, moisture sensors, and water entry points at specified deficiencies are provided below in Figures 4.1 to 4.3 respectively.

4.1.1.1 PRESSURE TAPS

Pressure taps are located in six wall portions (Figure 4.1), with the first portion located at the left extremity of the wall (facing the weather-side). Typically in each portion, taps are located both in the wall cavity between the stucco and the sheathing and in the stud space. Additionally, taps have been added to obtain measurements of pressure differential at points of water entry.

4.1.1.2 AIR BARRIER SYSTEM LEAKAGE

Air barrier system (ABS) leakage was regulated by introducing a series of 7-mm diameter holes in the ABS (Figure 4.1), a series of seven (one in each stud cavity) representing an equivalent leakage area (ELA) of 269-mm^2, providing a nominal wall assembly leakage of 0.2 L/s-m^2. A wall assembly leakage of 0.5 L/s-m^2 (ELA 808-mm^2) was achieved using twenty-one holes of the same diameter, three in each stud cavity. The desired nominal leakage through the wall assembly was achieved by “opening” or “closing” the appropriate number of holes in the ABS

Table 4.1 – Wall assembly types and key wall components

WA	Wall Type	Drainage Mechanism	Insulation Attachment	Water Resistive Barrier	Sheathing
6	Barrier wall + source drainage at window	Proprietary engineered sill	Latex acrylic adhesive	None	OSB (11-mm)
7	Dual barrier wall	None	Galvanized steel fasteners and polypropylene washers	60 min. building paper	OSB (11-mm)
8	Dual barrier wall + source drainage at window	Sill drip flashing	Polymer cement adhesive	Polymer cement coating	Glass mat gypsum board (12-mm)
9	Drained screen wall	6 x 30-mm vertical grooves @ 300-mm o.c. in EPS insulation	Polymer cement adhesive	Polymer cement coating	Glass mat gypsum board (12-mm)
10	Drained screen wall	3-mm nylon drainage mat	Galvanized steel fasteners and polypropylene washers	Non-cementitious moisture barrier coating	OSB (11-mm)

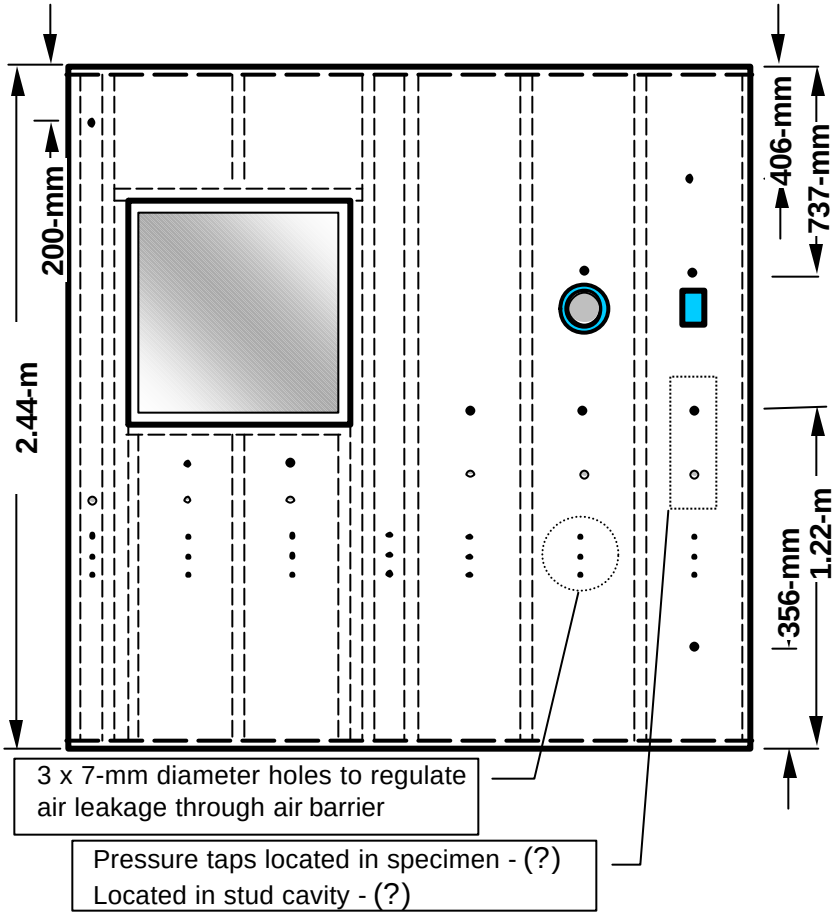

Figure 4.1 - Location of pressure taps and air leakage openings.

4.1.1.3 Moisture sensors in sheathing board

The location of moisture sensors is shown in Figure 4.2. A total of forty (40) moisture pin pairs have been imbedded in the specimen. Sixteen (16) pin pairs have been placed in the sheathing board to ½ the sheathing thickness (e.g. see schematic, Fig. 4.2; green icons) at locations where either water might first accumulate or at the base of the wall. A further 16 pairs have nominally been placed at the interface between the EPS insulation board and the water resistive barrier (yellow icons). The remaining eight (8) pairs have been imbedded in the EPS insulation board, of which four (4) have been imbedded to ½ the thickness of the board (red icons) and final group of four (4) have been placed at the interface between board and the finish coat (black icons).

The sensors are calibrated such that a light diode, located between the pairs of pins, is activated if the moisture content in the OSB reaches or exceeds ca. 14%. Over a test period, note is taken of the time and conditions under which the light is first activated.

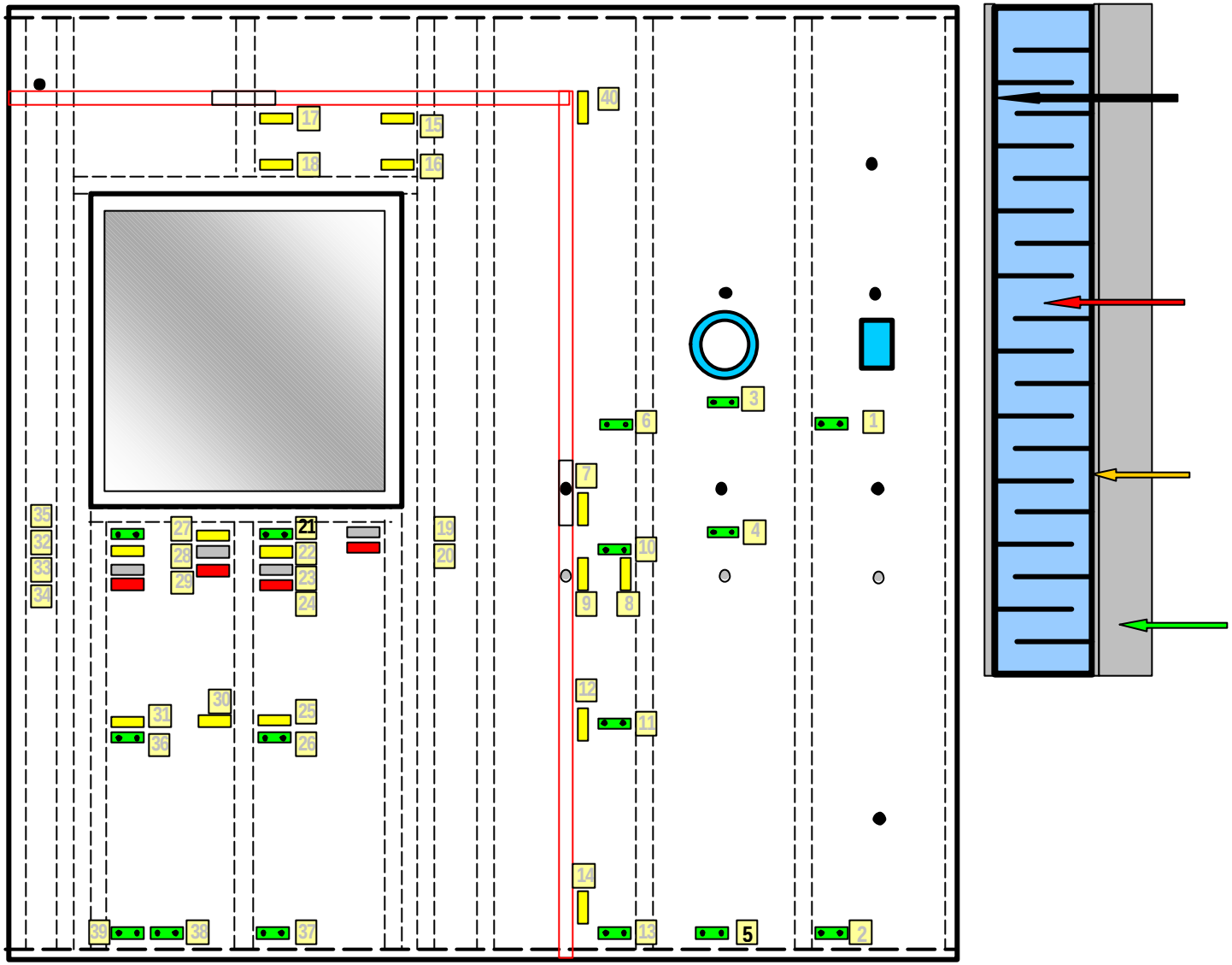

Figure 4.2 - Location of moisture sensors

4.1.1.4 WATER ENTRY POINTS AT SPECIFIED DEFICIENCIES

Water entry points at specified deficiencies (Figure 4.3), representative of those typically found at the joint seal located at the interface between wall components, are located in the following areas:

- Above the electrical outlet – a nominal 50-mm length of sealant is missing between the outlet cover and the wall.
- Above the ventilation duct – a nominal 50-mm length of sealant is missing between the duct and the wall.
- Below the window sill and between finishing strips – a 50-mm length of sealant is missing between the ending strips.
- Along the horizontal joint located above the window and mid-way between joint extremities – a 90-mm length of sealant is missing
- Along the vertical joint located mid-height between joint extremities – a 90-mm length of sealant is missing

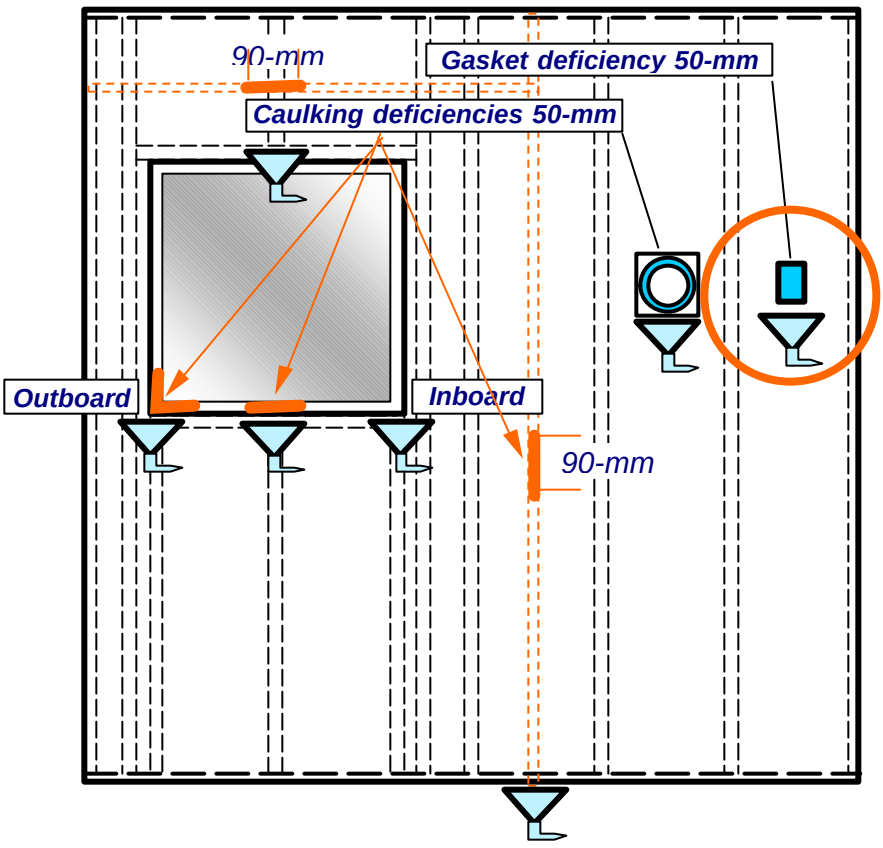

Figure 4.3 - Location of water collection points at specified deficiencies and collection troughs

4.2 Results

Results from water penetration trials (Stages 2 and 3) are presented in section 4.2.1 and water entry (Stages 5 to 7 - previously 4) in section 4.2.2. Water penetration tests on EIFS-Clad Walls – Stage 2. Note that water penetration trials do not include specified deficiencies in the wall specimen whereas these are part of the assessment protocol for water entry tests. When reference is made in this chapter to “deficiencies”, in all instances this is referring to specified deficiencies.

4.2.1 WATER PENETRATION TRIALS - INTRODUCTION

Performance tests were used to qualify the degree to which wall assemblies were able to maintain their watertight integrity when being subjected to static or dynamic pressure differentials concurrent with water spray using the dynamic wall test facility (DWTF). This series of tests were similar those currently used in industry to assess the likelihood of water penetration under extreme simulated climatic conditions and were conducted at levels comparable to, or in excess of, current industry requirements and standards.

The results obtained during water penetration trials (Stage 2) are essentially qualitative in nature. Observations were made as to where penetration occurs on the inside of the assembly (e.g. around windows, electrical outlet, and ventilation duct or through the sheathing board) and when it occurs over the course of the test sequence. Test conditions (static or mean dynamic pressure differential) when penetration occurs were noted and these provided a benchmark from which comparisons could then be made. Moisture sensors (MS) placed in the sheathing board at specific locations of the wall assembly indicated whether moisture had penetrated beyond the second line of defence. Activated moisture sensors registered lit if the presence of moisture was detected in the close proximity to the sensor.

4.2.1.1 WATER PENETRATION ABOUT THROUGH-WALL PENETRATIONS

An overview of results obtained from water penetration trials is provided in Table 4.2 below. Instances of water penetration are noted for observations of water entry at the window, electrical outlet, ventilation duct and sheathing board. For each instance, test conditions at which the water penetration was observed are provided, in particular the static pressure differential and the time, in minutes, after attaining the stated pressure level. In the case of water penetration at the window, entry at the left (L) or right corner (R) are also labelled.

Of the five EIFS wall assemblies evaluated, WA-8 and WA-9 did not exhibit any noticeable water entry about any of the through-wall penetrations nor through the sheathing board. In

contrast, WA-7 had water entry observed at the window, electrical outlet and through the sheathing board about moisture sensor (MS) No. 8. Water entry was also observed through the sheathing board in WA-6 at the joint between adjacent sheathing panels. WA-6 exhibited entry about either side of the window at ca. 500 Pa pressure difference whereas entry about the window was evident at 1000 Pa pressure difference in WA-10

Table 4.2 - Water penetration trials of EIFS WA-6 to WA-10 (no deficiencies)
Observed entry at window, electrical outlet, ventilation duct or sheathing board

WA	Window	Electrical outlet	Ventilation duct	Sheathing board
6	L-500 Pa @ 4 min. / R-500 Pa @ 4 min.	**NIL**	**NIL**	300 Pa at joint between sheathing panels
7	R-500 Pa / L-1000 Pa	300 Pa @ 1 h 10 m	**NIL**	150 Pa @ MS-8
8	**NIL**	**NIL**	**NIL**	**NIL**
9	**NIL**	**NIL**	**NIL**	**NIL**
10	R-1000 Pa	**NIL**	**NIL**	**NIL**

WINDOWS — It is useful to note that for this series of penetration trials, most of the observed entry points occurred about the window as opposed to entry about the electrical or ventilation duct. Three of the five wall assemblies exhibited water entry at either window corner, although, notably, these occurrences were observed at pressure differences well in excess (i.e. = 500 Pa) of the rated window performance of 300 Pa. Entry was observed at 500 Pa pressure difference in WA-6 (L and R) and WA-7 (R) whereas entry occurred at 1000 Pa pressure difference in WA-7 (L) and WA-10 (R).

ELECTRICAL BOX AND VENTILATION DUCT — No water entry was observed to occur about the ventilation duct and only WA-7 had noticeable water entry about the electrical outlet. In the later instance, entry occurred at a 300 Pa pressure differential. Entry about these locations is not expected given that the joint at their interfaces should be properly sealed. However entry evidently does occur regardless of the efforts made to seal the joints at the exterior of these penetrations and this is indicative of how difficult it is to insure absolute water-tightness when face-sealing cladding.

EVIDENCE OF WATER PENETRATION OF SHEATHING BOARD — Water penetration through the wall proper, i.e. beyond the second line of defence was evident in WA-7 at MS-8 (middle stud cavity at mid-height of wall and adjacent to vertical joint; see Fig. 4.2). Penetration was also observed in WA-6 in the stud cavity below the ventilation duct at the joint between adjacent

sheathing panels. Penetration commenced at a static pressure difference of 300 Pa and continued throughout the remaining portion of the static test.

4.2.1.2 WATER PENETRATION AS OBSERVED FROM RESULTS FROM MOISTURE SENSORS

A summary of results from moisture sensors is provided in Tables 4.3 and 4.4 below with additional information regarding results of WA-7 at different static pressures provided in Table 4.4. For each wall specimen, information is given on the whether a specific sensor lit during a particular test sequence, be it under static, dynamic or over the continuous water spray period of 16 hours. Pressure levels at which sensors lit also are provided.

Table 4.3 - Water penetration trials of EIFS WA-6 to WA-10: Observed activation of moisture sensor lights

Wall Assembly	Static	Dynamic	16-hour continuous
WA-6	#4 @ 500 Pa	#11, 14, 21 @ 300 ± 150 Pa	#'s 3, 19
WA-7	Multiple - see below	#'s 9 ,11, 12, 15, 17, 18 @ 700 ± 300 Pa	No additional lights
WA-8	#'s 19, 22, 30 @ 500 Pa #'s 20, 37, 38 @ 1 kPa	#'s 21, 39 @ 75 ± 40 Pa # 35 @ 150 ± 60 Pa	#'s 1, 2, 4, 10, 12, 13, 17, 32, 33, 36
WA-9	None	None	None
WA-10	# 13 @ 150 Pa # 20 @ 300 Pa	# 6 @ 300 ± 150 Pa # 23, 24, 28 @ 700 ± 300 Pa	#29

There is no possibility for the wall to dry out in the period between test sequences. Hence, sensor numbers are only given once since once they are lit, they remain so given that the test sequences follow one another from static to dynamic and then to the continuous sixteen (16) hour spray.

For WA-6, under static conditions, only MS-4 was activated – this is the sensor in closest proximity to the point of water entry between adjacent sheathing panels (refer to Figure 4.2) in the stud cavity beneath the ventilation duct. Under dynamic conditions, a further 3 sensors activated; MS-11, -14, and –21 at the 300 ± 150 Pa pressure level. Both sensors 11 and 14 are adjacent to the vertical joint possibly indicating some water entry about unidentified deficiencies along its' length. However, no other sensors were activated in proximity to the joint at higher pressure levels hence this evidence can not be considered conclusive. Evidence that moisture may be present beneath the window is indicated by MS-21 and as well, MS-19 that activated over the course of the 16-hour continuous test. MS-3 also activated during the 16-hour continuous test and this is consistent with observations of water entry about the ventilation duct.

As mentioned previously, details regarding the time and test conditions for moisture sensor activation over the course of testing WA-7 are provided in Table 4.4. Of the 40 moisture sensors used in the penetration tests, 23 were activated over the course of the static tests alone, a further six during the dynamic sequence, for a total of 29 activated sensors. Of these, all four sensors, nominally located at the interface between the expanded polystyrene (EPS) and the exterior finish (Fig. 4.2; re: black icons in closest proximity to the front of the EPS), activated either in the initial stages of the test (pressure difference 75 Pa) or the following stage carried out at 150 Pa (see Table 4.4). Likewise, all sensors located in the bulk of the EPS (red icons, Fig. 4.2) activated; two at 75 Pa pressure difference (MS-24, -34) and the remaining two at 500 Pa. (MS-20, -29). The location of the sensors and the time and conditions under which they were activated suggest that beneath the window there exist paths for water entry to the interstitial spaces between adjacent EPS panels. The movement of water is aided by increased pressure differences. That is, an additional number of sensors are activated as the pressure differential is increased. Twelve of the 13 sensors located directly beneath the window were activated over the course of the static test, of which 5, 3, 2 and 2 were sensors activated at pressure levels of 75, 150, 300 and 500 Pa respectively.

Table 4.4 - Water penetration static trials EIFS WA-7: Observed moisture sensor lights

Pressure difference	Black (19, 23, 28, 33)	Red (20, 24, 29, 34)	Yellow			Green
			J-V	J-H	W	
75 Pa	23, 33	24, 34			32	
150 Pa	28, 19		14		31, 38(b)*	35
300 Pa			8, 12		22, 27, 30	
500 Pa		20, 29			25	2(b), 5(b), 6
1000 Pa					39(b)	

- (**b**) – sensor located at **b**ase of wall

Over the course of the dynamic test, an additional 6 sensors were activated (Table 4.3) all of them at the most severe pressure fluctuations, i.e., 700 ± 300 Pa. These were sensors located in proximity to either the vertical (e.g. MS-9, -11, -12) or horizontal joints (e.g. MS-15, -17, -18) suggesting that such joints are most vulnerable to the imposed deficiencies when subjected to severe climatic conditions. No additional sensors were activated during the 16-hour test.

For WA-8, in which there were no observed points of water entry about the electrical outlet, ventilation duct or window, a total of 19 sensors were activated; 6 over the course of the static tests, a further 3 during the dynamic tests and the remaining 10 occurred from continuous

testing over the 16-hour period. The results suggest that water is present at the interface between the sheathing membrane and sheathing board. Over the course of the static test MS-19 (black icon), -22 (yellow), and –30 (yellow) were activated at 500 Pa pressure difference and MS-20 (red), -37 (green), and -38 (green) at 1000 Pa. All sensors are located in the stud cavities beneath the window. Sensors MS-19 and 20 are in proximity to one another and are located beneath the right corner (facing specimen) of the window; MS-22 is also located beneath the window (refer to Fig. 4.2). Sensor MS-30 is located mid-way between the wall base and the underside of the window and MS-37 and 38 are both located at the base of the wall. The activation of MS-37 and –38 is due to water ingress at the base of the wall at high pressure differentials.

Under dynamic conditions, three additional sensors were activated: MS-21 and -39 at 75 ± 40 Pa and MS-35 at 150 ± 60 Pa. MS-21 is located beneath the window and adjacent to MS-22 whereas MS-39 is situated at the base of the wall in proximity to MS-38 and in the stud cavity beneath the window. Hence the patterns for moisture penetration are consistent with that observed from the static tests in that those areas that showed indications of moisture penetration in the initial test sequence provided similar evidence of moisture penetration in dynamic tests.

Results from the 16-hour continuous spray for WA-8 indicated that a good number of additional sensors were activated in contrast to the other wall specimens tested in this series (Table 4.3); here 10 more sensors were activated over the course of the test as compared to 2 sensors for WA-6, 1 sensor for WA-10 and none for the remaining two wall specimens.

For WA-9, no sensors were activated in any of the tests sequences and neither was any water observed to enter about the electrical outlet, ventilation duct or window. This suggests that this wall assembly as compared to the other EIFS wall assemblies is the least susceptible to water penetration under these specific test conditions. The results appear to further suggest that for this drained screen wall assembly the vertical grooves in the EPS insulation provided some drainage from the sheathing membrane when subjected to these test conditions.

In the case of WA-10, only two sensors were activated during the static test sequence; MS-13 (green-in sheathing board) at 150 Pa and MS-20 (red-in EPS) at 300 Pa. Sensor MS-13 is located at the base of the wall in the stud cavity in which there is a vertical joint (Fig. 4.2). Sensor MS-20 is located beneath the right window corner (facing specimen) and this assembly is noted to be one that experienced penetration about the window at this location, albeit at much higher pressure levels. It appears that this particular result is consistent with that observed over the course of the static test. However, in the case of MS-13 it is not evident that moisture is due

to entry at the wall base exclusively given that no other sensors located in the base of the wall were activated over the course of this or any other test sequence.

Under dynamic conditions, a series of four (4) sensors were activated; MS-6 (green) at 300 ± 150 Pa and MS-23 (black), -24 (red), and –28 (black) at 700 ± 300 Pa. The sensor MS-6 is located in proximity to the vertical joint but above the deficiency whereas MS-23, -24 and –28 are located in the stud cavities beneath the window. For sensors located beneath the window results are consistent with that observed from the static test (MS-20) noted above. Water nominally entering about window corners is being forced along interstitial spaces between adjacent EPS panels.

The only sensor activated over the course of the 16-hour test sequence was MS-29 (red), adjacent to MS-28 (black) located in the stud cavities beneath the window. This result appears consistent with that observed in the previous tests.

4.2.1.3 SUMMARY OF RESULTS – WATER PENETRATION

- Water entry was observed about inherent openings (imperfections) in the cladding at the electrical outlet and window penetration; no penetration was observed at the ventilation duct.
- Certain walls did not exhibit any signs of water penetration into the stud cavity (WA-8 and WA-9); WA-8 is a dual barrier wall using vertical grooves in the adhesive layer to aid the drainage process; WA-9 uses grooves in the EPS to help achieve the same result.
- Water entry about the window penetration occurred in three of the five wall assemblies and at pressure levels well in excess (i.e. > 500 Pa) of the rated window performance (300 Pa).
- Water penetration was observed between sheathing boards of WA-6, in the stud cavity beneath the ventilation duct; the duct is the likely source of water entry.
- Irrespective of whether water was observed entering the stud cavity at through-wall penetrations, based on results from moisture sensors water was present in the EPS, and in the sheathing board.
- Most of the activity occurred in sensors located beneath the windows; this is consistent with observed water penetration at the window corners in three of five wall assemblies.
- Of the five EIFS wall assemblies tested, WA-7 appeared to be most affected by water penetration in the bulk of the wall cladding; 29 of 40 sensors activated over the course of the test and the conditions in which they were activated suggests that this wall assembly is most susceptible to water penetration under these test conditions.
- WA-8 also had a number of sensors activated (19/40) over the course of the test although most of these occurred in the final performance test in which the specimen is subjected to a

continuous water spray under pressure differential for 16 hours; this suggests that the process of water penetration and migration continues even under less severe conditions.

- WA-10 had a limited number of sensors activated (6) in particular sensors located beneath the window; these results are consistent with observations of water entry about the window.
- WA-6 had the least number of sensors activated; the activation of these sensors is consistent with that observed from water entry points between sheathing boards, about the ventilation duct and window penetrations.
- WA-9 did not have any sensors activated; this suggests that the wall assembly is the least susceptible to water penetration under these specific test conditions. Furthermore, the results appear to suggest that for this drained screen wall assembly the vertical grooves in the EPS insulation provided some drainage from the sheathing membrane when subjected to these test conditions.

4.2.2 WATER ENTRY ASSESSMENTS THROUGH SPECIFIED DEFICIENCIES

4.2.2.1 INTRODUCTION

Water entry assessments were used to determine the quantities and rates of water that might enter specified deficiencies of known type, size and location on the cladding when subjected to simulated climatic extremes, likewise using the DWTF. Levels of water spray and pressure differential were consistent with related climatic data of rainfall and wind speed that might occur in an extreme climatic event within a 10 year period in North America. This information provided a basis for a systematic and consistent means of transferring input to hygIRC, the hygrothermal model used in the MEWS simulation studies. Note that when reference is made to “deficiencies”, in all instances this is referring to specified deficiencies.

An overview of the results obtained from water entry assessments for WA-6 to WA-10 for the various assessment stages (i.e. stages 5 to 7) is provided in Table 4.5. The differences between stages are evident from the way in which the joint between the ventilation duct and wall cladding is configured. Specifically, Stage 5 incorporates a joint having both a backer rod and sealant surrounding the periphery of the duct with the exception of a 2-mm by 50-mm opening located at the underside of the joint. The backer rod is placed between the sheathing board and duct and the sealant bead is then applied around the periphery of the duct. An opening of appropriate size is then cut at the underside of the duct. This opening permits the passage of air however, the passage of water may in certain instances be reduced. Stage 6 is an intermediate stage in which the sealant has been removed and the joint between the duct and sheathing board has simply the backer rod in place. Stage 7, is equivalent to the previously

reported results from Stage 4 assessments on stucco clad walls. This is the stage where there is neither sealant nor backer rod in place.

General trends as to the changes in rate of entry in relation to increases in spray rate or static differential pressure (ΔP_s) are also noted. For the purposes of this work, it was deemed acceptable to generate what trends could be discerned based on these results given the time and resources available to carry out the work.

Water entry through deficiencies about the electrical outlet (Table 4.5, col. **E**) was evident for all Stages in WA- 7 and -9 and in Stage 5 for WA-10. No water entry was recorded for WA-6 and WA-8. In instances where water entry was observed in all stages (i.e. WA-7 and –9), rates of entry in relation to static pressure differential are provided in §4.2.2.2. Whereas in the case of WA-8 in which no water entered the electrical outlet, suggestions are provided regarding the likely path of water flow based on observations made over the course of the test.

For results derived from water entry through deficiencies about the ventilation duct, no water entry was observed for WA-8, in Stage 5 of WA-9 and in Stages 5 and 7 of WA-10. Information regarding the rates of water entry in relation to pressure differentials across the assembly is provided for WA-6, -7 and -9 as well as distinctions between results obtained in stages 5 and 7 of the assessment trials.

In regards to results obtained for water entry thought the vertical joint, no water entered the joint in WA-6 or –8. Results were obtained in Stage 5 for all other wall assemblies. With the exception of WA-6, no water was collected about windows for any of the other wall assemblies. A summary of the salient points regarding results of these test trials follows the discussion of results on water entry under dynamic pressure fluctuations.

Table 4.5 – Water entry assessments EIFS WA-6 to WA-10: Observed entry at electrical outlet (E), ventilation duct (V), Vertical joint (V-J), or window (W) at given test Stages

WA	Stage	E	V	V-J	Window		
					W-L	W-R	W-S
6	5	NIL	YES	NIL	YES	YES	NIL
	6	NIL	YES	NIL	YES	YES	NIL
	7	NIL	YES	NIL	YES	YES	NIL
7	5	YES	YES	YES	NIL	NIL	NIL
	6	YES	YES				
	7	YES	YES				
8	5	NIL	NIL	NIL	NIL	NIL	NIL
	6	NIL	NIL				
	7	NIL	NIL				
9	5	YES	NIL	YES	NIL	NIL	NIL
	6	YES	YES				
	7	YES	YES				
10	5	YES	NIL	YES	NIL	NIL	NIL
	6	NIL	YES				
	7	NIL	NIL				

4.2.2.2 WATER ENTRY ABOVE ELECTRICAL OUTLET

Results for water entry through a specified deficiency above an electrical outlet are given in Figures 4.4 to 4.6 of which a summary is provided in Tables 4.6 and 4.7. The values in Table 4.6 relate to WA-7 (see Table 4.1: dual barrier wall -no drainage mechanism- with spun bonded polyolefin membrane on 11-mm OSB sheathing) and Table 4.7 to WA-9 (drained screen wall with vertical grooves in EPS having a polymer cement coating membrane on 12-mm glass mat gypsum board).

As provided in Table 4.6 and shown in Figure 4.4, rates of water entry through the deficiency above the electrical outlet for WA-7 at either spray rate are very similar in that the response to increased pressure difference and the range of average values obtained between 0 and 300 Pa is about the same (e.g. Range : 0.052 vs. 0.049 L/min. at 1.7 and 3.4 L/min.-m^2). Slightly lower rates of entry occur at the lower spray rate be they the maximum values or average values attained at 0 and 300 Pa. Increases in rates of water entry in relation to corresponding increases in pressure difference across the assembly are evident at both spray rates. Notably, significant rates of water enter when no pressure is present across the wall. (i.e. 0.181 and 0.200 L/min. at spray rates of 1.7 and 3.4 L/min.-m^2 respectively).

Table 4.6 – WA-7: Water entry rates through deficiency above electrical outlet

Spray *Rate L/min.-m^2*	**Rate of water entry, L/min.**			
	Maximum	*Avg. at 0 Pa*	*Avg. at 300 Pa*	*Range*
1.7	0.254	0.181	0.233	0.052
3.4	0.272	0.200	0.249	0.049

For WA-9 (Table 4.7 and Figure 4.5) rates of water entry are comparatively lower than those of WA-7 at given spray rates and pressure differentials. For example, at a spray rate of 1.7 L/min.-m^2, the maximum water entry rate attained for WA-9 is roughly 4 times lower than the rate observed for WA-7. Similarly, rates of entry for WA-9 under no pressure differential are about 4.5 times less that of WA-7 at either spray rate. As was found for WA-7, rates of water entry at given spray rates increase in relation to corresponding increases in pressure difference across the assembly. However, given the range of values attained between 0 and 300 Pa pressure difference, this response (evident in Figure 4.5) is less evident at the lower (0.015 L/min.) as compared to the higher spray rate (0.069 L/min.).

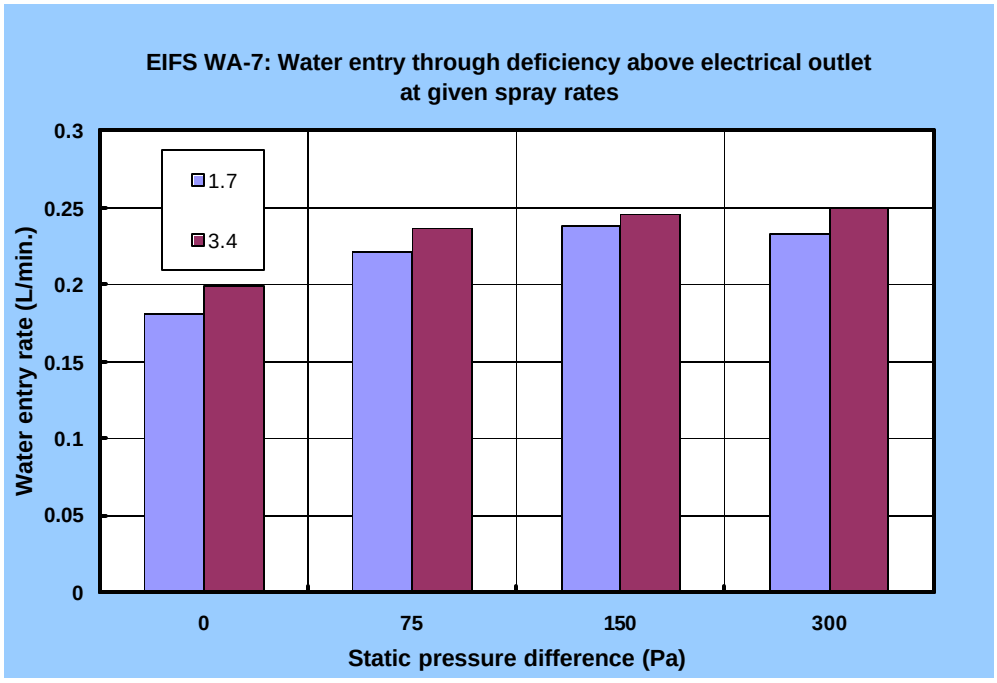

Figure 4.4 – EIFS WA-7 : Water entry under static pressure differential through deficiency above electrical outlet

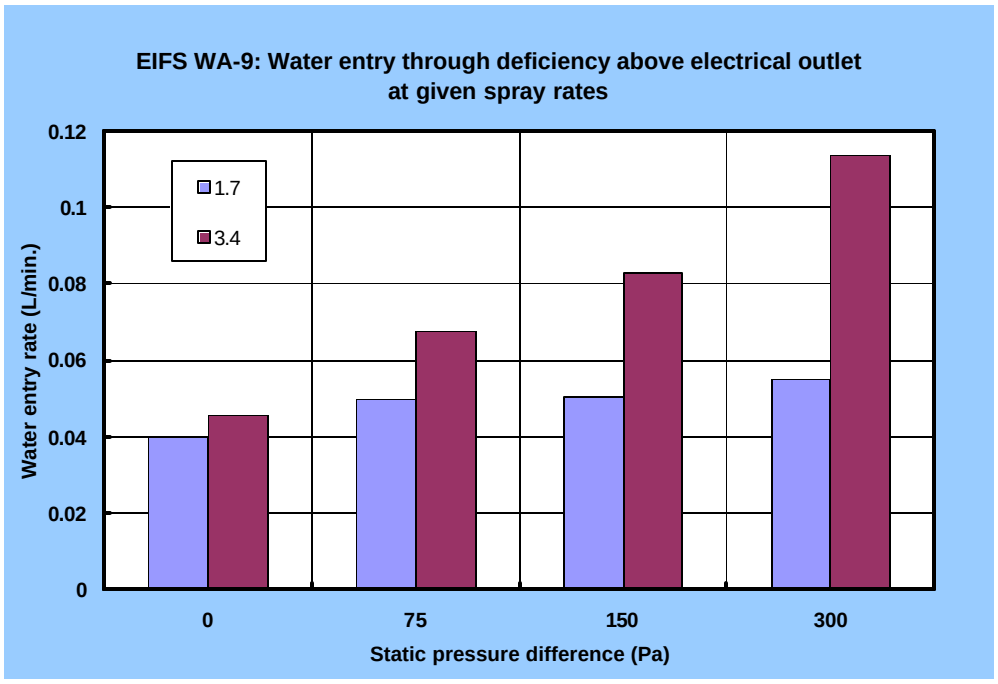

Figure 4.5 – EIFS WA-9 : Water entry under static pressure differential through deficiency above electrical outlet

Table 4.7 – WA-9: Water entry rates through deficiency above electrical outlet

***Spray** Rate L/min.-m^2*	**Rate of water entry, L/min.**			
	Maximum	*Avg. at 0 Pa*	*Avg. at 300 Pa*	*Range*
1.7	0.063	0.040	0.055	0.015
3.4	0.123	0.045	0.114	0.069

As was noted previously, no water was collected about the electrical outlet for WA-8. However, water was nonetheless observed to be entering through the deficiency above the outlet and draining in between the EPS and sheathing membrane (polymer cement coating) apparently down through vertical grooves formed in the adhesive layer (polymer cement coating). Figure 4.6 shows the stud cavity in which is located the water collection trough for the electrical outlet at an instance, over the course of the test, where drainage was observed to occur between EPS insulation and membrane.

It is not possible to estimate what quantities of water may have been drained at the interface, however it is certain that water was present at the interface given the previously reported results from penetration tests and as noted above, the observations made during the water entry assessments.

Figure 4.6 – EIFS WA-8 : Water entering through deficiency above electrical outlet but draining between gypsum board and EPS insulation.

4.2.2.3 WATER ENTRY ABOVE VENTILATION DUCT

Results for rates of water entry through deficiencies above a ventilation duct were obtained for WA-6, -7 and -9 for which results are presented in Figures 4.9, 4.10 and 4.13 respectively. It is worthwhile noting once again (re: Table 4.5) that no water entered the deficiency above the ventilation duct of WA-8 and in the case of WA-10 entry only occurred in Stage 6 (no sealant at the duct-sheathing board interface – backer rod in place). In Stage 7 for this wall assembly (WA-10: no sealant or backer rod in place), water entered the deficiency but was drained by and down the mesh; hence, no water was collected in this stage for WA-10.

An overview of results is provided in Tables 4.8 to 4.10.

Table 4.8– EIFS Stage 5: Water entry rates through the deficiency above the ventilation duct at given spray rates for WA-6, -7 and -9.

Spray Rates *L/min.-m²*	**Rate of water entry, L/min.**			
	Max. at 0 Pa	*Max. at 300 Pa*	*Range*	
1.7	0.083	0.140	0.057	
3.4	0.066	0.218	0.152	

Table 4.9 – EIFS Stage 6: Water entry rates through the deficiency above the ventilation duct at given spray rates for WA-6, -7 and -9.

Spray Rates *L/min.-m²*	**Rate of water entry, L/min.**			
	Max. at 0 Pa	*Max. at 300 Pa*	*Range – Min.*	*Range – Max.*
1.7	0.064	0.116	0.002	0.052
3.4	0.060	0.220	0.013	0.160

Table 4.10– EIFS Stage 7: Water entry rates through the deficiency above the ventilation duct at given spray rates for WA-6, -7 and -9.

Spray Rates *L/min.-m²*	**Rate of water entry, L/min.**			
	Max. at 0 Pa	*Max. at 300 Pa*	*Range – Min.*	*Range – Max*
1.7	0.133	0.180	0.0206	0.133
3.4	0.154	0.281	0.05	0.137

The following was noted:

- Water enters when no driving pressure is applied across the wall assembly (i.e. at a $?P_S = 0$ Pa) in all stages, although greater rates of entry occur when no barriers to entry are present at the interface between the ventilation duct and sheathing board (Stage 7). Maximum values for rates of water entry at 0 Pa are essentially the same for Stages 5 and 6. For example, 0.066 and 0.060 L/min. at a spray rate of 3.4 L/min.-m^2 for Stages 5 and 6 respectively as compared to 0.154 L/min. in Stage 7.
- Maximum values attained at 300 Pa $?P_S$ at the given spray rates are comparable although the highest rates were attained in Stage 7 for which there are no barriers to water entry. This suggests that entry is limited by the size of the deficiency above the ventilation duct and not by the barrier at the interface between the ventilation duct and the sheathing board.
- The range of values (difference in results obtained at 0 and 300 Pa ?P) are lower at lower spray rates; this is in keeping with the observation that entry is limited by the size of the deficiency.

WA-8 — For those walls not exhibiting any water entry, as in the case of WA-8, evidence of where water drained is provided in Figure 4.7 below. This figure shows water coming through the deficiency and draining between the sheathing board (glass mat gypsum) and the insulation. The grooves provided by the application of a cementitious coating using a notched trowel offer vertical drainage paths into which water can flow.

Figure 4.7 – EIFS WA-8 : Stage 7 - at test initiation, water coming through deficiency above ventilation duct and slowly draining between glass mat gypsum board and insulation

A schematic of this effect is provided in Figure 4.8. It shows the entry point for water at the deficiency (located above the ventilation duct) and the presumed path for water entry and drainage. Note that the figure below represents Stage 5 and in this configuration, the backer rod and sealant form the joint between the ventilation duct and sheathing board. The lines and arrows drawn in the figure suggest that the path for water entry is blocked by the sealant and backer rod and that the only means of drainage is down vertical grooves formed in the cementitious adhesive layer that is used to bind the EPS to the assembly. This layer forms the interface between the EPS and the weather resistive barrier, a barrier prepared using a polymer cement coating. In fact water will always find the path of least resistance. Hence even without the sealant or backer rod in place (i.e. Stage 7), water drained down vertical grooves as was shown in Figure 4.7.

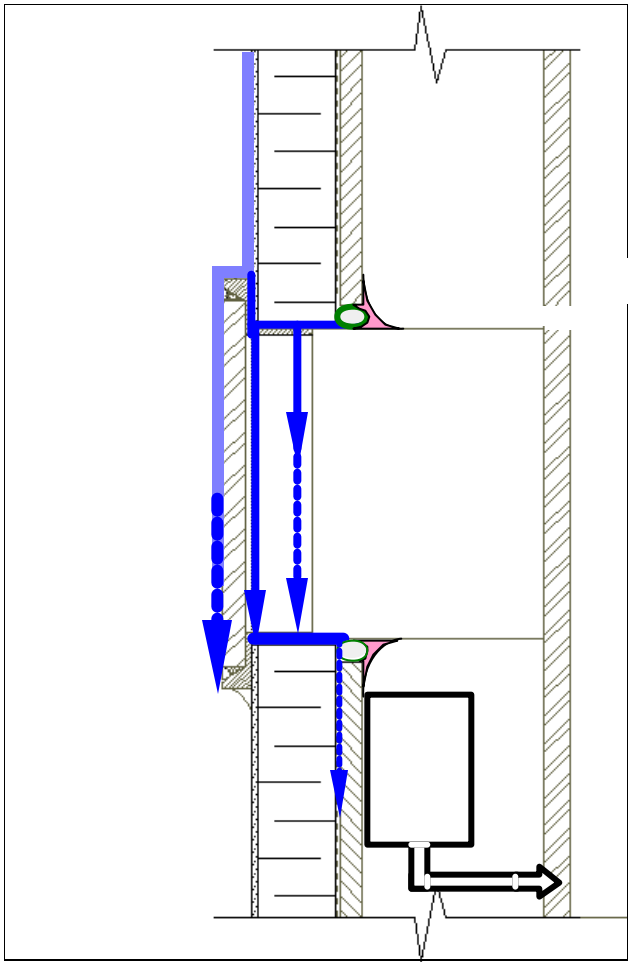

Figure 4.8 – EIFS WA-8: deficiency above vent duct presumed water entry path – caulking and backer rod in place – no water entry; probable drainage through vertical channels between adhesive layer and cementitious membrane coating

WA-6 — Rates of water entry for WA-6 are given in Figure 4.9 below. The rates of entry are provided as a function of the spray rate and pressure difference at which tests were conducted and for each nominal spray rate (0.85, 1.7 and 3.4 L/min.m^2), results from individual stages are also identified as being derived from Stages 5, 6 or 7 along the top of the plot.

For this wall assembly, little or no water enters at the lowest spray rate (0.85 L/min.-m^2) and the amounts that are observed are evident only in Stage 7. In this test stage, there are no barriers to water entry at the joint between the ventilation duct and sheathing boards. A slight increase in the amount of water collected is observed at the next level of spray rate (1.7 L/min.-m^2) and water entry occurs not only in Stage 7 but also at comparatively reduced rates in Stage 6 (backer rod in place). The greatest amounts of water are observed to enter at the highest spray rate (3.4 L/min.-m^2) where results were recorded in all test stages with rates increasing in relation to the degree of obstruction at the joint and the pressure applied across the wall assembly. Hence at this spray rate, the lowest rates of entry were observed in Stage 5 which is characterised by the use of both a sealant and backer rod to form the joint at the interface between the duct and sheathing board. In this stage, no water entry was observed when no pressure was applied across the assembly (i.e. 0 Pa ?P), but rates of entry increase with corresponding increases in $?P_S$ (e.g. from 0.003 at 75 Pa to 0.022 L/min. at 300 Pa $?P_S$ – a ca. 10 fold increase). In Stage 6 (backer rod in place) at this spray rate, rates of entry increased over those observed in Stage 5 (backer rod + sealant) and entry was also observed to occur when no pressure was applied (i.e. 0.028 L/min. at 0 Pa $?P_S$). Increases in rates of entry in relation to pressure differences are clearly evident: rates changed from 0.028 to 0.058 L/min. between 0 and 300 Pa $?P_S$. The highest rates of entry were observed in Stage 7 in which no sealant or backer rod is present at the joint interface: rates varied from 0.062 to 0.112 L/min. between 0 and 300 Pa $?P_S$.

A comparison of rates of entry of WA-6 (Figure 4.9) to that of WA-7 (Figure 4.10) and WA-9 (Figure 4.13) in Stage 7 (no sealant or backer rod in place) shows that the maximum rate of entry attained in WA-6 (0.112 L/min.) is roughly half of that achieved in WA-7 (0.185 L/min.) or WA-9 (0.281 L/min.). Given the observed entry of water between sheathing boards beneath the ventilation duct of WA-6 clearly suggests that rates of entry are affected by the path of water flow being diverted from the collection trough to the exit point between sheathing boards, as shown in Figures 4.11 and 4.12 below. In all stages of the test, water was observed to be exiting at this point (Figure 4.11) and as well was being forced through openings in the sheathing board proper (OSB) (Figure 4.12).

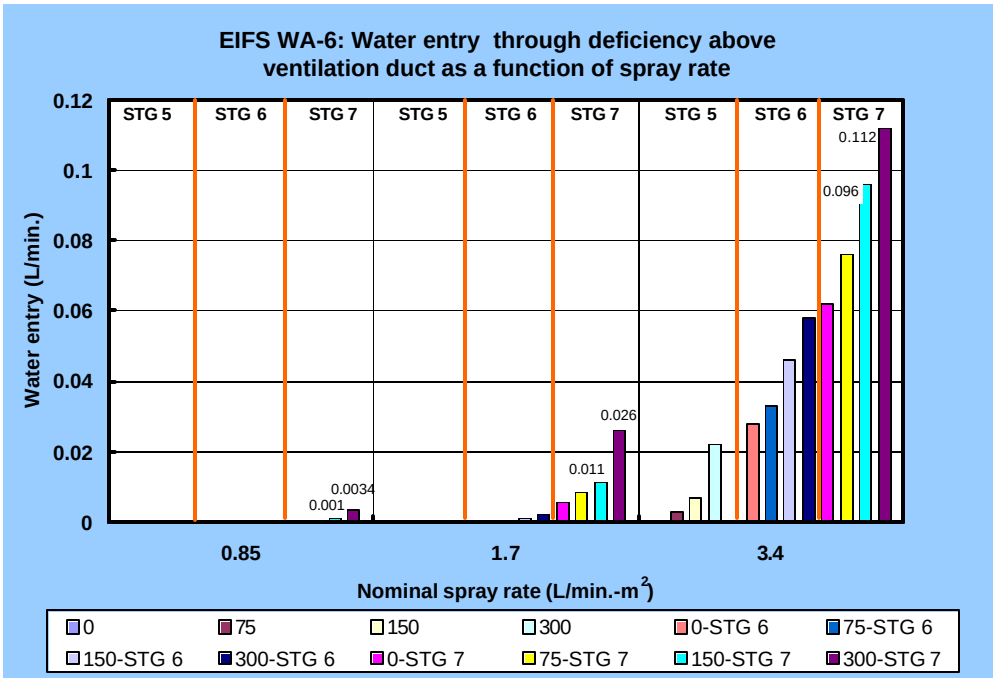

Figure 4.9 – WA-6: Water entry ventilation duct - Stages 5 through 7

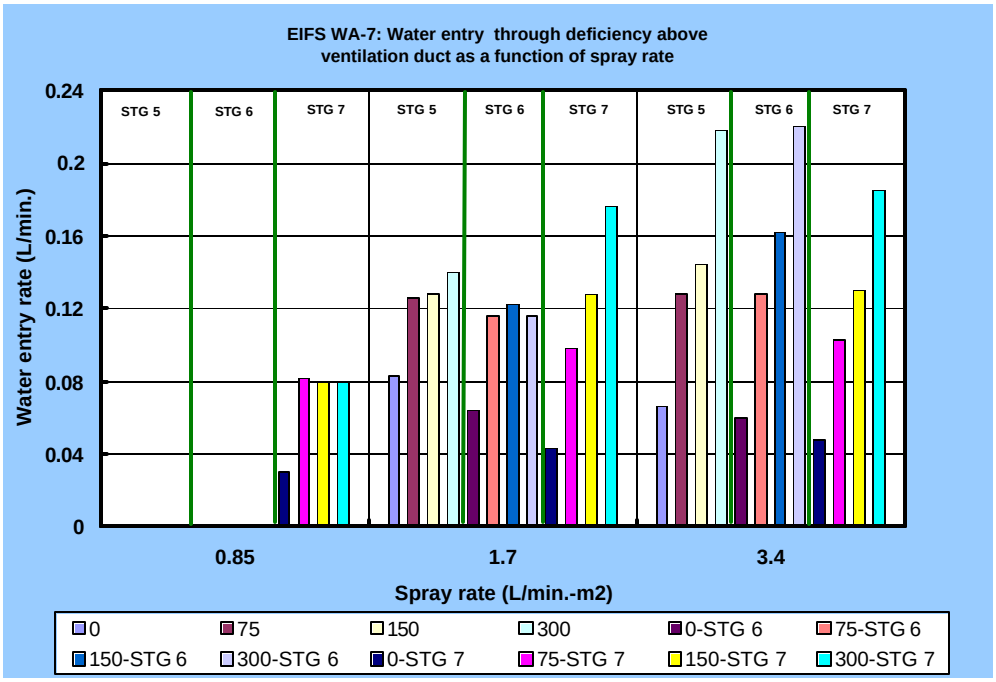

Figure 4.10 – WA-7: Water entry ventilation duct - Stages 5 through 7

Figure 4.11 – EIFS WA-6 : Water coming through deficiency above ventilation duct and between top and bottom sheathing boards (Stage 5- sealant and backing rod in place). Conditions - Static pressure difference: 300 Pa; Spray rate: 3.4 L/min.-m^2; Air Barrier System Leakage: 0.2 L/s-m^2

Figure 4.12 – EIFS WA-6 Stage 6 (sealant removed and backing rod in place): Cavity beneath ventilation duct. Water coming through pores in sheathing at the start of test – continued throughout Stage 6 and thereafter in Stage 7.

WA-7 — Rates of water entry for WA-7 are given in Figure 4.10. There is a lower incidence of water entry at the lowest spray rate as compared to the subsequent levels of higher spray rate. Thus in general, increased amounts of water enter the deficiency with a corresponding increase in the spray rate. At the lowest spray rate (0.85 L/min.-m^2), water enters under no pressure differential only in Stage 7 where no backer rod or sealant is present to restrict the passage of water from the deficiency to the collection trough. At this rate of spray and stage, rates of entry vary between 0.03 L/min. at 0 Pa ?P_S and 0.07 L/min. at 300 Pa ?P_S.

At the next level of spray rate (1.7 L/min.-m^2), water enters in all stages with about the same response to entry in stages 5 and 6. The maximum rate of entry in either of these stages is 0.140 and 0.122 L/min. respectively. Response to changes in driving pressure are only evident in Stage 7 in which there is seen to be a regular increase in rates of entry (i.e. from 0.043 to 0.176 L/min.) in relation to changes in pressure differential between 0 and 300 Pa. Interestingly at this spray rate, rates of water entry when no pressure is applied across the assembly diminishes from Stage 5 to Stage 7.

At the highest spray rate (3.4 L/min.-m^2), water enters in all stages and under all pressure conditions, including when no pressure is present. Responses of entry rates to changes in driving pressure are regular and the highest rates of entry are obtained at the highest pressure. Minimum values at 0 Pa ?P vary between 0.048 and 0.066 L/min. as compared to maximum values achieved at 300 Pa ?P; these vary between 0.185 to 0.220 L/min.

WA-9 — Results for WA-9 are given in Figure 4.13. Of note is that no water enters in Stage 5 (sealant and backer rod at joint interface). A comparison of all entry rates in Stage 6 and 7, irrespective of the spray rate, reveals that in Stage 6 entry rates varied between 0.010 and 0.037 L/min., whereas rates varied between 0.108 and 0.281 L/min. in Stage 7. Hence there was a 10-fold increase in rates of entry from Stage 6 to 7. In this instance, the presence of a joint at the interface had a marked effect on rates of entry. Rates of entry in Stage 7 are responsive to changes in pressure difference; increases in ?P_S bring about increase in rates of entry at all spray rates. As well, at given pressure levels, increases in rates of spray likewise increase the rates of water entry.

Rates of entry in Stage 7 for this wall assembly (WA-9) are in the same order of magnitude as those observed in the same stage of WA-7; e.g. at 300 Pa ?P, in WA-7 entry varies from 0.085 to 0.185 L/min. as compared to 0.132 to 0.281 L/min. for WA-9.

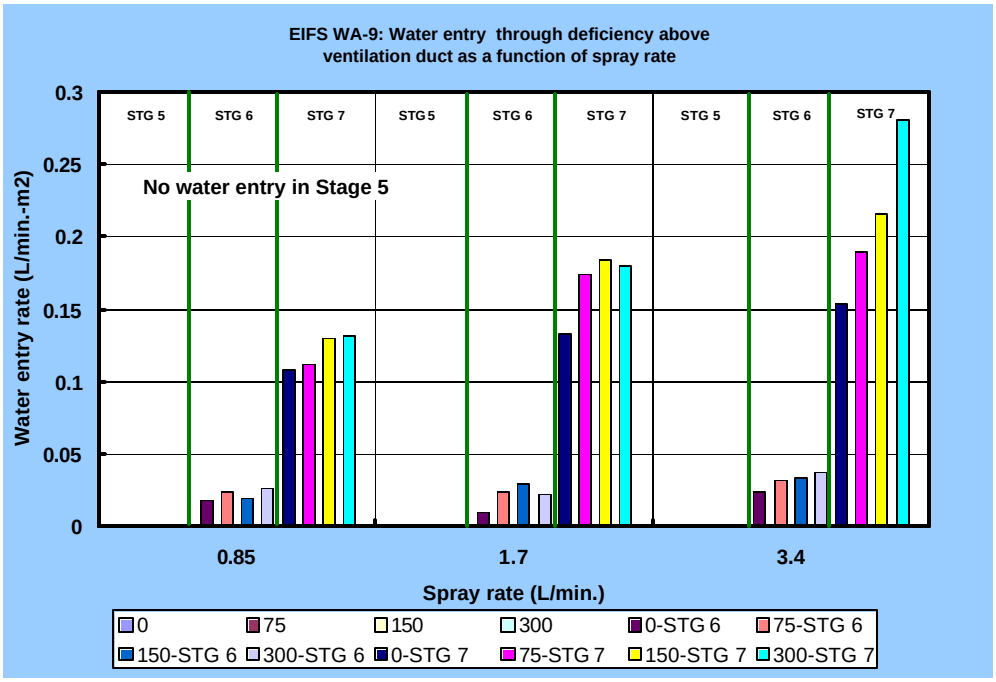

Figure 4.13 – EIFS Water entry - WA-9: vent duct - Stages 5 through 7

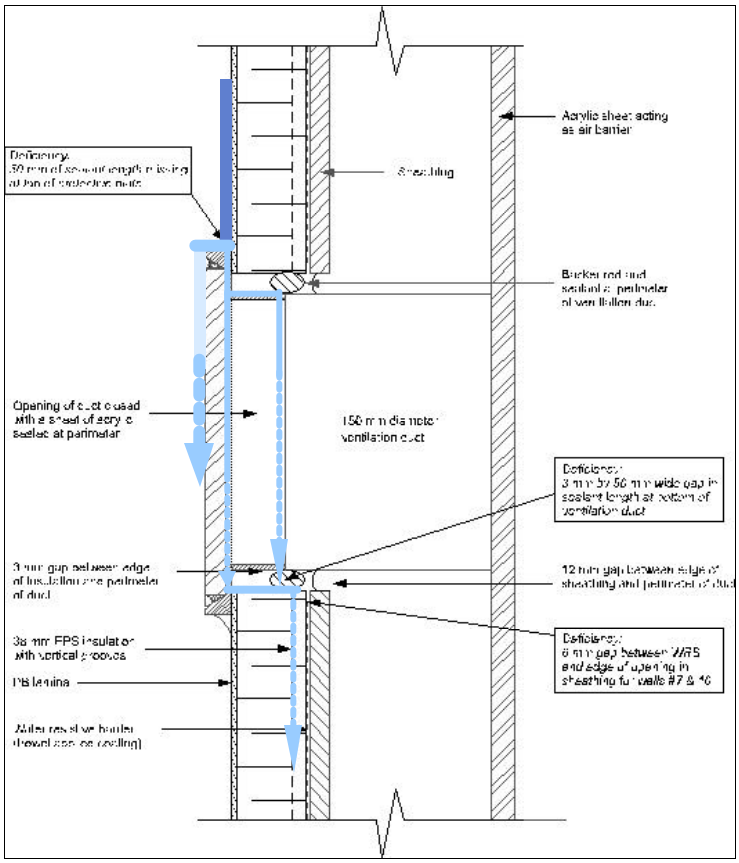

Figure 4.14 – WA-9 EIFS: water entry through vent duct - presumed water entry path

That no water was collected in Stage 5 of the test can be attributed to the sealing of the joint interface of WA-9, as depicted in Figure 4.14. The presumed water entry and drainage paths are shown in the figure; water does not pass the restricted 3-mm by 50-mm opening at the base of the ventilation duct, but drains through grooves present in the EPS insulation panel.

WA-10 — Results for WA-10 are provided in Figure 4.15 for which only values for Stage 6 were obtained; no collection was made in either Stage 5 or 7. WA-10 has a 3-mm nylon drainage mesh incorporated in the non-cementitious coating that acts as a moisture barrier. That no water entered Stage 5 can be attributed to the seal at the interface whereas it is not immediately known why no water appeared in Stage7 when no barriers to entry were present, in particular when collection was made in Stage 6. It was observed in Stage 7 that entry via the ventilation deficiency was evident and that drainage was occurring through the mesh. It may be that the backer rod was positioned such that drainage through the mesh was not possible and the path of least resistance was around the backer rod.

Nonetheless, results from Stage 6 show no water entry when no pressure is present and increased rates at higher pressures. The maximum value at 300 Pa ?) is ca. 0.05 L/min. which is comparable to that observed for Stage 6 in WA-6 (0.058 L/min.) and WA-9 (0.037 L/min.) and ca. 4 times less than that found for WA- 7 (0.220 L/min.).

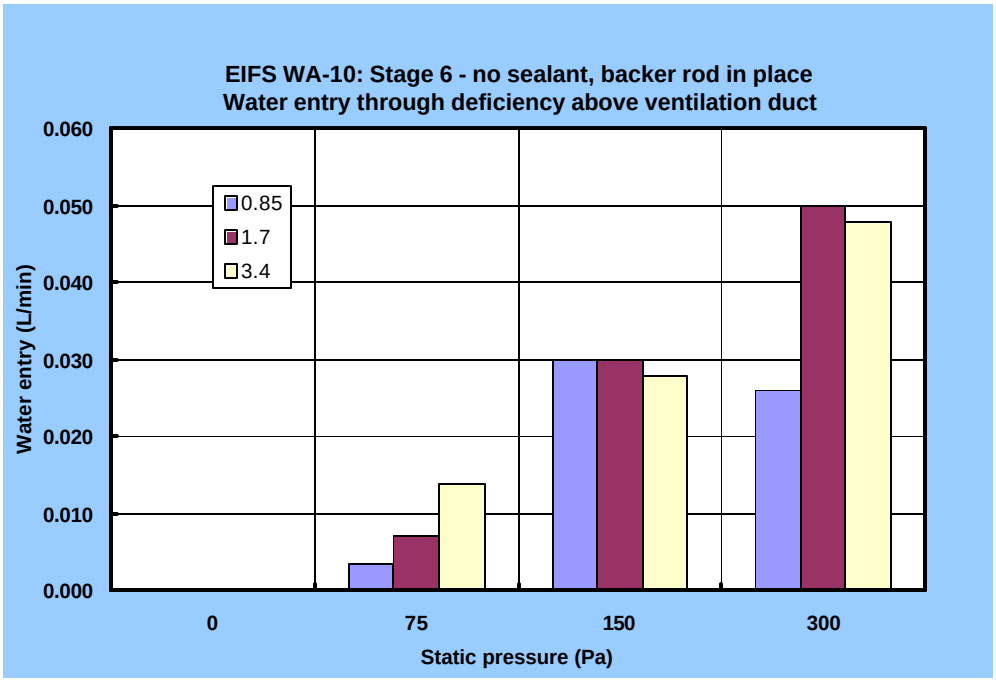

Figure 4.15 – EIFS Water entry - WA-10: vent duct - Stages 5 through 7

4.2.2.4 WATER ENTRY ABOUT WINDOWS

Results for water entry about window penetrations for WA-6 are provided in Figures 4.16 and 4.17. The information is arranged in terms of entry rates as a function of spray rate at given levels of static pressure differential; results at each test stage (5, 6 and 7) are grouped within each spray rate. Nominally, there should be no difference in test conditions to which the windows are subjected at any given level given that differences between stages relate to the interface details at the ventilation duct and not the window.

The rates of entry for the left side of the window (LS) are provided in Figure 4.16 whereas those for the right side (RS) in Figure 4.17. Overall, entry rates for either side are in general below those obtained for the ventilation duct (no entry about electrical outlet in WA-6). Values range from 0.001 to 0.02 L/min. with most of the rates below 0.01 L/min. as compared to values reaching, for example, ca. 0.11 L/min. for the ventilation duct. Entry was observed under conditions of no pressure differential.

Rates of entry on the LS were more consistent than those derived for the RS; for the LS, water was collected over almost all of the test stages when subjected to different spray conditions whereas collection was intermittent (Figure 4.16) on the RS. It can only be surmised that the load on the LS was more consistent than that on the RS and this is dependent on the manner in which water cascades over the cladding surface, interacting with protuberances, projections and natural vertical channels upstream from potential points of water entry.

On the LS (Fig. 4.16), rates of entry in general increased at higher spray rates. Hence the lowest aggregate rates of entry for the LS were obtained at the lowest spray rate (0.85 L/min.-m^2) and correspondingly higher rates of entry at spray rates of 1.7 and 3.4 L/min.-m^2. The average rates of entry at spray rates of 1.7 and 3.4 L/min.-m^2 was ca. 0.005 and 0.008 L/min. respectively with maximum values reaching 0.02 L/min. (at 300 Pa).

The intermittent nature of results for the RS is evident in Figure 4.17. Of the 24 results recorded, 75% of these were equal to or less than 0.001 L/min., ca. 88% were below 0.004 L/min. and the maximum reached was 0.005 L/min. The results suggest that if water is present at the entry point then rates of entry can reflect these loads however given the intermittent nature of the results quantities of water available at the deficiency may considerably vary. This in turn is related to quantity of water flowing over entry points and as mentioned above, the nature of water delivery to openings in the cladding.

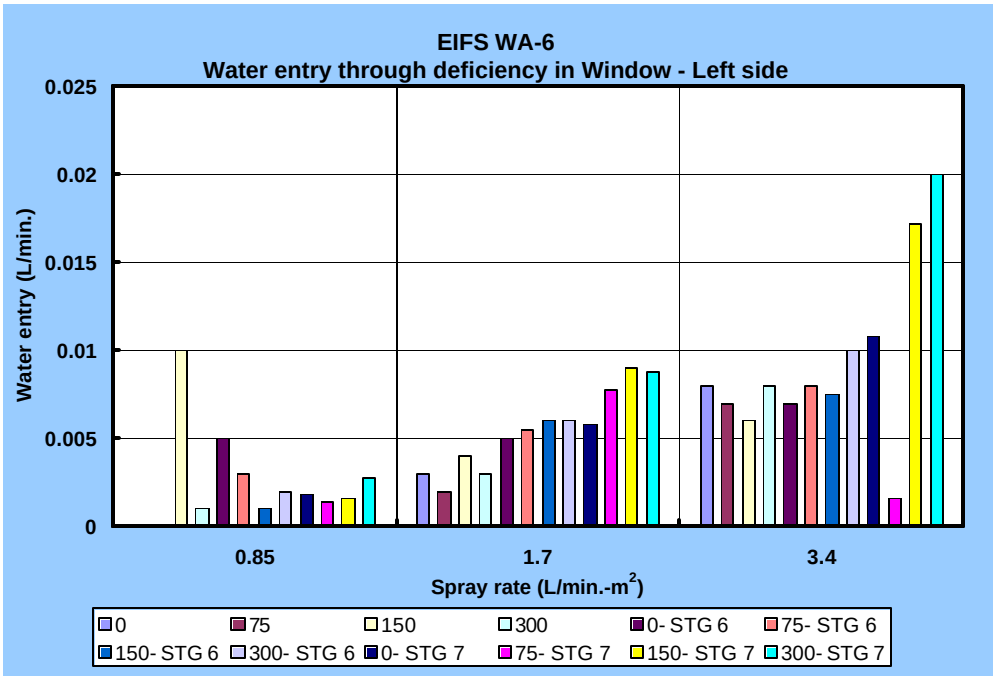

Figure 4.16 – EIFS WA-6: Water entry at various spray rates and at given static pressure differentials through deficiency at RS of window

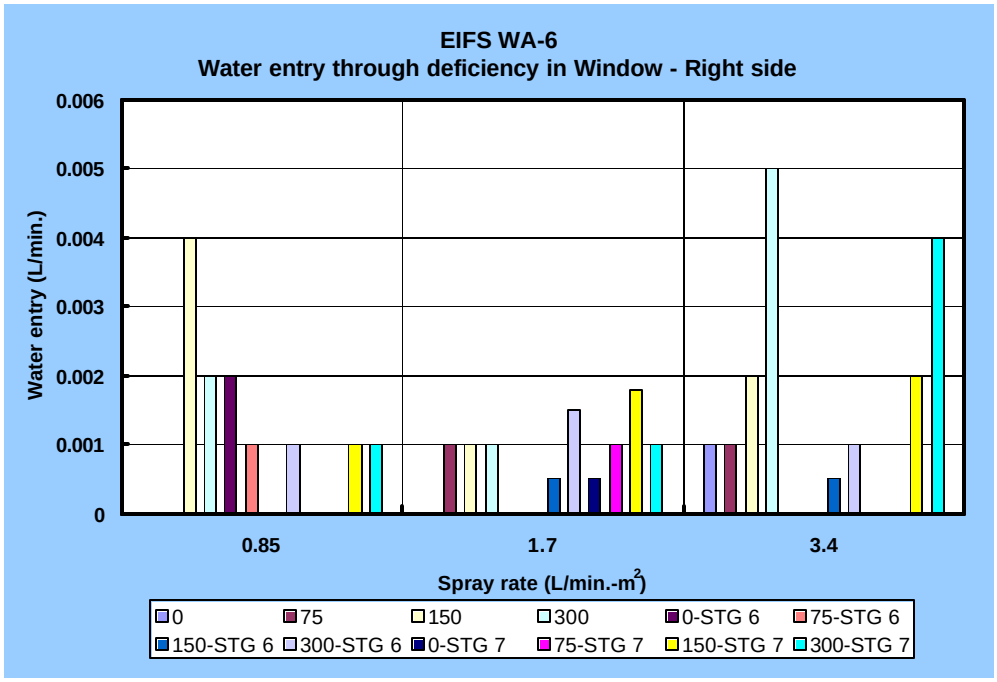

Figure 4.17 – EIFS WA-6: Water entry at various spray rates and at given static pressure differentials through deficiency at LS of window

4.2.2.5 WATER ENTRY ABOUT VERTICAL JOINTS

Of the three wall assemblies for which data was recorded (i.e. WA-7, -9 and -10; Figures 4.18 to 4.20 respectively.) considerable entry occurred when no pressure was evident across the assembly. This was particularly evident for the entry rates through the deficiency of the joint in WA-10 in which rates of entry at 0 Pa varied between ca. 0.24 and 0.37 L/min. over the range of spray rates as compared to rates in the order of 0.1 L/min. for the joints in the other wall assemblies.

Rates of entry were not dependent on the driving pressure as rates remained essentially the same irrespective of the pressure difference across the assembly. The exception to this observation was for WA-7 (Figure 4.18) where rates remained comparatively constant at test pressures of 0, 75 and 150 Pa (between 0.089 to 0.108 L/min.) but increased (between 0.132 to 0.298 L/min.) when the assembly was subjected to 300 Pa pressure difference.

With the exception of that noted above, rates of entry for WA-7 and WA-9 have a similar range, roughly between 0.09 and 0.15 L/min whereas WA-10 had the highest entry rates varying between 0.24 and 0.39 L/min. over the range of test pressures and spray rates.

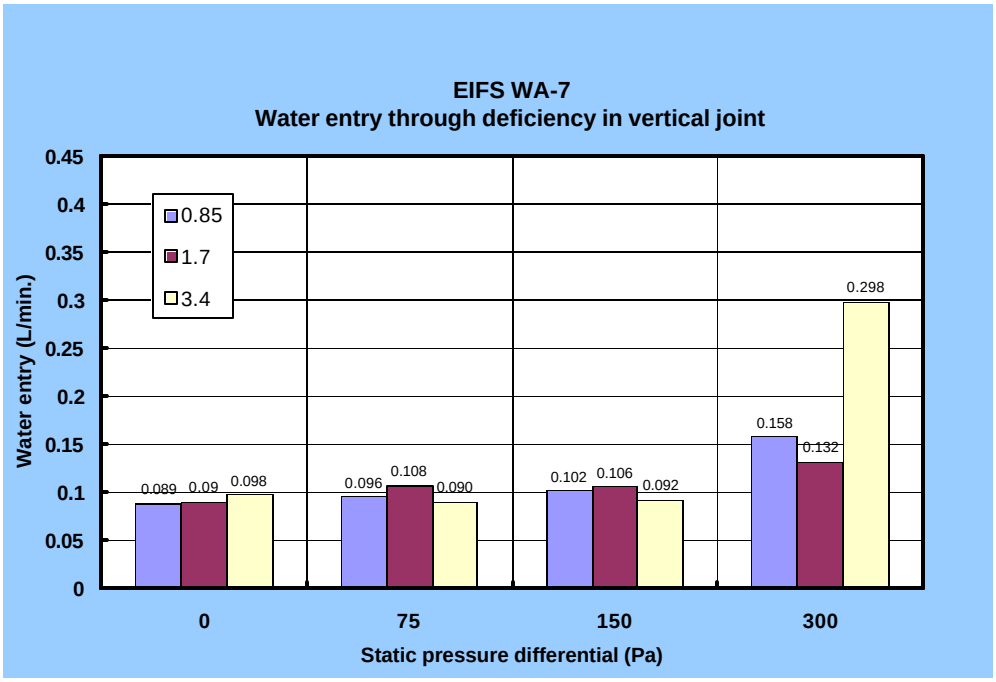

Figure 4.18 – EIFS WA-7: Water entry under static pressure differential through deficiency in vertical joint

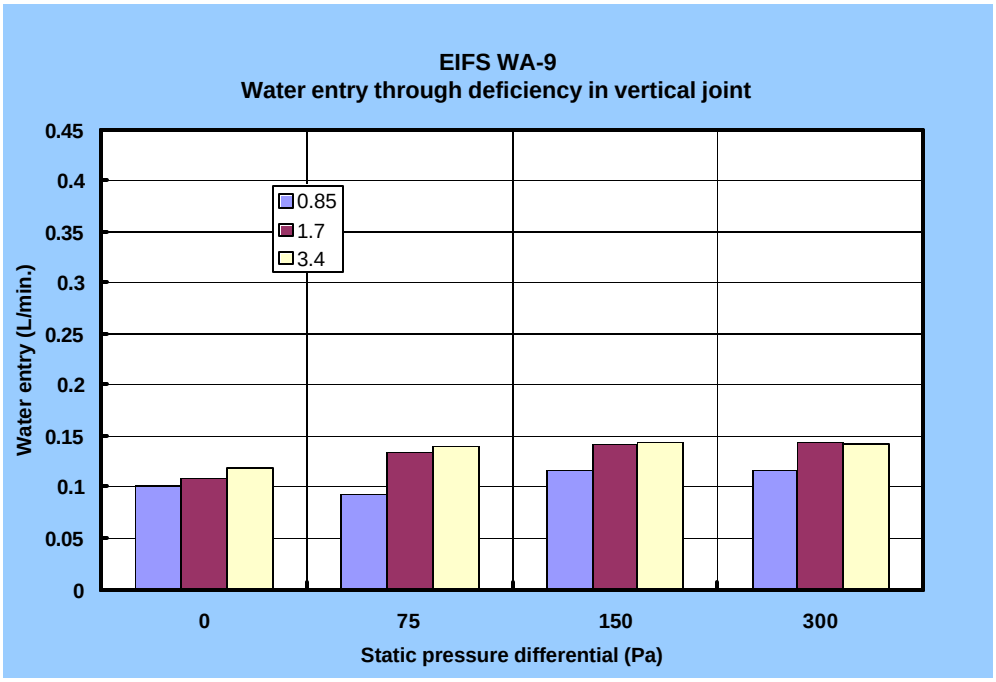

Figure 4.19 – EIFS WA-9: Water entry under static pressure differential through deficiency in vertical joint

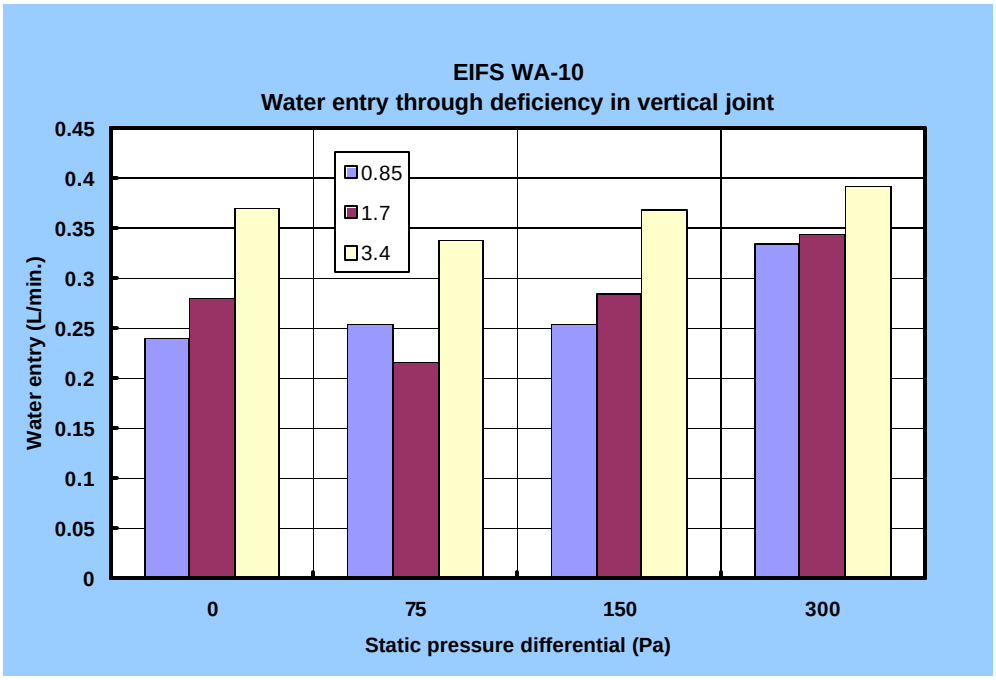

Figure 4.20 – EIFS WA-10: Water entry under static pressure differential through deficiency in vertical joint

Dependence on spray rates at given pressure levels was not evident in WA-7 (Figure 4.18) and only slightly so in WA-9 (Figure 4.19) whereas this was more apparent in WA-10 (Figure 4.20). For example, rates increased from ca. 0.24 to 0.37 L/min. at 0 and 150 Pa, and at 300 Pa from 0.34 to 0.39 L/min.

4.2.2.6 WATER ENTRY UNDER DYNAMIC PRESSURE FLUCTUATIONS – ELECTRICAL OUTLET

Results for water entry through deficiencies above the electrical outlet under dynamic pressure fluctuations are provided in Figures 4.21 and 4.22 and a summary provided in Table 4.11.

For dynamic tests at the lower spray rate (1.7 L/min.-m^2):

- Maximum value was 0.084 L/min. (at 300 Pa ΔP_s);
- Average value at 300 Pa was 0.074 L/min.

These results reflect the slightly higher values obtained under dynamic conditions as compared to those derived from tests under static testing. However, these values might be expected given that in the dynamic mode pressure levels fluctuate about a mean value and specimens are thus subjected to higher pressures as compared to a given pressure level in the static test mode.

At the higher spray rate (3.4 L/min.-m^2):

- Maximum value was 0.132 L/min.; as compared to static tests (0.123 L/min).
- The average rate at 300 Pa ΔP_s was 0.123 L/min. with a range of 0.083 L/min.

All of these values are essentially comparable to those obtained in static tests with the higher values being obtained under dynamic conditions.

Of importance as well is that rates of water entry when no pressure is applied across the assembly are significant; ca. 0.04 L/min. for WA-9 and up to ca. 0.17 for WA-7.

Table 4.11 – Comparison of water entry rates obtained under static and dynamic tests

Test Mode	Water entry rate (L/min.)					
	Spray rate - 1.7 (L/min.-m^2)			*Spray rate – 3.4 (L/min.-m^2)*		
	Maximum value	Avg. value at 300 Pa*	Range from 0-300 Pa	Maximum value	Avg. value at 300 Pa*	Range from 0-300 Pa
Static	0.063	0.055	0.015	0.123	0.114	0.074
Dynamic	0.084	0.074	0.034	0.132	0.123	0.083

- under dynamic testing, the values were obtained under a fluctuating pressure differential of 300 ± 125•sin ($2\pi ft$) Pa, with nominal mean pressure of 300 Pa.

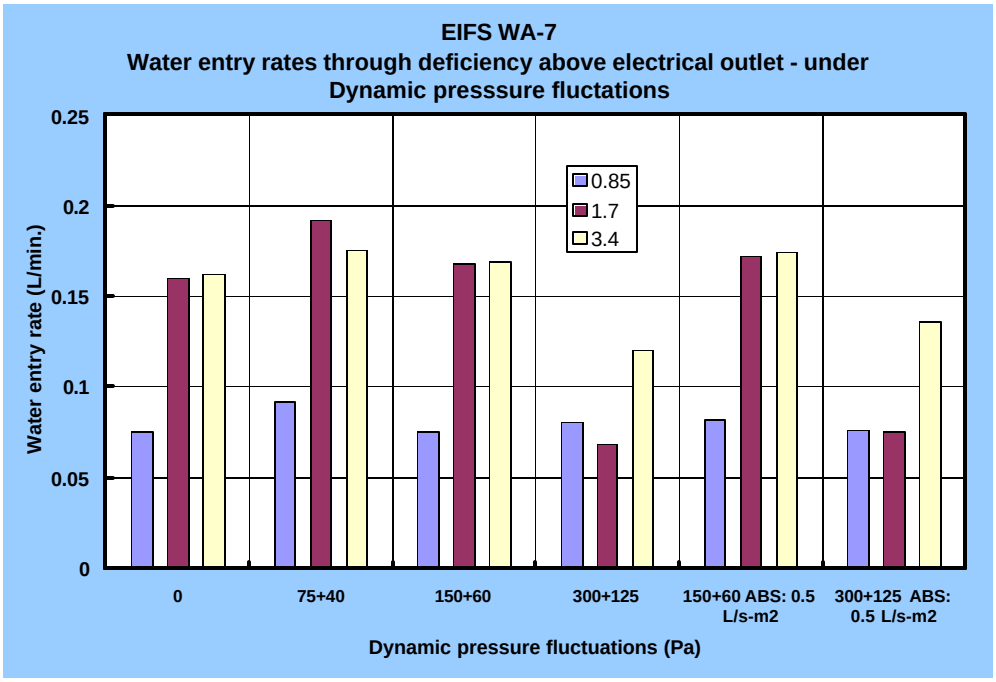

Figure 4.21 – EIFS WA-7: Water entry rates under dynamic pressure fluctuations through deficiency above electrical outlet

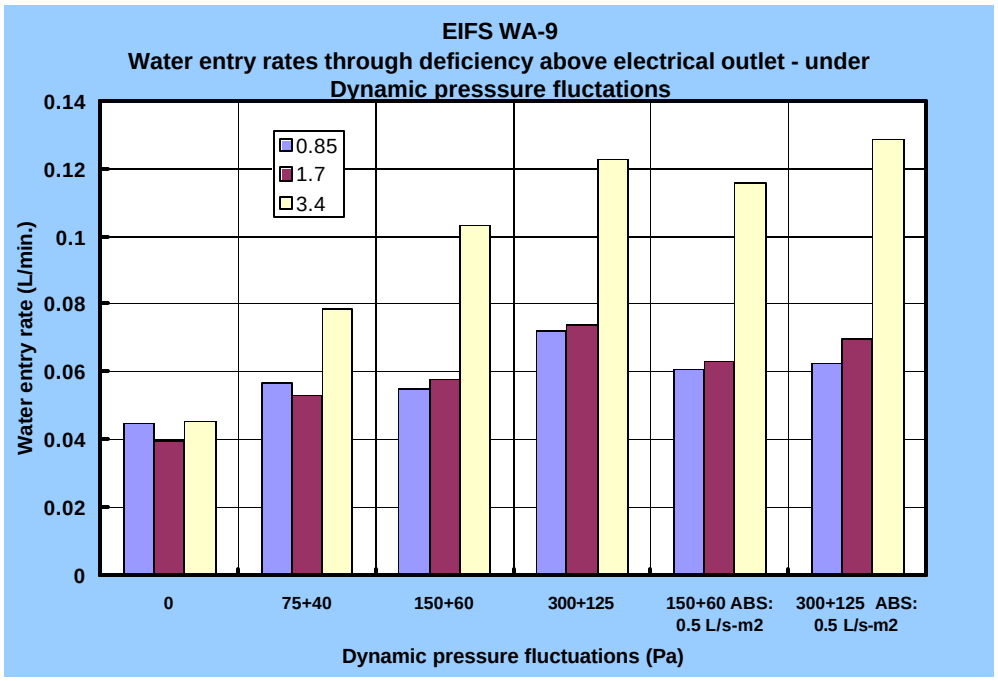

Figure 4.22 – EIFS WA-9 : Water entry rates under dynamic pressure fluctuations through deficiency above electrical outlet

Results for WA-7 do not show a dependency between water entry rates and levels of pressure fluctuation. Results at different pressure fluctuations show essentially the same response at the 0, 75±40, and 150±60 Pa levels with water entry increases at a given level related to increases in spray rate. However, the rate of water entry at the 300±125 level is less than that of the lower pressure levels.

In the case of WA-9, there appears to be a regular increase in rates of water entry at progressively higher levels of pressure fluctuation and as well, at a given pressure level, rates increase in relation to increases in spray rate.

The effect of changing the nominal air barrier system leakage (ABSL) on water entry rates is also provided for both walls. Note that the ABS leakage was undertaken at nominal values of 0.2 and 0.5 L/s-m^2. In WA-7 (Figure 4.21), a comparison of rates of entry at either the 150±60 or 300±125 Pa pressure levels shows no significant effect when the ABS is increased from 0.2 to 0.5 L/s-m^2. Likewise, for WA-9 (Figure 4.22) the variations shown between results do not appear to be significant. A more refined picture could be obtained by reviewing the driving pressures in proximity to the points of water entry.

4.2.2.7 Summary - Water entry assessments through specified deficiencies:

Water entry assessments were used to determine the quantities and rates of water that might enter specified deficiencies of known type, size and location on the cladding when subjected to simulated climatic extremes, using the Dynamic Wind and Wall Test Facility (DWTF).

Results revealed that:

- Water entry through specified deficiencies about the electrical outlet was evident for all Stages in WA-7 and -9 and in Stage 5 for WA-10; no water entry was recorded for WA-6 and WA-8.
- Water entered through specified deficiencies under gravity alone, i.e. instances when there was no driving pressure across assembly.
- Rates of entry through the specified deficiency for the electrical outlet are primarily dependent on the amount of water deposited on the wall; increased rates of entry were evident for corresponding increases in rates of water sprayed onto the cladding surface.
- In the case of WA-8, for which water entering the specified deficiency about electrical outlet did not collect in the stud cavity, the likely path of water subsequent to entry was drainage between the adhesive layer and water-resistant barrier (polymer cement coating) down through vertical channels located in the adhesive.

- No water entry was observed through specified deficiency about the ventilation duct for WA–8, in Stage 5 (sealant and backer rod in place) of WA-9 and in Stages 5 and 7 (no sealant or backer rod in place) of WA-10.
- Rates of entry for the specified deficiency at the ventilation duct are primarily dependent on the amount of water deposited on the wall; increased rates of entry were evident for corresponding increases in rates of water sprayed onto the cladding surface.
- Similar rates of water entry at the ventilation duct were found for EIFS walls as compared to results derived from tests on stucco walls.
- For water entry thought the specified deficiency at the vertical joint, none entered the joint in WA–6 or –8; water entry results were obtained for all other wall assemblies
- For assemblies having water entry about the specified deficiency at the vertical joint, rates of entry were dependent on pressure differences across the assembly
- With the exception of WA–6, no water was collected about windows for any of the other wall assemblies.

Chapter 5

Results from Masonry Wall Assemblies

TABLE OF CONTENTS

— CHAPTER 5 —

Results from Masonry Wall Assemblies

LIST OF FIGURES

LIST OF TABLES

CHAPTER OVERVIEW

MEWS methodology incorporates the performance testing and characterisation of full-scale wall assemblies to determine air leakage, dynamic response, water-tightness performance and water entry characteristics for each of the wall cladding types being evaluated in this study.

Performance tests were used to qualify the degree to which wall assemblies were able to maintain their watertight integrity when being subjected to static or dynamic pressure differentials concurrent with water spray using the dynamic wall test facility (DWTF). This series of tests were similar those currently used in industry to assess the likelihood of water penetration under extreme simulated climatic conditions and were conducted at levels comparable to, or in excess of, current industry standards.

Water entry assessments were used to determine the quantities and rates of water that might enter deficiencies of known type, size and location on the cladding when subjected to simulated climatic extremes, likewise using the DWTF. Levels of water spray and pressure differential were consistent with related climatic data of rainfall and wind speed that might occur in an extreme climatic event within a 10 year period in North America. This information provided a basis for a systematic and consistent means of transferring input to hygIRC, the model used in the MEWS simulation studies.

In this test series of masonry wall assemblies, four (4) different types of masonry-clad wall assemblies were subjected to performance and water entry assessments tests that included testing under different pressure differentials across the assembly and varying rates of water sprayed onto the cladding surface. Tests were completed in conformance with a protocol derived explicitly for this study and provided in Chapter 1 (T6-02-R8).

Results from water penetration assessments indicate that water ingress at through-wall penetrations was evident for all locations, in particular windows (3 of 4 walls); however no water was observed to have penetrated to the stud cavity. This is an expected result given the presence and size of the drainage space incorporated in each of these walls. On the basis of these tests, no apparent advantage is offered a wider space (i.e. 50-mm vs. 25-mm) in regard to reducing water entry to the space. The low level of moisture sensor activity in these walls is indicative of reasonable water management attributes incorporated in the assembly. Results clearly show that inadvertent water entry is highly likely if care is not taken to properly seal joints at the interfaces with penetrations. All of the water ingress activity at the various points of entry are indicative of the significant amounts of water that can collect in a short period of time under unfavorable climate conditions (i.e. high and prolonged intensity of wind-driven rain).

The water entry trials indicated that for the electrical outlet there was no dependence on pressure differential and little or no dependence on spray rate; maximum value of water entry rate was 0.16 L/min. However, gross amounts passing opening above electrical outlet collected in trough “D” or “T1”, each trough located in the drainage cavity. For the ventilation duct, entry rates were partially dependent on spray rate; maximum value of water entry rate was 0.185 L/min. It was also noted that the pressure differential across plane of the sheathing board drives water to trough “L”, the trough located in the stud cavity. In the case of water collection about the windows, rates of water entry were loosely dependent on spray rates; maximum rates attained in dynamic mode was 0.12 L/min.

5.1 Introduction

A series of four masonry veneer walls (Figure 5.1) were constructed and subsequently tested for water penetration trials and water entry assessments using the dynamic wall test facility. The pressure response of the wall assemblies and air leakage characteristics were also determined.

Details regarding the fabrication of the specimens, material specifications and specified deficiencies are provided in report T2-13. An overview of the different specimens showing the key components of the wall assemblies is provided in Table 5.1. Details regarding the location of pressure taps, of moisture sensors, of water entry points through specified deficiencies and means of water collection are outlined in the section on test specimens.

Results from water penetration trials (Stages 2 and 3) are first presented followed by those obtained for water entry assessments. (N.B. Stage 5, 6 and 7 – replace Stage 4). Tests were conducted according to the test protocol described in Chapter 1 (§1.2). Selected results from air leakage and dynamic response (Stage 1) of wall assemblies are also provided.

Table 5.1 – Wall assembly types and key wall components

WA#	Cavity size	WRB	Sheathing	Type of window	Extension	Type of sill
11	25 mm	None	25 mm XPS (ship lap joints)	Box	2 5/8"	Stone
12	25 mm	1 layer 30-min. paper	OSB	Flange	1 3/8"	Rowlock
13	25 mm	1 layer 30-min. paper	Asphalt-impregnated fiberboard	Box (with elastomeric pan flashing)	1 3/8"	Stone
14	50 mm	Micro-perforated HDPE / LDPE	Glass mat Gypsum board	Flange	2 5/8"	Rowlock

5.1.1 TEST SPECIMENS

The test configuration showing the location of pressure taps, moisture sensors, and water entry points through specified deficiencies are provided below in Figures 5.2 to 5.4 respectively.

5.1.1.1 PRESSURE TAPS

Pressure taps are located in six wall portions (Figure 5.1), with the first portion located at the left extremity of the wall (facing the weather-side). Typically in each portion, taps are located both in the wall cavity between the stucco and the sheathing and in the stud space. Additionally, taps have been added to obtain measurements of pressure differential at points of water entry.

5.1.1.2 AIR BARRIER SYSTEM LEAKAGE

Air barrier system (ABS) leakage was regulated by introducing a series of 7-mm diameter holes in the ABS (Figure 5.2), a series of seven (one in each stud cavity) representing an equivalent leakage area (ELA) of 269-mm^2, provided a nominal wall assembly leakage of .2 L/s-m^2. A wall assembly leakage of 0.5 L/s-m^2 (ELA 808-mm^2) was achieved using twenty-one holes of the same diameter, three in each stud cavity. The desired nominal leakage through the wall assembly was achieved by “opening” or “closing” the appropriate number of holes in the ABS

5.1.1.3 MOISTURE SENSORS IN SHEATHING BOARD

The location of moisture sensors is shown in Figure 5.3. A total of sixteen (16) moisture pin pairs have been imbedded in the sheathing board in various locations as a means of indicating the presence of moisture in the board material. Over a test period, note is taken of the time and conditions under which the light is first activated.

5.1.1.4 WATER ENTRY POINTS

Water entry points through specified deficiencies (Figure 5.3 and 5.4), representative of those joints that seal the interfaces between wall components, are located:

- Above the electrical outlet – a nominal 50-mm length of sealant is missing between the outlet cover and the wall.
- Above the ventilation duct – a nominal 50-mm length of sealant is missing between the duct and the wall.
- Below the windowsill and between finishing strips – a 50-mm length of sealant is missing between the ending strips.
- Along the horizontal joint located above the window and mid-way between joint extremities – a 90-mm length of sealant is missing
- Along the vertical joint located mid-height between joint extremities – a 90-mm length of sealant is missing

Figure 5.1 - Masonry walls assemblies (WA-11, -12, -13, -14) in various stages of fabrication

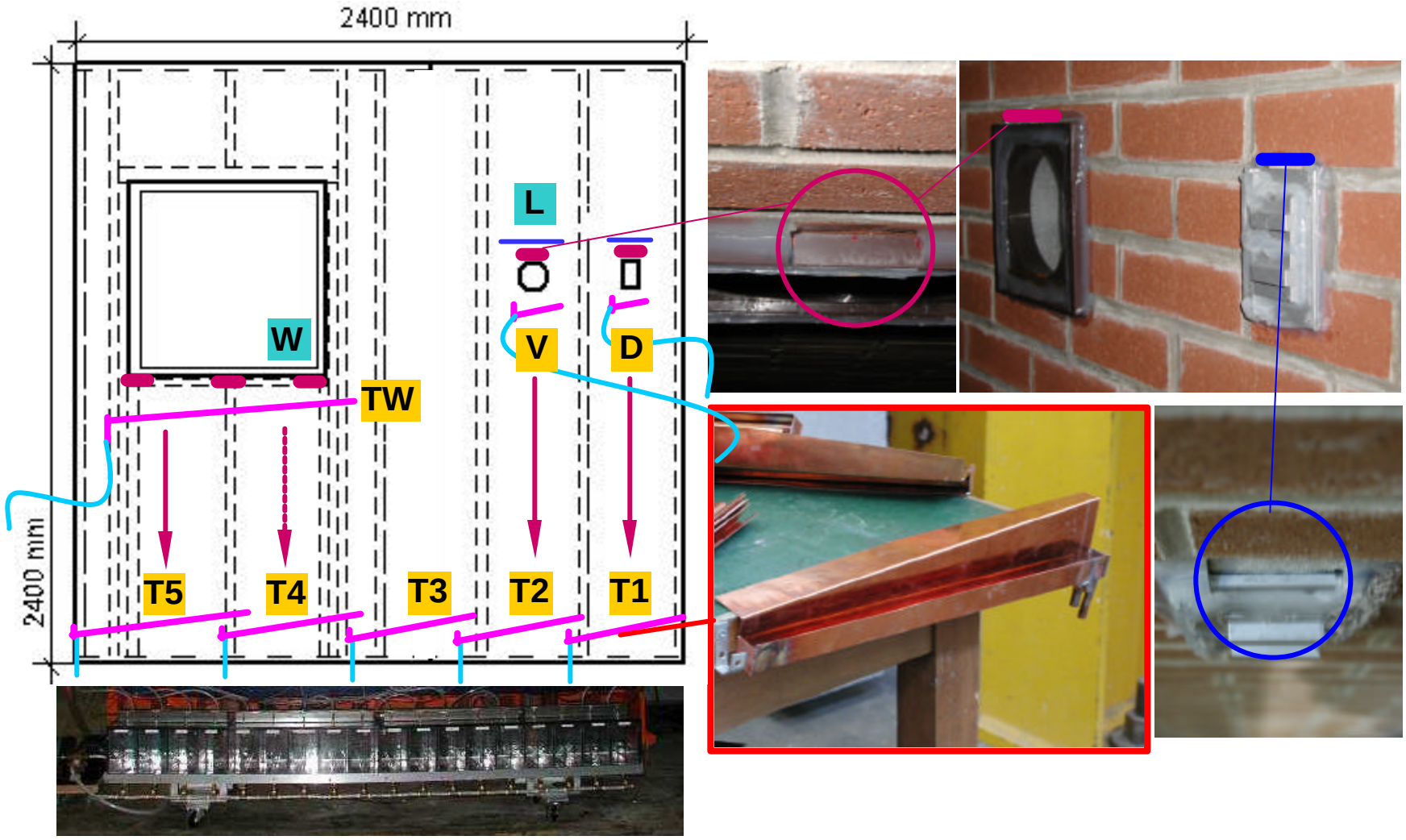

Figure 5.2 - Location of water collection points and troughs in ventilation–drainage space between brick cladding and sheathing.

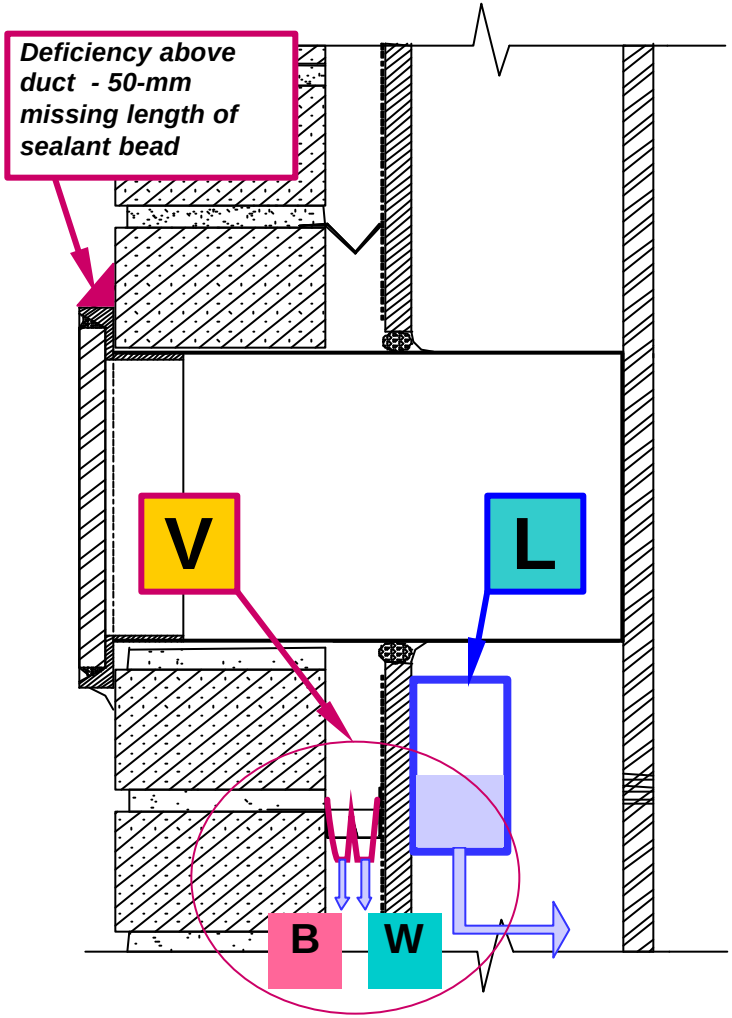

Figure 5.3 – Sectional view of wall assembly at ventilation duct showing location of water entry point and collection troughs. Troughs V-B, V-W: Water collected from behind duct along brick [B] cladding or wall [W] surfaces; Trough [L], located in the stud cavity, collects water passing the sheathing board.

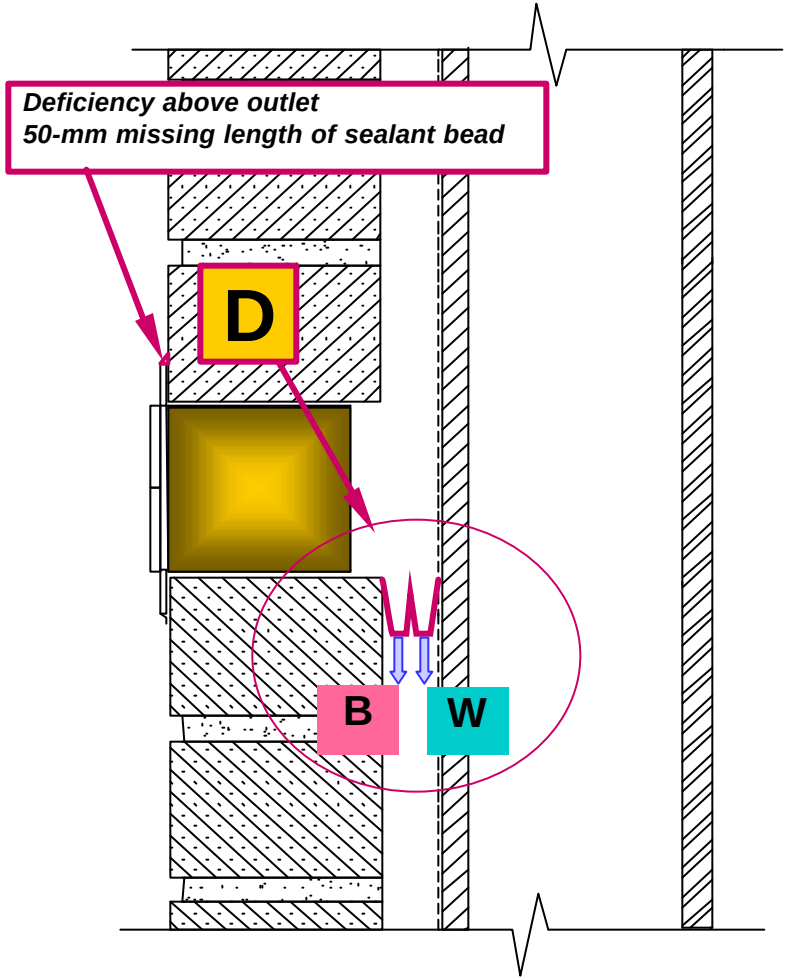

Figure 5.4 – Sectional view of wall assembly at electrical outlet showing location of water entry point and collection troughs. Troughs D-B, D-W: Collect water from behind outlet along brick [B] cladding or wall [W] surfaces

5.2 Results

Results from water penetration trials (Stages 2 and 3) are presented in section 5.2.1 and information is presented in relation to the results from a specific wall assembly following in sequence from WA-15 to WA-17. Summary information regarding specimen components is provided in Table 5.1 and a summary of the results is first presented in Table 5.2. Information related to the performance of each assembly when subjected to either static or dynamic test conditions is provided and a summary of the water penetration results is provided in section 5.2.1.6.

Note that water penetration trials do not include specified deficiencies in the wall specimen whereas these are part of the assessment protocol for water entry tests. When reference is made in this chapter to “deficiencies”, in all instances this is referring to specified deficiencies.

Results from assessments of water entry through specified deficiencies are provided in section 5.2.2. Specific information related to the collection of water in troughs located in proximity to the electrical outlet, ventilation duct and window is presented as is the collection of water in troughs located in the ventilation drainage space.

With the exception of WA-17 (hardboard-clad siding incorporating a drainage space), this series of four wall specimens (WA-11 to WA-14 inclusive) was the only one for which water collection was made from troughs located in the ventilation drainage space.

Results from water entry are presented in sequence where entry rates about specified through-wall penetrations are reviewed for all wall assemblies in relation to the range of values obtained in static and dynamic conditions a summary of which is given in Table 5.6.

5.2.1 WATER PENETRATION TESTS ON MASONRY-CLAD WALLS – STAGES 2 AND 3

5.2.1.1 INTRODUCTION

Results from water penetration tests in stages 2 and 3 of the test protocol are provided in Table 5.2 and Table 5.3 and Figures 5.5 to 5.8. Table 5.2 also gives information on the wall properties in respect to type of sheathing used and the size of a drainage space. Observed water penetration is indicated for each of the entry locations (see Figure 5.2) that include all of the troughs as well as the sheathing board. Information is also offered on moisture sensor (MS) activity and the number of sensors activated during the trials in relation to the number of functional sensors (i.e. X of Y). Assemblies were constructed with four different types of sheathing board including 25-mm extruded polystyrene (X), oriented stand board (O), Asphalt-impregnated fiberboard (F) and glass-mat gypsum board (G).

The most evident result from water penetration trials on this series of assemblies is that no water entered any of the through-wall penetrations to the stud cavity; no observations were made of water entry at trough L (located beneath ventilation duct), or W (beneath window on sill). Nor was water observed to have penetrated the sheathing board (Sh-Brd) for any of the walls in any tests. Notably, water did accumulate in the various troughs located in the drainage space directly behind the brick masonry veneer and outboard of the sheathing membrane (i.e. in troughs D, V, TW, and T1-T5, as shown in Figure 5.2).

Table 5.2 — Masonry-clad wall assemblies: Observed water penetration at various locations and siding assembly properties

	Masonry clad wall properties*				
	Sheathing Drainage Cavity	X Y Y	O Y Y	F Y Y	G Y Y
Observed Entry Location	**WA**	**11**	**12**	**13**	**14**
E**		⊖	⊖	⊖	⊖
V		⊖	⊖	⊖	⊖
W		◉	◉	⊖	⊖
Sh-Brd		⊖	⊖	⊖	⊖
MS		2/12	3/12	7/12	6/12

* X – 25 mm XPS ship lap joints; O – OSB; F – Asphalt-impregnated fiberboard; G – Glass mat Gypsum board

** Electrical outlet (E), ventilation duct (V), window (W), sheathing board (Sh-Brd) and activation of moisture sensors (MS)

Activation of moisture sensors was slight (Table 5.3) if one takes into account the false positive results obtained during the tests Note that false positive results indicate moisture sensors that have been inadvertently activated from incidental water deposition on their electrical leads (*identified as italicised results*). With the exception of WA-14, that indicated up to 6 MS activated, the remaining walls had either one or two moisture sensors activate during the tests, most of these due to activity following the 16-h of continuous spraying (Stage3).

Additional details regarding results of water penetration of specific wall assemblies is provided in the subsequent sections.

Table 5.3 - Moisture sensor activation in various wall assemblies during water penetration assessments for Stages 2 and 3*

WA-11		**WA-12**		**WA-13**		**WA-14**	
XPS *25-mm air space*		***OSB*** *25-mm air space*		***Fibre-B*** *25-mm air space*		***Gypsum-B*** *50-mm air space*	
S and D*	16-h	S and D	16-h	S and D	16-h	Static	16-h
MS-21	MS-11	None	MS-2	None	MS-2	None	MS-4
			MS-26		MS-5	Dynamic	
			MS-37		*MS-13*	MS-6	
					MS-37	MS-10	
					MS-38	MS-11	
					MS-39	MS-26	
					MS-26	MS-38	

* Stage 2 – Static and Dynamic test sequences; 16-h: Stage 3 of "continuous" (16-h) water spray and pressure; italicised MS information indicted false positive results

5.2.1.2 WATER PENETRATION WA-11 -CALD WALL ASSEMBLIES:

Information regarding the results of the water penetration trials of WA-11 is provided in Table 5.2 and Table 5.3 and Figure 5.5. Water was observed from the onset of the tests to penetrate imperfections in sealant jointing around the perimeter of the window, in particular the flange above the window, however entry was also observed at the base of the window. The later observation likely resulted in the eventual activation of MS-21 located beneath the window well. Over the course of the continuous16-h test sequence (Stage 3), MS-11 was activated, most likely due to a build up of water at the base of the test specimen.

5.2.1.3 WATER PENETRATION WA-12 -CALD WALL ASSEMBLIES:

Results on moisture sensor activation are provided in Figure 5.6; additional information is given in Table 5.2 and Table 5.3.

Over the course of the static and dynamic test sequences no moisture sensors were activated although MS-21 did indicate the presence of moisture but was subsequently found to be inoperative. There was considerable evidence of water entry as a number of troughs collected water. Entry was observed to occur at the 500 Pa ΔP_S; additional water flowed to the troughs at the 1000 Pa ΔP_S. Following the static test sequence, the quantities of water collected in the different troughs during this test was determined and the results are provided in Table 5.4.

The greatest amounts of water were collected about the window; trough TW-W located directly beneath the deficiency collected 130 mL and the adjacent trough (TW-B), used to collected water from the back of the cladding, collected 14 mL. Both of these troughs are directly above trough T4 in which considerable water was collected over the course of the test sequence; 138 mL in T4-B and 56 mL in T4-W. These values should be compared to those obtained for the electrical outlet, D-B (70 mL) and the ventilation duct, V-B (45 mL) both of which collected significant amounts of water.

Table 5.4 - WA-12: Collection of water in troughs during water penetration trials

Tr.	Water entry, mL	
	Location	
	B	W
D	70	
V	45	
W		
TW	130	14
T1	20	70
T2		30
T3		15
T4	56	138
T5		92

Other troughs for which results are tabulated include, 70 mL in T2-W and T1-B respectively, 30 mL and 20 in trough T2-B, 15 mL in T3-B and 92 mL in T5-B

The majority of the collection was in troughs servicing the backside of the cladding (troughs “B”) although significant amounts were collected in TW-W (130mL) as previously stated. That a good potion of water entry was collected in the “B” trough at the window, ventilation duct of electrical outlet is understandable given the configuration of the troughs in the drainage space and their proximity to potential points of water entry.

A limited number of sensors were activated during the 16-h continuous water spray sequence including MS-2, -26, and –37. Moisture sensors –2 and –37 were regarded as false positive results whereas MS-26 reflects the presence of moisture accumulation in the area beneath the window where it has already been determine that considerable moisture is present.

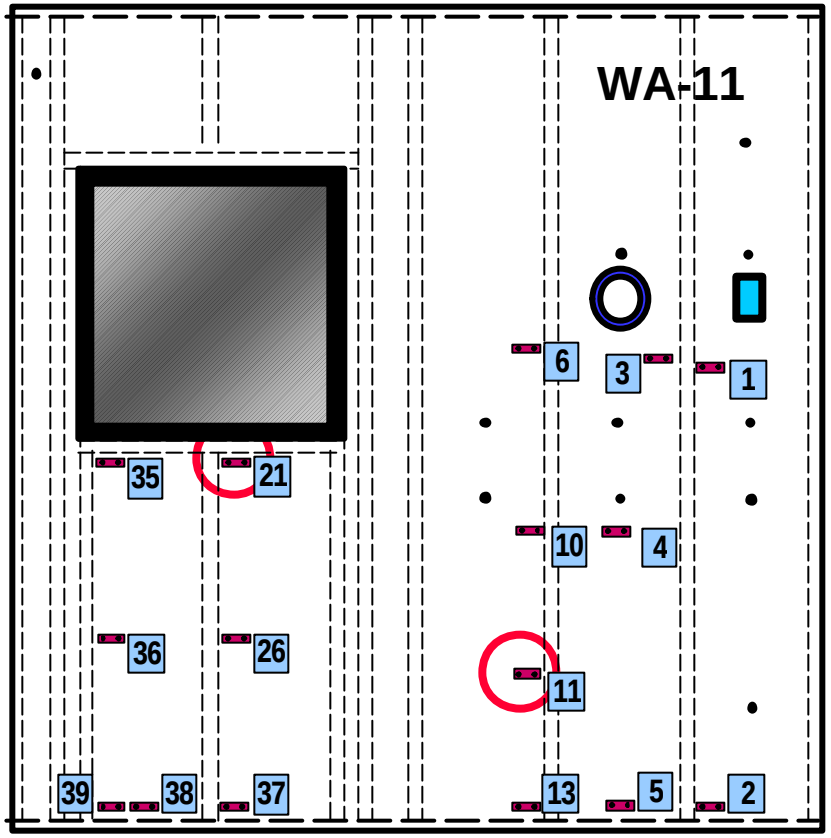

Figure 5.5 - WA-11: During static & dynamic tests - Water entry about window; MS-21activated; After continuous water spray of 16-h (0.4 L/min.-m^2 at 50 Pa) MS-11 activated.

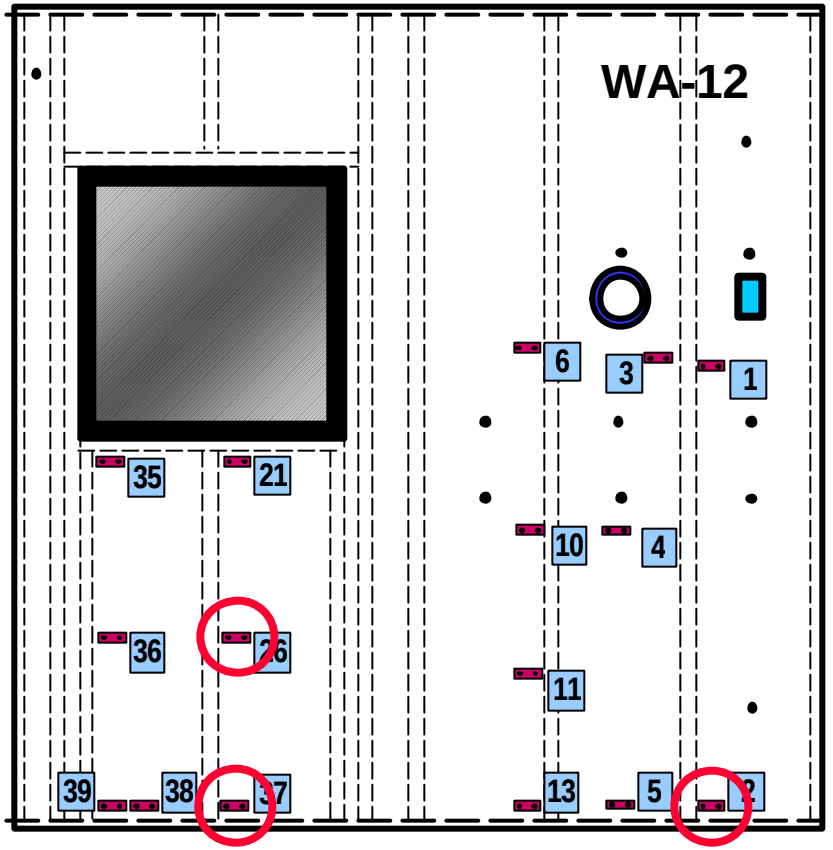

Figure 5.6 - WA-12 : No sensors activated over course of either static or dynamic trials; water entry observed at 500 Pa ΔP_S at electrical ; water entry @ 1000 Pa ΔP_S; water entry evident in other collectors; After 16-h continuous MS-2 and MS-37 - due to seepage at base; MS-26 - possible seepage about window

5.2.1.4 WATER PENETRATION WA-13 - MASONRY WALL ASSEMBLIES:

No water was observed in any of the collection troughs and neither were moisture sensors activated over the course of either the static or dynamic test sequences (MS-37 was activated but was inoperative). However a number of sensors were activated during stage 3 of the test protocol (16-h continuous water spray of 0.4 L/min.-m2 and 50 Pa pressure differential) as provided in Table 5.3 and Figure 5.7. Of the seven (7) sensors activated only MS-2 and MS-27 were activated due to local water penetration to the fiberboard in which the pin pairs were placed. The remaining five (5) moisture sensors were located at the base of the specimen and were determined as false positive results given the amount of water that had collected in the stud cavity at the base of the wall in their proximity.

5.2.1.5 WATER PENETRATION WA-14 MASONRY WALL ASSEMBLIES:

No water was collected in any of the troughs during stage 2 or 3 of the test (Table 5.2). Information regarding the activation of moisture sensors is provided in Table 5.5 and Figure 5.8. Of the sixteen (16) sensors used in the test five (5) of these were inoperative prior to the start of the test sequences. No activity was recorded in the static test sequence however, of the remaining eleven (11) functional moisture sensors, five were activated during the dynamic test sequence and included:

Table 5.5 – Activation of **moisture sensors (MS)** in WA-14

MS	**Time** (min.)	Δ**P$_D$***	**Spray rate**	**ABSL** *(L/s-m^2)*
MS-6	45	300	3.4	0.5
MS-10	21	150	3.4	0.5
MS-26	51	300	3.4	0.5
MS-11	70	700	3.4	0.2
MS-38	55	300	3.4	0.2

*ΔP_D : Dynamic differential pressure level

Following this test sequence, MS-4 (circled green in Figure 5.8) was activated during the 16-h of continuous water spray test. This sensor is located below the electrical outlet and although no water was recorded to have entered the trough servicing this component, it is likely that the outlet would be the source of moisture in proximity to the location of MS-4

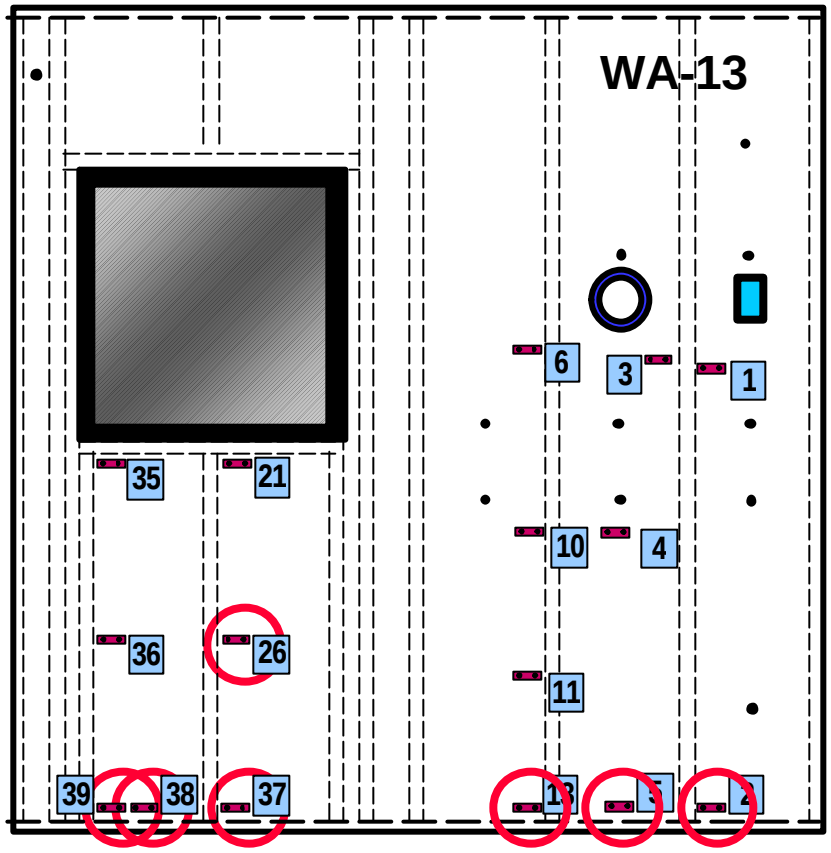

Figure 5.7 – WA-13: During static & dynamic tests - Water entry about window; After 16-h continuous spray: Moisture sensors activated: MS-26; Activated due to seepage at base of wall: MS-2, -5, -13, -37, -38, -39

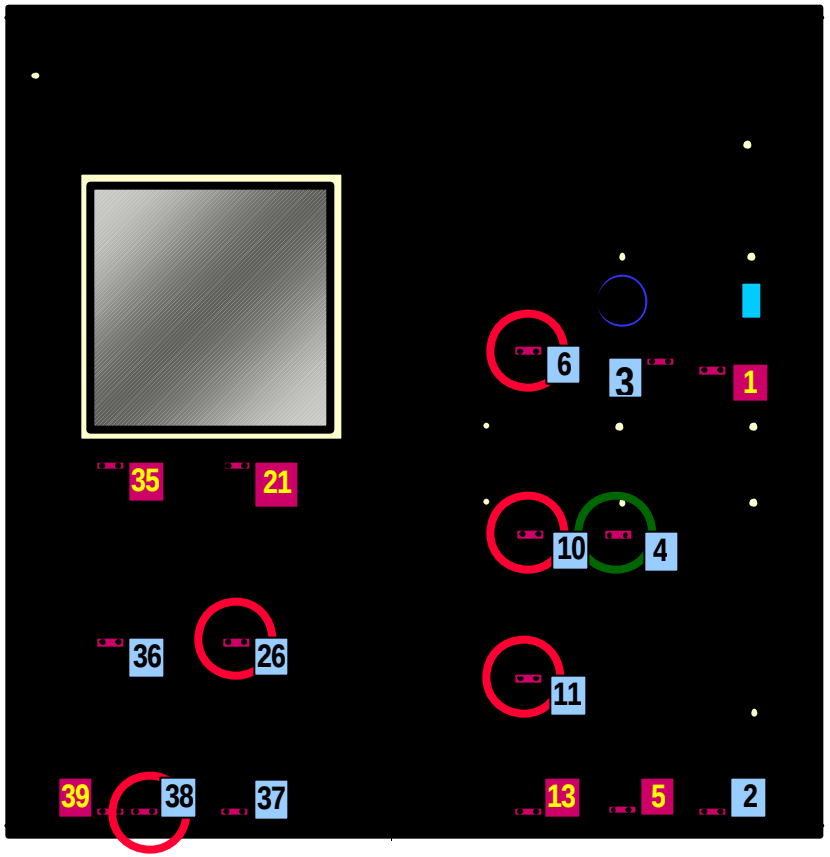

Figure 5.8 – WA-14: No water entry observed during static test; MS activation during dynamic trials, MS-6 (300 ± 125 Pa); MS-10 (150 ± 60 Pa); MS-11 (700 ± 300 Pa); MS-26 (300 ± 125 Pa); MS-38 (300 ± 125 Pa); MS-4 activated during 16-h continuous water spray

5.2.1.6 SUMMARY OF WATER PENETRATION FOR MASONRY WALL ASSEMBLIES

Water entry at through-wall penetrations was evident for all locations, in particular windows (3 of 4 walls); however no water was observed to have penetrated to the stud cavity. This is an expected result given the presence and size of the drainage space incorporated in each of these walls. Note that deficiencies are not yet incorporated in wall specimens when subjected to water penetration tests.

On the basis of these tests, no apparent advantage is offered a wider space (i.e. 25-mm vs. 50-mm) in regard to reducing water entry to the space. Although it is safe to assume that the wider space (50-mm) renders it less likely that water will access the sheathing membrane as compared to a 25-mm space. This aspect is dealt with in more detail in the section on water entry.

The low level of moisture sensor activity in these walls is indicative of reasonable water management attributes incorporated in the assembly. The results are hence to be expected given the nature, intensity and longevity of the performance test that notably exceed requirements set out in existing industry standards.

Results clearly show that inadvertent water entry is highly likely if care is not taken to properly seal joints at the interfaces with penetrations. All of the water entry activity at the various points of entry are indicative of the significant amounts of water that can collect in a short period of time under unfavorable climate conditions (i.e. high and prolonged intensity of wind-driven rain). Considering that every care had apparently been taken to insure the water tightness of the specimens by the sealing of joints at the different through wall penetrations (i.e. windows, electrical outlet, and ventilation duct) water nonetheless found a means to penetrate the joint seals and enter. This was particularly evident for WA-12. This wall assembly was the first of the four in the series to be tested. Greater care was taken in preparing the remaining specimens as was evident from the results reported in Table 5.2 that show a reduction in the number of incidents of water entry about the through-wall penetrations.

It is useful to reflect on the degree of care typically taken to assemble wall cladding in current construction practice as compared to that which was used in preparing the laboratory specimens and the expected ability of cladding and assemblies in the field to resist water penetration. Given the level of workmanship in practice issues of water tightness of the cladding will evidently continue to be of importance no matter what systems have been devised to mitigate the consequences of inadvertent water entry. However, those systems offering the

greatest redundancy with respect to the management of water passing the cladding likely provide the least potential for such issues to develop.

5.2.2 Assessment of Water entry through specified deficiencies

5.2.2.1 Introduction

Water entry assessments through specified deficiencies were used determine the quantities and rates of water that might enter deficiencies of known type, size and location on the cladding when subjected to simulated climatic extremes using the DWTF. Levels of water spray and pressure differential were consistent with related climatic data of rainfall and wind speed that might occur in an extreme climatic event within a 10 year period in North America. This information provided a basis for a systematic and consistent means of transferring input to hygIRC, the hygrothermal model used in the MEWS parametric analysis.

Results from water entry are presented in sequence where entry rates about specified through-wall penetrations are reviewed for all wall assemblies in relation to the range of values obtained in static and dynamic conditions. The review follows the sequence provide in Table 5.6 in which the collection of water, designated by the symbol (●), is identified for each of the troughs whereas instances where no water was collected in denoted by the symbol (✕).

Hence the initial review starts with water collection rates for troughs servicing the deficiency above the electrical outlet (D). Note that the outlet does not extend into the stud cavity hence no collection trough was included there.

The presentation of the subsequent results thus includes a similar treatment of the information for the ventilation duct (V and L), following which results are offered for troughs located about the windows (TW and W). These also include results obtained from troughs servicing the window (beneath frame and covering sill) located in the stud cavity (W).

An overview of results of water collection is provided in which a comparison is made of collection in troughs T1 to T5 offering an indication of the relative quantities collected in the different troughs and their significance in relation to the location of the deficiencies.

The final section provides a summary of the entry results including information regarding the water entry function.

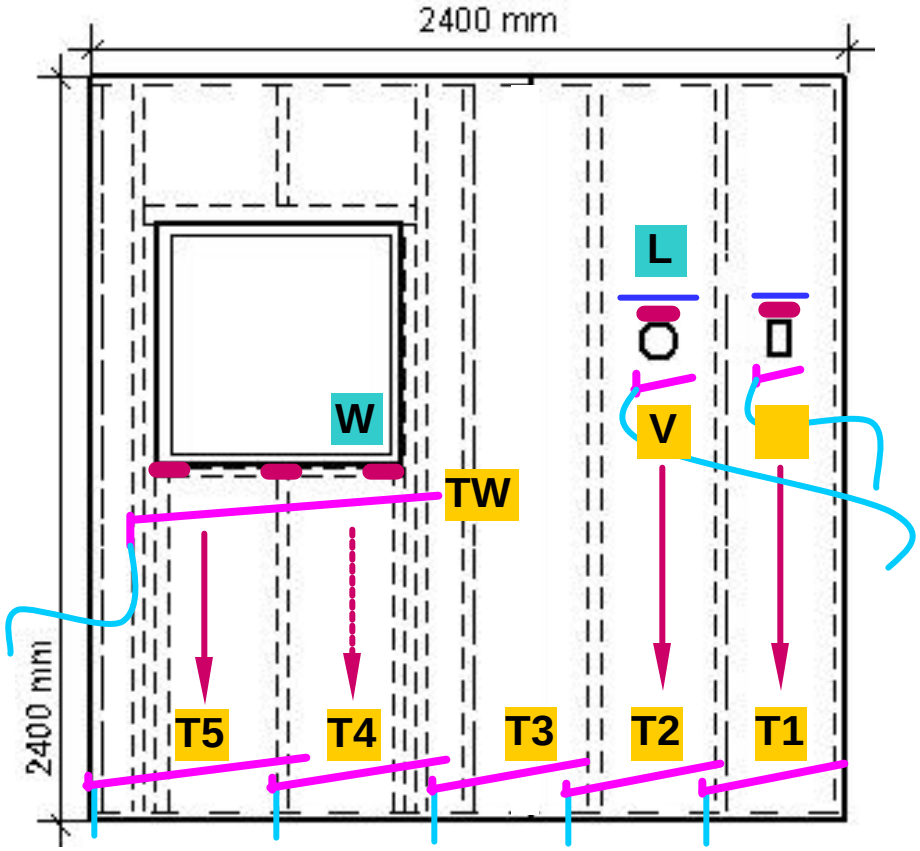

Figure 5.9 - Location of collection troughs

Table 5.6 – Collection of data in various troughs for brick masonry veneer walls

Trough Location		Masonry WA			
		11	12	13	14
D	B	●	●	×	●
	W	×	×	×	×
V	B	●	●	●	●
	W	×	×	×	×
TW	B	×	●	●	×
	W	×	●	●	×
T1	B	●	●	●	●
	W	●	●	●	×
T2	B	●	×	●	●
	W	×	●	●	●
T3	B	●	×	●	●
	W	×	●	●	×
T4	B	●	●	×	●
	W	×	●	●	×
T5	V	●	×	×	×
	W	×	●	●	×
L		●	●	×	●

● - water collected; × - no water collected

5.2.2.2 WATER ENTRY THROUGH SPECIFIED DEFICIENCIES AT ELECTRICAL OUTLET

Results from troughs D-B and D-W are provided in Table 5.7 and in Table 5.8 those results of troughs T1-B and –W located in the same space, but below that of trough D. The results of trough "T1" were included because substantial water was collected in this trough likely the uncollected run-off from trough D above it. Selected examples highlighting the particular trends observed from these results are further illustrated in Figures 5.10 and 5.11.

Results provided in Table 5.7 show that water is most likely to collect in trough "B" (back of brick cladding) as compared to "W" (adjacent to sheathing). Essentially, no water was collected in trough "W" of stage 5 and was only collected in "W" for stage 6 of WA-13 for both the static and dynamic test conditions. Even in this particular instance, results were sporadic in that collection was observed only at the higher spray rates (i.e. 3.4 L/min.-m^2).

Water that was collected in troughs "B" occurred for WA-11 and WA-12; WA-14 only provided results in the static conditions for stage 5 and limited results were obtained in stage 6 of WA-13.

The values obtained for WA-11 and WA-12 in stage 5 are comparable in that the range of values is the same; i.e. 0.11 to 0.16 L/min. collected in "D-B" of WA-11 as compared to 0.11 to 0.158 L/min. of the same trough of WA-12. The range of values between test carried out in static as compared with dynamic conditions were likewise similar for either WA-11 and WA-12 of stage 5 and in the case of WA-12, the similarity in range of values is extended as well to the results of stage 6.

Table 5.7 – Brick masonry veneer walls: Water entry rates through deficiency above electrical outlet collected in troughs "D-B" and "D-W" in static and dynamic test conditions - Stages 5 & 6

WA	Trough D	Water entry - Range of Values L / min.					
		Stage 5			Stage 6		
		Static	***Dynamic*** *ABSL 0.2 L/s-m^2*	***Dynamic*** *ABSL 0.5 L/s-m^2*	***Static***	***Dynamic*** *ABSL 0.2 L/s-m^2*	***Dynamic*** *ABSL 0.5 L/s-m^2*
11	**B**	0.11 – 0.16	0.112 – 0.16	0.115 – 0.16	N/C	N/C	N/C
	W	0	0	0	N/C	N/C	N/C
12	**B**	0.11 – 0.158	0.081 – 0.148	0.10 – 0.14	0.076 – 0.108	0.089 – 0.117	0.081 – 0.106
	W	0	0	0	0	0	0
13	**B**	0	0	0	0	0	0
	W	0	0	0	0 – 0.02	0 – 0.006	0 – 0.05
14	**B**	0 - 0.01	0	0	0	0	0
	W	0	0	0	0	0	0

Water entry results for trough T1 (Table 5.8) indicate that for stage 5, water was collected in the static and dynamic conditions and collection was made typically in both the “B” and “W” troughs with the exception of trough “W” of WA-14 in which no results were secured.

Interestingly, a comparison of results of trough T1 with those of D suggests that where water was not collected in the upper trough it might nonetheless be collected in the lower one. This is particularly relevant to WA-13 in which no collections at the upper troughs was made but for which comparatively significant values were recorded in the lower trough T1-B and less important amounts in T1-W. This suggests that the upper trough experiences some blockage and that the runoff from the blocked trough collected in the lower ones. The magnitude of the results from the lower trough appears to be comparable to say results obtained in the upper trough of WA-11 of WA-12, thus supporting this notion.

In any case, it is clearly evident that significant amounts of water can accumulate in the drainage space given merely the sustained presence of water on the cladding surface as shown in Figures 5.10 and 5.11. Illustrated in Figure 5.10 are the water entry rates to trough D-B (none obtained for D-W) at various spray rates and different static pressure levels. These results indicate that water entry rates when no pressure is applied across the assembly are as significant as when a pressure differential is applied. As well, rates of entry are essentially independent of the pressure level and neither are they directly related to the spray rate. Water appears to be as likely to enter at rates obtained at the lowest spray rate and pressure level as they are to for the highest spray rate and pressure level.

Table 5.8 – Brick masonry veneer walls: Range of water entry rates through deficiency above electrical outlet collected in troughs “T1-B” and “T1-W” in static and dynamic test conditions

WA	Stage5	COLLECTION TROUGH - T1		
	Trough **T1**	**Water entry - Range of Values L / min.**		
		Static	***Dynamic*** *ABSL 0.2 L/s-m^2*	***Dynamic*** *ABSL 0.5 L/s-m^2*
WA-11	B	0.020 - 0.026	0.020 - 0.021	0.020 - 0.021
	W	0.020 – 0.033	0.021 – 0.029	0.020 – 0.030
WA-12	B	0.035 – 0.040	0.027 – 0.030	0.025 – 0.030
	W	0.0006 – 0.005	0.005 – 0.011	0.004 – 0.012
WA-13	B	0.084 – 0.120	0.11 – 0.162	0.11 – 0.152
	W	0 – 0.010	0.001 – 0.015	0.009 – 0.016
WA-14	B	0.134 – 0.170	0.117 – 0.161	0.125 – 0.169
	W	0	0	0

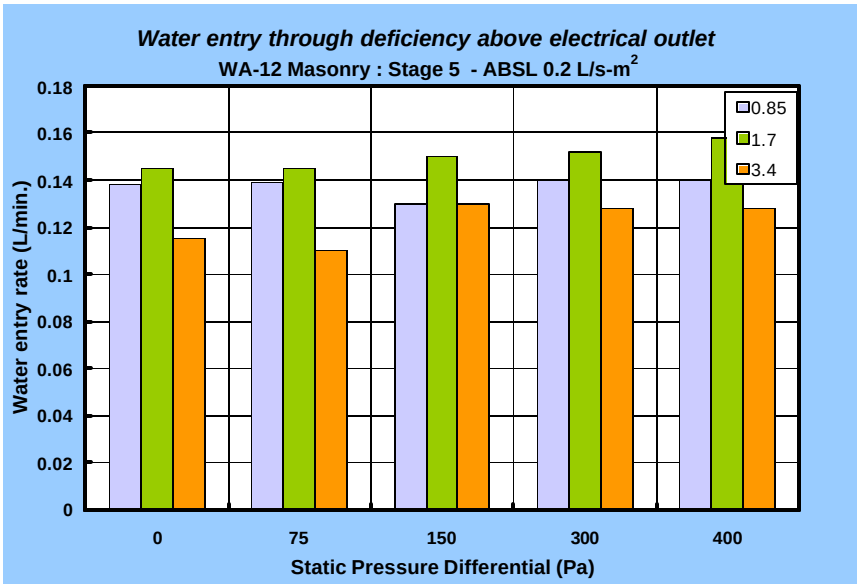

Figure 5.10– WA-12 (brick masonry veneer): Water entry rates through deficiency above electrical outlet as a function of static pressure and spray rates for Stage 5

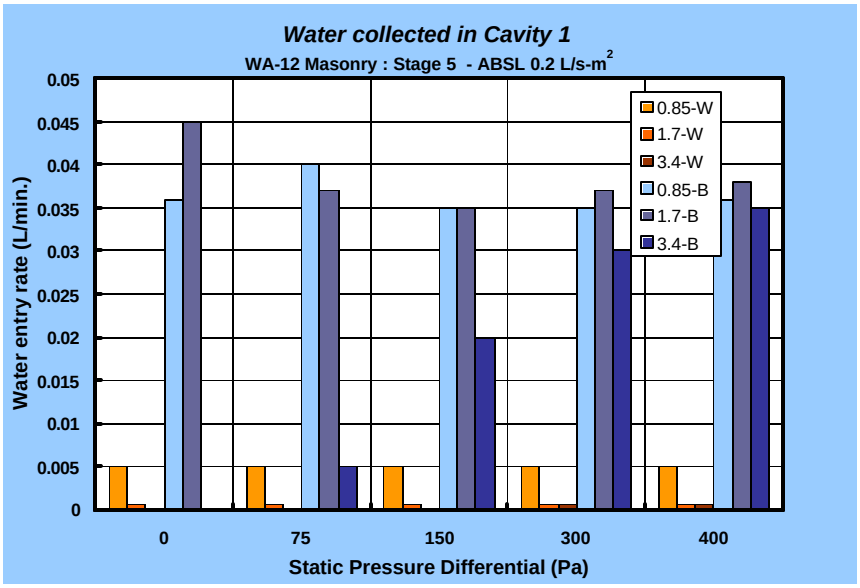

Figure 5.11– WA-12 (Brick masonry veneer): Water collection rates for troughs T1-B and T1-W (below electrical outlet) as a function of static pressure and spray rates for Stage 6

That the rates of entry are not a function of pressure differential is an expected result given that the cladding is vented and hence little or no differential likely exists across the entry points. That the rates of entry are neither related to the spray may be attributed to the size of the entry point. If the orifice at the point of entry is occluded by water deposition at the lowest spray rate, it is more than likely that at higher spray rates the same condition will hold and in the absence of

any driving pressure, no additional water can pass the opening. Hence the orifice at the entry point is passing the maximum quantity it can supply under gravity conditions and the spray rates employed in these test conditions.

Provided in Figure 5.11 are rates of entry to trough T1-B and –W as a function of spray rate and static pressure level. The maximum rates of entry to trough T1-B are about three times less than the upper trough (D-B) and the rates also appear not to be dependent on pressure levels or spray rate. The values for trough T1-W are considerably less important than those of the adjacent trough; rates of collection vary between ca. <0.001 and 0.005 L/min. or about an order of magnitude less than T1-B (Table 5.8).

5.2.2.3 WATER ENTRY THROUGH SPECIFIED DEFICIENCIES AT VENTILATION DUCT

Information for the ventilation duct, in which the range of water entry rates for V-B and –W as well as trough L are compared (Table 5.9) and results from trough T2, located in the space below trough V, are given in Table 5.10. Again, specific results are illustrated in Figure 5.12.

Note that no testing was completed for stage 6 (backer rod in place – no sealant) of WA-11 since it was determined from a test of Stage 7 (no sealant or backer rod in place) that completing this test was unlikely to offer additional insights into the comportment of the wall assembly.

Table 5.9 – Range of water entry rates for the Ventilation Duct (V) and Trough "L" in Stage 5 for masonry veneer clad assemblies

WA	Trough V	Water entry - Range of Values L / min.					
		Stage 5			Stage 6		
		Static	***Dynamic*** *ABSL 0.2 L/s-m^2*	***Dynamic*** *ABSL 0.5 L/s-m^2*	***Static***	***Dynamic*** *ABSL 0.2 L/s-m^2*	***Dynamic*** *ABSL 0.5 L/s-m^2*
11	**B**	0.009–0.185	0.02 – 0.17	0.02 – 0.173			
	W	0	0	0			
	L	0 – 0.01	0	0			
12	**B**	0.023 – 0.13	0.025 – 0.155	0.03 – 0.146	0.02 – 0.16	0.028 – 0.169	0.023 – 0.175
	W	0	0	0	0	0	0
	L	0 – 0.05	0 – 0.056	0 – 0.08	0 – 0.011	0 – 0.029	0 – 0.020
13	**B**	0 – 0.029	0 – 0.032	0 – 0.04	0 – 0.05	0 – 0.043	0 – 0.045
	W	0	0 – 0.045	0	0	0	0
	L	0	0	0	0	0	0
14	**B**	0.021–0.074	0.025 – 0.07	0.029–0.079	0.021 – 0.06	0.012 – 0.053	0.02 – 0.057
	W	0	0	0	0	0	0
	L	0 – 0.047	0 – 0.020	0 – 0.025	0	0 - 0.023	0 – 0.028

Water entry was recorded in trough “B” for all masonry wall assemblies and for both test stages 5 (sealant and backer rod in place) and 6. As was the case for the electrical outlet (trough D), little water was collected in troughs “W” (i.e. V-W) for all walls tested. However, irrespective of whether water was collected in trough “W”, the trough closet to the sheathing board, in stage 5 water entered trough “L” for both WA-12 and WA-14 and in limited amounts in static conditions for WA-11. This provides a clear indication of the path of water flow from the entry point at the top of the duct on the cladding proper to the underside of the duct and thereafter into trough L. The linkage provided by the duct is significant in that regardless of the presence of a drainage space, water can nonetheless enter into the stud cavity using the duct as a pathway.

Figure 5.12, provides a comparison of collection rates in troughs “B” and “L” as a function of static pressure differential and sprays rates for stage 5 in which both sealant and backer rod are in place. Only a small opening is available for water to pass at the base of the ventilation duct (i.e. 2-mm high x 50-mm long). At no and low pressure (75 Pa), entry to trough “B” is maximum and increases in relation to the spray rate; in comparison, entry to trough “L” in much less and only enters at the highest spray rate. As test pressures increase, so too do entry rates in trough “L” but again at the highest spray rate; rates of entry to trough “B” diminish at the higher spray rate in comparison to rates obtained at no pressure differential. This trend continues at the 150 and 300 Pa ΔP_s: rates of entry to “L” increase at all spray rates; entry rates diminish to “B” in like proportions.

Hence as illustrated in this figure, greater amounts are deposited in trough “L” at 300 Pa ΔP_s at the highest spray rate as compared to trough “B” at the same pressure level and spray rate. This further demonstrates that entry to within the wall cavity can readily occur and in significant amounts regardless of the presence of features such as drainage spaces provided there is present a through-path for water to flow and conditions are appropriate for flow to take place.

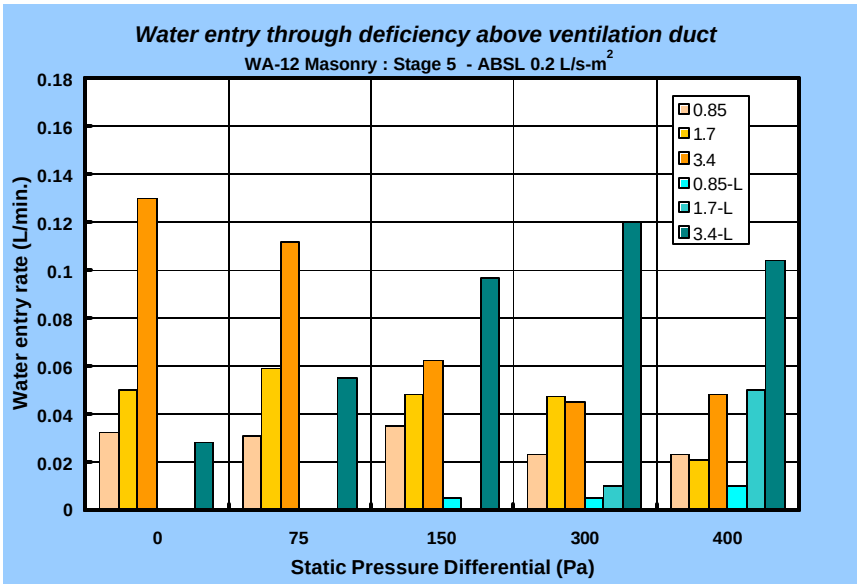

Figure 5.12– WA-12 (Brick masonry veneer) Water entry through deficiency above ventilation duct as a function of static pressure and spray rate – Stage 6 test conditions

The preceding example provides some insights into how water passes from the entry point at the deficiency to within the wall system given the precautions taken to seal the interface between through-wall penetrations, in this case the ventilation duct. The manner in which water entry occurs at this penetration when tested with different configurations at the interface seal as is provided in stages 6 and 7 is also of interest.

A review of the results from the various stages of WA-14 provides some useful indicators as to the conditions necessary for water entry. In WA-14, as was previously mentioned, water is always present in trough "V-B" for all stages and test conditions (i.e. static and dynamic), indicating that water freely enters the deficiency and hence can potentially access both the "W" and "L" troughs further within the wall assembly. Likewise, water is present at trough "L" for all stage 5 test conditions. In the case of stage 6 (backer rod in place – no sealant), water was present in "L" only in the dynamic test conditions and in these instances only at the higher spray rates and dynamic pressure level (ΔP_D). Finally, no water was observed in trough "L" for any of the test conducted in stage 7 (sealant and backer rod removed). The explanation for this is not evident however based on the information provided it appears that the pressure difference at the small opening at the base of the ventilation duct of stage 5 is sufficient to drive water through it whereas such potentials apparently are not evident in stage 7 given that no barrier to air flow exists at the perimeter of the duct at this test stage. The intermittent values obtained for entry in stage 6 suggest that some pressure difference exist at the interface due to the presence of the backer rod.

The path for water entry about the ventilation duct is illustrated in Figure 5.13 that show a sectional view of WA-12 at the duct. Water is seen to proceed from the entry point at the deficiency to the backside of the cladding where it might collect in trough “B”, as was demonstrated previously. It has also been shown that water might proceed to the underside of the duct and pass into the stud cavity to be collected in trough “L”. Water not passing at this point would collect in alternate troughs, potentially “W” (although no collection was observed) but also in the lower trough “T2” located in the drainage space beneath the ventilation duct.

These results clearly highlight the importance of adequate design and sealing practice of interface joints at through-wall penetrations even for wall assemblies that incorporate a drainage space and similar water management systems.

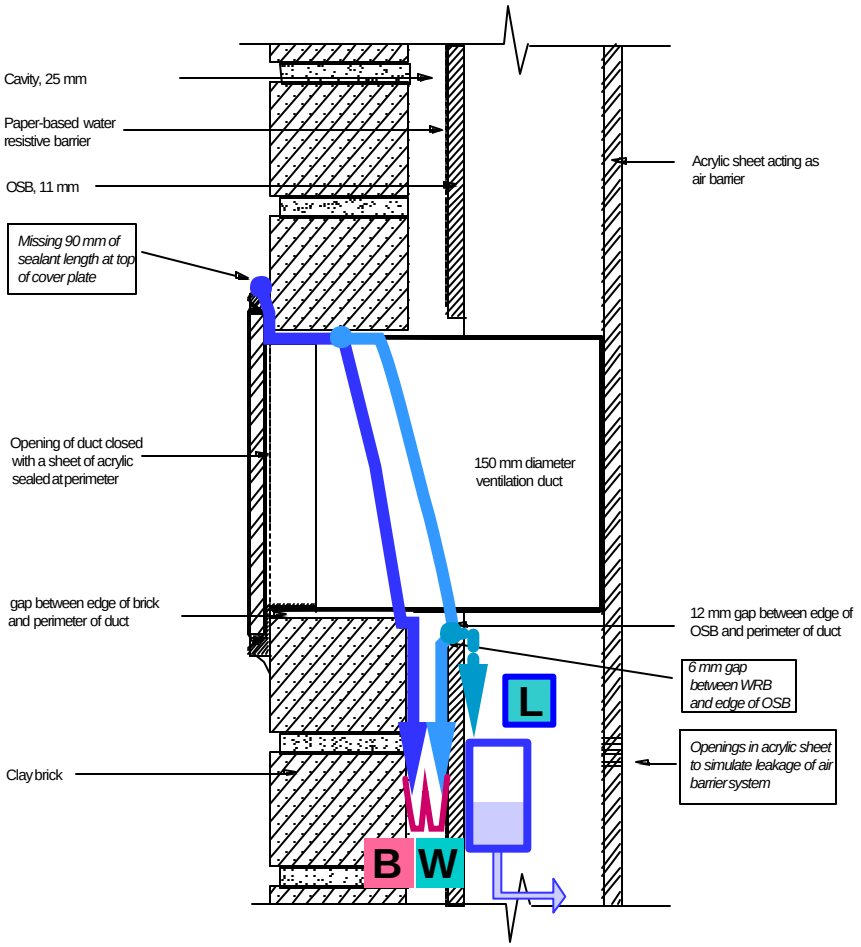

Figure 5.13– WA-12 (Brick masonry veneer) Sectional view through wall assembly at ventilation duct showing path of water entry into stud cavity and drainage space.

Results also show that comparable rates of entry are obtained for static as compared to dynamic test conditions in all stages where results were obtained for both test conditions. For example (Table 5.10):

- WA-11 provided a range of values for trough "V-B" in the static mode of 0.009 – 0.185 L/min. as compared to 0.02 – 0.17 L/min. in the dynamic mode (ABSL 0.2 L/s-m^2);
- WA-12 the range of values for the same trough was 0.023 – 0.13 in static as compared to 0.025 – 0.0155 L/min. in the dynamic mode;
- WA-13: 0 – 0.029 and 0 – 0.032 in the static and dynamic mode respectively;
- WA-14: 0.021 – 0.074 in static as compared to 0.025 – 0.07 L/min. in the dynamic mode.

A comparison of entry rates for the ABSL of 0.5 as compared to 0.2 L/s-m^2 shows that rates of entry are slightly greater when the ABSL is 0.5 L/s-m^2. For example, in Stages 5 and 6 the following information is provided from Table 5.9:

- Stage 5 □ : 0.5 L/s-m^2 | 0.2 L/s-m^2 0.029 – 0.079 | 0.025 – 0.070 L/min.;
- Stage 6 □ : 0.5 L/s-m^2 | 0.2 L/s-m^2 0.020 – 0.057 | 0.012 – 0.053 L/min.

Collection of water in the trough "T2" located beneath the ventilation duct in the drainage space provided results as shown in Table 5.10 for stage 5. Results from this stage are generally indicative of the range of results obtained in stages 6 and 7; water was collected prmari9y in trough "B" and rates of entry were roughly an order of magnitude less that in those obtained for trough "V-B" in the same space above. As well, results from dynamic tests are similar in range as those obtained in the dynamic test mode. For results obtained in the dynamic mode, the range of results for water entry for ABSL of 0.2 L/s-m^2 is similar to that retrieved at 0.5 L/s-m^2 for all walls evaluated.

Table 5.10 – Brick masonry veneer assemblies: Range of water entry rates in static and dynamic test mode for trough "T2" located beneath ventilation duct in drainage space for Stage 5

WA	Stage 5	Water entry - Range of Values L /min.		
	Collection Trough	***Static***	***Dynamic ABSL 0.2****	***Dynamic ABSL 0.5***
WA-11	B	0.010 – 0.025	0.017 – 0.022	0.015 – 0.024
	W	0	0	0
WA-12	**B**	0.017 – 0.043	0.005 - 0.021	0.011 – 0.019
	W	0	0	0
WA-13	**B**	0.041 – 0.10	0.060 – 0.112	0.060 – 0.118
	W	0 – 0.005	0 - 0.004	0 - 0.001
WA-14	**B**	0.018 – 0.075	0.039 – 0.088	0.050 – 0.090
	W	0 – 0.010	0 – 0.010	0 – 0.010

5.2.2.4 WATER ENTRY THROUGH SPECIFIED DEFICIENCIES AT WINDOW

Results from water entry at the window for stages 5 and 7 are proved in Table 5.11 and Figures 5.15. Figure 5.14 is a sectional view of WA-12 at the window opening and illustrates the path of water flow from the point of entry at the deficiency to the collection troughs "TW" located in the drainage space.

For WA-11 and WA-12, no tests were conducted in the dynamic mode of stage7 given that results obtained in the static mode yielded results that confirmed those obtained in stage 5. Results from stage 6 (not provided) were completed for WA-12, WA-13 and WA-14. The results obtained in this stage were similar to those obtained in stage 5; collection was made (or not) in the same troughs and within the same range of values of entry rate.

A review of the information provided in Table 5.11 shows that no water entry was observed in any of the troughs servicing the window of WA-14 in any of the stages or test conditions. This unexpected result suggests that either the entry points or collection trough were in some manner obstructed, as entry to "TW-B" should occur, as is evident from results of WA-12 and WA-13. A similar incident is apparent for WA-11 for which no water was collected in trough "TW-B". That water did enter the deficiencies about the windows is unmistakable given that water was collected in troughs "T4" and "T5" located in the drainage space directly below trough "TW". Hence it is likely that these upper troughs were indeed blocked and that water entry through the deficiency at the window-wall interface was made in troughs "T4" and "T5".

Table 5.11 – Masonry veneer clad assemblies: Range of water entry rates in static and dynamic test mode for troughs servicing windows for Stage 5 and 7

WA	Collect Tr.	***Water entry — Range of Values L / min.***					
		Stage 5			*Stage 7*		
		Static	***Dynamic*** *ABSL 0.2*	***Dynamic*** *ABSL 0.5*	***Static***	***Dynamic*** *ABSL 0.2*	***Dynamic*** *ABSL 0.5*
WA-11	**B**	0	0	0	0	N/C	N/C
	W	0	0	0	0	N/C	N/C
	LS	0 – 0.015	0 – 0.015	0 – 0.007	0	N/C	N/C
	RS	0.06 – 0.076	0.04 – 0.092	0.08 – 0.098	0.058 – 0.102	N/C	N/C
WA-12	**B**	0.036 – 0.042	0.03 – 0.032	0.028 – 0.032	0.022 – 0.009	N/C	N/C
	W	0.005	0.009	0.007 – 0.010	0.006 – 0.009	N/C	N/C
	LS	0	0	0	0	N/C	N/C
WA-13	**B**	0.03 – 0.086	0.04 – 0.10	0.045 – 0.12	0.074 – 0.09	0.09	0.115
	W	0 – 0.009	0	0	0	0	0
	LS	0	0	0	0	0	0
WA-14	**B**	0	0	0	0	0	0
	W	0	0	0	0	0	0
	LS	0	0	0	0	0	0

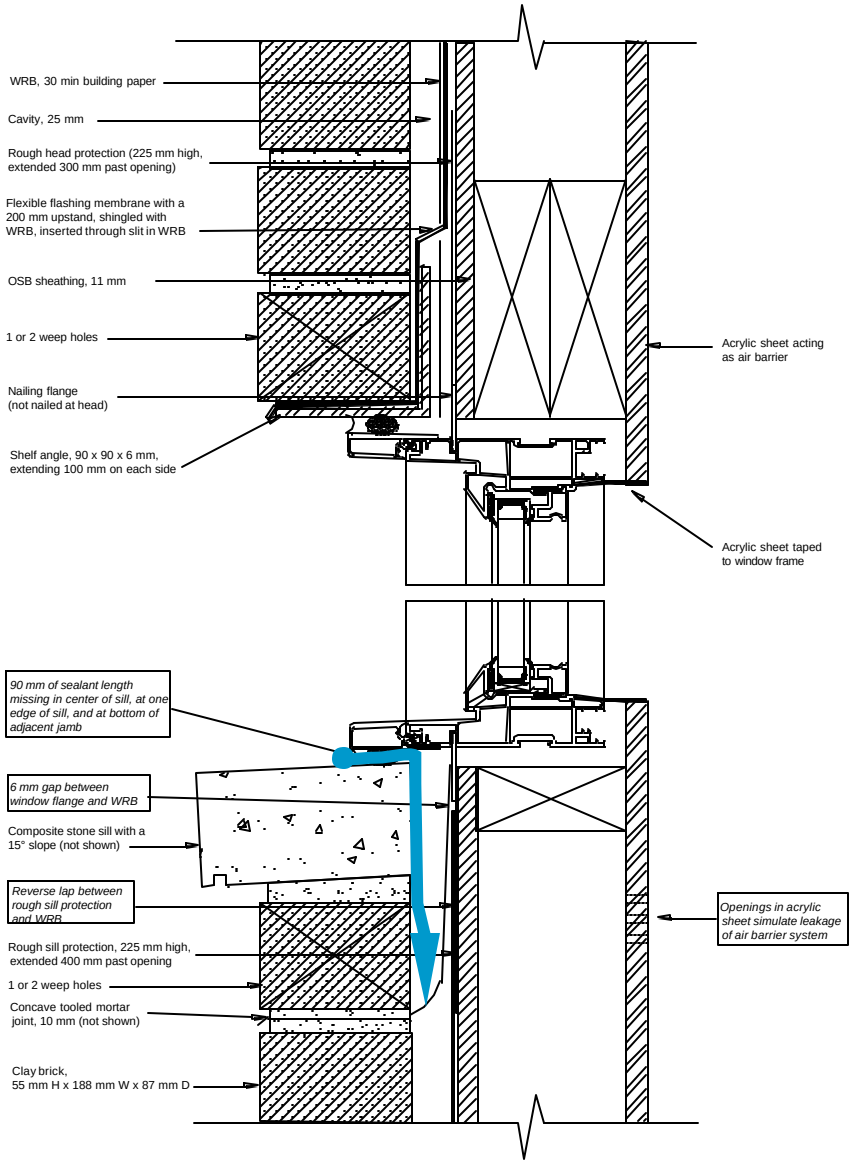

Figure 5.14– Section view of WA-12 at window opening showing water entry path from deficiency to collection troughs

Furthermore, the rates of collection in these two troughs were in the same range as those observed for "TW-B" of WA-12 and WA-13. For example, in the static mode (stage 5), the following results were obtained:

<u>"TW-B" (upper trough)</u>

- WA-12: 0.036 – 0.042 L/min.;
- WA-13: 0.03 – 0.086 L/min.;

<u>"T4-B" (lower trough in same space)</u>

- WA-11: 0.008 – 0.012 L/min.;
- WA-14: 0 – 0.012 L/min.

Of the wall assemblies tested, only WA-11 had water entry collected in troughs inside the stud cavity, namely troughs W-LS and W-RS. Water entry of both of these troughs is significant (e.g. 0 to 0.015 and 0.03 to 0.076 L/min. for W-LS and W-RS respectively at ΔP_S – stage 5) and further confirms the results revealed in the water penetration trials.

This is additional confirmation of the need to adequately prepare water management details for through-wall penetrations. In this instance, water entering the stud cavity at the sill should be drained to the space between the cladding and sheathing. The fabrication details of a "flanged" window, as were all windows in these wall specimens, are such that there is also a lower flange that hinders the placement of a drainage basin emptying into this space. However removal of this flange would provide the necessary clearance to install the sub-sill drainage "basin".

Typical trends for water entry to troughs "TW-B" and "TW-W" are provided in Figure 5.15 for which entry rates in stage 5 are given in relation to the static pressure levels and spray rates. These results show that rates of entry for TW-W are about three time less than those of TW-B; values for rates of entry (L/min.) range between 0.007 – 0.010 as compared to 0.029 - 0.035 for "TW-W" and "TW-B" respectively.

The results also indicate that considerable water can enter under gravity alone, where no pressure differential exists across the assembly (i.e. at 0 Pa). In this instance, rates of entry vary between 0.023 and 0.04 L/min. (at spray rates of 0.85 and 3.4 L/min.-m^2 res.).

In addition, the results suggest that rates of entry are independent of pressure level for either trough; no discernable increase in entry rates is apparent for corresponding increases in pressure level with the exception of entry rates in "TW-B" at the highest spray rate. In this instance, slight increases in entry rate are observed for corresponding increase in pressure level. This indicates that the entry point is not occluded at lower rates but becomes so at the higher spray rate.

Indeed, at most pressure levels, with the exception of the 400 Pa ΔP_S, entry rates are not contingent on spray rates although at 400 Pa ΔP_S there is slight dependence on the spray rate.

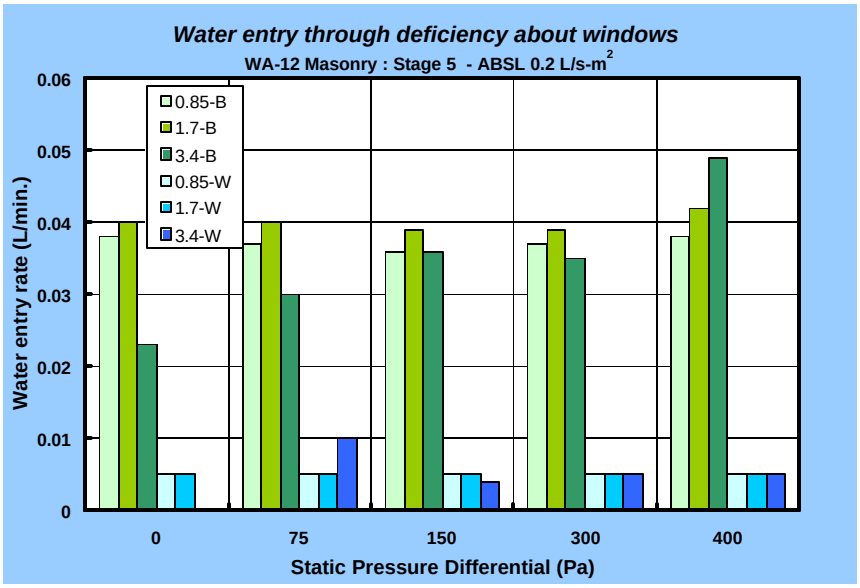

Figure 5.15– WA-12 (Brick masonry veneer) Water entry through deficiency about window as a function of static pressure level and spray rate for Stage 6

5.2.2.5 WATER COLLECTION AT TROUGHS IN VENTILATON-DRAINAGE SPACE

An overview of water collected in each trough located in the drainage space is given in Figure 5.16 in which the entry rates (L/min.) in stage 5 at 400 Pa ΔP_S are provided as a function of the various collection troughs and spray rates. The information clearly shows that where no through-wall penetrations exist, collection in the lower troughs likewise is effectively absent. This is evident for trough "T3" above which there are no penetrations, although some water was collected (circled), most likely from run-off of the adjacent and higher troughs located in proximity to the ventilation duct (i.e. "V-B" and "V-W").

The most significant rates were those collected in trough"T1-B" and reached 0.038 L/min.; this rate of entry is about 4 times less than that achieved by the trough directly above it, "D-B", at the same spray rate and static differential pressure level (1.7 L/min.-m^2 and 400 Pa).

That water collected in a "B" or "W" trough located in the lower portion of the wall is partially dependent on the rate of collection of the upper troughs. As was reported earlier, run-off from the upper troughs would necessarily collect in the lower ones although not preferentially on one side or the other of the space. That is, if water run-off occurred in an upper trough "B", located on the backside of the cladding, it could potentially collect in either the "B" or "W" troughs not necessarily the "B" trough from where it originated. This accounts in part for the different locations and varying rates (i.e. "B" or "W") at which water collected in these lower troughs.

The information is also useful in that it provides some measure of the magnitude of moisture loads in the drainage space.

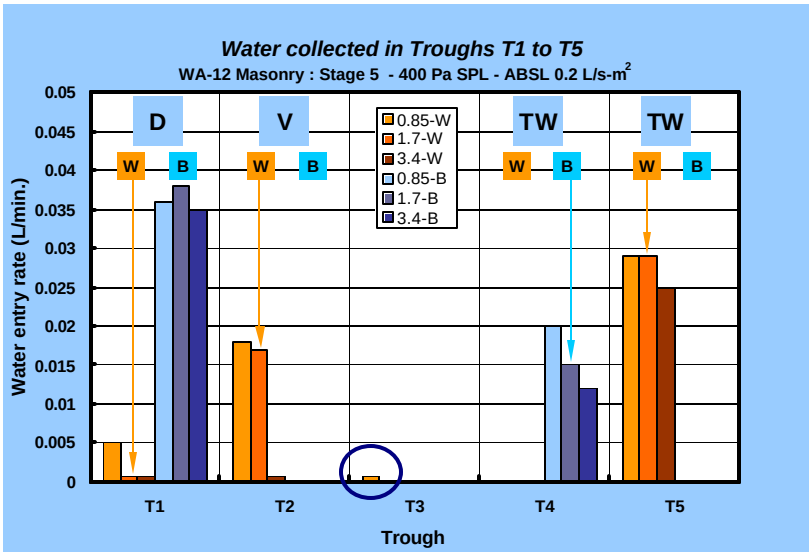

Figure 5.16 – WA-12 (Brick masonry veneer) Water collection rates troughs T1 to T5 for Stage 6 in static pressure conditions

5.2.2.6 SUMMARY OF RESULTS FROM WATER ENTRY THROUGH SPECIFIED DEFICIENCIES

An overview is provided in Figure 5.17 of rates of entry in relation to static pressure differential for WA-12 (0.85 L/min.-m^2 and stage 5) for all collection troughs. With the exception of trough "D-B", all remaining troughs had collection rates of ca. 0.04 L/min. or lower and this rate was about 3 times less than that observed for trough D-B. As well, rates of entry are not dependent on pressure levels as might generally be expected given the nature of construction of the wall assembly.

Following these water entry trials the following may characterize the entry at deficiencies located about different through-wall penetrations, that include the:

i.) Electrical outlet -

- No dependence on pressure differential and little or no dependence on spray rate; maximum value of water entry rate was 0.16 L/min.
- Gross amounts passing opening above electrical outlet collect in trough "D" or "T1", each trough located in the drainage cavity.

ii.) Ventilation duct -

- Entry rates partially dependent on spray rate; maximum value of water entry rate was 0.185 L/min.
- pressure differential across plane of the sheathing board drives water to trough "L"

iii.) Windows -

- water entry rates loosely dependent on spray rates; maximum rates attained in dynamic mode was 0.12 L/min.

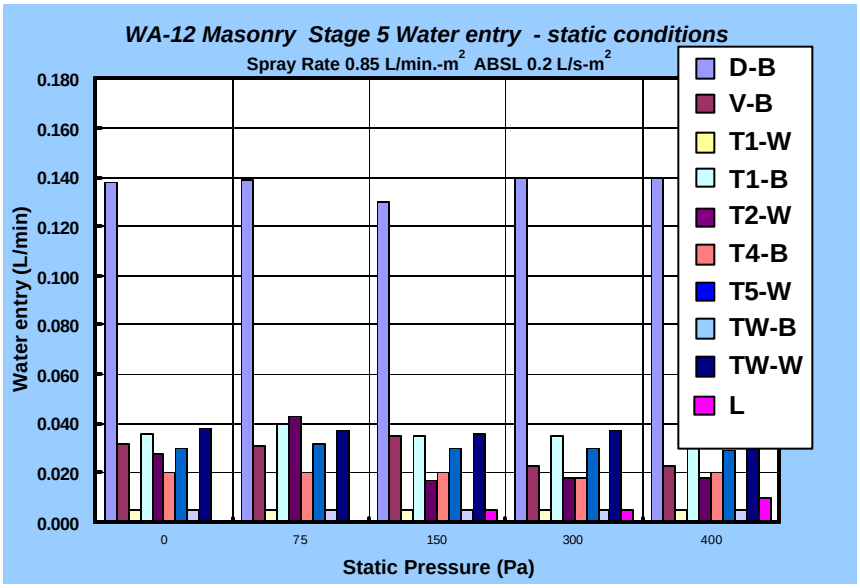

Figure 5.17– WA-12 (Brick masonry veneer) Water collection rates troughs T1 to T5 for Stage 6 in static pressure conditions

5.2.2.7 WATER ENTRY FUNCTION

For brick masonry wall assemblies an entry function was derived from results of water entry through the deficiency above the ventilation outlet as opposed to that for the electrical outlet, as was done for the other three wall types. The derivation was based on values of entry through the ventilation duct for stage 5 of WA-12 subjected to static pressure differentials. As described previously the function relates estimates of rates of entry to the stud cavity in relation to static pressure and spray rates. It is used as the basic water entry parameter for hygIRC simulations undertaken in Task 7 of the MEWS project. The function permits estimating the quantity of water entering the cavity per unit time for climate variables such as wind speed and rainfall intensities.

The water entry function derived for the ventilation duct for brick masonry veneer walls is:

$$dq/\,dR_p\,(Pa) = -1.471\,E^{-07}\,(?P)^2 + 1.722\,E^{-04}\,(?P) + 0.0155$$

The curve is plotted in Figure 5.18 in which the values of dq / dR_p, ranging between 0 and 0.06 (L/min.)(L/min.-m^2)$^{-1}$ are provided in relation to the static pressure differential in Pa (0-400 Pa). The value of fit was $R^2 = 0.9893$, indicating the curve readily characterises the data.

The value of 0.0155 (L/min.)(L/min.-m^2)$^{-1}$ in the equation is that amount of water entry 'potential' provided when no pressure difference occurs across the assembly. The implications with respect to entry into the stud cavity given that spray rates might average say 0.019 L/min.-m^2 over a wet season (for Wilmington say), are that average entry rates over the hour would be ca. 0.018 L/hr or about 20 mL (ca. 1/20 of a cup of water).

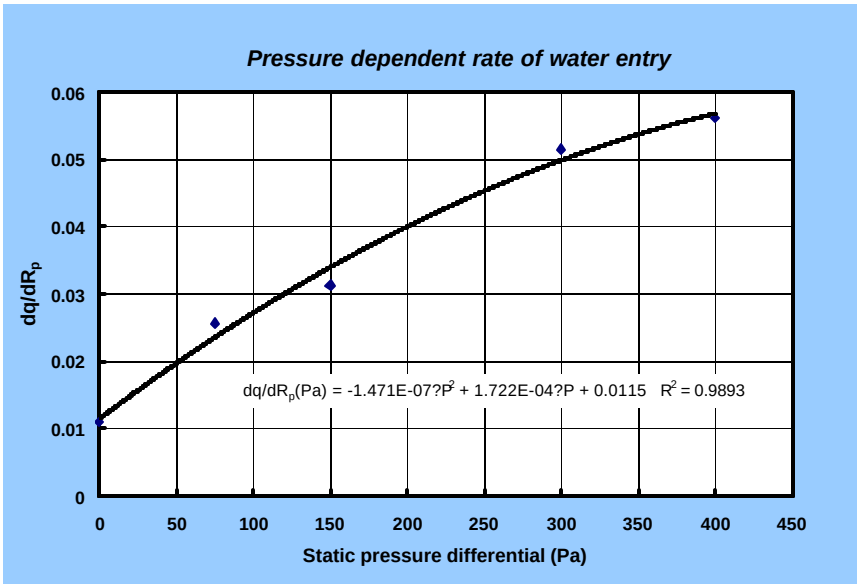

Figure 5.18 – Water entry function for brick veneer wall based on entry of water through ventilation duct

Chapter 6

Results from Siding Wall Assemblies

TABLE OF CONTENTS

? **CHAPTER 6 ?**

Results from Siding Wall Assemblies

LIST OF FIGURES

LIST OF TABLES

CHAPTER OVERVIEW

MEWS methodology incorporates the performance testing and characterisation of full-scale wall assemblies to determine air leakage, dynamic response, water-tightness performance and water entry characteristics for each of the wall cladding types being evaluated in this study.

Performance tests were used to qualify the degree to which wall assemblies were able to maintain their watertight integrity when being subjected to static or dynamic pressure differentials concurrent with water spray using the dynamic wall test facility (DWTF). This series of tests were similar those currently used in industry to assess the likelihood of water penetration under extreme simulated climatic conditions and were conducted at levels comparable to, or in excess of, current industry standards.

Water entry assessments were used to determine the quantities and rates of water that might enter deficiencies of known type, size and location on the cladding when subjected to simulated climatic extremes, likewise using the DWTF. Levels of water spray and pressure differential were consistent with related climatic data of rainfall and wind speed that might occur in an extreme climatic event within a 10 year period in North America. This information provided a basis for a systematic and consistent means of transferring input to hygIRC, the model used in the MEWS parametric analysis.

In this test series, three (3) different types of siding-clad wall assemblies were subjected to performance and water entry assessments tests that included testing under different pressure differentials across the assembly and varying rates of water sprayed onto the cladding surface. Tests were completed in conformance with a protocol derived explicitly for this study and provided in Chapter 1.

Results indicate that in regard to water penetration, the wall assemblies are vulnerable to water ingress at high levels of dynamic loading. However, under static conditions and lower levels of dynamic load, the wall assemblies were reasonably watertight and performed adequately without evident water penetration.

No entry at the electrical outlet was obtained for WA-15 and WA-16 (wall assembly incorporating a ventilation-drainage cavity). In the case of WA-15, water was seen entering the deficiency but not passing the sheathing board or collecting in the trough located in the stud cavity. Water entering this deficiency sought passage to the interstitial space between the cladding and the sheathing. For WA-16, the provision of a 19-mm space between the cladding and the sheathing effectively prevented water from collecting in the trough located in the stud cavity, as might be expected. In the case of WA-17 for which water was collected, rates of water entry ranged between 0.065 to 0.167 L/min. These values are consistent with those obtained for other wall assemblies at this deficiency.

Water was collected for WA-15 and WA-16 however only traces of water were collected for WA-17. For WA-15, water enters under no pressure differential and in significant quantity and at substantially higher rates of entry at increased spray rates. For WA-16 (having a ventilation-drainage cavity), the space between the cladding and the sheathing affected results. Portions of water were collected in the trough located in the drainage space and adjacent to the sheathing, or in the lower collection troughs of the drainage space, before eventually accumulating in the trough located in the stud cavity.

Water entry about windows was evident for WA-15 (W-LS) and WA-16, although for WA-16 little or no water was observed to enter into the stud cavity; no water was recorded for WA-17. A good portion of the water accumulated in the ventilation-drainage space between the cladding and the sheathing

6.1 Introduction

A series of three siding walls (Nos. 15, 16, 17) were constructed and subsequently tested for water penetration trials and water entry assessments using the dynamic wall test facility. The pressure response of the wall assemblies and air leakage characteristics were also determined.

Details regarding the fabrication of the specimens, material specifications and specified deficiencies are provided in the report found in Appendix A. An overview of the different specimens showing the key components of the wall assemblies is provided in Table 6.1 below. Details regarding the location of pressure taps, of moisture sensors, of water entry points through specified deficiencies and means of water collection are outlined in the section on test specimens.

Results from water penetration trials (Stages 2 and 3) are first presented followed by those obtained for water entry assessments on specimens that incorporate specified deficiencies (N.B. Stage 5, 6 and 7 – replace Stage 4). Tests were conducted according to the test protocol described in Chapter 1 (§1.2). Selected results from air leakage and dynamic response (Stage 1) of wall assemblies are also provided.

Table 6.1 – Wall assembly types and key wall components

WA	Type of siding	Cavity	Water Resistive Barrier	Sheathing
15	Hardboard	None	Airguard	Asphalt impregnated fiberboard
16	Hardboard	19 mm (PT wood strapping)	2 layers 30-min paper	Glass mat gypsum board
17	Vinyl	None	None	36 mm XPS insulation

6.1.1 Test specimens

The test configuration showing the location of pressure taps, moisture sensors, and water entry points through specified deficiencies are provided below in Figures 6.1 to 6.3 respectively.

6.1.1.1 Pressure taps

Pressure taps are located in six wall portions (Figure 6.1), with the first portion located at the left extremity of the wall (facing the weather-side). Typically in each portion, taps are located both in the wall cavity between the stucco and the sheathing and in the stud space.

Additionally, taps have been added to obtain measurements of pressure differential at points of water entry.

6.1.1.2 AIR BARRIER SYSTEM LEAKAGE

Air barrier system (ABS) leakage was regulated by introducing a series of 7-mm diameter holes in the ABS (Figure 6.1), a series of seven (one in each stud cavity) representing an equivalent leakage area (ELA) of 269-mm^2, provided a nominal wall assembly leakage of 0.2 L/s-m^2. A wall assembly leakage of 0.5 L/s-m^2 (ELA 808-mm^2) was achieved using twenty-one holes of the same diameter, three in each stud cavity. The desired nominal leakage through the wall assembly was achieved by "opening" or "closing" the appropriate number of holes in the air barrier system.

6.1.1.3 MOISTURE SENSORS IN SHEATHING BOARD

The location of moisture sensors is shown in Figure 6.2. A total of sixteen (16) moisture pin pairs have been imbedded in the sheathing board in various locations as a means of indicating the presence of moisture in the board material. Over a test period, note is taken of the time and conditions under which the light is first activated.

6.1.1.4 WATER ENTRY POINTS

Water entry points at specified deficiencies (Figures 6.3 and 6.4), representative of those found at the joint seal located at the interface between wall components, are located:

- Above the electrical outlet – a nominal 50-mm length of sealant is missing between the outlet cover and the wall.
- Above the ventilation duct – a nominal 50-mm length of sealant is missing between the duct and the wall.
- Below the windowsill and between finishing strips – a 50-mm length of sealant is missing between the ending strips.
- Along the horizontal joint located above the window and mid-way between joint extremities – a 90-mm length of sealant is missing
- Along the vertical joint located mid-height between joint extremities – a 90-mm length of sealant is missing

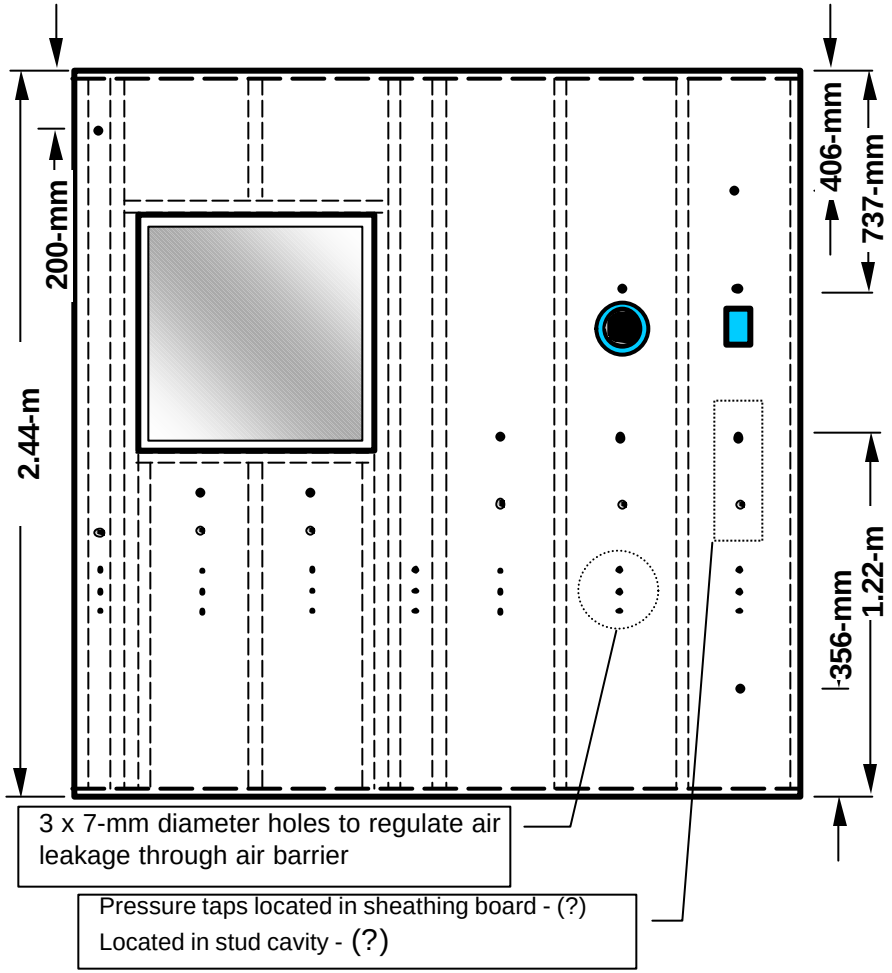

Figure 6.1 - Location of pressure taps and air leakage openings.

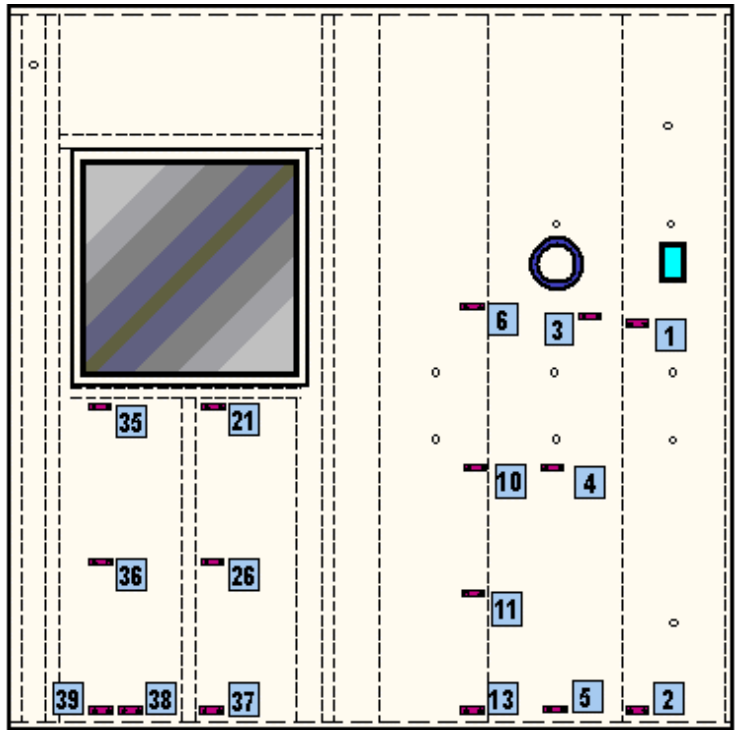

Figure 6.2 - Location of moisture sensors

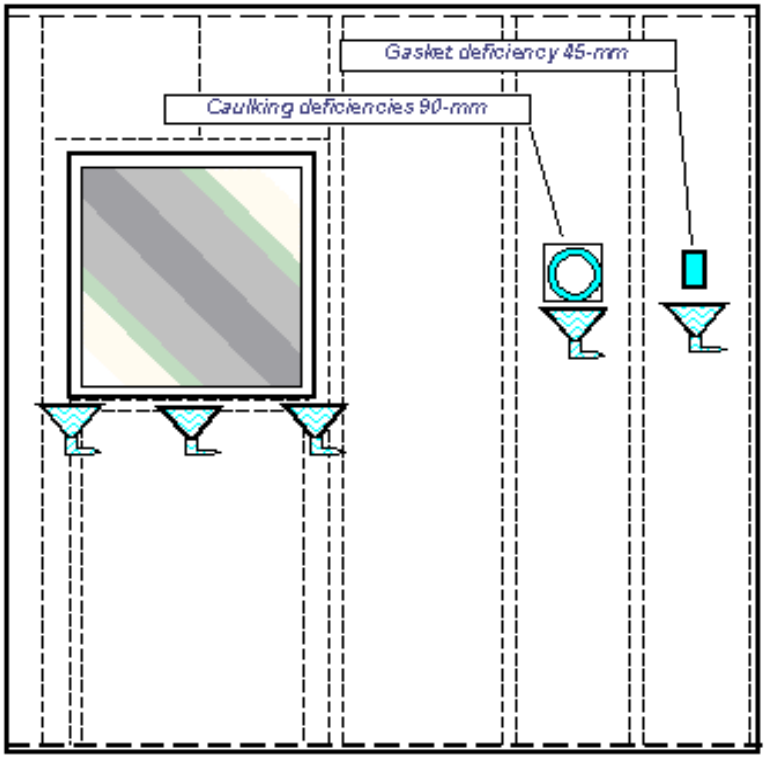

Figure 6.3 – WA-15 & WA-17:
Location of water collection points and troughs

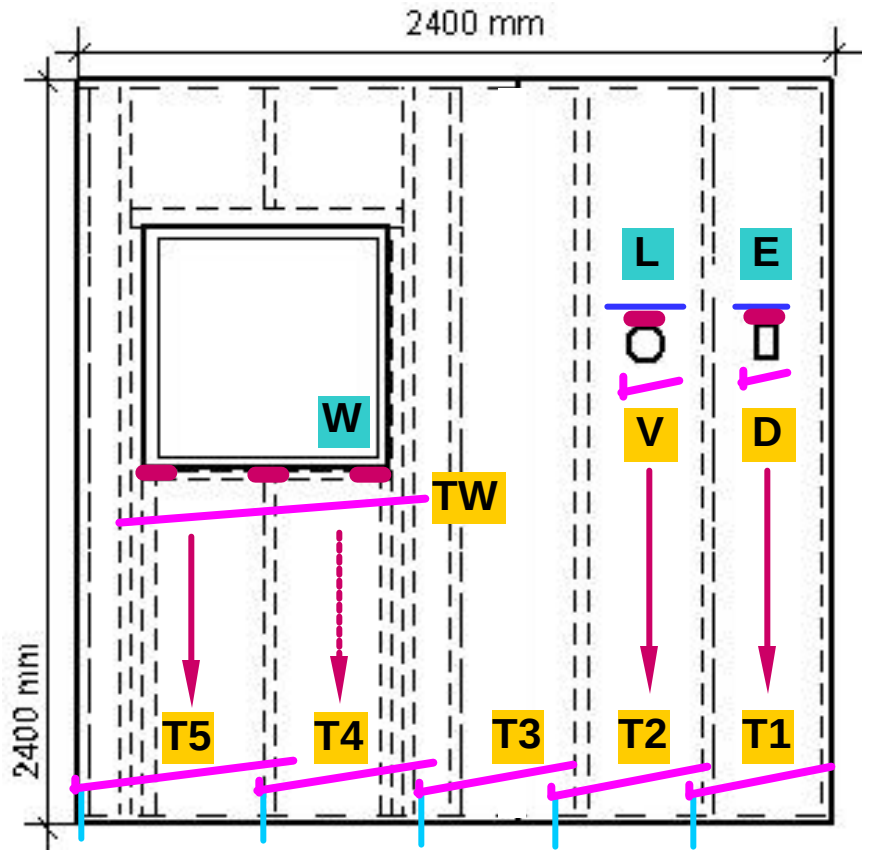

Figure 6.4 – WA-16: Location of water collection points and troughs

6.2 Results

Results from water penetration trials (Stages 2 and 3) are presented in section 6.2.1 and information is presented in relation to the results from a specific wall assembly following in sequence from WA-15 to WA-17. Summary information regarding specimen components is provided in Table 6.1 and a summary of the results is first presented in Table 6.2.

Information related to the performance of each assembly when subjected to either static or dynamic test conditions is provided and a summary of the water penetration results is provided in section 6.2.1.5. Note that water penetration trials do not include specified deficiencies in the wall specimen whereas these are part of the assessment protocol for water entry tests. When reference is made in this chapter to “deficiencies”, in all instances this is referring to specified deficiencies.

Results for water entry through specified deficiencies (Stages 5 to 7 - previously 4) are provided in section 6.2.2 a summary of which is offered in Table 6.3. Thereafter, information is presented in order of wall assembly starting with WA-15. Results, as applicable to the specific wall assembly, are presented for the electrical outlet, ventilation duct, and window. Special consideration is given WA-16 given that additional water collection troughs were fitted in the ventilation-drainage space between the cladding and the sheathing. In this instance, the information specific to a given through-wall penetration is augmented with that offered by the collection of water in this space.

Results obtained in static pressure conditions are compared to those in dynamic conditions. As well, results obtained in the dynamic test mode are evaluated in regard to the effects of changing the nominal air barrier system leakage.

Where necessary, results from the different test stages (i.e. 5, 6 or 7) are reviewed and contrasted. Note that Stages 5 and 6, described below, are variations of Stage 4 (described in Chapter 1), whereas Stage 7, likewise described below, replaces Stage 4. Stage 5 provides for a perimeter seal at the ventilation duct sheathing board interface consisting of a backer rod and sealant. The seal is continuous with the exception of a small opening in the sealant (2-mm high x 50-mm long) at the base of the duct. For Stage 6 a seal is provided in the same location however, the sealant is removed leaving only the baker rod in place around the ventilation duct. In Stage 7 (previously Stage 4), no sealant or backer rod is in place around the duct.

A summary of results for water entry through deficiencies is presented in section 6.2.2.5.

Selected results from air leakage determinations and pressure response tests (Stage1) are provided in sections 6.2.3 and 6.2.4 respectively.

6.2.1 WATER PENETRATION TESTS ON SIDING-CLAD WALLS – STAGES 2 AND 3

6.2.1.1 INTRODUCTION

Performance tests were used to qualify the degree to which wall assemblies were able to maintain their watertight integrity when being subjected to static or dynamic pressure differentials concurrent with water spray using the dynamic wall test facility. This series of tests were similar those currently used in industry to assess the likelihood of water penetration under extreme simulated climatic conditions and were conducted at levels comparable to, or in excess of, current industry requirements and standards. Note that no specified deficiencies were incorporated in the specimens.

The results obtained during water penetration trials (Stages 2 and 3) are essentially qualitative in nature. Observations were made as to where penetration occurs on the inside of the assembly (e.g. around windows, electrical outlet, and ventilation duct or through the sheathing board) and when it occurs over the course of the test sequence. Test conditions (static or mean dynamic pressure differential) when penetration occurs were noted and these provided a benchmark from which comparisons could then be made. Moisture sensors (MS) placed in the sheathing board at specific locations of the wall assembly indicated whether moisture had penetrated beyond the second line of defence. A red indicator light on the sensor was activated if the presence of moisture was detected in the close proximity to the sensor.

An overview of the water penetration trials is provided in Table 6.2. Observed water entry locations include the electrical outlet (E), ventilation duct (V), window –any location – (W), and sheathing board (Sh-Brd). Had any moisture sensors (MS) been activated over the course of the test sequence, then the number of activated (X) in relation to the number of functional sensors (Y) is reported as X of Y (e.g. 8/13 : 8 of 12). Where no activity is recorded, a null symbol is offered (Ø), whereas activity over the range of test values is indicated by the symbol (●). Where only a single occurrence of the penetration event was recorded, the test mode (i.e. static or dynamic) and pressure level are given (e.g. 300 D: dynamic test mode and the $300 + 125 \sin(2\pi ft)$ Pa level).

The table also provides basic information on siding properties that involves the type of sheathing board used in the fabrication of the assembly (i.e. F – fiberboard; G – exterior grade gypsum board; X – XPS; Extruded polystyrene), the presence of a cavity and the possibility of drainage.

.

Table 6.2— Siding-clad wall assemblies: Observed water penetration at various locations and siding assembly properties

	Siding properties			
	Sheathing	F	G	X
	Drainage	N	Y	N
	Cavity	N	Y	N
Observed Entry Location	**WA**	**15**	**16**	**17**
E		⊖	300D	◉
V		⊖	700D	◉
W		700D	⊖	⊖
Sh-Brd		⊖	⊖	◉
MS	**X of Y**	⊖	8/10	2/12

Electrical outlet (E), ventilation duct (V), window (W), sheathing board (Sh-Brd) and activation of moisture sensors (MS)

6.2.1.2 WATER PENETRATION WA-15 HARDBOARD-CLAD WALL ASSEMBLIES:

Results indicated that WA-15 was little affected by the penetration trials. No water was observed at any of the through-wall locations with the exception of water collection beneath the window at the beginning of the dynamic test sequence at the 700 Pa dynamic pressure level (i.e. pressure fluctuations of 700 ± 300 sin (2πft) Pa).

6.2.1.3 WATER PENETRATION WA-16 HARDBOARD-CLAD WALL ASSEMBLIES:

This WA is the one that incorporates a ventilation and drainage space of 19-mm width between the backside of the cladding and the sheathing barrier. It did not exhibit any evidence of water penetration at the window or through the sheathing board. However, water was collected in troughs servicing the electrical outlet and ventilation duct. In both instances this occurred in the dynamic test mode at the 300 dynamic pressure level (i.e. pressure fluctuations of 300 ± 125 sin (2πft) Pa) in the case of the trough servicing the electrical outlet, and at 700 Pa dynamic pressure level for the ventilation duct.

Moisture sensor (MS) activity was significant given that 8 of 12 moisture sensors were activated over the course of the penetration trials, of which six (6) were activated in the static and dynamic test sequences (Figure 6.5; MS- 2, 10, 13, 21, 36, 39 – MS circled in red) and the remaining two (2) were activated during 16-h of continuous water spraying (Stage 3 of test protocol; MS-3 and –11; MS circled in green). Note that darkened labels indicate sensors inoperable at the start of the test (i.e. MS-4, 6, 26, 38).

The first functional moisture sensor was activated after 10-min. of testing (MS-37), and is located at the base of the wall. This was subsequently deemed to be a false positive reading as was MS-5 that was activated after 15-min. at the same test conditions. Subsequently during the test, five (5) moisture sensor were activated at the 75 Pa static pressure level (MS-2, 10, 21, 36, 39) and the sixth moisture sensor (MS-13) activated after 46-min. of testing at 150 Pa static pressure level.

The activation of MS-21 and –36 is indicative of water penetration about the window and that of MS-3, 10 and –11 likely as a result of water ingress at the electrical outlet. Those moisture sensors located at the base of the WA (i.e. MS-2, -13, -39) may be false positive readings given that a good deal of water accumulated at the base of the walls – this would not normally be the case in-service.

6.2.1.4 WATER PENETRATION WA-17 VINYL CLAD WALL ASSEMBLIES:

This WA is one of two WA's tested that include extruded polystyrene (XPS) as the sheathing board (the other is WA-13, brick masonry veneer). As provided in Table 6.6, water was observed to penetrate at the ventilation duct and electrical outlet. Significant penetration occurred through the sheathing board in the dynamic mode; none was observed about the window location.

Of the twelve (12) functional moisture sensors, two (2) were activated over the course of the static and dynamic test sequences (MS-21 at 35-min. and 75 Pa static pressure level and MS-1 at 48-min. and 150 Pa static pressure level). Both of these sensor locations are circled in Figure 6.6. Following this test sequence, four (4) additional sensors were activated including MS-11, -36, -38 and –39. Moisture sensors –38 and –39 were determined as false positive results whereas the activation of MS-11 may be indicative of water entry at the electrical outlet that subsequent trickled down towards the area in proximity to the activated moisture sensor. Activation of MS–36 may be due to water entry about the window opening that likewise made a path downwards towards sensors located further down along the wall.

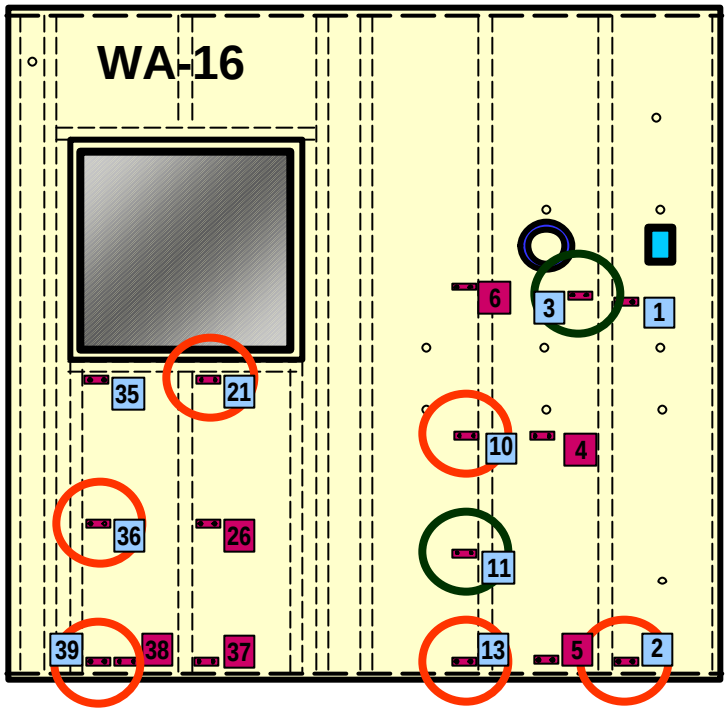

Figure 6.5– WA-16 Hardboard: Water collection in troughs E and V; Following static & dynamic tests - Sensors : # 2, # 10, # 13, # 21, # 36, # 39; Following 16-h continuous - Sensors: # 3 and # 11

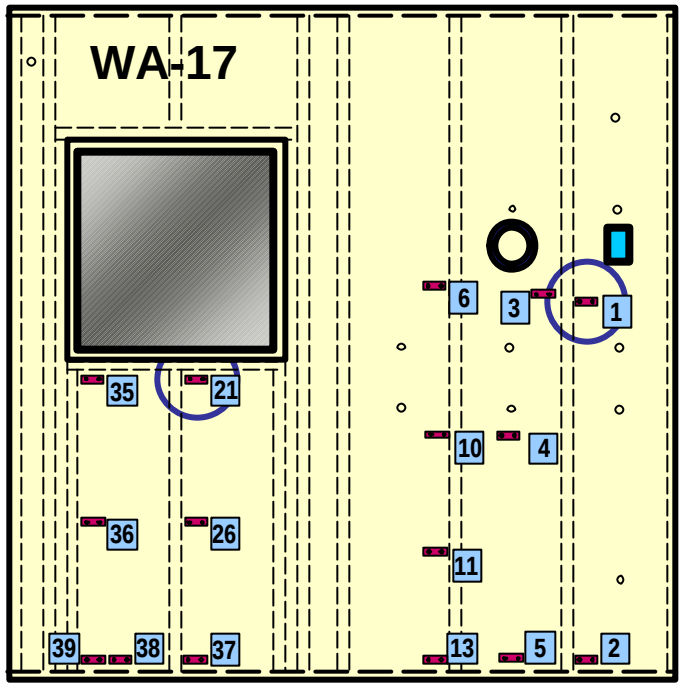

Figure 6.6– WA-1 WA-17 Vinyl: Water collection in troughs E and V; Following Static test – Sensors # 1 and # 21; Dynamic test @ 700±300 Pa - Water entry of XPS at ship-lap joint; Following 16-hrs continuous - No additional sensors activated

The water entering the horizontal joint between adjacent XPS panels occurred in the dynamic test mode and at the 700 Pa dynamic pressure level. The exact point of entry was at the extreme edge of the test specimen where the horizontal joint meets the outermost wood stud of the specimen; this vertical stud delineates the extremity of the specimen. Water appears to have passed the outer edge seal between the cladding and the test frame and thereafter found its way behind the cladding and through the horizontal joint between adjacent panels in the sheathing board. The presence of openings along this horizontal joint is worth some discussion.

The rigidity of the wall, and hence the degree to which it flexes under load (i.e. air pressure fluctuations), is in part dependant on the rigidity of the sheathing board and the degree to which the board is affixed to the wood frame. In general then, a high degree of rigidity with minimal flexure is expected for a rigid board (e.g. OSB sheathing) affixed to the frame in the conventional manner. When the sheathing board offers reduced rigidity in flexure, as is the case with an XPS board, the overall flexural rigidity of the WA is likewise reduced. Consequently walls using XPS would typically flex to a significantly higher degree than those walls incorporation OSB when subjected to similar loading schemes. The degree of flexure in XPS sheathing walls is such that horizontal joints located at the extreme point of bending of the panel (mid-height) open under flexural loads and thus provide significant points for air and, potentially, water to enter.

6.2.1.5 SUMMARY OF WATER PENETRATION TRIALS—

Water penetration tests were conducted on three different siding-clad wall assemblies, one of which included a drainage and ventilation cavity (WA-16). The following observations were made:

WA-15 (hardboard–clad with fibreboard sheathing board)

- Water entry was observed about window in dynamic mode at high pressure; otherwise
- This wall assembly was reasonably watertight under the prevailing test conditions.

WA-16 (hardboard–clad with gypsum sheathing board)

- Water entry was observed about the electrical outlet and ventilation duct;
- Moisture sensors activated in dynamic mode at high pressures - susceptibility of wall to dynamic loads.

WA-17 (vinyl – clad with XPS sheathing board)

- Water entry was observed about the electrical outlet and ventilation duct ; and
- in the dynamic mode significant water entry was evident at high pressure differentials.
- The reduced wall rigidity from the use of XPS sheathing may have contributed the water entry in the dynamic mode.

6.2.2 ASSESSMENT OF WATER ENTRY THROUGH SPECIFIED DEFICIENCIES

6.2.2.1 INTRODUCTION

The assessment of water entry through specified deficiencies was used determine the quantities and rates of water that might enter deficiencies of known type, size and location on the cladding when subjected to simulated climatic extremes using the Dynamic Wall Test Facility. Levels of water spray and pressure differential were consistent with related climatic data of rainfall and wind speed that might occur in an extreme climatic event within a 10 year period in North America. This information provided a basis for a systematic and consistent means of transferring input to hygIRC, the hygrothermal model used in the MEWS simulation studies.

Table 6.3– Water entry assessments:
Observed entry at various trough locations

	Siding properties			
	Sheathing	F	G	X
	Drainage	N	Y	N
	Cavity	N	Y	N
Observed Entry Location	**WA □**	**15**	**16**	**17**
E*		Ø	◉	◉
V		◉	◉	Ø
W-L		◉	Ø	Ø
W-R		Ø	Ø	Ø
W-S		75S/150D	Ø	Ø

* Electrical outlet (E), Ventilation duct (V), Window left side (W-L); W-right side (W-R); W-sill (W-S)
** No data: Ø; Water entry data: ◉ S: Static pressure level; D: Dynamic pressure level

6.2.2.2 WATER ENTRY THROUGH SPECIFIED DEFICIENCIES FOR WALL ASSEMBLY 15 (WA-15)

Collection of water was possible for the electrical outlet, ventilation duct and four separate troughs beneath the window, two at window corners (LS and RS) and two beneath the window at the sill (L-sill; R-sill). The left (L) and right (R) designations refer to the respective location of troughs about the window when one faces the specimen interior.

No water was collected for the electrical outlet although water was observed to be entering the deficiency and thereafter, to flow into interstitial spaces between the cladding and the sheathing paper (Figure 6.7). Neither was water collected for the RS trough and only intermittent results were obtained for either the R-sill or L-sill troughs. For example, water was collected in the R-sill (Table 6.4) and L-sill (Table 6.5) troughs in the following five and four instances respectively (of 45 possible entries over three stages for each trough) over the course of water entry trials undertaken in static pressure mode. These results show that intermittent water entry is more likely in conditions of high pressure differential (= 300 Pa), although clearly, water entry may nonetheless occur when only spray is applied (e.g. entry #1, both tables).

Table 6.4 – Water collection in right window sill trough (R-sill)

#	Static pressure (Pa)	Spray rate (L/min-m^2)	Collection rate (L/min.)
1	0	1.7	0.0072
2	75	1.7	0.0150
4	400	0.85	0.0030
3	400 (S6)	3.4	0.0012
5	400 (S5)	3.4	0.0014

Table 6.5 - Water collection in left window sill trough (L-sill)

#	Static pressure (Pa)	Spray rate (L/min-m^2)	Collection rate (L/min.)
1	0	1.7	0.0021
2	300	0.85	0.0028
3	400	0.85	0.0014
4	400	3.4	0.001

Consequently, more extensive results are presented for the ventilation duct and the LS window.

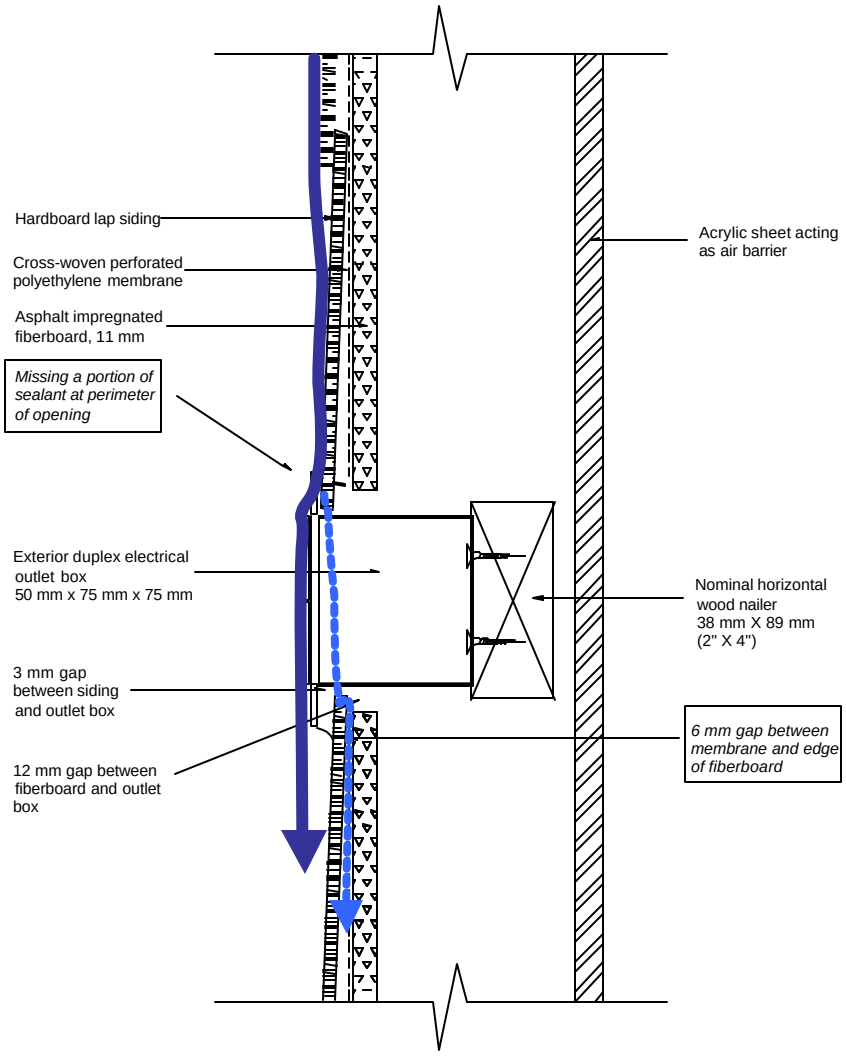

Figure 6.7– WA-15 Hardboard siding: sectional view showing detail for electrical outlet and water entry path to interstitial space between cladding and sheathing

6.2.2.2.i WATER ENTRY THROUGH SPECIFIED DEFICIENCIES AT THE VENTILATION DUCT

Results recorded for water entry about the ventilation duct in either static or dynamic mode are respectively summarised in Tables 6.6 and 6.7 and illustrated in Figures 6.7 to 6.9.

Water enters under no pressure differential and in significant quantity either in static or dynamic mode and at substantially higher rates of entry at increased spray rates. In the static pressure mode (Table 6.6), a review of the range of values of entry rates in relation to changes in spray rates at a given pressure level (i.e. Avg. 0 and 400 Pa ΔP_S) in comparison to variations in rates of entry at a given spray rate (i.e. range) suggest that rates of entry are primarily dependent on the spray rate and not the pressure difference across the assembly.

Table 6.6– WA-15: Water entry rates through deficiency above ventilation duct – *Static pressure mode* – summary of results from three stages (Stages 5, 6 & 7)

Spray *Rate* *L/min.-m²*	**Rate of water entry, L/min.**			
	Maximum	*Avg. at 0 Pa*	*Avg. at 400 Pa*	*Range*
0.85	0.0192	0.0177	0.0162	0.0078
1.7	0.030	0.0173	0.0249	0.0238
3.4	0.062	0.0453	0.0473	0.024

Table 6.7– WA-15: Water entry rates through deficiency above ventilation duct – *Dynamic pressure mode* – summary of results from three stages (Stages 5, 6 & 7)

Spray *Rate* *L/min.-m²*	**Rate of water entry, L/min.**							
	Maximum		*Avg. at 75 ± 40 Pa*		*Avg. at 300 ± 125 Pa*		*Range*	
	*0.2**	*0.5*	*0.2*	*0.5*	*0.2*	*0.5*	*0.2*	*0.5*
0.85	0.0186	0.021	0.016	0.016	0.0166	0.0166	0.0044	0.008
1.7	0.0246	0.028	0.0215	0.0212	0.0215	0.0253	0.0060	0.008
0.34	0.086	0.080	0.0277	0.0313	0.0548	0.0577	0.0730	0.055

* Tests conducted with nominal wall assembly leakage of 0.2 and 0.5 L/s-m²

This is clearly evident from the results depicted in Figures 6.8 and 6.9 that show rates of water entry collected in the ventilation duct trough in stages 5 and 7 respectively. Rates of water entry in either instance do not increase in relation to corresponding increases in static pressure differential but do markedly increase in value from the lowest to the highest spray rates. This effect is systematic in the case of stage 7 (Fig. 6.9) where at each static pressure level there is an increase in rate of collection that directly corresponds to changes in spray rate. Note that the apparent reason for the divergence in results between stages is that in stage 7 there are comparatively no barriers to entry (sealant and backer rod removed from joint between duct and sheathing board) to that of stage 5. In this stage only a small opening is available (2-mm x 50-mm) for water to penetrate the second line of defence (e.g. Fig. 6.17) and both the backer rod and sealant are present around the remainder of the joint between the duct and sheathing board. Water must work its way from the opening at the deficiency, located at the top of the duct and along its length to the underside of the duct.

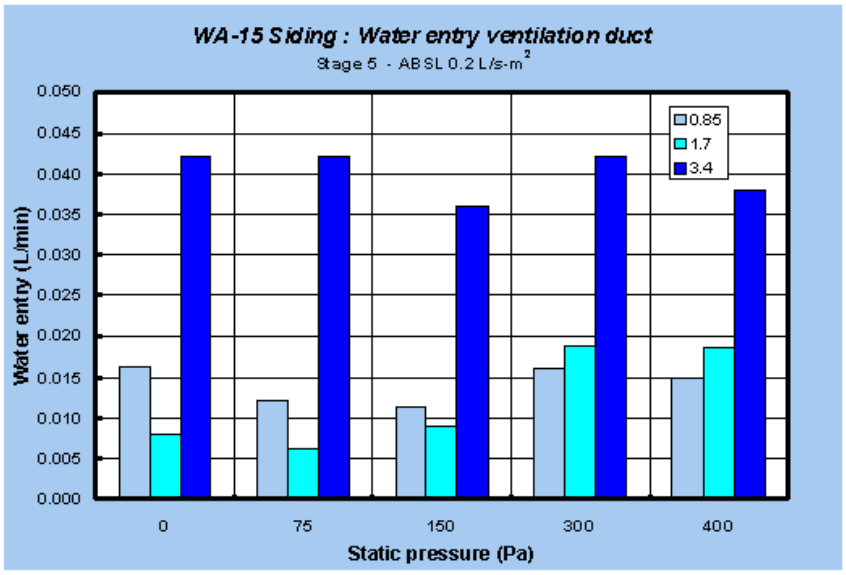

Figure 6.8– Siding WA-15 : Stage 5 - Water entry under static pressure differential through deficiency above vent duct

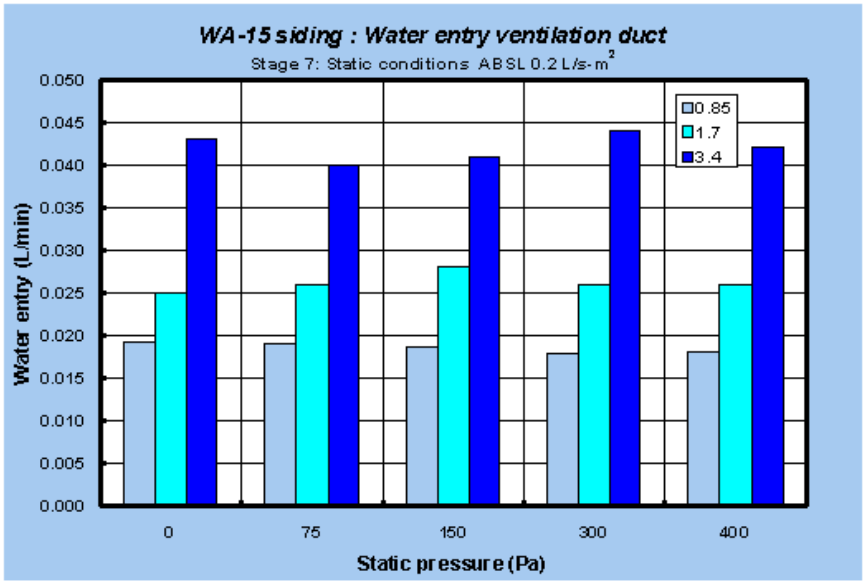

Figure 6.9– Siding WA-15 : Stage 7 - Water entry under static pressure differential through deficiency above vent duct

Comparison of rates of entry in Stage 7 in the dynamic test mode is offered in Figure 6.10. In this instance the nominal wall assembly air leakage is 0.2 L/s-m^2. The characteristic response is similar to that shown for the static test mode; an increase in pressure level has no discernible effect on rates of water entry whereas the response is characterised by increases in water entry rates in relation to corresponding increases in spray rates. As well, the rates of entry calculated in the dynamic mode are reasonably similar to those obtained in the static test mode (e.g. 0.03 L/min. at 75 Pa ΔP_D vs. 0.04 L/min. at 75 Pa ΔP_S).

.

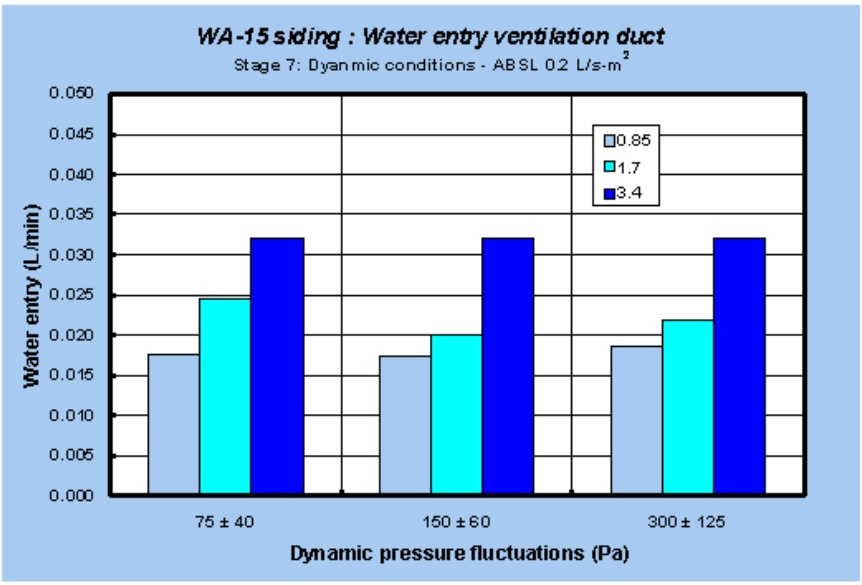

Figure 6.10– Siding WA-15 : Water entry rates under dynamic pressure fluctuations through deficiency above ventilation duct

6.2.2.2.ii WATER ENTRY THROUGH SPECIFIED DEFICIENCIES AT THE WINDOW – TROUGH LS

Results for water entry to the LS window are given in Table 6.8 and 6.9 and Figure 6.10. Under static pressure conditions there was little or no water collected at 0 Pa static pressure level although values for entry at the highest pressure attained on average 0.0.113 L/min. with maximum values ranging between 0.0126 to 0.0154 L/min.

In the dynamic test mode, maximum values attained are similar to those achieved in the static mode; greater rates of entry were evident for nominal ABSL (air barrier system leakage) of 0.5 as compared to 0.2 L/s-m^2. This later observation is also apparent for rates of entry obtained at 75 Pa and the 300 Pa ΔP_D.

Table 6.8– WA-15: Water collection rates in window trough LS – *Static pressure mode* – summary of results from three stages (Stages 5, 6 & 7)

Spray *Rate L/min.-m^2*	**Rate of water entry, L/min.**			
	Maximum	*Avg. at 0 Pa*	*Avg. at 400 Pa*	*Range*
0.85	0.0154	<0.001	0.0096	0.0154
1.7	0.0126	<0.001	0.0096	0.0126
3.4	0.0134	0	0.0113	0.0134

Table 6.9– WA-15: Water collection rates in window trough LS – *Dynamic pressure mode* – summary of results from three stages (Stages 5, 6 & 7)

Spray *Rate L/min.-m^2*	**Rate of water entry, L/min.**							
	Maximum		*Avg. at 75 ± 40 Pa*		*Avg. at 300 ± 125 Pa*		*Range*	
	*0.2**	*0.5*	*0.2*	*0.5*	*0.2*	*0.5*	*0.2*	*0.5*
0.85	0.0140	0.0178	0.001	0.0045	0.0094	0.0141	0.014	0.018
1.7	0.0120	0.0180	0.0026	0.0035	0.0083	0.0124	0.012	0.016
3.4	0.0115	0.0158	0.0026	0.0033	0.0084	0.0138	0.0115	0.016

* Tests conducted with nominal wall assembly leakage of 0.2 and 0.5 L/s-m^2

As provided in Figure 6.11, rates of water collected in the trough on the LS of the window vary in accordance with pressure differential; changes in spray rate as such do not affect the results. The reason for this is straightforward. In contrast to the water entry path through the wall offered by the deficiency above either the electrical outlet or the ventilation duct, there is no similar direct path for water entry in the case of windows. As such, the amount of water collected is limited by the comparatively smaller interstitial spaces that exist between the widow

pane and glazing, the glazing and the window frame, as well as the interface between the window and the wall. These spaces more than likely are filled to capacity even at the lowest spray rate hence additional water sprayed on the cladding has no direct affect on water collection rates. However, given that the pathways are likely saturated, increases in collection rates are possible given increases in pressure differential across the wall assembly; the increase in pressure forces water through the spaces and eventually by the window frame. Hence rates of collection increase in proportion to corresponding pressure increases as clearly demonstrated in Figure 6.11.

Note as well, water also enters under no pressure differential; this significant item clearly demonstrates that significant amounts of water can accumulate simply by virtue of water being present on the surface of the cladding. For example, at an average rate of water collection of 0.0026 L/min. the left side (LS) of the window would accumulate in the order of 150 mL of water in an hour if spray impinged on the surface of the cladding at an average rate of 0.85 L/min.-m^2.

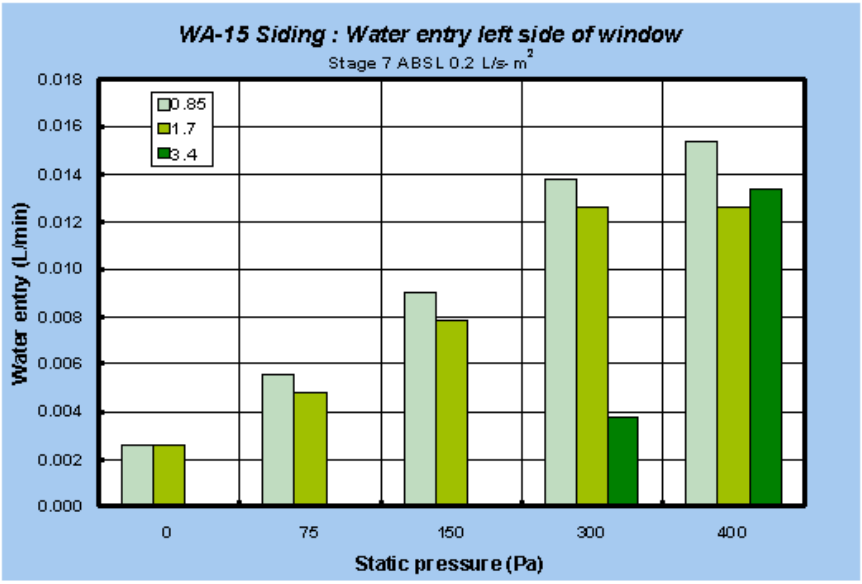

Figure 6.11: Siding WA-15 – Water entry at various spray rates and at given static pressure differentials through deficiency at Left Side (LS) of window

6.2.2.3 WATER ENTRY THROUGH SPECIFIED DEFICIENCIES FOR WALL ASSEMBLY 16 (WA-16)

An overview of results is provided in Table 6.10; locations for each of the collection troughs are given in Figure 6.12. Note that troughs were located in the 19-mm space between the cladding and the sheathing (i.e. in the ventilation and drainage cavity) permitting the collection of water entering deficiencies and passing the cladding proper. These troughs were located beneath each of the penetrations and include that servicing the deficiency above the electrical outlet (D), the ventilation duct (V) and the window (TW).

Above each of troughs V and D were deflectors that were used to prevent any water inadvertently entering the respective troughs from above to dilute the entry results. Those troughs used inside the stud cavity behind each wall penetration remain to collect water passing the cladding and sheathing board; this is trough E servicing the electrical outlet, trough L for the ventilation duct and troughs W (i.e. RS, LS, R-sill, L-sill) at the window proper.

As well, at the base of the wall there is another series of troughs, T1 to T5. Trough T1 collected water in the cavity delineated by the breadth of the stud space; water not collected by trough D would collect here. Likewise for trough T2, any water not collected by trough V would collect in trough T2. The locations of each of the troughs, showing the respective collection 'zones' are depicted in Figure 6.12.

Finally, each of the troughs located in the ventilation-drainage cavity were constructed and installed so that water could be collected from the back of the cladding (designated as trough location "B") or collected from the sheathing barrier (trough location "W"). This configuration of troughs offered over 20 collection points from which rates of water entry could be determined. As well, for those deficiencies located above either the electrical outlet or ventilation duct, the arrangement of a successive series of troughs permitted obtaining some idea of the likelihood of water entering the deficiency and thereafter, passing beyond the sheathing board given the substantial gap between the cladding and sheathing.

A review of results offered in Table 6.10 shows that water was collected in trough L, the trough located beneath the ventilation duct in the stud cavity, in trough V-W, located beneath the ventilation duct in the ventilation-drainage space adjacent to the membrane, but not in trough V-B, also located beneath the ventilation duct in the drainage space but placed against the back of the cladding.

Table 6.10- Water collection in troughs

Tr.	Trough location		
	S	B	W
D		●	○
V		–	●
L	●		
E	○		
W	–		
TW		●	●
T1		–	●
T2		●	●
T3		–	–
T4		–	○
T5		○	●

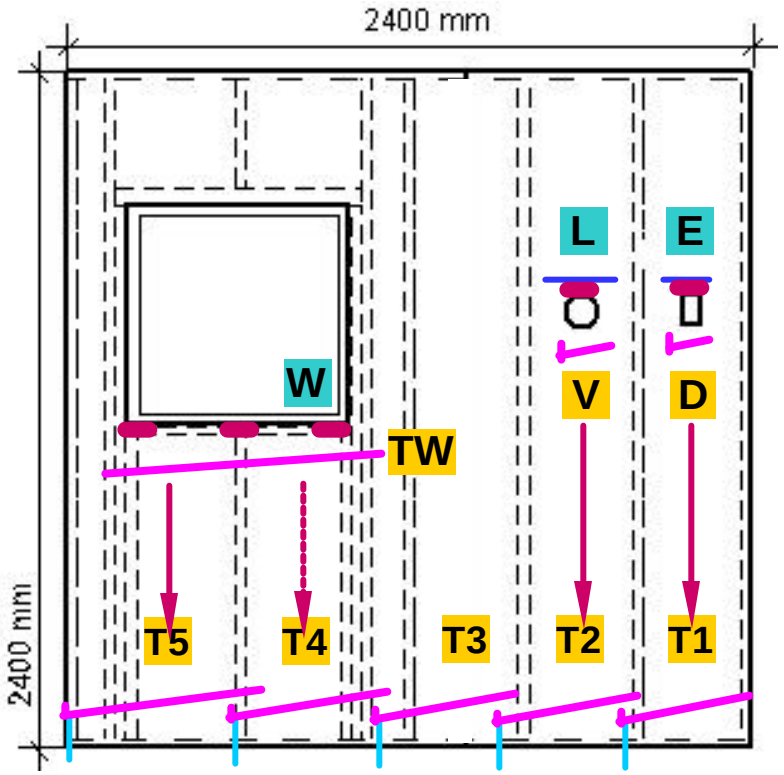

Figure 6.12– WA-16 Hardboard siding: water entry points and collection of data

Similarly for the electrical outlet, trough E provides only intermittent results, whereas the bulk of the water entering the deficiency above the electrical outlet was collected in trough D-B, located in the ventilation-drainage space beneath the outlet and adjacent to the back of the cladding. Hence few instances were recorded of water being collected in trough D-W (trough in ventilation-drainage space, beneath electrical outlet and adjacent to sheathing).

Any overflow from collection in troughs D or V (-W or -B) would collect in troughs T1 and T2 respectively, as shown in Figure 6.12. Trough T3 is the only trough for which no deficiencies are located above it. Notably, no water was collected from this trough suggesting that water entry via the interstitial spaces between cladding boards is minimal and that most water entry likely emanates from entry through deficiencies.

Water was collected in both the B and W locations of trough TW located in the ventilation-drainage space just beneath the lower edge of the window frame. Collection was evident in troughs T4 and T5 although no collection was observed for trough T4-B, located at the back of the cladding.

Results are presented in relation to the type of through-wall penetration being considered (i.e. electrical outlet, ventilation duct, and window) and with all the contributing results from those troughs affected by entry through a deficiency for a given type of through-cladding penetration. Hence results are presented such that the effects of entry through the deficiency located above the electrical outlet are first considered and include results from the collection in troughs E, D-B, D-W and T1-W. Selected results from this series are provided in Table 6.11 to 6.14 and Figures 6.13 and 6.15.

Thereafter, the effects of entry through the deficiency located above the ventilation cut are reviewed and include results from water collection in troughs L, V-W, T2-B and T2-W. Selected results are provided in Table 6.15 and illustrated in Figures 6.16 and 6.17.

Finally, a review of results of water entry through deficiencies in the window are presented and include information obtained from troughs TW-B, TW-W, T4-W, T5-B, T5-W and W. Figures 6.20 and 6.21 provide useful highlights from results of this series of troughs.

6.2.2.3.i WATER ENTRY THROUGH SPECIFIED DEFICIENCIES AT THE ELECTRICAL OUTLET

The number of test trials in relation to the number of events for which water was collected in troughs E and D-W is given, for the static mode, in Table 6.11 and dynamic mode in Table 6.12.

Table 6.11– Number of test trials for which water was collected in troughs E and D-W for various stages under *static pressure test conditions*

Trough	Stage			Total	%
	5	6	7		
E	2/15	2/15	0/15	4/45	9
D-W	3/15	4/15	9/15	16/45	36

Table 6.12– Number of test trials for which water was collected in troughs E and D-W for various stages under *dynamic test conditions*

Trough	Stage						Total	%
	5		6		7			
ABSL*⇨	0.2	0.5	0.2	0.5	0.2	0.5		
E	0/9	1/9	1/9	0/9	0/9	0/9	4/54	7.5
D-W	0/9	0/9	6/9	6/9	3/9	3/9	18/54	33

* ABSL – nominal value of 0.2 or 0.5 L/s-m^2

As might be expected the likelihood of entry diminishes with each successive in-board trough from a 100% likelihood of water collection in trough D-B to 36% in trough D-W and finally to ca. 9% in trough E under static conditions. In the dynamic mode, the results are similar. However, the probability of water collection in troughs E or D-W is slightly less in this mode; ca. 33% for D-W as compared to ca. 36% in static mode and for trough E, ca. 7.5 in the dynamic as compared to ca. 9% in the static mode. These results also indicate that the probability is greater that water will be collected at higher pressure levels (i.e. twice as likely at 150, 300, or 400 Pa as at 75 Pa static pressure level) and spray rates (i.e. almost three time more likely at 3.4 as compared to 0.85 L/min.-m^2).

Rates of entry in trough D-B obtained in static and dynamic mode are summarised in Tables 6.13 and 6.14 respectively. In static conditions, maximum values attained in all stages at spray rates of 0.85, 1.7 and 3.4 L/min.-m2 are 0.15, 0.162 and 0.179 L/min. respectively.

Table 6.13– WA-16: Water entry rates through deficiency above electrical outlet to trough "B"– *Static pressure mode* – summary of results from three stages (Stages 5, 6 & 7)

Spray *Rate* *L/min.-m²*	**Rate of water entry, L/min.**			
	Maximum	*Avg. at 0 Pa*	*Avg. at 400 Pa*	*Range*
0.85	0.150	0.135	0.126	0.032
1.7	0.162	0.145	0.140	0.033
3.4	0.179	0.148	0.150	0.06

Table 6.14– WA-16: Water entry rates through deficiency above electrical outlet to trough "B"– *Dynamic pressure mode* – summary of results from three stages (Stages 5, 6 & 7)

Spray *Rate* *L/min.-m²*	**Rate of water entry, L/min.**							
	Maximum		*Avg. at 75 ± 40 Pa*		*Avg. at 300 ± 125 Pa*		*Range*	
	*0.2**	*0.5*	*0.2*	*0.5*	*0.2*	*0.5*	*0.2*	*0.5*
0.85	0.140	0.145	0.133	0.135	0.133	0.133	0.012	0.033
1.7	0.158	0.168	0.144	0.143	0.143	0.145	0.028	0.037
3.4	0.168	0.175	0.151	0.157	0.153	0.151	0.043	0.045

* Tests conducted with nominal wall assembly leakage of 0.2 and 0.5 L/s-m²

Results from tests in the dynamic mode are similar to those obtained under static conditions; little or no dependence of entry rates for increases in dynamic pressure level and a greater effect on entry rates from increases in spray rate.

A change in the nominal air barrier leakage of the wall assembly from 0.2 to 0.5 L/s-m² does not appear to change the entry results at this trough. Given the nature of the design of the cladding it is expected that most water would accumulate in trough D-B, a reduced amount in D-W and little or on water should be collected in E. As well, changes in the ABSL (air barrier system leakage) should not greatly affect pressure differentials at the entry points given that the cladding is assembled to provide not only adequate drainage, but as well, pressure moderation. The pressure moderation effect reduces pressure differences across both the cladding and the other barriers of the wall assembly.

What is of interest is comparing results obtained in the dynamic mode at different test stages. The seal at the ventilation duct also affects the pressure distributions in adjacent stud cavities as well as that of the ventilation-drainage space. For example, no results were recorded for water entry in trough D-W in stage 5 as compared to a 6/9 chance in stage 6 and 3/9 in stage 7 irrespective of the level of ABSL; water in all instances was collected in trough D-B. This suggests that proper sealing of all passages for air leakage helps mitigate the effects of water entry through deficiencies in the cladding.

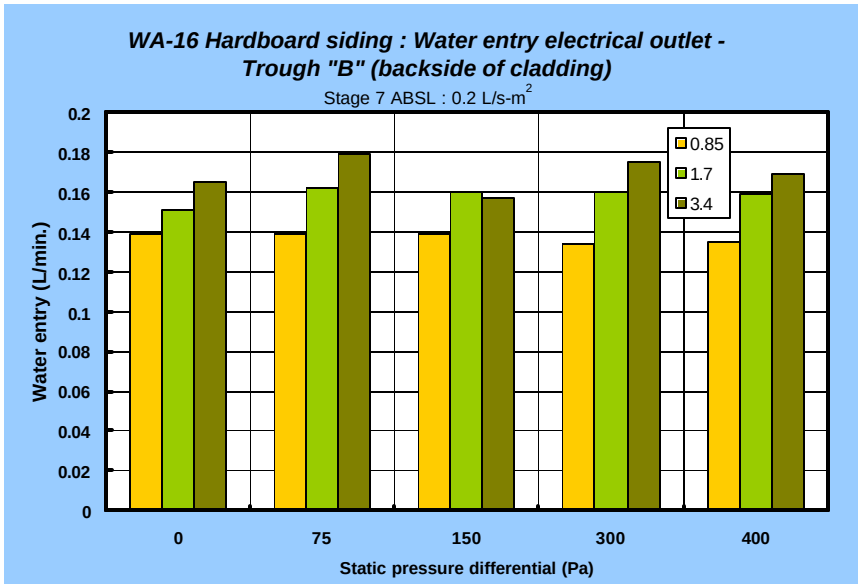

Figure 6.13– Siding WA-16 : Water entry under static pressure differential through deficiency above electrical outlet. Water collected in trough "B" (backside of cladding)

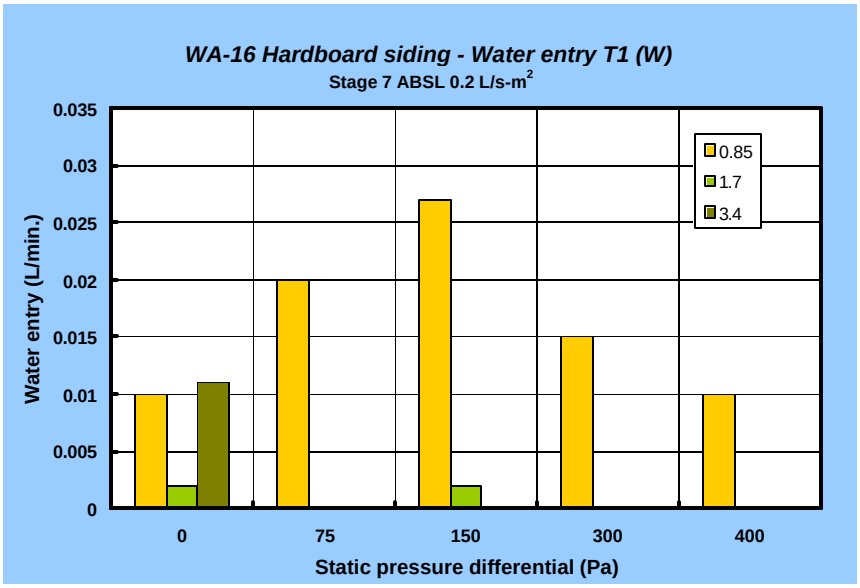

Figure 6.14– Siding WA-16 : Water entry under static pressure differential through deficiency above electrical outlet. Water collected in trough "T1" (W)

Water not collected in troughs D-B or D-W would collect below in trough T1. Provided in Figure 6.13 are entry rates in static conditions for trough T1-W that match those provided for D-B of Figure 6.12. The results show that most of the accumulation was collected at the lowest spray rate; little or no water was collected in this trough at spray rates of either 1.7 or 3.4 L/min.-m^2 for any of the pressure levels. Note that the rates of entry of trough T1 vary between 0 and 0.027 L/min. whereas rates for the trough above it vary between 0.134 and 0.169 L/min., roughly an order of magnitude difference between collection rates. Essentially, the lower trough represents the excess not collected in the trough above. This same pattern is evident for troughs beneath both the ventilation duct and window.

6.2.2.3.ii WATER ENTRY THROUGH SPECIFIED DEFICIENCIES AT THE VENTILATION DUCT

An overview of results obtained for the ventilation duct is provided in Table 6.15 and Figures 6.16 and 6.17. No water was collected in the trough beneath the ventilation duct in the ventilation-drainage space and closest to the cladding (i.e. trough V-B). However, water entering the deficiency above the ventilation duct was collected either in trough V-W (trough beneath duct adjacent to sheathing board in ventilation–drainage space), L (in stud cavity) or in troughs T2 located at the base of the wall directly below the duct.

Table 6.15 – Water entry at ventilation duct

Trough	Static test conditions Water entry L/min.			Dynamic test conditions Water entry L/min.					
				ABSL – 0.2 L/s-m^2			ABSL – 0.5 L/s-m^2		
	Stage			*Stage*			*Stage*		
	5	**6**	**7**	**5**	**6**	**7**	**5**	**6**	**7**
V-B	0	0	0	0	0	0	0	0	0
V-W	0-0.017	3 values	0-0.020	0-0.029	1 value	3 values	0.004-0.025	1 value	0-0.04
L	0-0.032	0-0.042	0-0.032	0-0.040	0-00.13	0-0.020	0-0.156	0.005-0.070	0-0.01
T2-B	0.001-0.058	0.012-0.058	0-0.073	0.017-0.051	0.020-0.058	0-0.070	0-0.052	0-026-0.080	0-0.10
T2-W	0.008-0.06	0-0.102	0.009-0.061	0.026-0.233	0.028-0.290	0.018-0.279	0.010-0.290	0.030-0.242	0.015-0.336

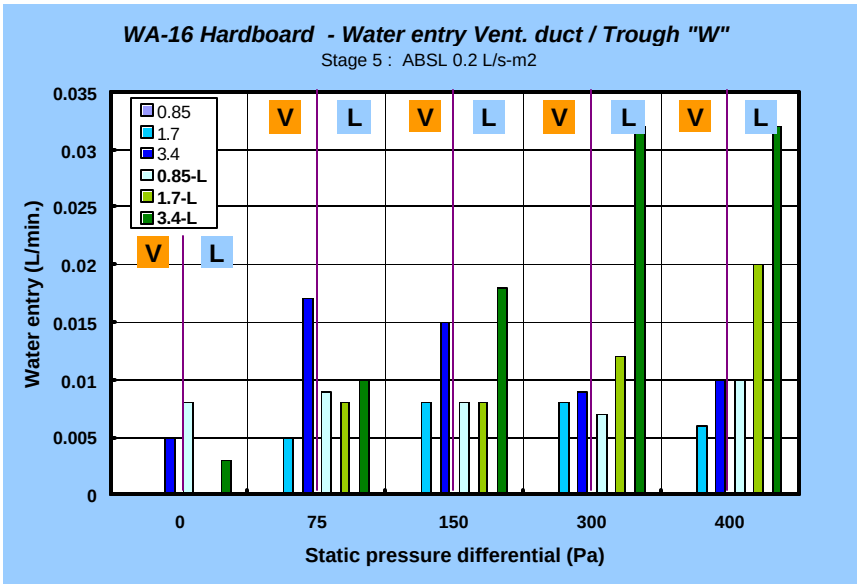

Figure 6.15–WA-16 hardboard siding: Stage 5 - Water entry under static pressure differential through deficiency above vent duct (Trough "W")

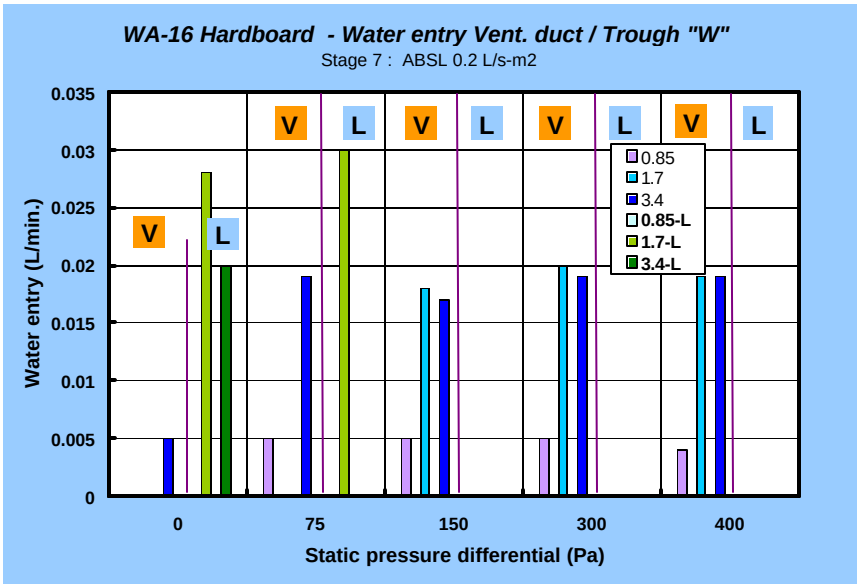

Figure 6.16–WA-16 hardboard siding: Stage 7 - Water entry under static pressure differential through deficiency above vent duct (Trough "W")

Of the water entering this deficiency, the more significant rates were obtained in stage 5 for trough L, located in the stud cavity where water must pass the sheathing board and enter via a small opening located at the underside of the duct in the joint between the duct and the board (see Figure 6.18). In this stage, both sealant and backer rod are used to seal the joint with the exception of this small opening (ca. 2-mm wide x 50-mm long) whereas in stage 7, the sealant and backer rod are removed. Results for stage 6 show that little or no water collected in trough V-W, but considerable more was in troughs L and T2-W. The rates at which water was collected in trough L (stage 6) are comparable to those obtained in stage 5, however in stage 6 little or no water was collected when the spray rate was 0.84 L/min.-m^2. Finally, in stage 7, most of the water was collected in troughs V-W and T2-W or –B but not L. Hence it appears that the air flow and pressure differentials that prevail in stage 5 at the ventilation duct tend to drive water through to the stud cavity whereas these conditions are not sufficient to do so in the latter stages of the test (i.e. stages 6 and 7).

This situation is evident when comparing results from stages 5 and 7 for troughs V-W and L at the various pressure levels and spray rates, as shown in Figures 6.16 (stage 5) and 6.17 (stage 7) respectively. In stage 5 (Fig. 6.16) rates of entry to trough V-W tend to be reasonably the same at each pressure level; increases in spray rate tend to slightly increase the rates of entry to this trough. The dependency of rates of entry on spray rate is more evident for trough L in particular at pressure levels of 150, 300 and 400 Pa. The situation in stage 7 (Fig. 6.17 – no sealant or backer rod) is now different owing to the change in pressure conditions within the ventilation-drainage space; at higher pressure levels (i.e. 150, 300 and 400 Pa) no water is collected in trough L whereas rates of collection to trough V-B are dependant in part, on spray rates.

Results obtained in the dynamic test mode are similar to those retrieved in static mode; collection of water was made in trough L for stages 5 and 6 with a reduced likelihood of collection in stage 7. For trough V-W in the dynamic mode, water was primarily collected in stage 5, little or no water being collected in stages 6 and 7. This was apparent whether the nominal ABSL (air barrier system leakage) was 0.2 or 0.5 L/s-m^2. However, rates of entry in stage 5 were generally greater when the ABSL was 0.5 as compared to 0.2 L/s-m^2. Hence, the effect of an increased in the ABSL on an increase in water entry rate is again evident. In the case of trough L, similar comments apply to the preceding water entry results obtained for trough V-W.

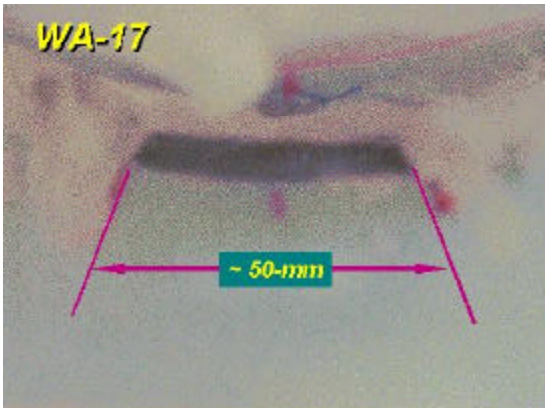

Figure 6.17– WA-17 : Stage 5 - Close-up view of opening (~ 4-mm x 50-mm) beneath the ventilation duct

6.2.2.3.iii WATER ENTRY THROUGH SPECIFIED DEFICIENCIES AT THE WINDOW

A summary of results obtained for water entry to troughs TW-W, TW-B located beneath the window frame in the ventilation-drainage space between the cladding and the sheathing board is provided in Table 6.16, and Figures 6.18 and 6.19. As well, information regarding collection in troughs T4-B, -W and T5-B, and -W are also given in the table.

Table 6.16– Summary of water entry to troughs located in proximity to window and at base of wall assembly in ventilation-drainage space

Trough	Static test conditions Water entry L/min.			Dynamic test conditions Water entry L/min.					
				ABSL – 0.2 L/s-m^2			ABSL – 0.5 L/s-m^2		
	Stage			*Stage*			*Stage*		
	5	**6**	**7**	**5**	**6**	**7**	**5**	**6**	**7**
TW-B	0.005-0.08	0.04-0.14	0.22-0.29	0.09-0.40	0.14-0.37	0.21-0.35	0.03-0.20	0.09-0.16	0.03-0.14
TW-W	0.006-0.15	0.11-0.29	0.13-0.31	0.07-0.29	0.16-0.32	0.19-0.27	0.09-0.40	0.14-0.37	0.21-0.35
T4-B	Ø	Ø	Ø	Ø	Ø	Ø	Ø	Ø	Ø
T4-W	1 value	Ø	1 value	1 value	Ø	Ø	Ø	1 value	3 values
T5-B	Ø	1 value	0-0.02	1 value	0-0.04	Ø	1 value	0-.10	Ø
T5-W	0-0.14	0-0.11	0-0.15	0.03-0.10	0.01-0.10	0.03-0.20	0.02-0.23	0.005-0.16	0.08-0.28
W-LS	2 values	Ø	Ø	Ø	Ø	Ø	Ø	Ø	Ø

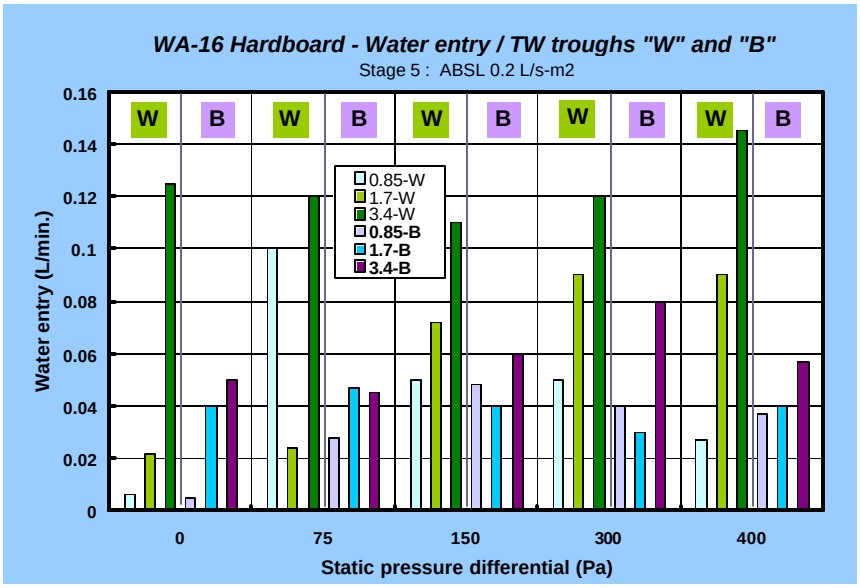

Figure 6.18: Siding WA-16 – Water collection in trough "TW" for both the W-wall side and B-back of cladding at various spray rates and for given static pressure differentials.

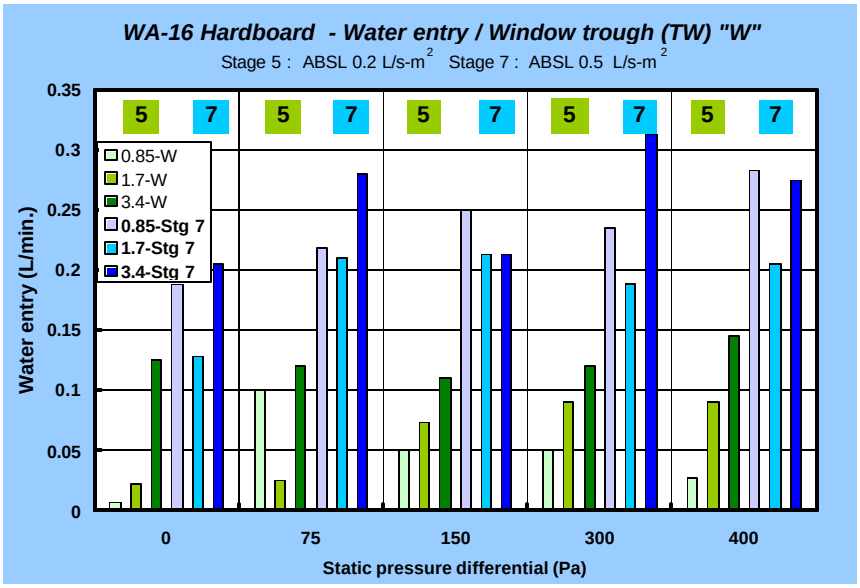

Figure 6.19: Siding WA-16 – comparison between water collection rates of stages 5 and 7 in trough "TW" on the W-wall side at various spray rates and for given static pressure differentials.

Essentially no water was collected in any of the W troughs that are located beneath the window frame on the sill and serve to collect water that might penetrate the window assembly to the joints of the window-wall interface.

Water entering the deficiencies at the base of the window frame primarily found its way to trough TW-W, that is the trough located closest to the sheathing board. However, significant rates of entry were obtained for trough TW-B as depicted in Figure 6.18. In general, rates of entry were observed when no pressure differential was applied to the wall and in increasing amounts to corresponding increases in spray rate for either trough.

A comparison of entry rates to trough TW-W in stages 5 and 7 is provided in Figure 6.19. Greater rates were obtained in stage 7 as compared to stage 5; in stage 7, as in stage 5 rates were not dependent on pressure levels but to a lesser extent, dependent on spray rate. The increase in rates of water entry to this trough can in part be attributed to the variation in cavity pressure brought about by changes in sealing the interface between the ventilation duct and the sheathing board.

6.2.2.4 WATER ENTRY THROUGH SPECIFIED DEFICIENCIES FOR WALL ASSEMBLY 17 (WA-17)

6.2.2.4.i STATIC PRESSURE LEVELS

Water was collected only for the trough serving the electrical outlet. No significant amounts were collected in any of the remaining troughs although traces were observed in the collection trough used for the ventilation duct. Results for collection rates of water entering the deficiency above the electrical outlet under static test conditions are given in Table 6.17 and Figure 6.20 and in dynamic test conditions in Table 6.18.

In regard to test results obtained under static pressure conditions, water entry was observed under no pressure differential; values for rates of water entry ranged between 0.056 L/min. (spray rate, SR = 0.85 L/min.-m^2) to 0.167 L/min. (SR= 3.4 L/min.- m^2).

As well, there is in general, a dependency of both pressure differential and spray rate on water entry rates. This tendency is however more pronounced in the case of spray rate as compared to pressure differential. For example, the magnitude of the range of values for rates of water collection in relation to the range of test pressures (at a given spray rate) varies between 0.004 and 0.027 L/min. Whereas the magnitude in this same range of values in relation to the range of spray rates (at given pressure level) varies between 0.04 and 0.102 L/min. Hence the effect of spray rate is about half to a full order of magnitude more significant than that of pressure on water collection rates at this electrical outlet.

Table 6.17– WA-17: Water entry rates through deficiency above electrical outlet – *Static pressure mode* – summary of results from three stages (Stages 5, 6 & 7)

Spray *Rate* *L/min.-m²*	**Rate of water entry, L/min.**			
	Maximum	*Avg. at 0 Pa*	*Avg. at 400 Pa*	*Range*
0.85	0.097	0.070	0.079	0.041
1.7	0.106	0.086	0.099	0.024
3.4	0.159	0.145	0.154	0.029

Table 6.18– WA-17: Water entry rates through deficiency above electrical outlet – *Dynamic pressure mode* – summary of results from three stages (Stages 5, 6 & 7)

Spray *Rate* *L/min.-m²*	**Rate of water entry, L/min.**							
	Maximum		*Avg. at 75 ± 40 Pa*		*Avg. at 300 ± 125 Pa*		*Range*	
	*0.2**	*0.5*	*0.2*	*0.5*	*0.2*	*0.5*	*0.2*	*0.5*
0.85	0.098	0.120	0.082	0.083	0.069	0.101	0.047	0.062
1.7	0.108	0.200	0.096	0.100	0.100	0.182	0.023	0.113
3.4	0.182	0.295	0.144	0.151	0.160	0.282	0.051	0.158

* Tests conducted with nominal wall assembly leakage of 0.2 and 0.5 L/s-m²

This trend is clearly depicted in Figure 6.20 that shows water entry rates for the electrical outlet in stage 6 of the test sequence and in which the nominal air leakage of the wall assembly is 0.2 L/s-m². The rates of entry are shown in relation to the five static pressure levels and each spray rate. It is evident that very slight increases in rates of entry occur at a given spray rate whereas at each given pressure level there is a marked increase in rate of entry for a corresponding increase in spray rate.

6.2.2.4.ii WATER ENTRY THROUGH SPECIFIED DEFICIENCIES UNDER DYNAMIC PRESSURE FLUCTUATIONS

Results from dynamic tests reflect patterns observed for results obtained under static conditions. Rates of water entry increase more significantly in relation to increases in spray rate as compared to increase in pressure level. As well, rates of entry are essentially comparable to those obtained in static conditions. For example, at a given ABSL (air barrier system leakage) of 0.2 L/s- m², variances between maximum and minimum values for rates obtained in either the dynamic or static mode are small; a variance of 0.004 L/min. for the minimum rate of entry and 0.023 L/min. for the maximum rate of entry.

A comparison of rates of entry in the dynamic mode under different nominal wall assembly leakage conditions reveals that greater entry rates were obtained in most test sequences

(25/27) when the ABSL (air barrier system leakage) was 0.5 as opposed to 0.2 L/s- m^2. This is an expected result given that nominally at the higher leakage rates, pressure differentials across entry points are likely to be greater thus increasing the likelihood of water entry when water is present at the deficiency.

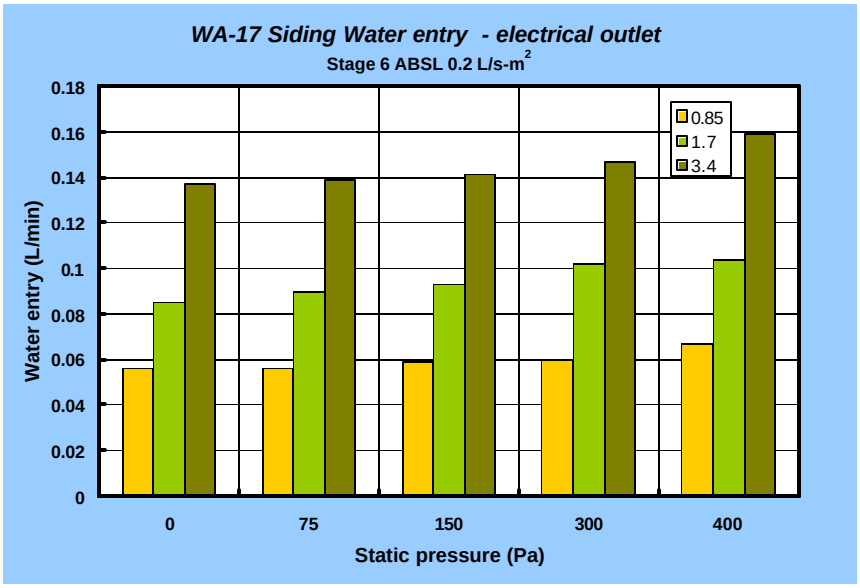

Figure 6.20 – Siding WA-17 : Water entry under static pressure differential through deficiency above electrical outlet

6.2.2.5 SUMMARY – ASSESSMENT OF WATER ENTRY THROUGH SPECIFIED DEFICIENCIES

A brief review is offered in regard to the water entry assessments in which results for the electrical outlet will be followed by those obtained for the ventilation duct and then the window. As well, the entry function for the electrical outlet is provided, as this information was important to the parametric studies undertaken in Task 7 of the MEWS project.

6.2.2.5.i SUMMARY WATER ENTRY THROUGH SPECIFIED DEFICIENCIES — ELECTRICAL OUTLET

No entry at was obtained for WA-15 and WA-16. In the former case, water was seen entering the deficiency but not passing the sheathing board or collecting in the trough located in the stud cavity. Water entering this deficiency sought passage to the interstitial space between the cladding and the sheathing.

For WA-16, the provision of a 19-mm space between the cladding and the sheathing effectively prevented water from collecting in the trough located in the stud cavity, as might be expected. Water that did enter collected in the trough located direct behind the cladding. The rates of entry were found to be dependent on the spray rates to which the cladding was subjected; greater rates of water entry were achieved for corresponding increases in spray rate.

Hence water entry rates for the electrical outlet have only been collected for WA-17. The rates of entry are consistent with those obtained for stucco-clad wall assemblies; values ranged between 0.065 to 0.167 L/min. The more significant effect on water entry rates was the spray rate as compared to the pressure differential.

An entry function for the electrical outlet located in siding-clad wall assemblies was based on average values of entry for all stages. The function relates estimates of rates of entry to the stud cavity in relation to static pressure differentials and spray rates and is used as the basic water entry parameter for hygIRC simulations undertaken in Task 7 of the MEWS project. The entry function permits estimating the quantity of water entering the cavity per unit time for climate variables such as wind speed and rainfall intensities. The wind speed is related to a pressure difference across the assembly and the rainfall to a spray rate. With both these climatic data, and using the function, the rates of entry are estimated.

The water entry function derived for the electrical outlet of this wall assembly is the following:

$$dq/\,dR_p\,(Pa) = 1.115\,E^{-10}\,(?P)^3 - 3.3885\,E^{-8}\,(?P)^2 + 1.618\,E^{-5}(?P) + 0.0422$$

The curve is plotted in Figure 6.21 in which the values of $dq\,/\,dR_p$, ranging between 0.041 and 0.06 $(L/min.)(L/min.\text{-}m^2)^{-1}$ are provided in relation to the static pressure differential in Pa (0-400 Pa). The value of fit was $R^2 = 0.9999$, indicating a strong fit of data to the curve.

The value of 0.0422 $(L/min.)(L/min.\text{-}m^2)^{-1}$ in the equation is that amount of water entry 'potential' provided when no pressure difference occurs across the assembly. This implies that if rain is deposited on the cladding when little or no wind occurs, entry will nonetheless take place and an approximate rate of 0.0422 L/min. per unit of spray rate. The implications with respect to entry into the stud cavity given that spray rates might average say 0.019 $L/min.\text{-}m^2$ over a wet season (for Wilmington say), are that average entry rates over the hour would be ca. 0.048 L/hr or about 50 mL (ca. 1/10 of a cup of water).

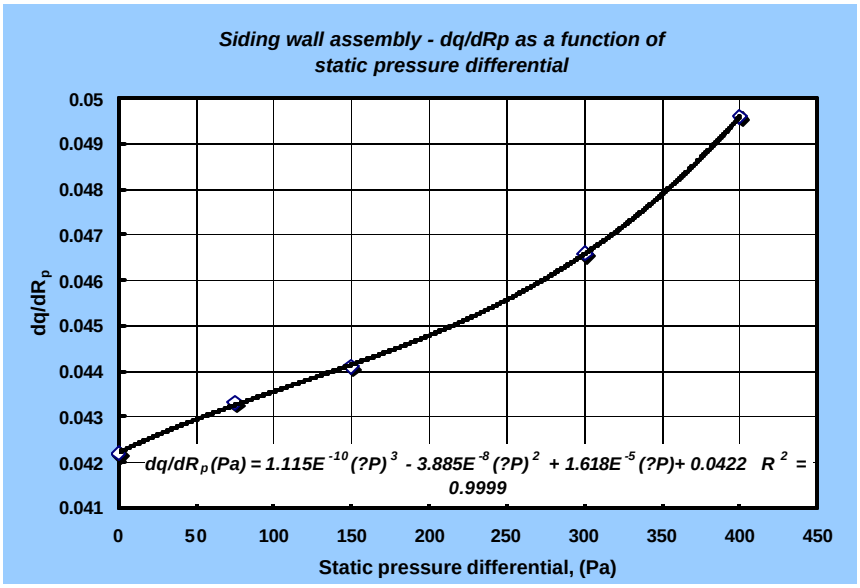

Figure 6.21: Siding WA – Water entry function derived from results of water entry through the electrical outlet of WA-17

6.2.2.5.ii SUMMARY WATER ENTRY THROUGH SPECIFIED DEFICIENCIES — VENTILATION DUCT

Water was collected for WA-15 and WA-16 however only traces of water were collected for WA-17. For WA-15, water enters under no pressure differential and in significant quantity (Maximum Avg. at 0 Pa: 0.045 L/min.) and at substantially higher rates of entry at increased spray rates. Indeed, rates of entry are primarily dependent on the spray rate and not the pressure difference across the assembly. Results from the dynamic mode are similar to those obtained in static mode, with values of maximum rate of entry ranging between 0.019 to 0.086 L/min in the dynamic as compared to a range of 0.019 to 0.062 L/min. in the static mode. As well, the joint seal at the interface between the sheathing and the ventilation duct affects the nature of the entry but not the maximum values attained. Results from Stage 7, where no seal exists, are similar to those obtained for stage 5 for which both a backer rod and sealant are used to seal the joint (e.g. maximum values Stage 5 : Stage 7 • 0.042 L/min. : 0.044 L/min.).

For WA-16, the space between the cladding and the sheathing affected results as portions of water were collected in the trough adjacent to the sheathing, in the troughs below before eventually accumulating in the trough located in the stud cavity. Rates of collection in the trough located in the stud cavity ranged up to 0.032 L/min.

6.2.2.5.iii SUMMARY WATER ENTRY THROUGH SPECIFIED DEFICIENCIES — WINDOW

Water entry about windows was evident for WA-15 (W-LS) and WA-16, although for WA-16 little or no water was observed to enter into the stud cavity; no water was recorded for WA-17.

A good portion of the water accumulated in the ventilation-drainage space between the cladding and the sheathing.

For WA-15, maximum values ranged between 0.0126 to 0.0154 L/min. In the dynamic test mode, maximum values attained are similar to those achieved in the static mode; greater rates of entry were evident for nominal ABSL (air barrier system leakage) of 0.5 as compared to 0.2 L/s-m^2. Rates of water collected in the trough on the LS of the window vary in accordance with pressure differential; changes in spray rate as such do not affect the results.

Chapter 7

Overview of results from water penetration trials and water entry assessments

TABLE OF CONTENTS

? CHAPTER 7 ?

Overview of results from water penetration trials and water entry assessments

LIST OF FIGURES

LIST OF TABLES

7.1 Introduction

- An overview of the different wall assemblies and their respective components is provided in

- Table 7.1.
- A comparison of results from the water penetration trials is provided in section 7.2.1. The review is made on the basis of results on penetration observed adjoining the window, the electrical outlet and ventilation duct, or through-wall penetration of the sheathing board.
- A comparison of results of water entry trials is given in section 7.2.2. Results obtained from the different wall assemblies for entry at the various penetration points are reviewed, specifically those for the electrical outlet, ventilate duct, adjoining the window and vertical joint.
- Section 7.2.3 provides the Derivation of Water entry functions and input to hygIRC and related information on water entry rates
- The final section offers some insights into the implications and limitations of the entry functions.

Note that water penetration trials do not include specified deficiencies in the wall specimen whereas these are part of the assessment protocol for water entry tests. When reference is made in this chapter to “deficiencies”, in all instances this is referring to specified deficiencies.

Table 7.1 – Wall assembly types and key wall components

WA-#	System description	Drainage Space	WRB	Sheathing board	Window type
1	Stucco - concealed barrier 19 mm, lime-cement plaster / self-furring expanded metal lath	None	Cross-woven perforated polyethylene membrane	OSB (11 mm)	Flange
2	Stucco - concealed barrier, 19 mm, lime-cement plaster / self-furring woven metal lath	None	1 layer 60-min. rated building paper	OSB (11 mm)	Flange
3	Stucco - concealed barrier, 19 mm, lime-cement plaster / self-furring welded wire metal lath	None	Spun-bonded polyolefin membrane	OSB (11 mm)	Flange
4	Stucco - 12 mm, fibre-reinforced plaster pre-mix with acrylic finish / self-furring expanded metal lath	None	2 layers 30-min. rated building paper	OSB (11 mm)	Flange
5	Stucco - Drained system with top and bottom vents of 19 mm, 3 coats Portland cement plaster (BC BERC)	10-mm PT wood strapping	2 layers 30-min. rated building paper	OSB (11 mm)	Flange
6	EIFS Barrier wall +source drainage at window (i.e. Proprietary engineered sill)	None	None	OSB (11 mm)	Flange
7	EIFS Dual barrier Wall	None	1 layer 60 min. rated building paper	OSB (11 mm)	Flange
8	EIFS Dual barrier Wall + local drainage at window (Sill drip flashing)	None	Polymer cement coating	Glass mat gypsum board (12 mm)	Flange
9	EIFS Drained wall	6 mm X 30 mm vertical grooves	Polymer cement coating	Glass mat gypsum board (12 mm)	Flange
10	EIFS Drained wall	3 mm nylon drainage mat	Non-cementitious coating	OSB (11 mm)	Flange
11	Masonry / 90mm brick veneer / Stone sill	25 mm	None	25 mm XPS (ship lap joints)	Box
12	Masonry / 90 mm brick veneer / Rowlock sill	25 mm	1 layer 30-min. paper	OSB (11 mm)	Flange
13	Masonry / 90 mm brick veneer / Stone sill	25 mm	1 layer 30-min. paper	Asphalt-impregnated fiberboard	Box elastomer pan flashing
14	Masonry/ 90 mm brick veneer / Rowlock sill	50 mm	Micro-perforated HDPE / LDPE	Glass mat Gypsum board (12 mm)	Flange
15	Siding - Hardboard Composite wood lap siding	None	Micro-perforated HDPE / LDPE	Asphalt-impregnated fiberboard	Flange
16	Siding - Hardboard Composite wood lap siding	19 mm, PT wood strapping	2 layers 30-min. rated building paper	Glass mat Gypsum board (12 mm)	Flange
17	Siding -Vinyl	None	None	36 mm XPS	Flange

7.2 Review of test results

7.2.1 Water Penetration trials - Comparison of results

A summary of results from water penetration trials is provided in Table 7.2 in which the occurrence (or not) of penetration at specific points of entry are given in relation to the seventeen (17) wall assemblies. As well, information on the individual assemblies is provided, including the generic type (i.e. stucco, EIFS, brick masonry, and siding), type of sheathing, the presence and type of drainage space between the cladding and the sheathing, should any be provided. The distinction offered in regard to drainage is essentially one that only affects the EIFS wall assemblies. The other wall assembly types either have the possibility of 'free' drainage in the space between the cladding and the sheathing, or in the absence of a space, are not considered to provide adequate drainage as such. In the case of EIFS wall assemblies then, although no evident drainage space exists, as compared to those assemblies for which a space has specifically been provided (e.g. WA-16; 19-mm space), the symbol L denotes local drainage, VG - vertical grooves, and DM – drainage mat (i.e. 3-mm nylon drainage mat).

The occurrence of penetration was observed at the various entry points including the electrical outlet (E), ventilation duct (L), and adjoining the windows (W) as well as through the sheathing board (Sh-Brd). Activation of functional moisture sensors (MS) over the course of the trials was noted and the number of activated (X) in relation to the functional sensor (Y) is given as X of Y.

For each wall assembly then, observed penetration at the various entry points or through the sheathing board is given the symbol (◉) whereas a null symbol (⊖) indicates that no entry was observed during the trials. In addition to providing information on the degree of MS activity, information is also offered as to the test mode (static or dynamic –D) and pressure level (Pa) at which penetration was first observed. For example, for Stucco WA-2A, penetration was first observed to occur in the sheathing board at the 500 Pa static pressure level (denoted as 500) whereas in the case of WA-16, penetration of the siding-clad wall assembly was observed at 300 Pa dynamic pressure level (denoted as 300D).

A review of the summary provides a measure of the number of penetration 'events' observed during the trials. Hence, penetration occurred at the electrical outlet in 4 of 17 walls, the ventilation duct in 3 of 17 walls, adjoining the window in 9 of 17 walls and through the sheathing board in 4 of 17 walls. Evidently for the specimens investigated in this study, these results suggest that the most vulnerable area for water penetration is the window.

Table 7.2 – Summary of results from water penetration trials

	Stucco						EIFS					Brick masonry				Siding		
Sheathing[1]	O	O	O	O	O	O	O	O	G	G	O	X	O	F	G	F	G	X
Drainage[2]	N	N	N	N	N	Y	L	N	VG	VG	DM	Y	Y	Y	Y	N	Y	N
D-Space	N	N	N	N	N	Y	N	N	N	N	N	Y	Y	Y	Y	N	Y	N
WA-#	**1**	**2A**	**2B**	**3**	**4**	**5**	**6**	**7**	**8**	**9**	**10**	**11**	**12**	**13**	**14**	**15**	**16**	**17**
Entry points[3]																		
(D) E	⊖	◉	500	⊖		⊖	⊖	**300**	⊖	⊖	⊖	⊖	⊖	⊖	⊖	⊖	**300D**	◉
(V) L	⊖	◉	500	⊖		⊖	⊖	⊖	⊖	⊖	⊖	⊖	⊖	⊖	⊖	⊖	**700D**	◉
(TW) W	700D	300	700	500	500	⊖	**500**	**500**	⊖	⊖	**1000**	◉	⊖	⊖	⊖	700D	⊖	⊖
Sh-Brd	⊖	**75 / 500**	**500D**	⊖		⊖	**300**	**150**	⊖	⊖	⊖	⊖	⊖	⊖	⊖	⊖	⊖	700D
(X of Y) MS	7/15	16/16	4/16	11/16	4/16	nil	6/40	29/40	19/40	Nil	7/40	2/12	3/12	7/12	6/12	⊖	8/10	2/12

1.) O – OSB; G – glass mat gypsum board; X – XPS; F – asphalt impregnated fibreboard
2.) N – no drainage; Y – drainage; L – local drainage; VG – vertical grooves (see Table 7.2); DM – nylon drainage mat (Table 7.2)
3.) E – Electrical outlet; V – Ventilation duct; W – window; Sh-Brd – Sheathing board; MS – moisture sensors (X of Y : sensors activated of Y functional sensors)

7.2.1.1 WATER PENETRATION ADJOINING WINDOW

The susceptibility of the window and adjoining window-wall interface to water penetration can not be attributed to the wall design as such or indeed the presence or not of a drainage space between the cladding and the sheathing. Walls containing a drainage space also experienced entry about the window although this was not as likely as for wall assemblies not incorporating a space. Hence this emphasises that interface details about windows (indeed all details about through-wall penetration) need proper consideration regardless of the type of wall assembly given the possibility that leakage will likely occur at the window-wall interface and the window proper.

7.2.1.2 WATER PENETRATION OF ELECTRICAL OUTLET AND VENTILATION DUCT

Water penetration observed about the electrical outlet was notably absent in walls incorporating a drainage space with the exception of WA-16 (siding – 300 Pa dynamic pressure level). That is, one wall of six (1/6) assemblies having a drainage space had penetration about the electrical outlet. Similar results were observed for penetration about the ventilation duct (i.e. 1 of 6 WA). As well, in both instances where penetration occurred in the case of a wall assembly having a drainage space, these were during the dynamic test mode for the siding wall assembly. Although these results were only evident at higher-pressure levels (i.e. 300 Pa and 700 Pa dynamic pressure level), they nonetheless suggest that details at the through-wall and cladding penetrations of siding wall assemblies (i.e. electrical outlet and ventilation duct) are somewhat vulnerable to water penetration. Hence these should be reviewed to insure adequate performance.

7.2.1.3 WATER PENETRATION OF SHEATHING BOARD

Observed penetrations through the sheathing board notably did not occur in any of the wall assemblies incorporating a drainage space. This is an expected result as access to the sheathing board from direct entry of water through the cladding is evidently less likely in walls incorporating a drainage space. This does not imply that the sheathing board is not vulnerable in a wall where a space exists given that water may nonetheless accumulate on the sheathing membrane from run-off at the through-wall penetrations or deposition in the interstitial space between the membrane and board. This occurrence was evident in WA-11 to WA-16, wall assemblies that include a drainage space and in which moisture sensor activity was nonetheless evident.

Actual through-wall penetration was only apparent for certain stucco and EIFS wall assemblies (i.e. WA-2A, WA-2B, and WA-7). In other instances, water was seen to penetrate at the horizontal joint between adjacent sheathing boards (i.e. WA-6, and WA-17). In the case of WA-6, penetration at

the horizontal joint between boards was due to water entry above the joint from water entering at the ventilation duct. Water had penetrated the interstitial space between the insulation and the sheathing board and found an opening at the joint.

For WA-17, the horizontal joint between XPS sheathing boards was the vulnerable joint; the contributing factors to water penetration in this instance was the lack of rigidity of the wall assembly and the ease of access of water to the back of the vinyl cladding. It was apparent that a lack of rigidity induced a significant deflection at the mid-height of the wall when the specimen was subjected to dynamic pressure fluctuations. This, in turn, causes the ship-lap joint to rotate, open, thereby allowing movement of air and, if water is present behind the cladding, water.

In the case of the stucco wall assemblies, through wall penetration was evident for WA-2A and WA-2B; for EIFS wall assemblies, WA-7. For WA-2A, penetration occurred at 75 Pa static pressure level (ΔP_S) and thereafter in another location at 500 Pa ΔP_S (Figure 7.1). In the case of WA-2B, penetration was observed at 300 Pa dynamic pressure level (ΔP_D) whereas this occurred at 150 Pa ΔP_S for WA-7 (in proximity to MS-8).

Stucco wall assemblies incorporate a metal lath or similar metal lattice to which stucco is applied. The lath itself is affixed directly to the wall assembly using staples. The staples traverse the sheathing membrane and pierce the sheathing board and in a good number of instances completely pass through the board. These are potential points of water penetration. As illustrated in Figure 7.1, if any water is present at the sheathing board, penetration is likely when the wall assembly is subjected to a heightened pressure differential.

Micro-droplets of the type illustrated in the figure formed over the course of the penetration trials. The rate of deposition of micro-droplets (Figure 7.1) in the stud cavity was estimated from observations carried out over the course of tests undertaken at a static pressure level of 250 Pa. This suggests that in an hour in these same conditions about 50 mL would accumulate in the stud cavity or about 15-20 mL under average conditions that might prevail in an hour in a light rain (i.e. 25 Pa ΔP_S).

The nature of the entry through the OSB sheathing in WA-7 was similar to that observed for WA-2A and WA-2B. Micro-droplets were seen to be forming at a point where a staple leg penetrated the sheathing board. What is of significance for WA-7 is the number of moisture sensors activated over the course of the test. Of the EIFS wall assemblies this was the only one that had neither drainage space or specified system for managing inadvertent water intrusion (other than the designation ‘dual barrier’). The performance of the wall assembly is in contrast for example to that of WA-9 in which no moisture sensors were activated. It is evident that wall assemblies characterised by WA-7 are vulnerable to water penetration when subjected to test conditions of the penetrations trials.

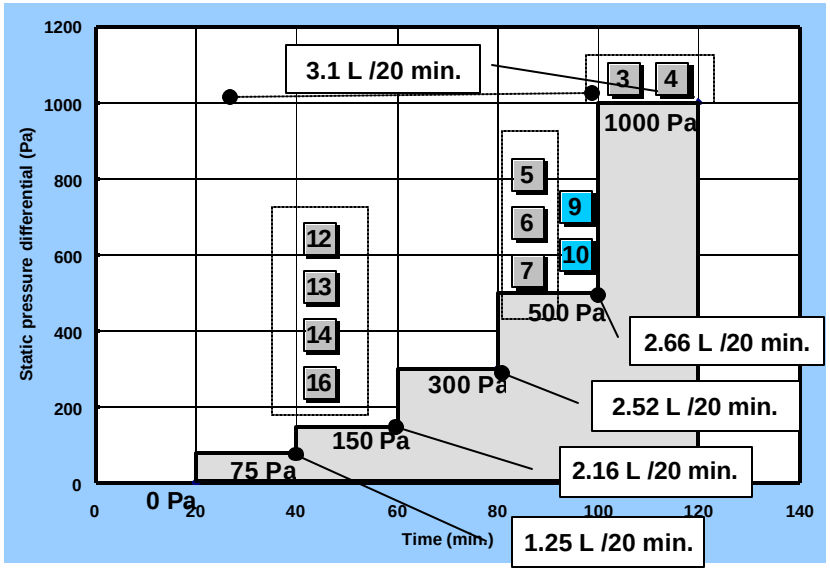

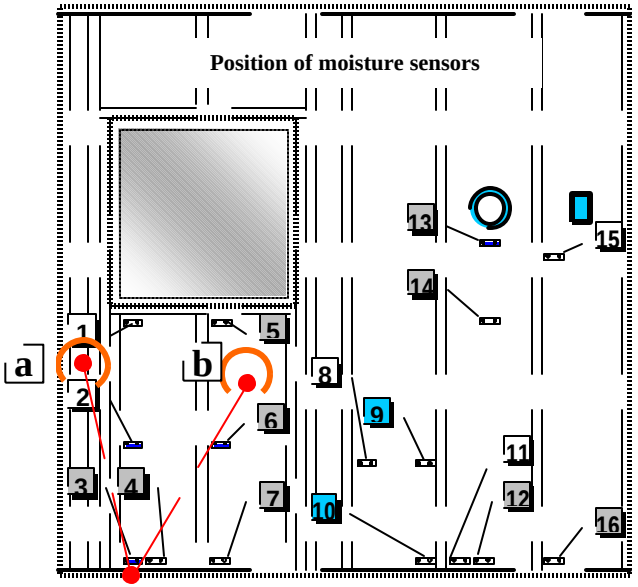

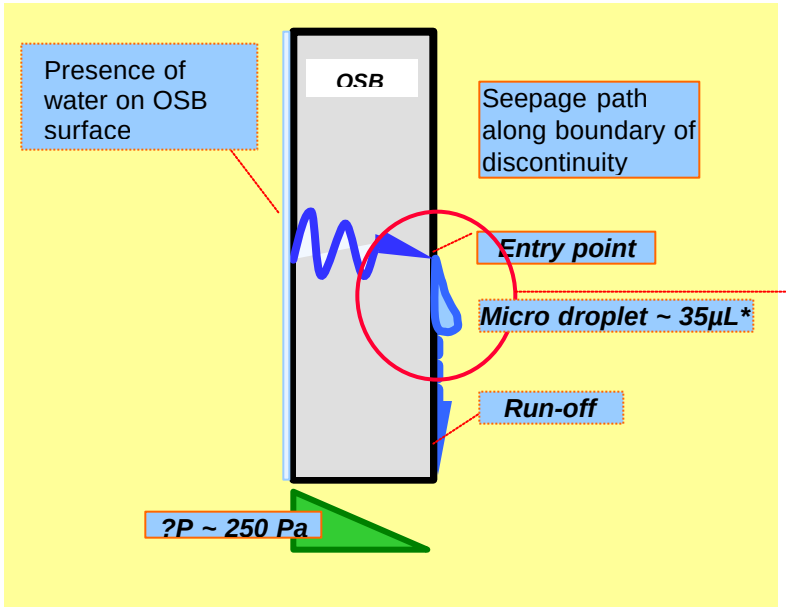

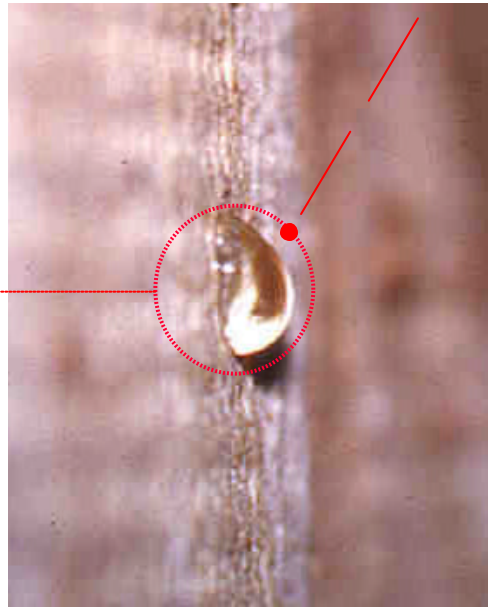

Penetration of sheathing board at (**a**) - 35 min. and in cavity at (**b**) beneath window - 90 min.

Figure 7.1 - Water penetration trials – evidence of water penetration through OSB sheathing board in Wa-2A, WA-2B and WA-7.

7.2.1.4 WATER PENETRATION TRIALS - OVERVIEW

Of the seventeen wall evaluated WA-2A, WA-2B (Stucco) and WA-7 (EIFS) were clearly vulnerable to water penetration in conditions to which they were subjected in the penetration trials. The susceptibility of WA-2A to water penetration is confirmed by a subsequent test on WA-2B. The difference between WA-2A and -2B is that WA-2A was the first of the seventeen walls to be tested and hence was subjected to severe test conditions over the course of developing and refining the test protocol; the construction of both wall assemblies was nominally the same.

Those wall assemblies offering the greatest redundancy in performance in respect to management of water intrusion and hence the least vulnerable to water penetration were those incorporating a drainage space. These wall assemblies showed the fewest instances of water penetration in any of the components and as well, some of the lowest activity of moisture sensors. This includes the masonry wall assemblies (WA-11 to WA-14 inclusive), WA-5 of the stucco-clad wall assemblies, and WA-16 of siding clad wall assemblies. As well, on the basis of these trials, EIFS wall assemblies that incorporated a drainage system, such as vertical grooves present in either the insulation or adhesive coating, had reduced likelihood of water penetration to the sheathing board.

These results are quite expected given what is presently known about the capabilities of the different wall systems to manage water intrusion. Indeed these results confirm the notion of reduced vulnerability of wall systems that incorporate a drainage space and further highlight the importance of adequate detailing about through-wall penetrations. This was in particular evident for windows, which were found to be the most sensitive components in regard to penetration.

These penetration trials help emphasise those wall assemblies that are vulnerable to water penetration, specifically WA-2A and WA-2B, WA-7 and WA-17. In the case of WA-17 the point should be made that penetration was brought about by the reduced rigidity of the wall from the use of XPS sheathing. Note that the ship-lap joint at the junction between adjacent panels was not taped and neither was there a sheathing membrane. The use of vinyl siding as such is not a factor in the overall comportment of the wall, however this combination of components should be further investigated as the breach occurred under significant test loads.

7.2.2 ASSESSMENT OF WATER ENTRY THROUGH SPECIFIED DEFICIENCIES - COMPARISON OF RESULTS

Entry points about the electrical outlet, ventilation duct and adjoining window are shown in Figure 7.2. Water entry points at specified deficiencies are representative of those typically found at the at the interface between wall components, and are located:

- Above the electrical outlet – a nominal 50-mm length of sealant is missing between the outlet cover and the wall.
- Above the ventilation duct – a nominal 50-mm length of sealant is missing between the duct and the wall.
- Below the windowsill and between finishing strips – a 50-mm length of sealant is missing between the ending strips.
- Along the horizontal joint located above the window and mid-way between joint extremities – a 90-mm length of sealant is missing
- Along the vertical joint located mid-height between joint extremities – a 90-mm length of sealant is missing

Troughs have been provided for collection of water in the stud cavity in proximity to the electrical outlet (E), ventilation duct (L) and the window (W). Troughs were also provided for water collection in a ventilation-drainage cavity for the masonry specimens (WA-11 to WA-14 inclusive) and one of the siding specimens (WA-17). This includes troughs adjacent to the electrical outlet (D), ventilation duct (V), window (TW) and a series of five (5) troughs (T1 - T5) located at the base of the wall, each extending across two vertical studs (i.e. ca. 400-mm). Shown in the figure above the troughs located in the ventilation-drainage cavity and adjacent to either the electrical outlet or ventilation duct are deflectors. These were used to prevent any water inadvertently entering above the level of specified deficiencies of either the electrical outlet or ventilation duct from being collected in their respective troughs.

Results of measurements from each of these points of entry are summarised and inferences made with respect to water entry and flow from the point to entry to within the wall assembly.

The range of maximum values for rates of water entry obtained for both the electrical outlet and ventilation duct is within the same order of magnitude (Table 7.3). Those for entry about points adjoining the window are in general lower as compared to the electrical outlet or ventilation duct, roughly an order of magnitude less. However, in certain instances the rate of entry adjoining the window extends to levels shown for either the electrical outlet or ventilation duct (i.e. 0.17 L/min. brick masonry at SR of 1.7 L/min.-m^2). The lower rates obtained in the case of the widow are to be expected given that direct paths for water entry are not evident for

flange windows as the flange itself is an obstacle to water flow. In instances where a box window was part of the assembly (i.e. in brick masonry wall assemblies), rates increased as water entry paths are less convoluted and offer direct access to collection troughs located beneath the window frame on the inside face of the sheathing membrane.

Table 7.3 – Maximum rates of water entry (L/min.) of wall assemblies at different points of collection

Trough	Stucco *		EIFS		Brick masonry		Siding	
	SR[1] 1.7	SR 3.4	SR 1.7	SR 3.4	SR 1.7	SR 3.4	SR 1.7	SR 3.4
E	0.086	0.33	0.254	0.272	0.16		0.106	0.159
V	0.51	0.56	0.133	0.154	0.185		0.03	0.062
W	0.087	0.037	0.01	0.02	0.17		0.0136	0.0134

1.) Spray Rate - SR (L/min.-m^2)

* When reference is made to wall assembly types (e.g. “Stucco”, “EIFS”, “Brick masonry”, “Siding”) this implies that results are derived from tests on a limited number of specimens – inferences are not being made in regard to generic types of wall assemblies unless specifically stated as such.

A summary of results obtained in static conditions is provided in Table 7.4 in which the occurrence of water entry at specific points of entry are given in relation to the seventeen wall assemblies. As was provided in the previous summary table for results of water penetration trials (Table 7.2), information is given on the configuration of individual assemblies.

Water entry points include the electrical outlet (E), ventilation duct (L), vertical joint (J), and collection troughs adjoining the window on the left (W-L) or right (W-R) sides or at the sill (W-S). The table does not include information on those troughs located in the drainage space between the cladding and sheathing (i.e. masonry wall assemblies and WA-16:siding) as all of these troughs located beneath the trough wall penetrations collected water.

In the case of the trough servicing the electrical outlet (E), it is noted that no results were recorded in the case of WA-5 (stucco wall with 19-mm drainage space) nor any of the brick masonry clad wall assemblies. This is simply because the electrical outlet did not extend into the stud cavity, hence no provision for a collection trough was evidently necessary at this location. However, troughs were located in the drainage space (D) that collected water entering at that location as depicted in Figure 7.2

As well, the summary reports on results for rates of entry obtained in static test conditions. Typically, if collection was made in static conditions, collection was also evident when walls were subjected to dynamic test conditions.

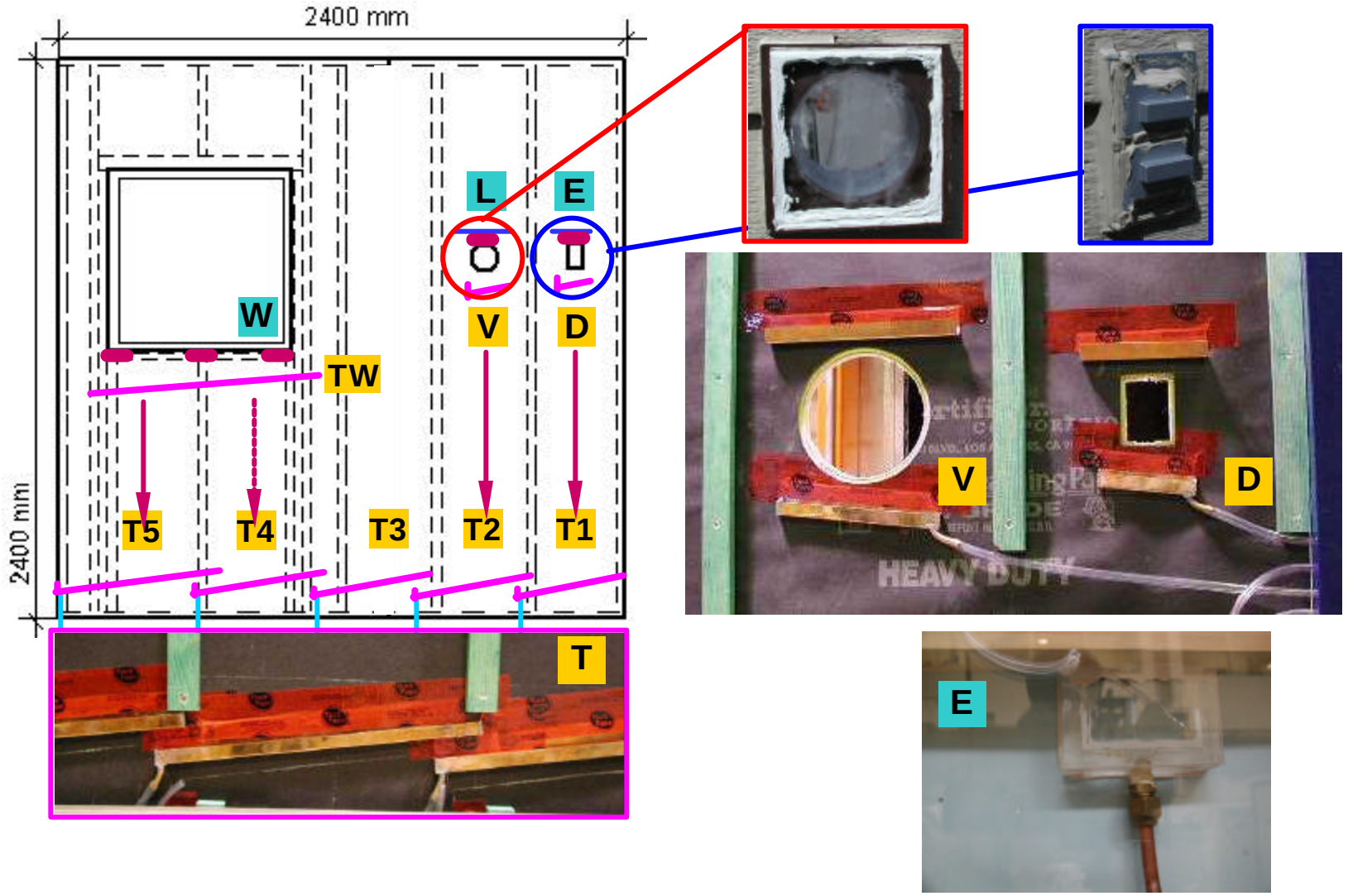

Figure 7.2 – Location of water entry points through specified deficiencies and identification of collection troughs

7.2.2.1 WATER ENTRY THROUGH DEFICIENCY ABOVE ELECTRICAL OUTLET

A review of the information provided in Table 7.4 reveals that 10 of 13 wall specimens provided data for entry of water through the deficiency above the electrical outlet. As mentioned previously, water was collected in troughs “D” located in the drainage space between the cladding and sheathing membrane.

For WA-15, water was observed behind the hardboard cladding; it subsequently drained to the interstitial space between the cladding and sheathing. Direct observation of water entry at the electrical outlet for either WA-6 or WA-8 was not made. It can only be assumed that in both these instances, whatever quantities of water entering the deficiency found a path to flow and drain from the area. In the case of WA-8, this may have been aided by the presence of vertical grooves in the EPS insulation.

Of importance in regard to entry rates are the maximum rates obtained when no pressure was applied across the assembly as well as the effect on rates of entry when increasing either the pressure or spray rate. Entry rates when no pressure is applied across the assembly are particularly significant since these suggest that even in instances when little driving pressure exists across the assembly, if water is present on the surface of the cladding water will enter the assembly through deficiencies.

All wall assemblies for which water entered the electrical outlet had water enter under no applied pressure differential. The maximum rates of entry to troughs servicing the electrical outlet when no pressure was applied across the assembly is given in Table 7.5. The rates (L/min.) are given for the different generic types of wall assemblies (stucco, EIFS, masonry, and siding) and spray rates applied to the cladding surface (i.e. 0.85, 1.7 and 3.4 L/min.-m^2). Note that no test data was collected for stucco walls at spray rate of 0.85 L/min.-m^2). As well, values given for the masonry walls are for trough “D-B”, the trough closest to the backside of the brick masonry cladding located in the drainage space.

Table 7.4- – Summary of results from assessments of water entry through specified deficiencies

	Stucco						EIFS					Brick masonry				Siding		
Sheathing[1]	O	O	O	O	O	O	O	O	G	G	O	X	O	F	G	F	G	X
Drainage[2]	N	N	N	N	N	Y	L	N	VG	VG	DM	Y	Y	Y	Y	N	Y	N
Space	N	N	N	N	N	Y	N	N	N	N	N	Y	Y	Y	Y	N	Y	N
WA-#	**1**	**2A**	**2B**	**3**	**4**	**5**	**6**	**7**	**8**	**9**	**10**	**11**	**12**	**13**	**14**	**15**	**16**	**17**
Entry points[3]																		
(D) E	◉	◉	◉	◉	◉		⊖	◉	⊖	◉	◉					⊖	◉	◉
(V) L	◉	◉	◉	◉	◉	⊖	◉	◉	⊖	◉	⊖	◉	◉	⊖	◉	◉	◉	⊖
J							N/A	N/A	N/A	◉	◉							
(TW) W-L	⊖	◉	◉	◉	⊖		⊖	⊖	⊖	⊖	⊖	◉	⊖	⊖	⊖	◉	⊖	⊖
W-R	⊖	◉	◉	⊖	⊖	⊖	◉	⊖	⊖	⊖	⊖	◉	⊖	⊖	⊖	⊖	⊖	⊖
W-S	⊖	◉	◉	⊖	⊖	⊖	⊖	⊖	⊖	⊖	⊖	⊖	⊖	⊖	⊖	⊖	⊖	⊖

1.) O – OSB; G – glass mat gypsum board; X – XPS; F – asphalt impregnated fibreboard
2.) N – no drainage; Y – drainage; L – local drainage; VG – vertical grooves (see Table 7.2); DM – nylon drainage mat (Table 7.2)
3.) E – Electrical outlet; V – Ventilation duct; W – window; Sh-Brd – Sheathing board; MS – moisture sensors (X of Y : sensors activated of Y functional sensors)

Table 7.5 – Maximum rates of entry (L/min.) to troughs servicing the electrical outlet at no applied pressure differential across wall assembly (i.e. 0 Pa $?P_S$)

WA type*	Spray rate (L/min.-m^2)		
	0.85	1.7	3.4
Stucco	N/D**	0.0765	0.047
EIFS	0.202	0.204	0.256
Masonry***	0.138	0.145	0.115
Siding	0.095	0.092	0.167

* refers to the type cladding of specimens investigated in this study
** N/D – no test conducted; ***values taken from trough "D-B", WA-12

These results demonstrate that significant quantities of water can readily accumulate within an hour (e.g. 0.25 L ~ 1 cup of water). Although there is some variation in the rates obtained for different wall assemblies, the values obtained are all within the same order of magnitude, ranging from 0.047 L/min. to 0.256 L/min.

The variation in rates of entry upon increases in spray rate is essentially the same as more when pressure differentials are increased. Table 7.6 shows the average rates of entry for the different wall assemblies at 0 and 300 Pa differential pressure across the assembly at spray rates of 1.7 and 3.4 L/min.-m^2. Differences in rates of entry between values achieved at 0 and 300 Pa pressure differential and at a spray rate of 1.7 are essentially the same as those obtained at 3.4 L/min.-m^2. Similarly, differences between values obtained at 1.7 and 3.4 L/min.-m^2 and at no pressure difference are about the same as at 300 Pa difference.

Table 7.6–Variation in maximum rates of entry (L/min.) to troughs servicing the electrical outlet at 0 (no) and 300 Pa applied pressure differential across wall assembly

	Spray rate (L / min.-m^2)			
	Static pressure differential (Pa)			
	1.7		**3.4**	
WA type*	*0*	*300*	*0*	*300*
Stucco	0.054	0.069	0.056	0.20
EIFS	0.181	0.233	0.200	0.249
Siding	0.086	0.099	0.145	0.154

* refers to the type cladding of specimens investigated in this study

7.2.2.2 DEFICIENCY ABOVE VENTILATION DUCT

Referring again to Table 7.4, values for water entry rate were obtained for 13 of 17 assemblies. Those not providing information included WA-5, WA-8, Wa-13, and WA-17.

The results from tests have been reported as those derived from three different stages in which stage 5 provided for a backer rod and sealant at the interface between the ventilation duct and the sheathing board. Entry to the collection trough "L" was possible at the underside of the duct through am opening in the sealant of nominally 2-mm by 50-mm, as shown in Figure 7.3.

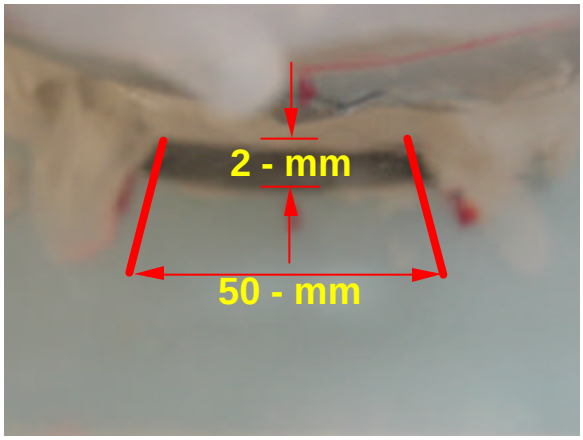

Figure 7.3 –Location of water entry point beneath ventilation duct

Maximum rates of entry under no applied pressure differential is provided in Table 7.7 and those obtained at 300 Pa applied pressure in Table 7.8. These results show that under no applied pressure, significant rates can be achieved irrespective of the test stage. Rates of entry among the different wall types vary between 0 and 0.109 L/min. at a spray rate of 0.85 L/min.-m^2 and at the highest spray rate of at 3.4 L/min.-m^2, between 0 and 0.256 L/min. Rates of entry obtained in general from tests on stucco wall specimens were higher as compared to results of water entry from tests on the other wall specimen types. E.g. the values for maximum entry rate of stucco walls in stages 5, 6 and 7 at a spray rate of 3.4 L/min.-m^2 was 0.254, 0.248, 0.256 L/min. respectively as compared to 0.066, 0.060 and 0.154 L/min. in the same stages respectively for the EIFS wall assemblies.

For any given wall specimen type, the rates of entry from one stage to the next are comparable or at least within an order of magnitude difference. Hence results from one stage to the next do not appear to be affected by variations in the treatment of the joint between the ventilation duct and sheathing board.

Rates of water entry in the different stages of the four masonry wall specimens were either non-existent or below those obtained for the other wall specimen types. In this instance, the presence of a wide drainage space appears to help reduce the likelihood of water entry to the stud cavity by this elongated path.

Table 7.7 – Maximum rates of entry (L/min.) to troughs servicing the Ventilation duct at no applied pressure differential across wall assembly (i.e. 0 Pa ?P)

WA type*	Water entry rates (L/min.) *Spray rate (L/min.-m2)								
	Stage 5			Stage 6			Stage 7		
SR* □	*0.85*	*1.7*	*3.4*	*0.85*	*1.7*	*3.4*	*0.85*	*1.7*	*3.4*
Stucco	0.066	0.191	0.254	0.095	0.180	0.248	0.109	0.160	0.256
EIFS	0	0.083	0.066	0.018	0.064	0.060	0.108	0.133	0.154
Masonry	0	0	0.028	0	0	0	0	0.014	0
Siding	0.016	0.008	0.042	0.018	0.019	0.051	0.019	0.028	0.043

* refers to the type cladding of specimens investigated in this study

The maximum water entry rates (Table 7.8) for the different wall assemblies at the higher pressure level (300 Pa) provide similar trends to those obtained in the case where no pressure is applied. However, the rates are, in general, greater at the higher pressure level as compared to that obtained under no pressure, as might be expected. These increases are relatively small in comparison to those achieved by increasing the spray rate. E.g. for the stucco wall specimens, a comparison between entry rates obtained at a spray rate of 0.85 and 3.4 L/min.-m^2, shows increase in rates of entry of 0.276, 0.196, and 0.211 L/min. in stages 5, 6, and 7 respectively. Whereas at a spray rate of 3.4 L/min.-m^2, entry rates obtained at 300 as compared to 0 Pa pressure level increase by 0.086, 0.042, 0.043 L/min. in stages 5, 6, and 7 respectively. The increases achieved at higher pressure levels are ca. 2-6 less important than those obtained for increases in spray rates.

Table 7.8– Maximum rates of entry (L/min.) to troughs servicing the Ventilation duct at 300 Pa applied pressure differential across wall assembly

WA type*	Water entry rates (L/min.) *Spray rate (L/min.-m2)								
	Stage 5			Stage 6			Stage 7		
SR* □	*0.85*	*1.7*	*3.4*	*0.85*	*1.7*	*3.4*	*0.85*	*1.7*	*3.4*
Stucco	0.064	0.113	0.340	0.094	0.161	0.290	0.088	0.178	0.299
EIFS	0	0.140	0.218	0.026	0.116	0.220	0.132	0.180	0.281
Masonry	0.050	0.018	0.120	0	0	0.030	0	0	0.012
Siding	0.016	0.019	0.042	0.015	0.042	0.062	0.018	0.026	0.044

* refers to the type cladding of specimens investigated in this study

7.2.2.3 WATER ENTRY THROUGH DEFICIENCIES ADJOINING WINDOW

Information provided in Table 7.4 indicates that 4 of 18 wall specimens experienced water entry about the “right” (W-R) and 5 of 18 walls about the “left” (W-L) corner of the window assembly. Only 2 of 18 wall specimens experienced water entry at the sill (W-S). The “left” and “right” designations pertain to the respective corners when viewing the wall assembly facing the inside of the wall (i.e. window would be to right of specimen). Results obtained in the case of the sill are few and intermittent. e.g. only three instances were recorded:

- WA-2B: 0.037 L/min. at 300 Pa ΔP_S and spray rate of 3.4 L/min.-m^2
- WA-15: 0.007 L/min. at 0 Pa ΔP_S and spray rate of 1.7 L/min.-m^2
- WA-15: 0.003 L/min. at 300 Pa ΔP_S and spray rate of 0.85 L/min.-m^2

Whereas results from the selected walls for trough W-L are presented in Table 7.9 and that for W-R in Table 7.10.

These results indicate that:

- Water was primarily collected in trough W-L (in five wall assemblies for W-L as compared to 4 for W-R);
- Water collected when no pressure was applied across the assembly and in the case of WA-6 at increasing rates for corresponding increases in spray rate;
- Increases in pressure (from 0 to 300 Pa ΔP_S) likewise induce increase in rates of entry for both W-L and W-R at a given spray rate;
- The most significant rate of entry (0.20 L/min.) was achieved in WA-6 at 300 Pa ΔP_S and a spray rate of 3.4 L/min.-m^2;
- There were noticeable changes in rates of entry for WA-6 between test stages as shown in Table 7.11.

Greater rates were obtained in Stage 7 in every instance for trough W-L irrespective of the pressure level or spray rate. This trend was similar for W-R at the 300 Pa static pressure level; at 0 Pa, the results were mixed. However, it is apparent from this that the variations in pressure across the assembly at and around the window and window – wall interface affect entry rates. The heightened leakage across the sheathing board characteristic of stage 7 (no backer rod or sealant in place at the ventilation duct joint) appears to induced additional entry at the window.

Table 7.9 – Maximum rates of entry (L/min.) to trough W-L servicing the Window – "Left" corner at 0 and 300 Pa applied pressure differential across wall assembly and specified spray rates

WA	Water entry rates (L/min.) *Spray rate (L/min.-m^2)					
	0 Pa ?P			300 Pa ?P		
	0.85	*1.7*	*3.4*	*0.85*	*1.7*	*3.4*
WA-2A	-	0.0069	0	-	0.087	0.074
WA-2B	-	0.001	0	-	0.024	0.023
WA-3	-	0.0026	-	-	0.053	0.054
WA-6	0.018	0.058	0.108	0.028	0.088	0.200
WA-15	0.003	0.003	0	0.014	0.013	0.004

Table 7.10– Maximum rates of entry (L/min.) to trough W-R servicing the Window – "Right" corner at 0 and 300 Pa applied pressure differential across wall assembly and specified spray rates

WA	Water entry rates (L/min.) *Spray rate (L/min.-m^2)					
	0 Pa ?P			300 Pa ?P		
	0.85	*1.7*	*3.4*	*0.85*	*1.7*	*3.4*
WA-2A	-	0	0	-	0.006	0.030
WA-6	0	0.005	0	0.010	0.010	0.040
WA-11	-	-	0.086	-	-	0.088

Table 7.11– Maximum rates of entry (L/min.) to trough W-R servicing the Window – "Right" corner for Stages 5 and 7 at pressure differentials of 0 and 300 Pa and specified spray rates

WA-6		Water entry rates (L/min.) *Spray rate (L/min.-m^2)					
		Stage 5			Stage 7		
		0.85	*1.7*	*3.4*	*0.85*	*1.7*	*3.4*
W-L	0 Pa	0	0.003	0.008	0.018	0.058	0.108
	300 Pa	0.001	0.003	0.008	0.028	0.088	0.200
W-R	0	0	0	0.001	0	0.005	0
	300 Pa	0.002	0.001	0.005	0.010	0.010	0.040

7.2.2.4 WATER ENTRY THROUGH DEFICIENCIES AT VERTICAL JOINTS IN EIF WALL SPECIMENS

A summary of the results obtained for water entry through deficiencies in the vertical joints of EIFS walls assemblies is provided in Figure 7.4. Results were recorded in only two of the five EIFS walls; WA-9 and WA-10. Water rates through the vertical joint are provided for each wall assembly in relation to the static pressure differential across the assembly and the spray rate applied to the wall cladding.

Results indicate that entry rates obtained for either wall are within the same order of magnitude, ranging between ca. 0.10 L/min. and ca. 0.40 L/min. over the range of spray rates and pressure differentials applied in these tests. In general rates of entry for WA-9 are lower than those of WA-10 by a factor ranging between 2 and 4; this may be simply due to the manner in which the deficiency was incorporated in the joint although nominally these would have been the same. Inspection of the joints following the tests did not reveal any evident differences to account for the divergence in results.

For either joint, rates at different pressure levels appear to be the same and changes in rates are affected by changes to the applied spray rate. This effect is more clearly evident for WA-10 as the rates of entry obtained for example at the lowest spray rate and 0 Pa pressure difference increase from 0.24 to 0.37 L/min. at the highest spray rate. Hence, the primary dependency of rates of entry are related to the spray rate. As well, rates of entry at 0 Pa are, notably, as significant as rates at the remaining pressure levels for either WA-9 or WA-10.

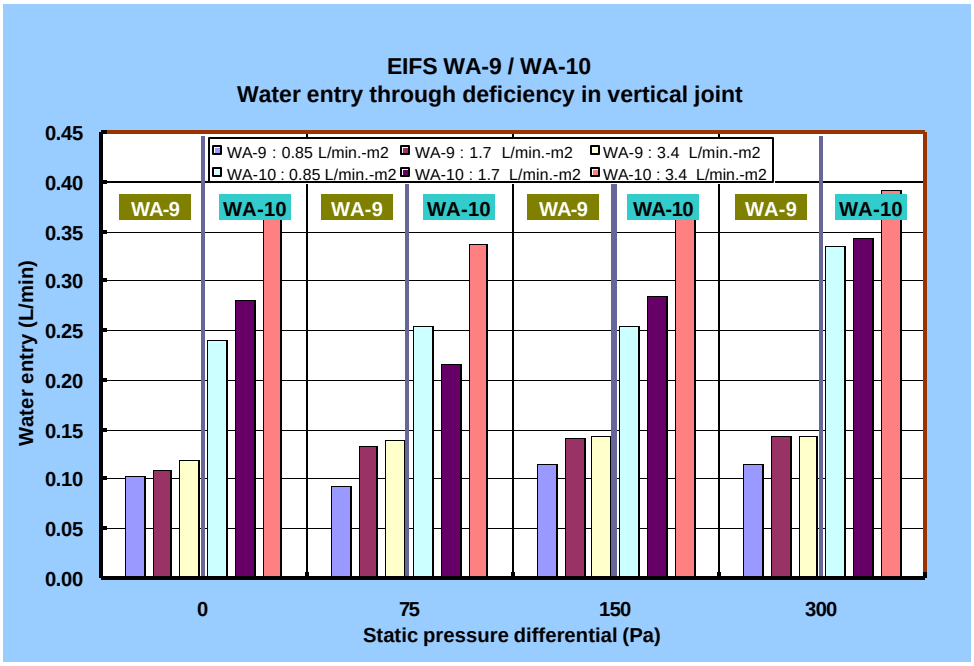

Figure 7.4 – Water entry rates through deficiencies in vertical joints of EIFS wall assemblies

7.2.3 WATER ENTRY FUNCTIONS AND INPUT TO HYGIRC

7.2.3.1 INTRODUCTION

The prediction of the consequences of accidental water entry into wall assemblies, using hygIRC, requires knowledge of the quantity of water entering through possible deficiencies located on the exterior face of the wall cladding. The amount of water entering is a function of the specific size of deficiency, the amount of water present in the vicinity of the deficiency and the air pressure differential across the deficiency, which is also a function of the pressure differential across the wall assembly. The quantity of water and air pressure differential are evidently directly related to a naturally occurring climatic phenomenon, i.e. wind-driven rain. Values of horizontal rainfall in mm/h at any particular location in North America can be obtained from weather data. Likewise, hourly average wind speeds for the same locations are available and can be converted to velocity pressures (pressure due to the velocity and density of the air). Hence, the wind-driven rain on the vertical surface of the wall can be readily estimated using, for example, Straube's equation as described in detail in the Task 4 report[1]. A schematic flow-chart of the process to depict the conversion of the climatic variables to the hygIRC input data is shown in Figure 7.5.

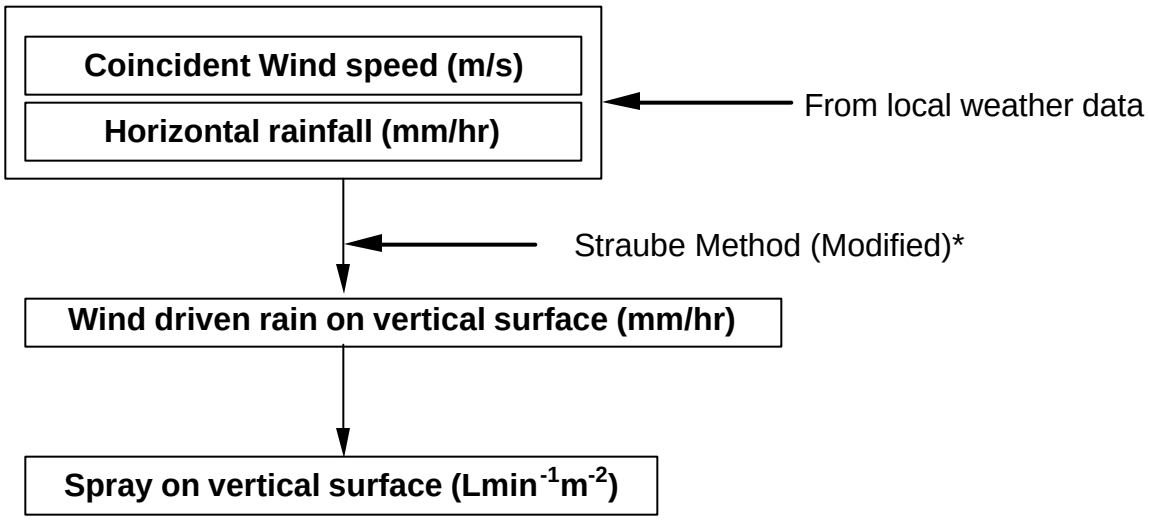

Figure 7.5 - A schematic flow-chart of the process to depict the conversion of the climatic variables to the hygIRC input data - * Modified Straube method was used as provided in the Task 4 report[11]

[1] Cornick, S.; Dalgliesh, A.; Said, N.; Djebbar, R.; Tariku, F.; Kumaran, M.K. Report from Task 4 of MEWS Project - Task 4-Environmental Conditions Final Report (IRC-RR-1130)

7.2.3.2 BASIS FOR COMBINING NATURAL PHENOMENA AND EXPERIMENTAL RESULTS

The basis for combining natural phenomena with experimental observation is shown in Figure 7.6. Natural phenomena, as presented schematically Figure 7.6-a, are wind speed and rainfall intensity. The wind speed can be converted to a pressure differential across the wall (i.e. $\Delta P = f(u)$) whereas the vertical hourly rainfall intensity (mm/h) provides a measure of the spray rate ($Lmin.^{-1}m^{-2}$) to which the wall is subjected. The experimental set-up for benchmarking trials of water entry for specific types of deficiencies on wall assemblies is shown schematically in the Figure 7.6-b. Tests were carried out at given spray rates and pressure differentials as described in previous sections.

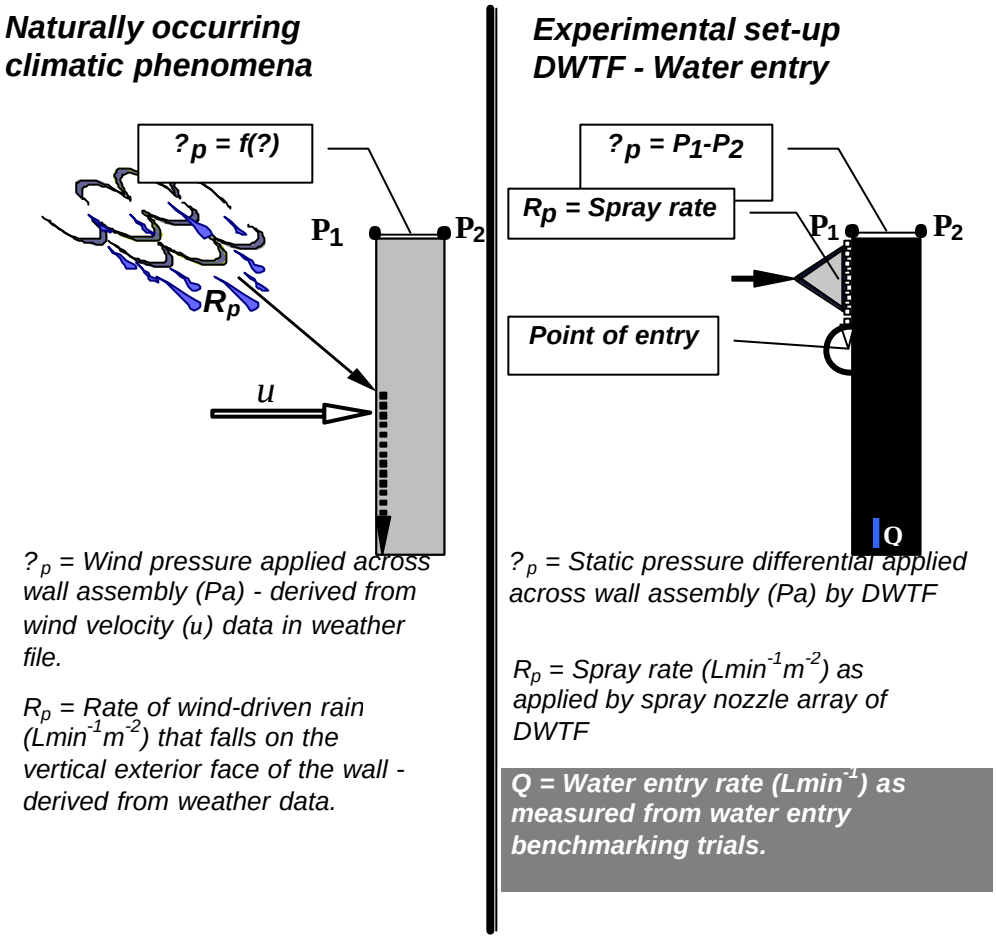

Figure 7.6 - Combining natural phenomena with experimental observation

7.2.3.3 OBSERVATIONS AND RESULTS FROM FULL-SCALE WALL TESTS

The degree to which water enters through specific deficiencies in full-scale walls has been benchmarked for each of the different types of wall specimens as provided in the previous sections and for a reference wall fabricated using acrylic sheathing (see Chapter 2 – Base-case WA). This offers a basis for estimating the amounts of water entry to be used in simulation.

Specifically, results from water entry through the deficiency located above the electrical outlet were used to derive entry functions for the Stucco, EIFS and siding wall specimens as well as the acrylic wall specimen. In the case of masonry wall specimens, the entry function was derived on the basis of entry through the deficiency above the ventilation duct as no collection was made for the electrical outlet. Given that the outlet did not extend into the stud cavity evidently precluded collecting water at that point.

7.2.3.4 WATER ENTRY THROUGH SIMULATED DEFICIENCIES UNDER STATIC CONDITIONS

As already described, water entry assessments for all assemblies of the test program were conducted under static pressure conditions at nominal spray rates of 1.7 L/min.-m^2 and 3.4 L/min.-m^2, whereas the full-scale acrylic specimen was subjected to a range of spray rates (1.7 to 4.5 L/min-m^2) and pressure differentials (75-1000 Pa).

The types of deficiencies included in the different generic wall assemblies are concordant with those incorporated in the acrylic wall assembly (Base-case) described in detail in Chapter 2. In other words, the deficiencies are placed at the same location on the wall, and the size and location of the openings above the electrical outlet are nominally the same as in the base-case.

Based on these tests, a comparison was made of rates of water entry through nominally the same type of deficiencies in the acrylic wall (base-case) as those of the stucco wall assemblies as shown in Figure 7.7.

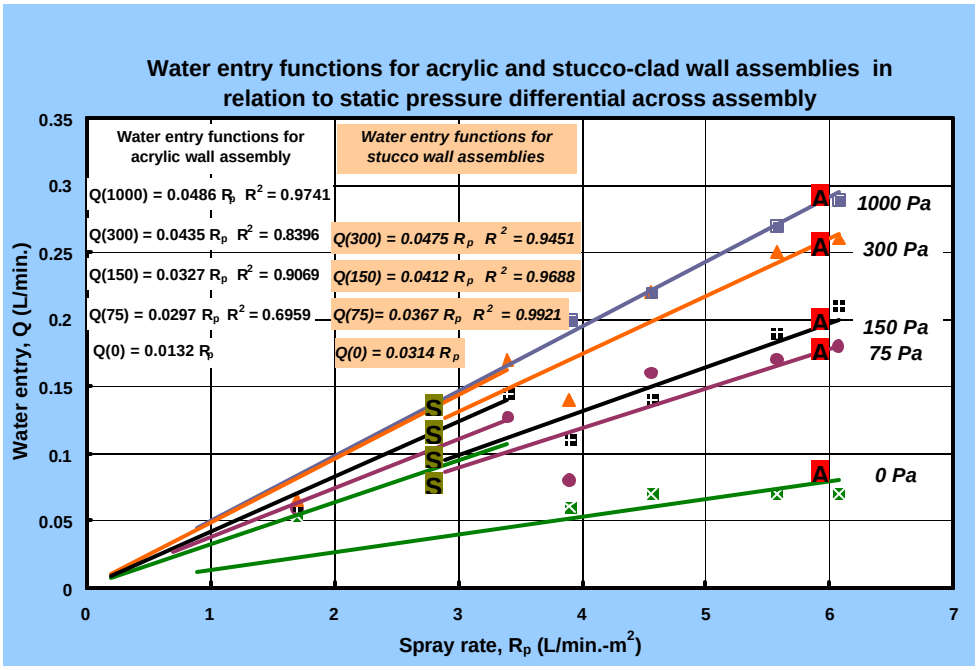

Figure 7.7 – Water entry rates in relation to spray rate at different pressure levels for acrylic (**A**) and stucco (**S**) wall assemblies

This figure depicts water entry through the electrical outlet in the base-case (acrylic) and stucco–clad walls as a function of spray rate. The lines labelled "**A**" in Figure 7.7 represent the water entry functions obtained for the acrylic-clad wall at four specific static pressure differentials, i.e., 75, 150, 300, 1000 Pa, and the lower bound results from tests conducted with zero pressure differential. Equations of the linear function fitted to the data points are also provided showing the regression coefficient as a measure of fit of the data. It is to be noted that the results are plotted in such a manner so that the line passes through the origin since no water entry is expected if water spray is not applied to the wall.

Results from water entry on stucco wall assemblies WA-1 to -4, exclusive of 5 (since no water entered through the electrical duplex in this case) are also provided in the same figure and are labelled "**S**". The results derived for the stucco-clad walls fit reasonably well at the higher pressure levels and over estimate the amount of water entry when no pressure is applied to the wall as compared to those obtained for the base-case wall (acrylic). In essence the values obtained for the stucco walls are bounded by the results derived from the tests on the base-case (acrylic) wall assembly. Hence, it is not unreasonable to assume that water entry functions based on results obtained from tests on different cladding systems can be depicted using the linear approximations derived for the base-case (acrylic) wall assembly.

7.2.4 WATER ENTRY RATE

Using the experimental observation of water entry in the base-case (acrylic) wall and, for example, the stucco clad assembly the relationship derived between water entry rate (Q in L min^{-1}), spray rate (R_p in $L \cdot min^{-1}\ m^{-2}$) for each level of static pressure difference (ΔP_S in Pa) is expressed as:

$$Q\ (\text{L min}^{-1}) = m_p \bullet R_p\ (\text{L} \cdot \text{min}^{-1}\ \text{m}^{-2})$$

In which the water entry potential, $m_p = dQ/dR_p$ ($L \bullet min.^{-1} / L \bullet min.^{-1}\text{-}m^{-2}$) for which the subscript p refers to the entry potential at a given pressure level. This linear expression correctly assumes that no water entry will occur when the spray rate, R_p, is zero, hence the function extends through the origin, as shown in Figure 7.7.

If the water entry potential ($m_p = dQ/dR_p$) is plotted as a function of static pressure level (ΔP_S), then empirical relations can be fitted to this data that yield the relationships given in Table 7.12 and shown, for each wall specimen type, in Figures 7.8-a to –d. Essentially, the water entry potential, (m_p) is assumed to be an empirical function of the static pressure differential, for which:

$$m_p\ (?P) = f\ (\text{static pressure difference}, ?P)$$

This is shown in Figures 7.8-a to -d for the acrylic wall specimen (a) as well as the other wall specimen types including stucco (a), EIFS (b), brick masonry (c) and siding (d).

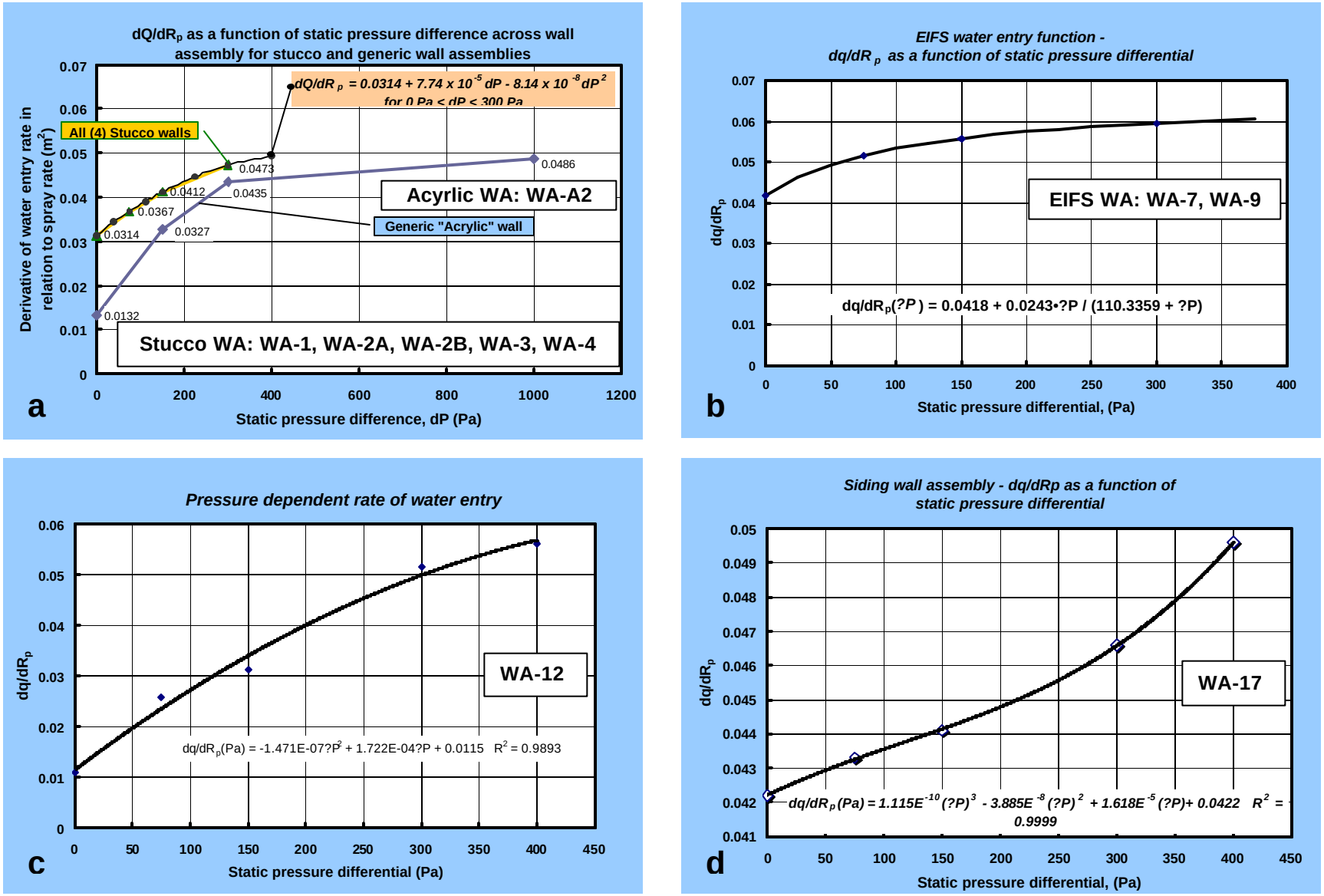

Figure 7.8 – Water entry functions for (a) stucco wall and acrylic (b) EIFS, (c) brick masonry veneer and (d) siding wall assemblies

Based on these relations, the water entry rate through a deficiency located above a through-wall penetration, such as an electrical outlet placed in a stucco clad wall, can be estimated from the spray rate (R_p), derived from weather data, and an empirical function that includes the coincident pressure differential across the wall (*?P*).

The list of water entry functions for the different wall assemblies is provided in Table 7.12.

Table 7.12 – Summary of water entry functions

WA type*	Water Entry Function dQ/dR_p ($L \cdot min.^{-1} / L \cdot min.^{-1}\text{-}m^{-2}$)
Stucco	$0.0314 + 7.7E^{-5}?P - 8.1E^{-8}?P^2$
EIFS	$0.0418 + 0.025\ ?P / (110 + ?P)$
Siding	$0.0422 + 1.62E^{-5}?P - 3.89E^{-8}(?P)^2 + 1.12E^{-10}(?P)^3$
Masonry**	$0.0115 + 1.72E^{-4}?P - 1.47E^{-7}(?P)^2$

* Refers to the type cladding of specimens investigated in this study

** Entry function for ventilation duct

Water entry functions for all generic wall assemblies are plotted in Figure 7.9. At no pressure differential, the entry to the stud cavity in the masonry wall provides the lowest potential (0.0115 $L \cdot min.^{-1} / L \cdot min.^{-1}\text{-}m^{-2}$) whereas the greatest potential is obtained for the siding wall assemblies (0.0422 $L \cdot min.^{-1} / L \cdot min.^{-1}\text{-}m^{-2}$). As shown in the figure, the potentials evidently increase as pressures increase and at, e.g. 150 Pa, water entry potentials are greatest for EIFS (0.0562 $L \cdot min.^{-1} / L \cdot min.^{-1}\text{-}m^{-2}$) and least for masonry (0.034 $L \cdot min.^{-1} / L \cdot min.^{-1}\text{-}m^{-2}$) wall assemblies. At the highest pressure level (400 Pa), potentials are most significant for EIFS wall assemblies, followed by masonry, stucco and siding wall assemblies.

The actual hourly load (L/min. x 60 min.) deposited into the wall would depend on the average hourly values of pressure (derived from wind speed) and spray rate (rainfall rate) co-existent on the wall for that period.

The location where water that enters the stud cavity is deposited was determined from experimental observations as described in detail in the Appendix B. Essentially, it was observed during these experiments that water entering the stud cavity of a stucco wall assembly under conditions of 75 Pa static pressure differential and a spray rate of 3.4 $L/min.\text{-}m^2$ collected at the base of the cavity on the base plate. Furthermore, the water had a tendency to spread out along the width of the cavity between vertical studs. Hence it was assumed that the comportment of all subsequent wall assemblies was similar to that observed of the stucco wall assembly. Simulations were carried out in accordance with these observations.

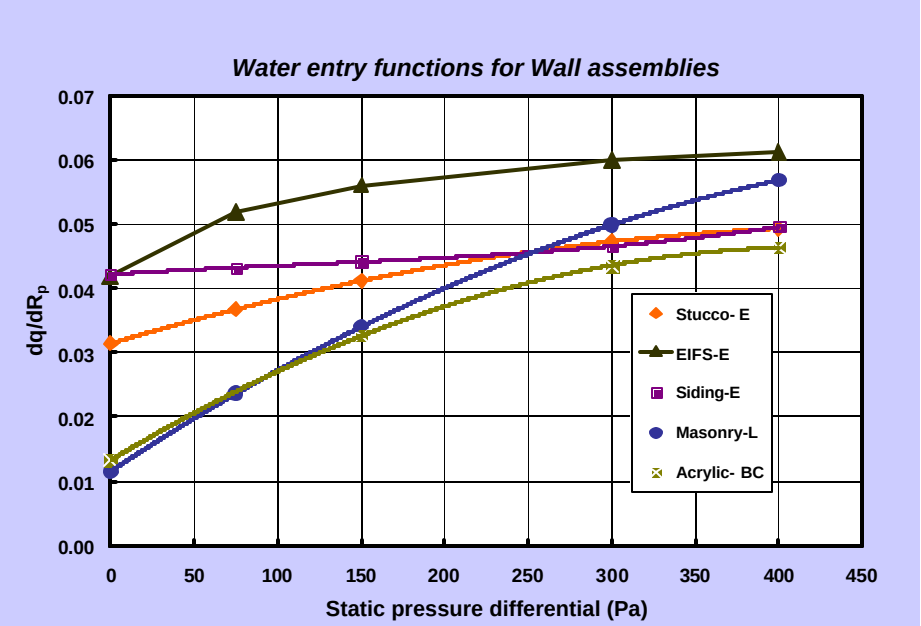

Figure 7.9 – Water entry functions for wall assemblies – dq / dR_p as a function of static pressure differential

7.2.4.1 IMPLICATIONS AND LIMITATIONS OF FUNCTIONS

An example of the application of the entry function to estimate the amount of water entry to stucco walls in a given hour for a Wilmington climate ("Wet' year) is provide in Figure 7.10. The step by step process demonstrates the manner in which an individual hourly entry of wind speed and rainfall data is converted to an hourly water entry load to the stud cavity. The initial step (1) extracts climate data from the hourly climate data files for the given location and specific year, in this case the Wilmington (SC) 'Wet' year. The data 'set' provided is a wind velocity (?) of 51 km/h and a coincident rainfall rate of 10.4 mm/h. This information is converted to pressure and spray rate information, for which pressure in simply ½??^{2} (assumes a conservation estimate of the pressure coefficient, C_p = 1) and the conversation of rainfall to spray rate uses the approach suggested in Figure 7.5, the modified Straube equation. The hourly climate conditions indicate a 47 Pa pressure and a spray rate of 0.115 L/min-m^2. Using the water entry function for stucco walls (Table 7.12) and a pressure of 47 Pa, the water entry potential is estimated (2) to be 0.0344 L/min./L/min-m^2. When this value combined (3) with a spray rate of 0.115, the entry, Q (L/min.) is estimated to be (4) 0.004 L/min. or 240 mL/hr.

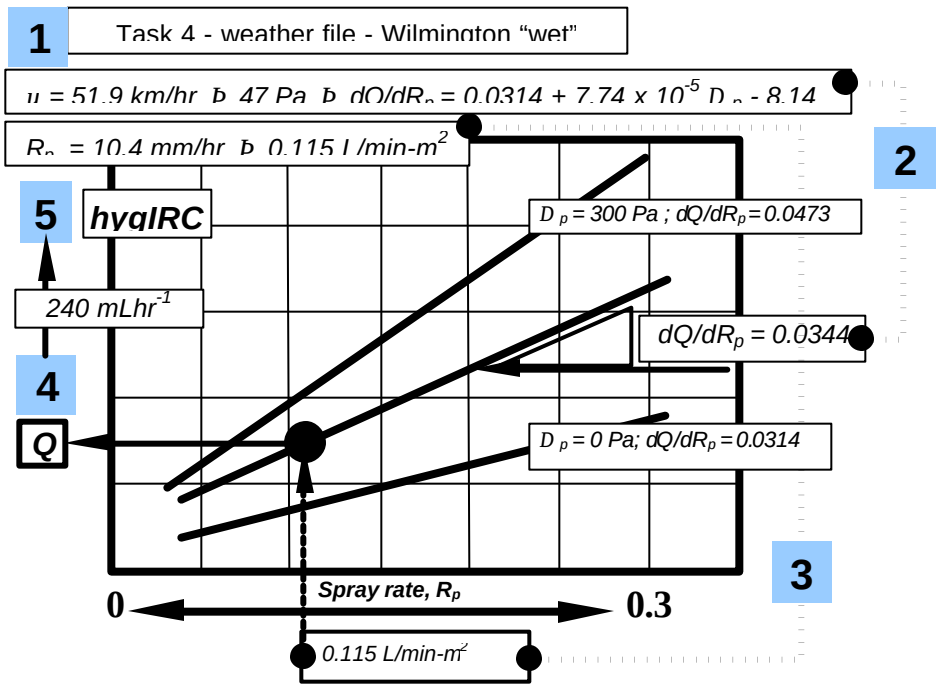

Figure 7.10 – An example of the application of the entry function to estimate the amount of water entry in an hour in a Wilmington 'Wet' year.

This provides information on a single hourly entry and indeed an extreme rain event for the Wilmington climate. However there are many hundreds of such hourly entries in any given climate year. An estimate of the maximum and minimum values provided by any of the water entry the functions can be obtained from information on the average hourly pressures and rainfall rates for a given climate. As an example of the range of hourly water entry rates that could be expected among the different wall assemblies, average hourly and derived climate data for Wilmington ('Wet' year), respectively consisting of spray rate and coincident wind pressures, is provided in Figures 7.11 and 7.13 respectively. This gives information on the range of hourly spray rates (calculated from the rainfall rates) for Wilmington over a 'wet' year in which there are more than 400 such rain 'events'. The average spray rate is given as 0.0186 L/min.-m^2. From Figure 7.12, the related average wind pressure is 27 Pa.

Using this information, and combining it with the water entry function for stucco walls (Table 7.12), provides the range of hourly rates of water entry into wall assemblies. As illustrated in Figure 7.13, a lower limit of 18 mLhr^{-1} is derived from the masonry walls, whereas an upper limit of 52 mLhr^{-1} is obtained from the EIFS walls. These loads are much lower than the 240 mLh^{-1} load obtained for the singular and extreme rain event described in the previous example and further illustrates the range of values to which the wall assemblies are subjected in this climate.

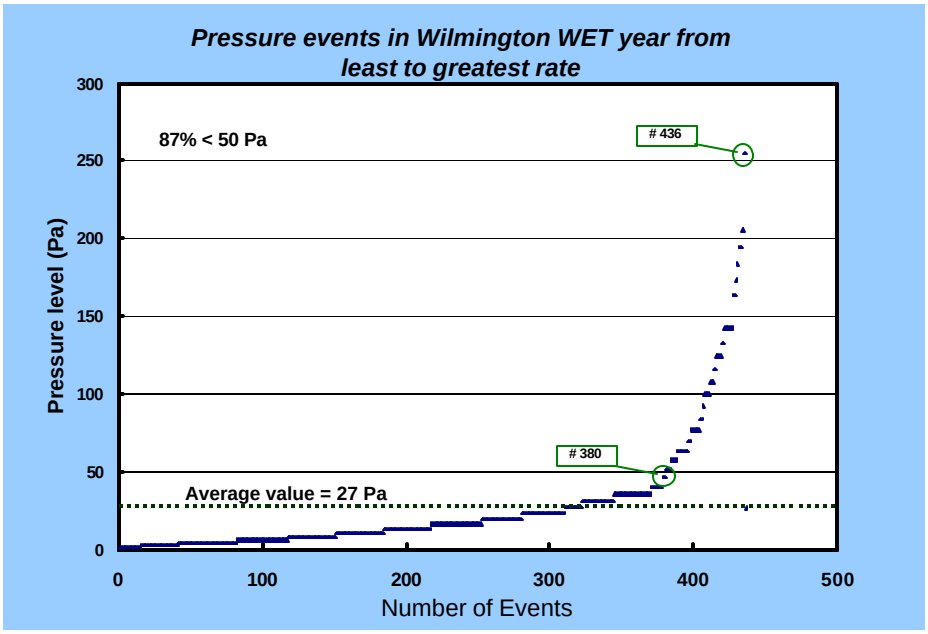

Figure 7.11 – Average spray rates

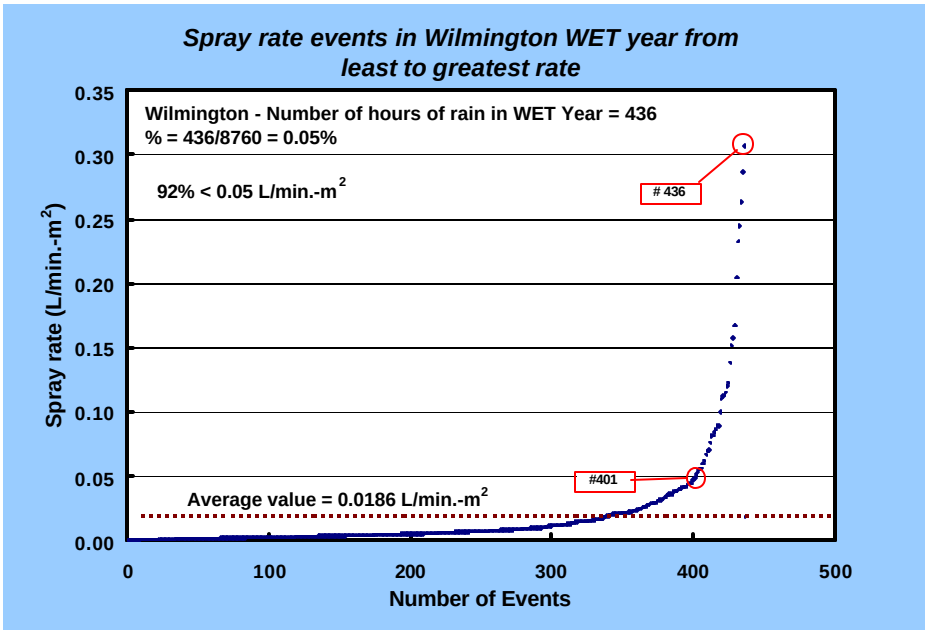

Figure 7.12 – Average wind speed and estimate pressure differential

The present exercise has provided a systematic means of estimating water entry loads based on experimental results on real wall assemblies and readily available climate information. Their respective long-term response to climate loads can only be ascertained through a thorough and systematic hygrothermal simulation and analysis as was carried out in Task 7

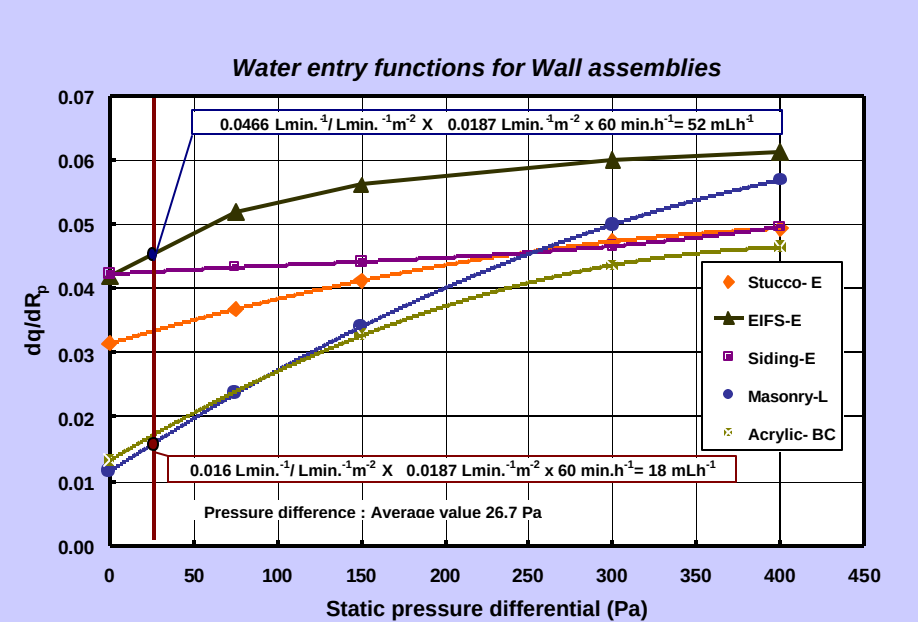

Figure 7.13 – Water entry functions for wall assemblies – expected limits of entry rates in relation to average pressure differentials

? M E W S ?

CONSORTIUM FOR MOISTURE MANAGEMENT FOR EXTERIOR WALL SYSTEMS

MOISTURE CONTROL PERFORMANCE OF WALL SYSTEMS & SUBSYSTEMS

APPENDIX A

RECOMMENDATION FOR THE SELECTION OF DEFICIENCIES FOR THE 17 WALL SPECIMENS TO BE INVESTIGATED FOR WATER INGRESS USING THE DYNAMIC WALL TESTING FACILITY

TG2 Working Group on Deficiencies

November 1999

APPENDIX A

Recommendation for the Selection of Deficiencies

Table of Contents

Preamble

In July 1999, TG 2 of MEWS formed a working group whose scope was to review the types of deficiencies that can occur in the four types of wall systems included in MEWS project, and from there, to propose a series of deficiencies to be included in the wall assemblies which are to be subjected to water entry tests in the IRC Dynamic Wall Testing Facility (DWTF). The output of the WG could also be useful to Task 8 for the development of guidelines.

The working group (WG) consisted of Madeleine Rousseau, Mark Bomberg, Adaire Chown, Guylaine Desmarais, Paul Maurenbrecher, Fadi Nabhan, Nadi Said and Michael Lacasse, all from IRC, as well as Sylvio Plescia (CMHC) and Don Onysko (DMO Associates).

The WG wrote a draft Technical note and circulated it to the MEWS partners via the MEWS website in August 1999. The Note described the methodology adopted by the Working Group for the selection of deficiencies as well as the preliminary series of deficiencies selected for the wall specimens[1]. Madeleine Rousseau presented the document during the September 21, 1999 evening forum of the MEWS meeting. At that September meeting, comments from partners focussed on deficiencies related to window flashings, and to the first line of defense in EIFS and stucco wall assemblies. In light of those comments and a better understanding of flashing practice in US, the recommendations were modified. This document reflects the changes agreed upon during the September meeting, and goes a step further in defining the deficiencies for the wall specimen.

The recommendations presented in this document were subsequently reviewed by Task Group 6. Task 6 members then determined the extent to which the proposed list of deficiencies could be implemented within the proposed scope for the water entry experiments using the dynamic wall test facility and within the expected timeframe for experimental evaluation.

♦ [1] Technical Note on the Selection of Wall Deficiencies, Document T2-WG-10, Sept.15, 1999. 15 p.

Terminology

Defining and using common terminology to express one's idea is critical to proper communication. The technical terms defined below and used in this document are meant to be "working" definitions for the purpose of the MEWS project.

Air barrier system: assembly installed to provide a continuous barrier to the movement of air[2]. The air barrier system must have low permeance to air (in Canada National Building Code requires that materials have less than 0.02 L/(s·m^2) at 75 Pa), be continuous over joints, junctions and penetrations and be able to resist 100% of the specified wind load (if the assembly is subjected to wind).

Box window: window that does not have a nailing flange. The window frame is fastened to the wall rough opening.

First line of defense: in the context of a multiple-element protection strategy against rain penetration in exterior walls, the cladding assembly constitutes the first line of defense. It is intended to minimize rainwater passage both through and around the cladding [3].

Flange-mounted window: window with a nailing flange located along the perimeter of the frame. The nailing flange is used to attach the window to the wall. Also called nail-on windows or windows with integral nail-on fin.

Flashing: components of the exterior envelope used to intercept and direct the flow of water to designed drainage paths. [4] The flashing assembly includes materials and joints that can shed water without allowing leakage. Flashings are usually made of sheet metal or flexible water-resistant or waterproof membranes. *Through-the-wall flashing,* located at the window head and sill, intercepts water from the inside of the window rough opening and directs water to the outside.

Inner boundary layer: as part of the second line of defense of the wall against rain penetration, the inner boundary layer's role consists of protecting the back-up wall from water penetration. This material has water-resistance properties. Some membranes, coatings or some insulation materials can perform this function.

Second line of defense: in the context of a multiple-element protection against rain penetration in exterior walls, the second line of defense can include a flashed, drained and vented air space, as well as a material with water resistance characteristics (see inner boundary layer) on the exterior face of the back-up wall. The essential feature of a second line of defense consists of having an inner boundary layer that exhibits water-resistance properties.

Sheathing membrane: This water-resistant membrane's main function consists of acting as a secondary protection against the passage of water to the interior. Term used in the national Building Code of Canada.

♦[2] National Building Code of Canada 1995, Part 1 Scope and Definitions, p.1.

♦[3] Evolution of Wall Design for Controlling Rain Penetration, IRC Construction Technology Update no 9, 1997

♦[4] *Flashings* Best Practice Guide –Building Technology, Canada Mortgage and Housing Corporation, Ottawa, 1998

Water-resistive barrier (WRB): Its main function consists of acting as a secondary protection against the passage of water to the interior. Term used in United States in the Uniform Building Code.

Window rough opening: framed opening in the wall, slightly larger than the window.

1- Types of penetrations through the wall specimens

The Working Group recommended that the following three types of penetrations and junctions be included in all wall specimens:

1) Window

Windows considered. Three types of window frames have been considered for the testing program: the flange-mounted window frame, the box frame with integral sill, and the basic box window. The technique used to attach the window to the rough opening in the wall determine the types of flashing details that can be implemented. Specifically, flange-mounted windows in which the flange is an integral part of the window frame cannot accommodate a through-the-wall flashing at the window sill and head because the nailing flange becomes a physical obstacle to obtaining a continuous flashing from inside to the outside. Truncation of such types of integral flanges to allow for a through-the-wall flashing could compromise the structural integrity of the window installation. Figures 1, 2 and 3 illustrate the conceptual approaches possible for flashing details with the three types of windows the group considered.

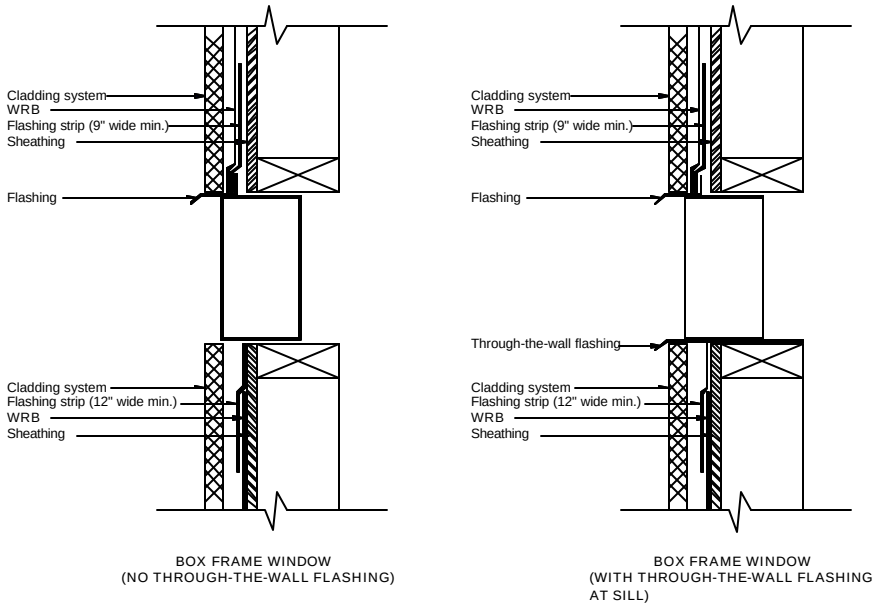

Figure A.1. Flange-mounted window and recommended overlap between flashing membrane and WRB

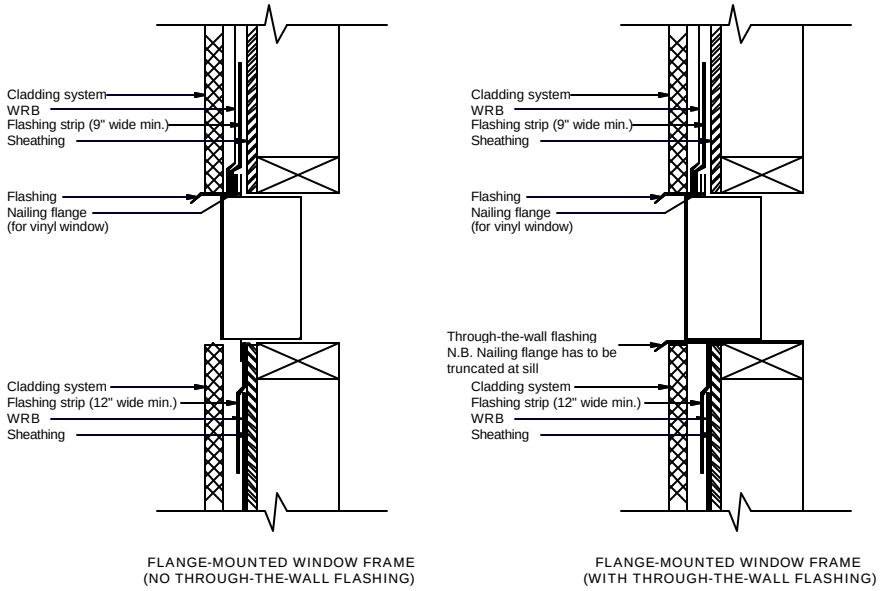

Figure A.2. Box frame window and recommended overlap between flashing membrane and WRB

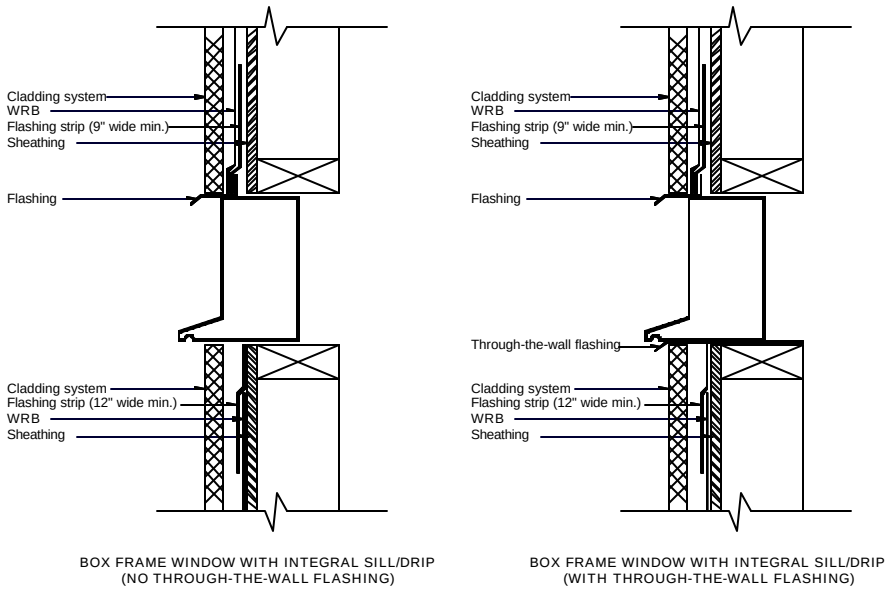

Figure A3. Box frame window with integral sill and recommended overlap between flashing and WRB

Window selected: a flange-mounted fixed vinyl (PVC) window measuring 755 mm by 755 mm (29 ¾ inches by 29 ¾ inches). Figure 4 describes the vinyl window with a nailing flange to be used in the water entry experiments using the base-case wall.

The flange-mounted window was selected for two reasons:

- it appears to have a large part of the market in US and some parts of Canada (e.g. BC), and
- it presents particular difficulties related to the drainage and evacuation of incidental water entering the wall specimen. The flashing at the window sill cannot be a through-the-wall flashing because the nailing flange of the window frame is in the way. The typical flashing installation directs water present at the outside face of the window flange to the water-resistive membrane. Water that might reach below the window sill (e.g., through leaky mitred corners of the window) may be trapped on the inner wall portion where water-susceptible materials are located.

The window should be configured to ensure that near zero air leakage occurs at the glazing/frame interface and controlled water leakage should be introduced through two openings, one at each mitred corner of the sill. One opening should allow water leakage between the first and second lines of defense (i.e. on the water-resistive membrane), while another opening should be located behind the flange to permit water entry behind the WRB (see Figure 4).

For all wall specimens, an air barrier system should be on the inside face of the studs, in the form of a rigid acrylic sheet. An opening in the air barrier material in proximity to its interface with the window frame would simulate defective sealing of that junction.

2) Exterior electrical duplex outlet

The outlet should penetrate through the 1st line of defense and possibly the 2nd line of defense (depending on the thickness of the cladding), but not the air barrier material located on the inside face of the wood studs.

3) Ventilation duct

A circular duct having a 150-mm diameter should penetrate directly through the first and second lines of defense as well as the air barrier system. An opening in the air barrier system in proximity to the duct inside termination would simulate defective sealing at the duct/air barrier interface.

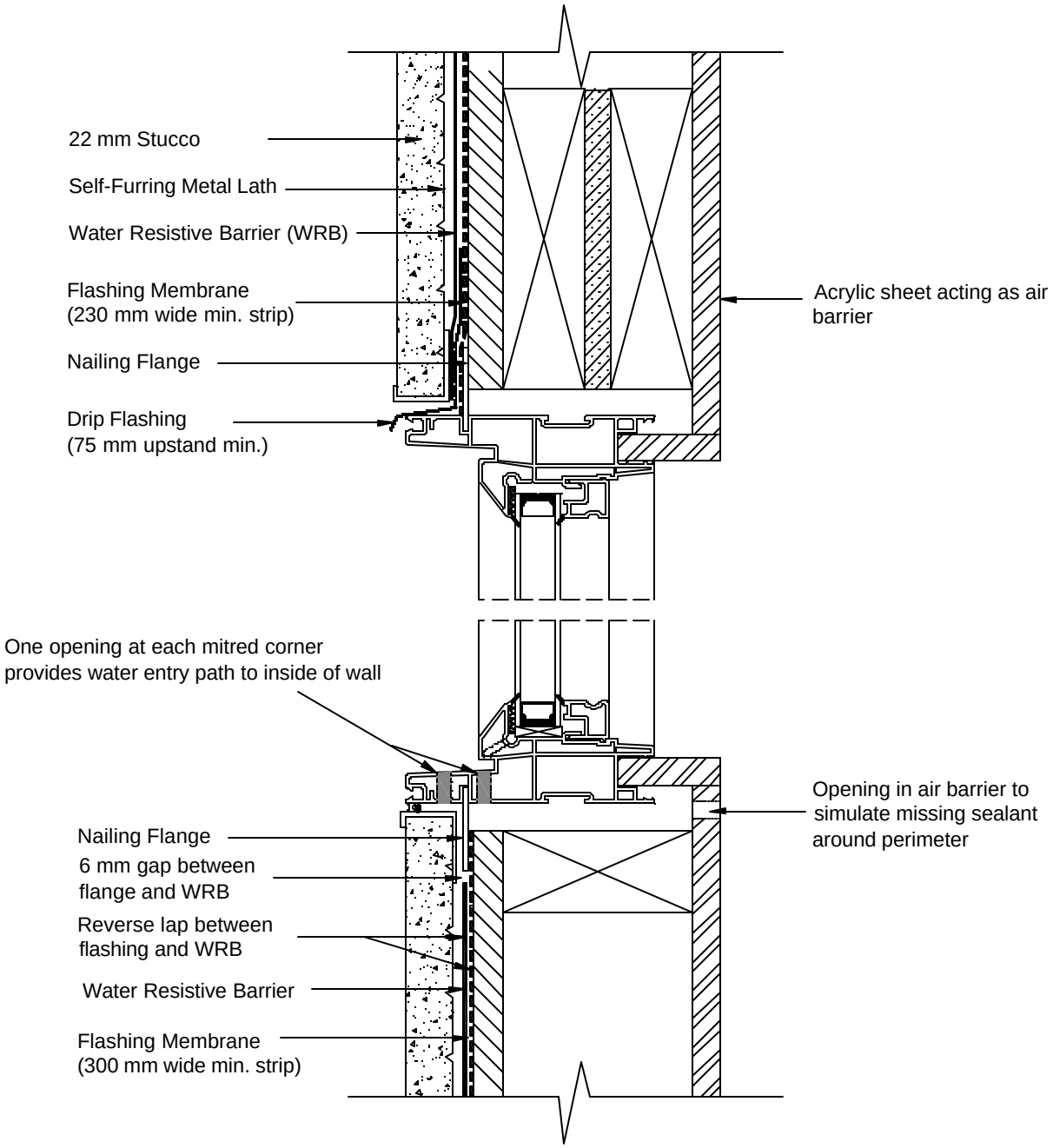

Figure A.4. Vertical section of flange-mounted vinyl window installed in a stucco-clad wood-frame wall. Location of holes in window sill for water entry into the wall assembly

2- Location & Size of Penetrations

It is proposed that the three penetrations be positioned in the wall specimens in the fashion similar to that provided in Figure 5. It is desirable that water runs down on the wall specimen before reaching the penetration in order to expose the penetration and its deficiencies to a significant quantity of water obtained by two types of wetting patterns (i.e. direct water spray and water running down a surface). It is assumed that 460 mm of wall specimen above the penetrations is the minimum band required for that purpose. The penetrations should be located in separate stud cavities in order to minimize interference between water leakage associated with each penetration.

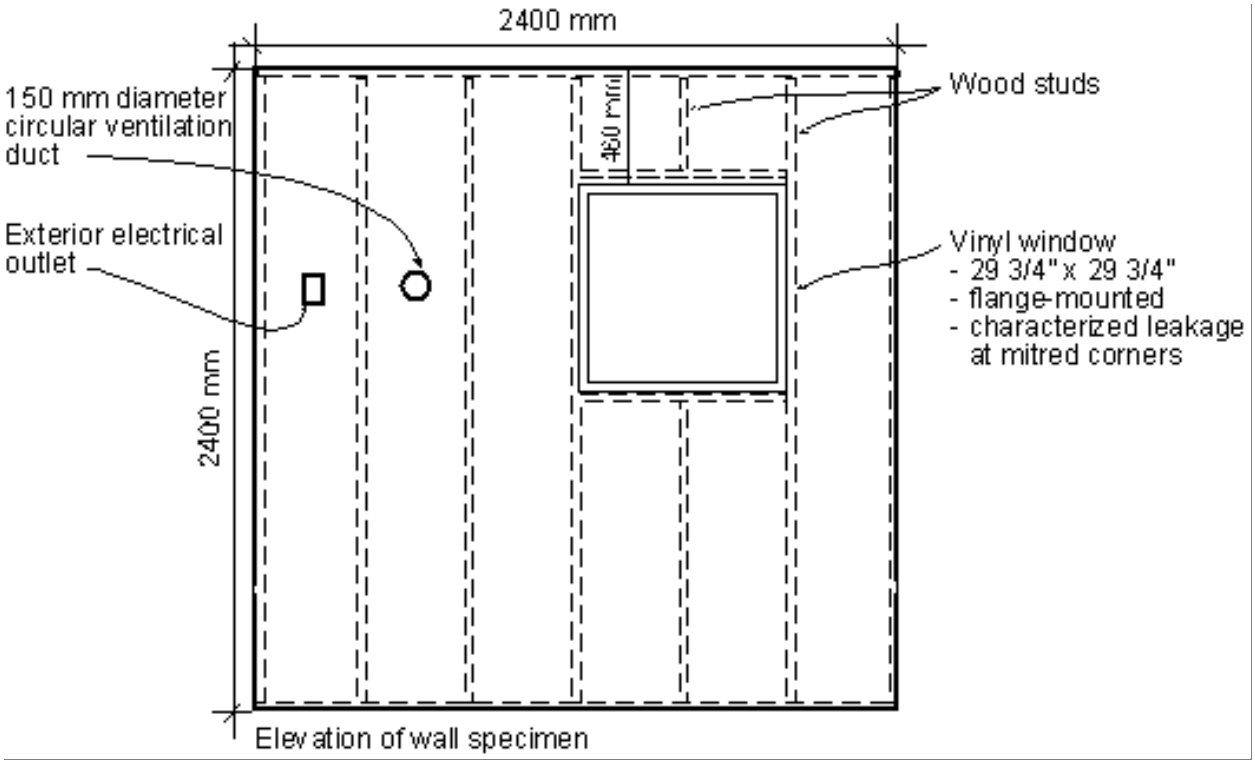

Figure A.5. Suggested positioning of penetrations in a typical wall specimen

3. Types of Deficiencies in the Wall Specimens

For the purpose of this project, a deficiency was defined as a characteristic of a material or of an assembly of materials within a wall assembly that prevents the material or the assembly from fulfilling its function in the context of a given moisture management strategy for the walls. In most instances a deficiency provides a water entry path towards the inside of the wall. This in itself may or may not lead to the deterioration of building materials; the outcome depends on the drying potential of the wall assembly (which in turn is a function of the climate and the construction of the whole wall assembly).

Two types of deficiencies were proposed for the water entry tests of wall specimens using the DWT facility:

- generic and
- assembly-specific deficiencies.

Both types were to be included in all specimens being evaluated. In was understood that all wall specimens should be subjected to the same generic deficiencies, whereas the assembly-specific deficiencies would vary with the type of cladding of the assemblies and the specificity of the assembly.

- Generic deficiencies

It was recommended that generic deficiencies should be introduced in each of the three parts of the wall assembly: in the first line of defense and in the second line of defense of the Rain Penetration Control Elements (RPCE), as well as in the Heat, Air Moisture and Structure elements (only the air barrier system is relevant to rain penetration control evaluation).

This way the different wall specimens would be subjected not only to the same environmental loads (water & air pressure differences) but also to the same “openings” allowing water entry. This approach would nominally permit a reasonable comparison of water management response among the different wall assemblies in terms of water infiltration and water drainage. A summary of the proposed generic deficiencies is provided in section 3.1.

- Assembly-type specific deficiencies

Certain deficiencies specific to a given wall assembly can be quite significant for water entry paths even though they cannot be replicated in all wall types of the testing program (e.g. cracks in cement plaster for a stucco-clad wall). For that reason, deficiencies specific to the nature of the cladding assembly should be introduced in the wall specimen. These are provided in section 3.2.

3.1 Generic deficiencies

The proposed generic deficiencies could be implemented in the following manner:

- in the first line of defense: some degree of discontinuity of sealant between the wall cladding and the interfacing component, e.g. window, duct, etc;
- in the second line of defense: some degree of discontinuity of the inner boundary layer (sheathing membrane/WRB) intended to intercept the water that bypassed the first line of defense.
- in the Heat, Air, Moisture and Structure elements (HAMS): some degree of discontinuity in the air barrier system that would introduce direct and indirect air flow patterns in a concentrated (not diffused) fashion i.e. holes should be made in the air impermeable material acting as the designated air barrier element. For all wall specimens, an air barrier system would be on the inside face of the studs, in the form of a rigid acrylic sheet.

The generic deficiencies proposed are presented in Table 1 and are illustrated in Figures 6 and 7.

Table A.1 Summary of recommended generic deficiencies for water entry evaluation of wall specimens

Interface/ Junction	Generic deficiency in RPCE		Generic deficiency in air barrier system (in HAMS)
	1st line of defense	2nd line of defense	
Wall-window A fixed vinyl, flange-mounted with simulated water leakage at corners of the window frame	♦ Missing a portion of seal length at the sill ♦ Missing seal at the jamb/sill junctions ♦ Missing a portion of seal length at the jamb/head junctions	♦ Reverse lap between the inner boundary layer material (WRB) and the flashing at window sill ♦ A 6 mm gap left between the WRB and the window flange along the window sill	♦ Openings of a given size in acrylic sheet to simulate a missing portion of seal length at the interface between the designated airtight element of the wall (acrylic sheet) and that of the window frame
Wall-ext. electrical outlet	♦ Missing a portion of seal length at the perimeter of the outlet	♦ A 18 mm gap left between the inner boundary layer material and the perimeter of the penetrating element ♦ No flashing in place	♦ None ♦ PS. The outlet box does not penetrate through the air barrier of the specimen
Wall- duct A 150-mm diameter circular ventilation duct	♦ Missing a portion of seal length at the perimeter of the duct	♦ A 18 mm gap left between the inner boundary layer material and the perimeter of the penetrating element ♦ No flashing in place	♦ Openings of a given size in acrylic sheet to simulate a missing portion of seal length at the interface between the designated airtight element of the wall (acrylic sheet) and that of the duct

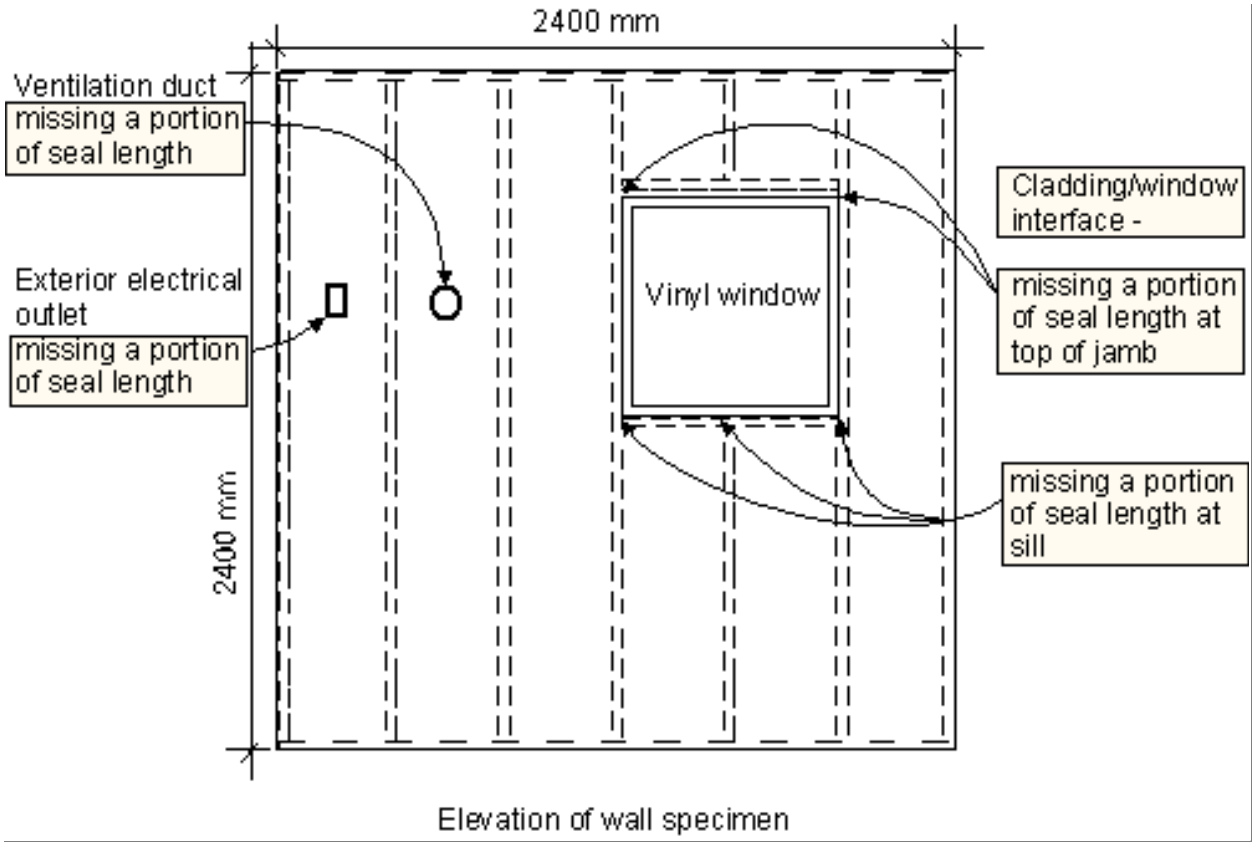

Figure A.6. Generic deficiencies in the first line of defense of a typical wall specimen

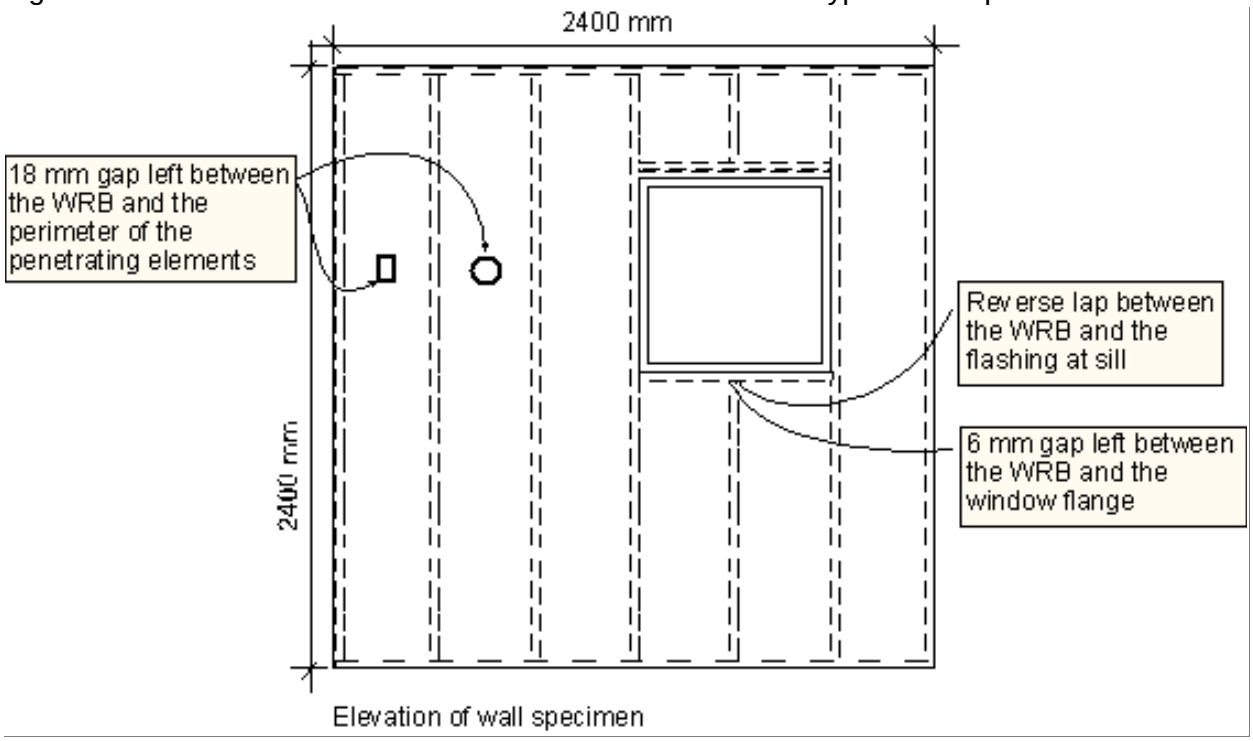

Figure A.7. Generic deficiencies in the second line of defense of a typical wall specimen

3.2 Assembly-specific Deficiencies

Table 2 presents the proposed assembly-specific deficiencies for evaluation in the water-entry experiments. Additional assembly-specific deficiencies could have been introduced in the actual test specimens once their design and details at the interfaces were completed. TG 2 undertook the production of additional documents that describe in detail the construction of the test specimens including the generic and assembly-specific deficiencies.

Table A.2 Summary of recommended assembly-specific deficiencies for water entry evaluation of wall specimens

Wall assemblies	Deficiencies
Stucco #1, 2, 3, 4	• Cracks along the interface between the cement plaster and the prefabricated metal strip for vertical & horizontal control joints • No end dam at window head drip flashing
Stucco #5	Cracks along the interface between the cement plaster and the prefabricated metal strip for a vertical control joint • No end dam at window head drip flashing • Blocked drainage openings at the bottom of wall
EIFS # 6	• Missing sealant at control joints • Cracks at the interface between the lamina and the V-shaped control/expansion joint • Blocked drainage openings at source drainage of window
EIFS # 8	• Missing sealant at control joints • Cracks at the interface between the lamina and the V-shaped control/expansion joint
EIFS #7, 9, 10	• Missing sealant at control joints • Cracks at the interface between the lamina and the V-shaped control/expansion joint • Blocked drainage openings at the bottom of wall
Masonry #11, 12, 13, 14	• Poor adhesion between mortar and bricks, causing cracking at the interface • Incomplete filling of head joints • Blocked weepholes • No end dam at window head drip flashing NB : These deficiencies are preliminary and will be confirmed when the Construction Practice Review chapter is completed
Wood siding #15, 16	• Open butt joint between boards • Open butt joint between boards and vertical corner trim • No back priming of the siding NB : These deficiencies are preliminary and will be confirmed when the Construction Practice Review chapter is completed
Vinyl siding #17	• Blocked drainage holes • A gap between the corner vertical trim and the siding board NB : These deficiencies are preliminary and will be confirmed when the Construction Practice Review chapter is completed

Appendix B

TABLE OF CONTENTS

LIST OF TABLES

LIST OF FIGURES

1. AIR LEAKAGE CHARACTERISATION

Air leakage - Stucco wall assemblies

Air leakage characteristics of stucco wall assemblies are provided in Figures B.1 to B.4. Air leakage of wall assemblies without deficiencies in the respective cladding systems are provided in relation to air barrier system leakage having nominally no air barrier (Figure B.1) in place or with the air barrier system leakage minimised (Figure B.2).

The assembly leakage in which there is no apparent ABS in place is roughly indicative of the leakage of the assembly at the second line of defence.

Air leakage of stucco wall assemblies without and with deficiencies at different values of nominal ABS leakage are provided in Figure B.3 and B.4 respectively.

System air leakage through the wall assembly given equivalent air leakage areas in the ABS of 168-mm^2 and 509-mm^2 are representative of nominal air leakage through the ABS of 0.2 L/s-m^2 and 0.5 L/s-m^2 respectively

Air leakage - EIFS wall assemblies

Air leakage characteristics of EIFS wall assemblies are provided in Figures B.5 to B.8. Air leakage of wall assemblies without deficiencies in the respective cladding systems are provided in relation to air barrier system leakage having nominally no air barrier (Figure B.5) in place or with the air barrier system leakage minimised (Figure B.6).

Air leakage of EIFS wall assemblies without and with deficiencies at different values of nominal ABS leakage are provided in Figure B.7 and B.8 respectively.

Air leakage – Brick masonry wall assemblies

Air leakage characteristics of brick masonry wall assemblies are provided in Figures B.9 to B.12. Air leakage of wall assemblies without deficiencies in the respective cladding systems are provided in relation to air barrier system leakage having nominally no air barrier (Figure B.9) in place or with the air barrier system leakage minimised (Figure B.10).

Air leakage of brick masonry wall assemblies without and with deficiencies at different values of nominal ABS leakage are provided in Figure B.11 and B.12 respectively.

Air leakage – Siding wall assemblies

Air leakage characteristics of siding wall assemblies are provided in Figures B.13 to B.16. Air leakage of wall assemblies without deficiencies in the respective cladding systems are provided in relation to air barrier system leakage having nominally no air barrier (Figure B.13) in place or with the air barrier system leakage minimised (Figure B.14).

Air leakage of siding wall assemblies without and with deficiencies at different values of nominal ABS leakage are provided in Figure B.15 and B.16 respectively.

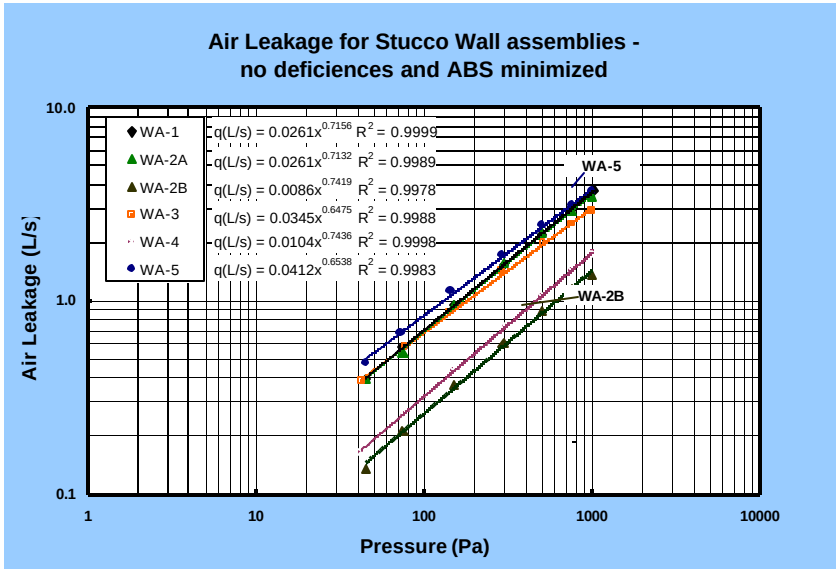

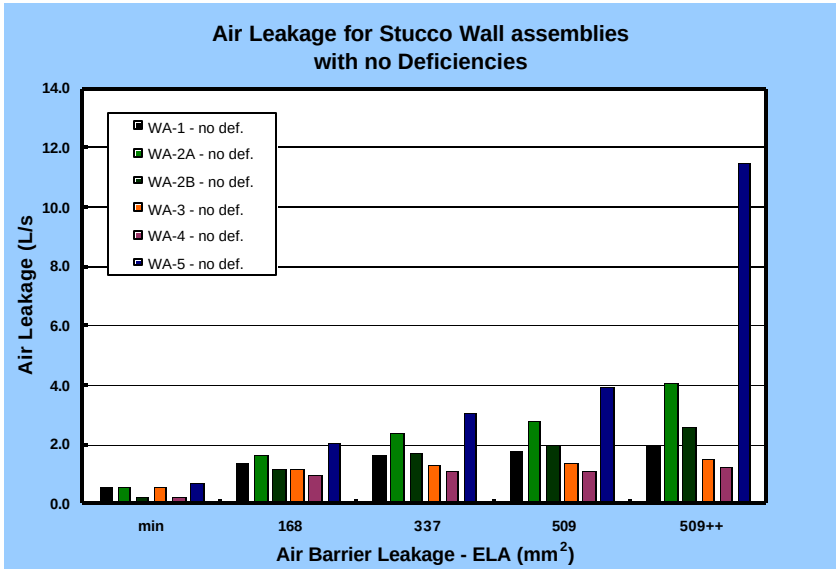

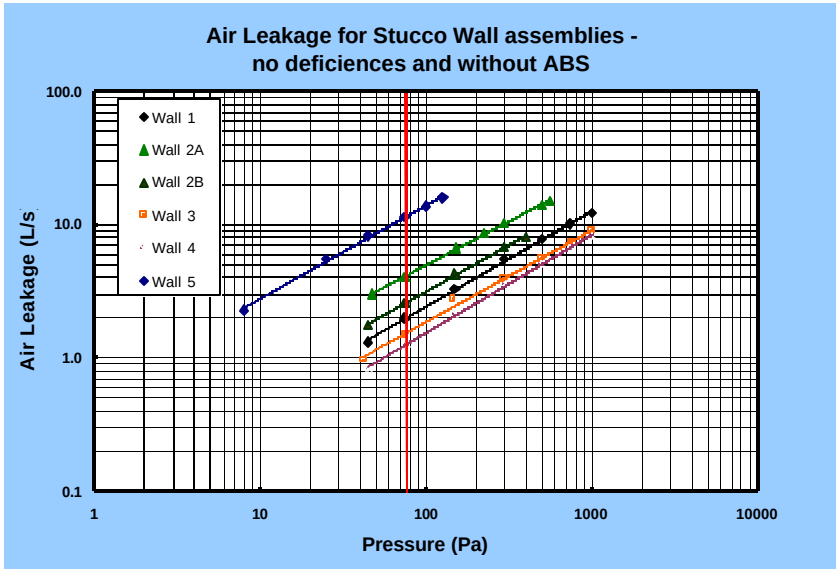

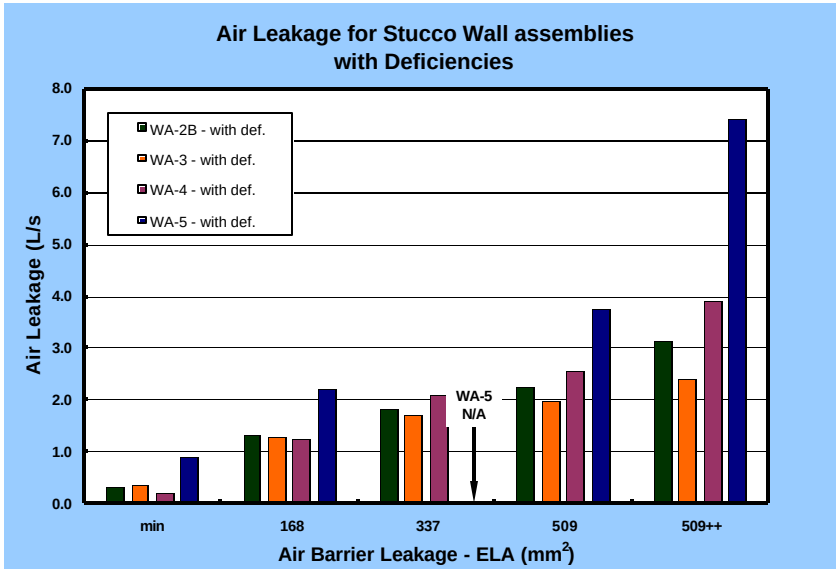

Figure B.1– Air leakage of stucco WA having no deficiencies and without air barrier system (ABS) in place

Figure B.2 – Air leakage of stucco WA having no deficiencies and air barrier system leakage (ABS) minimised

Figure B.3 – Air leakage of stucco WA having no deficiencies and in relation to the ELA of the air barrier system (ABS)

Figure B.4 – Air leakage of stucco WA having with deficiencies and in relation to the ELA of the air barrier system (ABS)

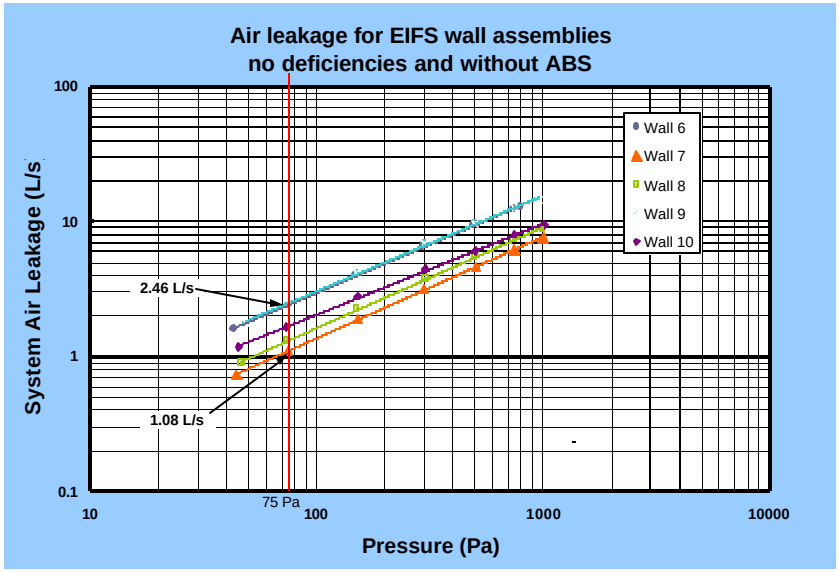

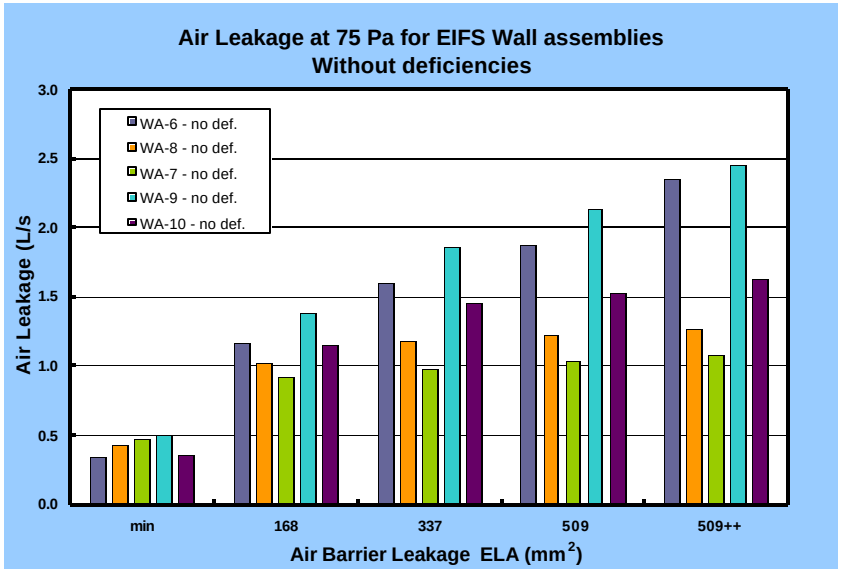

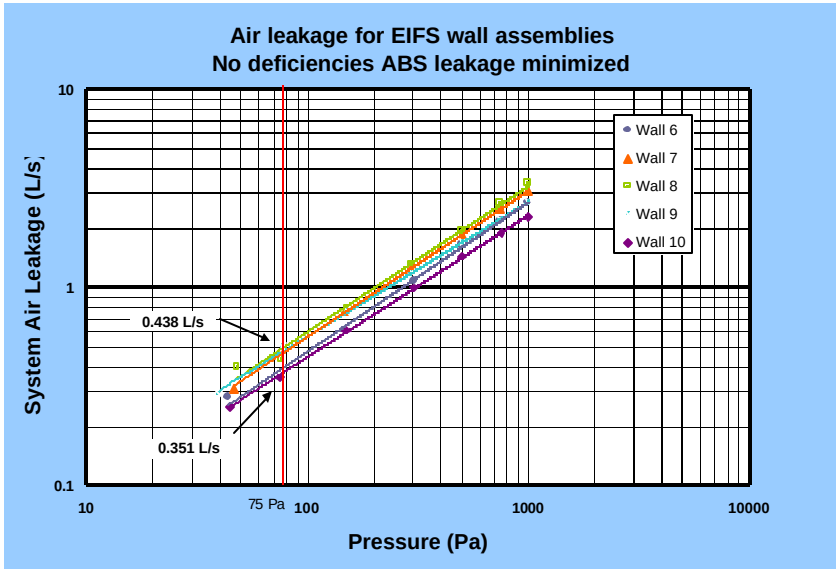

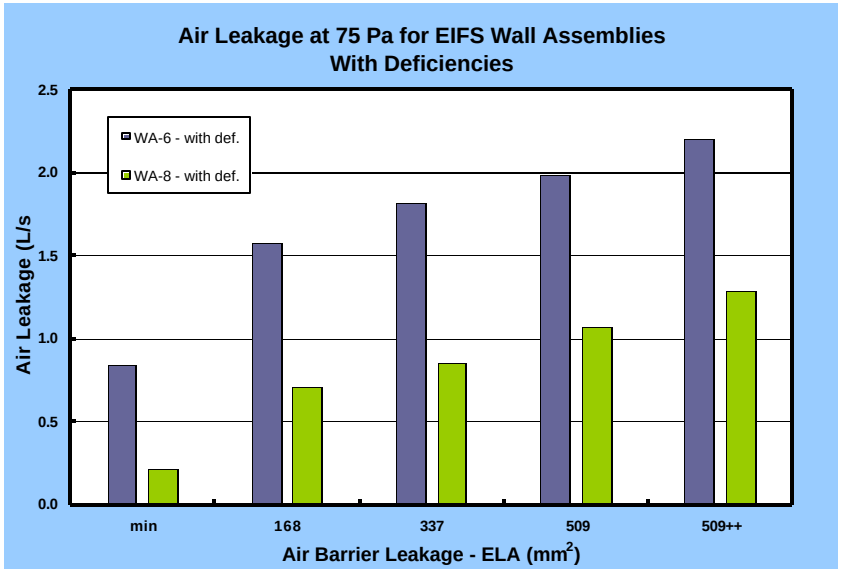

Figure B.5 – Air leakage of EIFS WA having no deficiencies and without air barrier system (ABS) in place

Figure B.6 – Air leakage of EIFS WA having no deficiencies and air barrier system leakage (ABS) minimised

Figure B.7 – Air leakage of EIFS WA having no deficiencies and in relation to the ELA of the air barrier system (ABS)

Figure B.8 – Air leakage of EIFS WA with deficiencies and in relation to the ELA of the air barrier system (ABS)

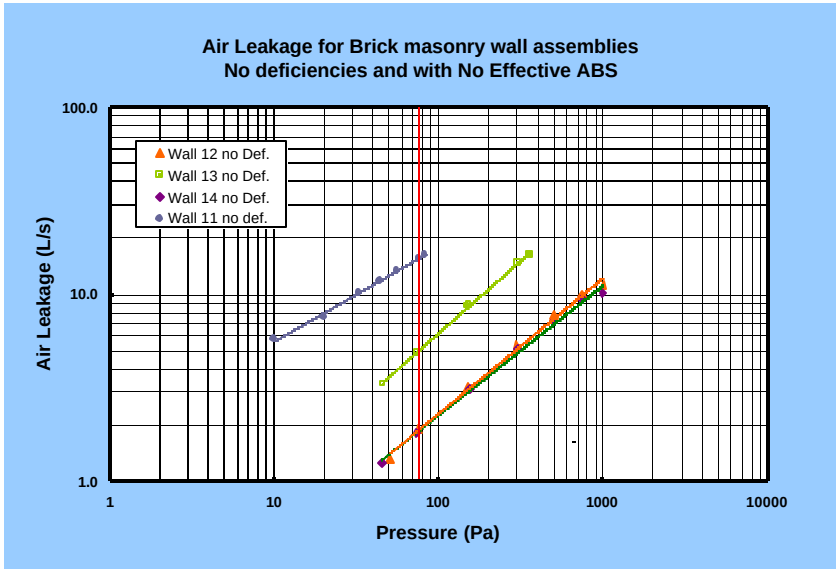

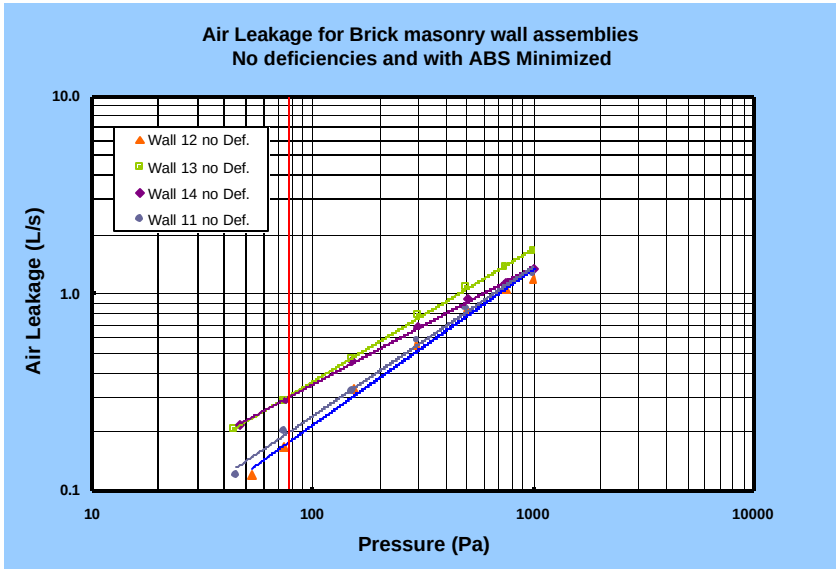

Figure B.9 – Air leakage of brick masonry wall assemblies having no deficiencies and without air barrier system (ABS) in place

Figure B.10 – Air leakage of brick masonry wall assemblies having no deficiencies and air barrier system leakage (ABS) minimised

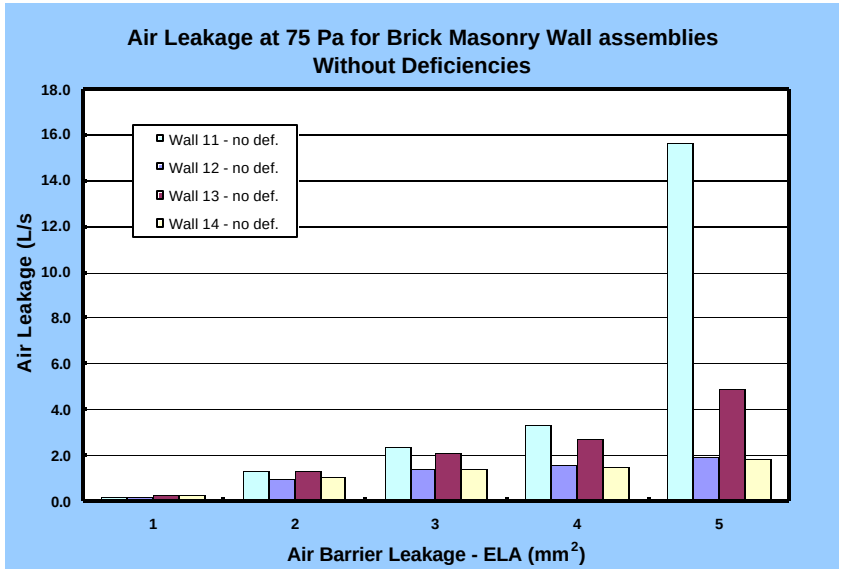

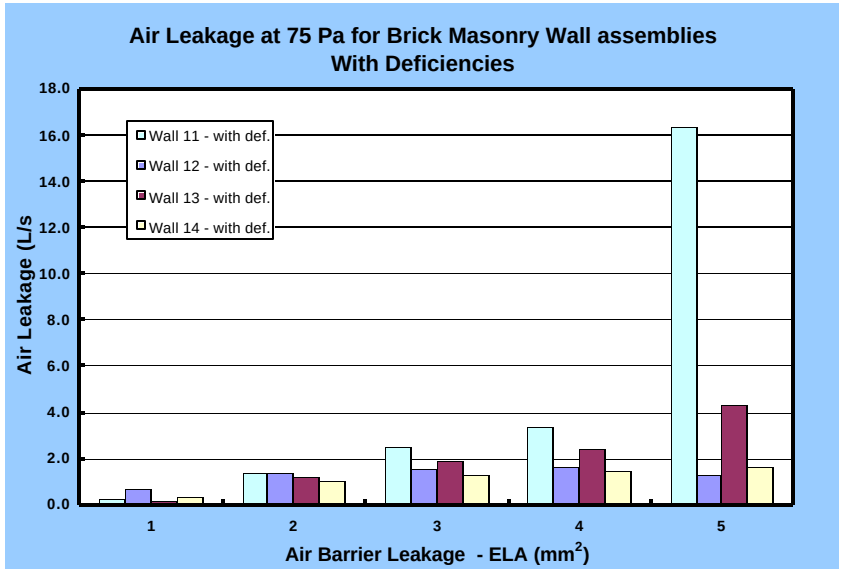

Figure B.11 – Air leakage of brick masonry wall assemblies having no deficiencies and in relation to the ELA of the air barrier system (ABS)

Figure B.12 – Air leakage of brick masonry wall assemblies with deficiencies and in relation to the ELA of the air barrier system (ABS)

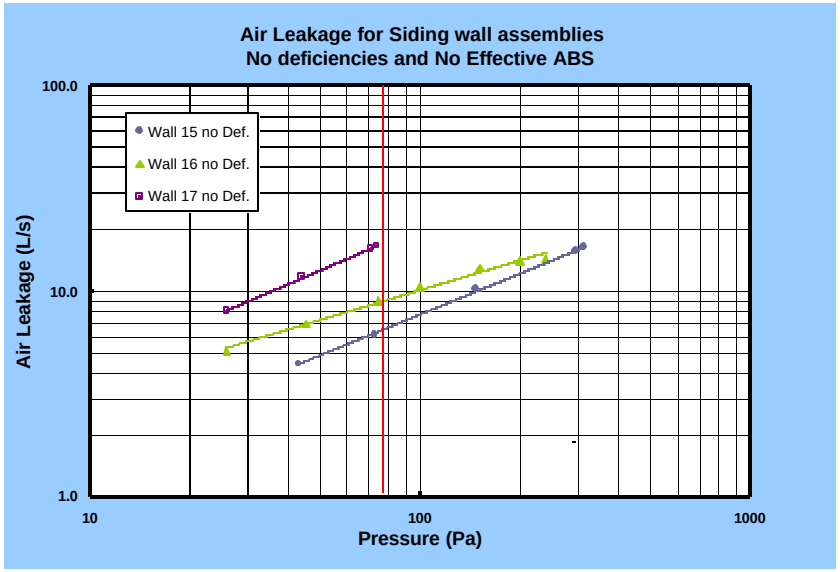

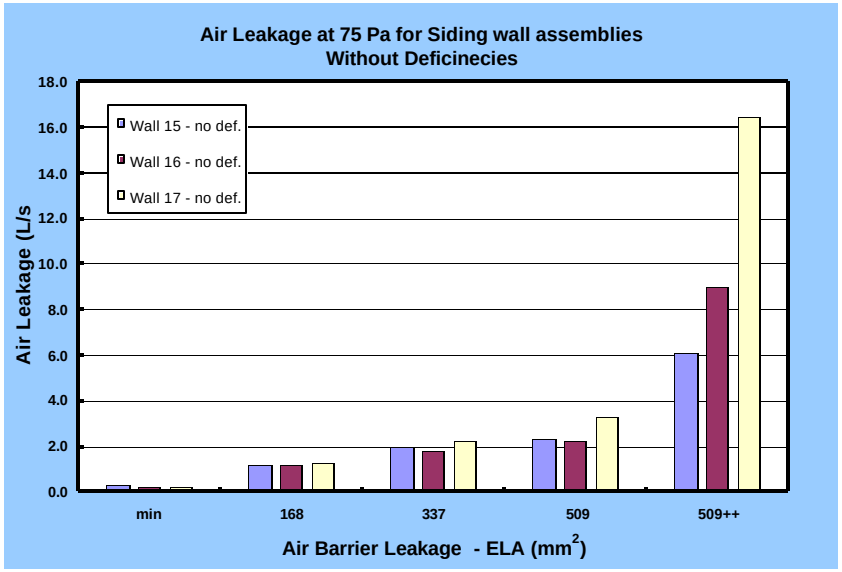

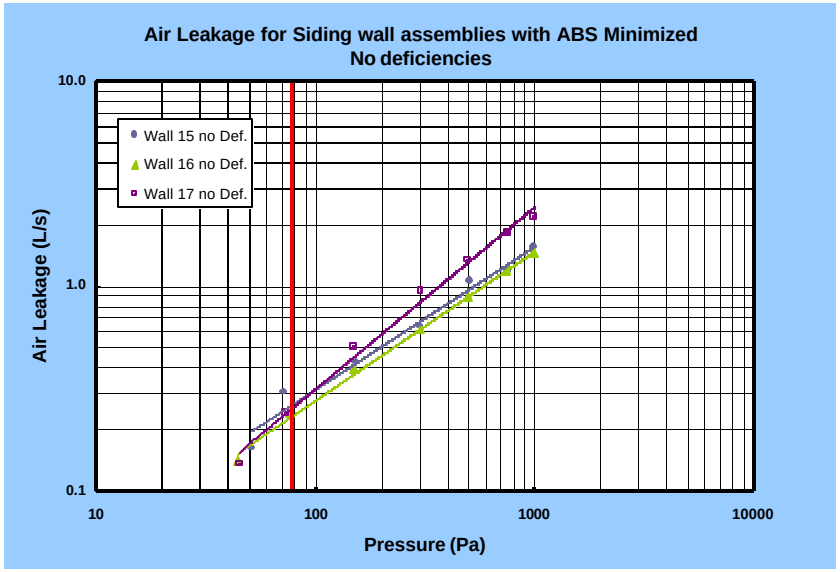

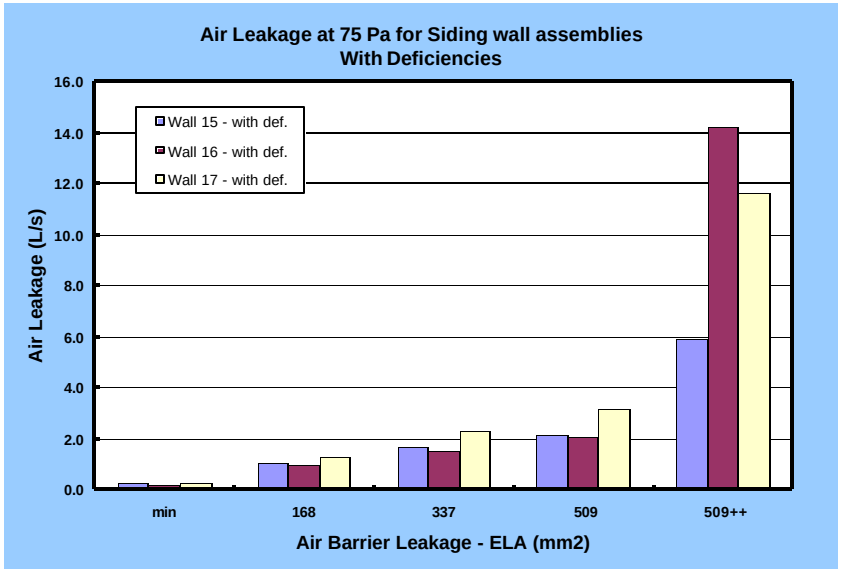

Figure B.13 – Air leakage of **siding** wall assemblies having no deficiencies and without air barrier system (ABS) in place

Figure B.14 – Air leakage of **siding** wall assemblies having no deficiencies and air barrier system leakage (ABS) minimised

Figure B.15 – Air leakage of **siding** wall assemblies having no deficiencies and in relation to the ELA of the air barrier system (ABS)

Figure B.16 – Air leakage of **siding** wall assemblies with deficiencies and in relation to the ELA of the air barrier system (ABS)

2. PRESSURE RESPONSE – STATIC AND DYNAMIC MODES

2.1 STATIC PRESSURE RESPONSE –

Static pressure response - Stucco wall assemblies

Static pressure response characteristics of stucco wall assembly WA-3 is provided in Figure B.18; WA-4 in Figure B.19.

Static pressure response - EIFS wall assemblies

Static pressure response characteristics of EIFS wall assembly WA-6 is provided in Figure B.19; WA-7 in Figure B.20; WA-8 in Figure B.21; WA-9 in Figure B.22; and, WA-10 in Figure B.23.

Static pressure response – Brick masonry wall assemblies

Static pressure response characteristics of Brick masonry wall assembly WA-11 is provided in Figure B.24; WA-12 in Figure B.25; WA-13 in Figure B.26; WA-14 in Figures B.27.

Static pressure response - Siding wall assemblies

Static pressure response characteristics of siding wall assemblies WA-15 is provided in Figure B.28; WA-16 in Figure B.29 and WA-17 in Figure B.30.

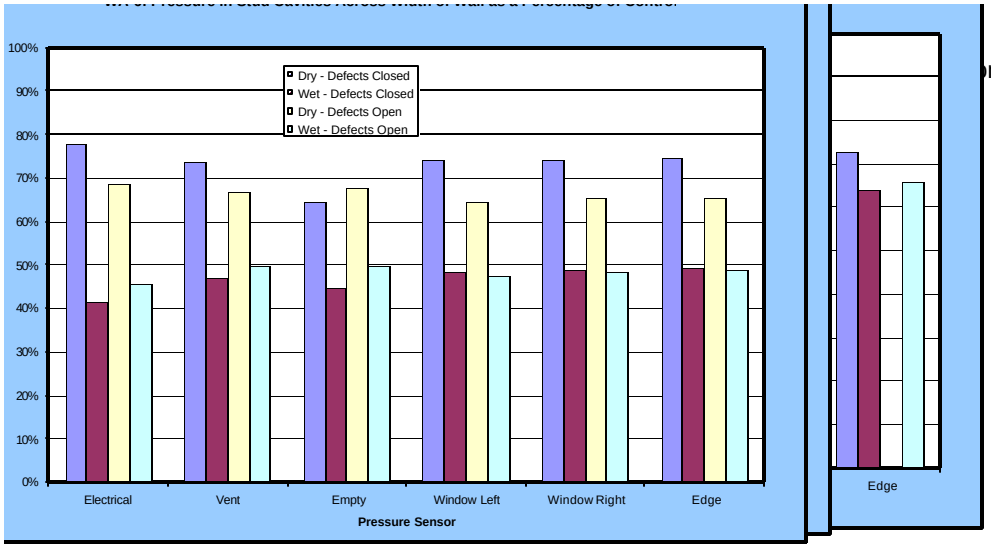
100%
90%
80%
70%
60%
50%
40%
30%
20%
10%
0%
Dry - Defects Closed
Wet - Defects Closed
Dry - Defects Open
Wet - Defects Open
Electrical
Vent
Empty
Window Left
Window Right
Edge
Pressure Sensor

Edge

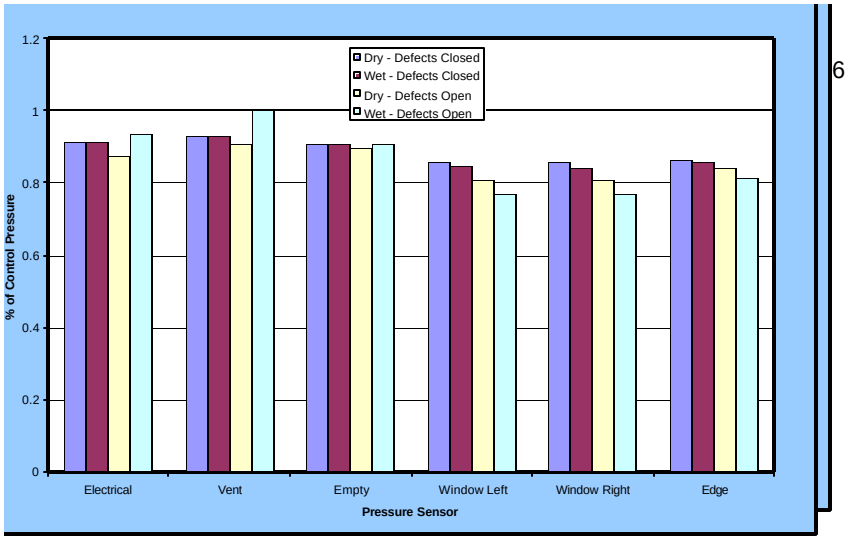

Figure B.25 – Pressure response WA-12 - across stud space

Figure B.26 - Pressure response WA-13 - across stud space

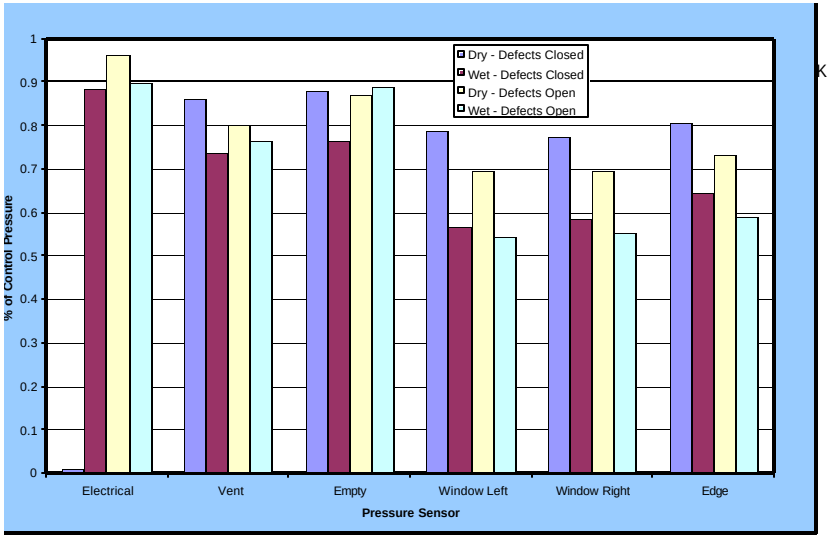

Figure B.27 - Pressure response WA-14 - across stud space

Figure B.28 - Pressure response WA-15 - across stud space

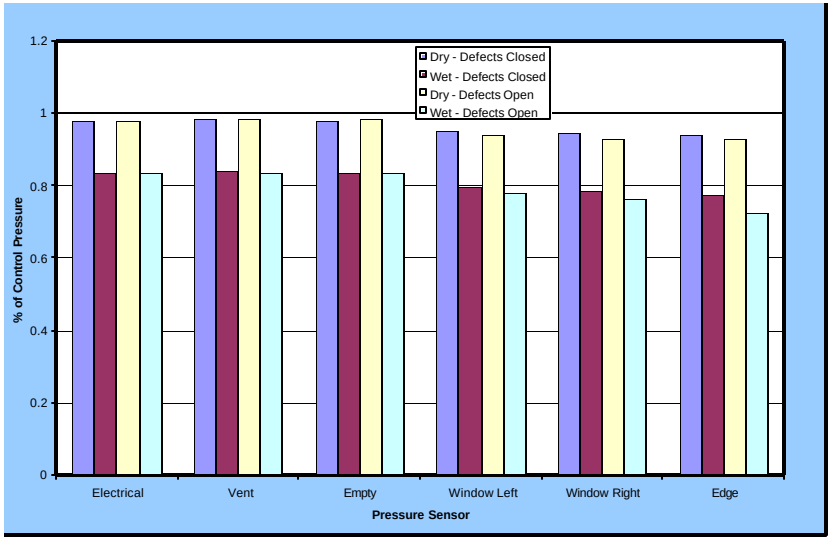

Figure B.29 - Pressure response WA-16 - across stud space

Figure B.30 - Pressure response WA-17 - across stud space

2.1.1 EIFS STATIC PRESSURE RESPONSE – ADDITONAL INFORMATION

The pressure response under static conditions in stud cavities located across WA-6 when the ABS leakage is either 0.2 or 0.5 L/s-m^2 is provided in Figures B.51 and B.52. Figure B.51 shows the pressure ratio at various driving pressures for specific pressure sensors or channels (CH) located within each of the stud cavities. Channel 6 (CH6) represents the left most stud cavity when facing the inside of the wall. Channel 10 is the adjacent cavity to the right of CH6 and so on across the wall. The pressure ratio is the ratio of actual pressure in the cavity under given conditions to the total or control (CTL) pressure across the assembly. The amount of pressure available to drive water through an opening is simply the difference between the total pressure and the pressure in the cavity. In terms of pressure ratios, the driving pressure ratio would be equivalent to one less the ratio at a given pressure level. The higher this value, the greater the potential driving pressure across the opening.

In Figure B.51, in which the ABS leakage is 0.2 L/s-m^2, the static pressure response of CH6 ranges from ca. 0.65 to 0.84 when the pressure difference across the assembly varies between 75 and 700 Pa. That is, the pressure in the left most stud cavity (CH6) is about 65% of 75 Pa and roughly 85% of 700 Pa under these conditions. These results are essentially the same for all stud cavities of this wall. The driving pressure ratios would hence vary between 0.35 and 0.26.

The pressure ratios are shown to diminish however (Figure B.52) when the system is evaluated with a nominal ABS leakage of 0.5 L/s-m^2. In this instance, ratios range from about 0.3 to 0.5 when the pressure difference across the assembly varies between 75 and 700 Pa. This implies that when the system leakage is changed from 0.2 to 0.5 L/s-m^2 the proportion of pressure available to drive water through openings on the outside of the wall likewise increases. The driving pressure ratios in this instance would vary between 0.6 and 0.5. This suggests that there is a greater likelihood of water entry for those systems having an ABS leakage of 0.5 as compared to 0.2 L/s-m^2

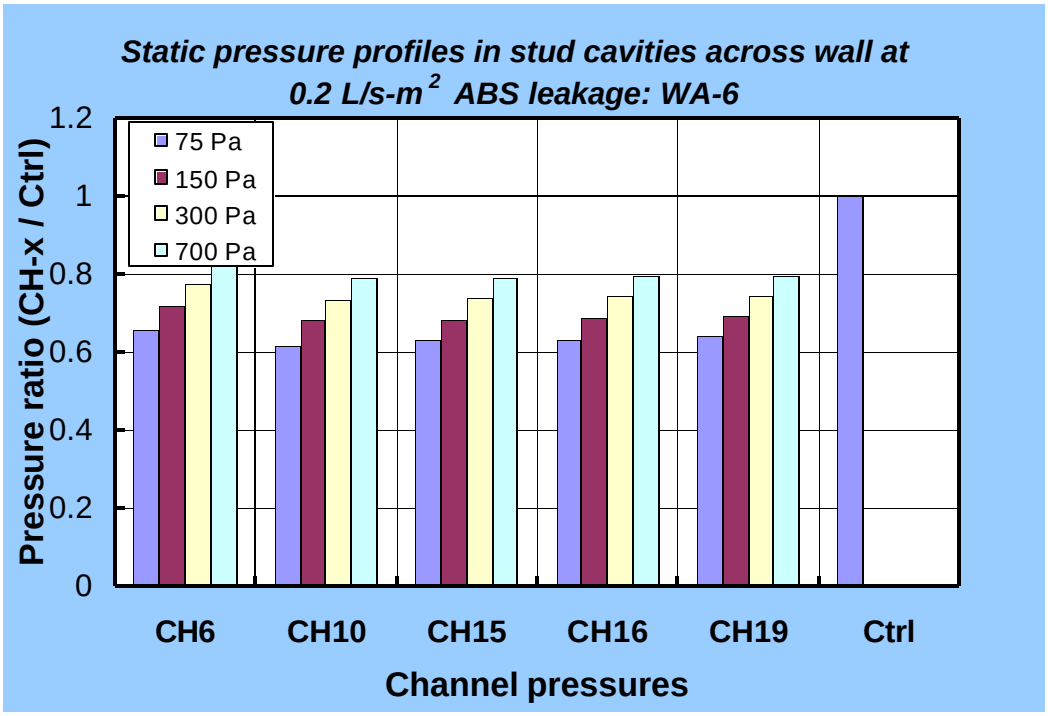

Figure B.31 – WA-6: Static pressure ratios over a range of driving pressures in stud cavities across width of wall. Nominal air barrier system leakage: 0.2 L/s-m²

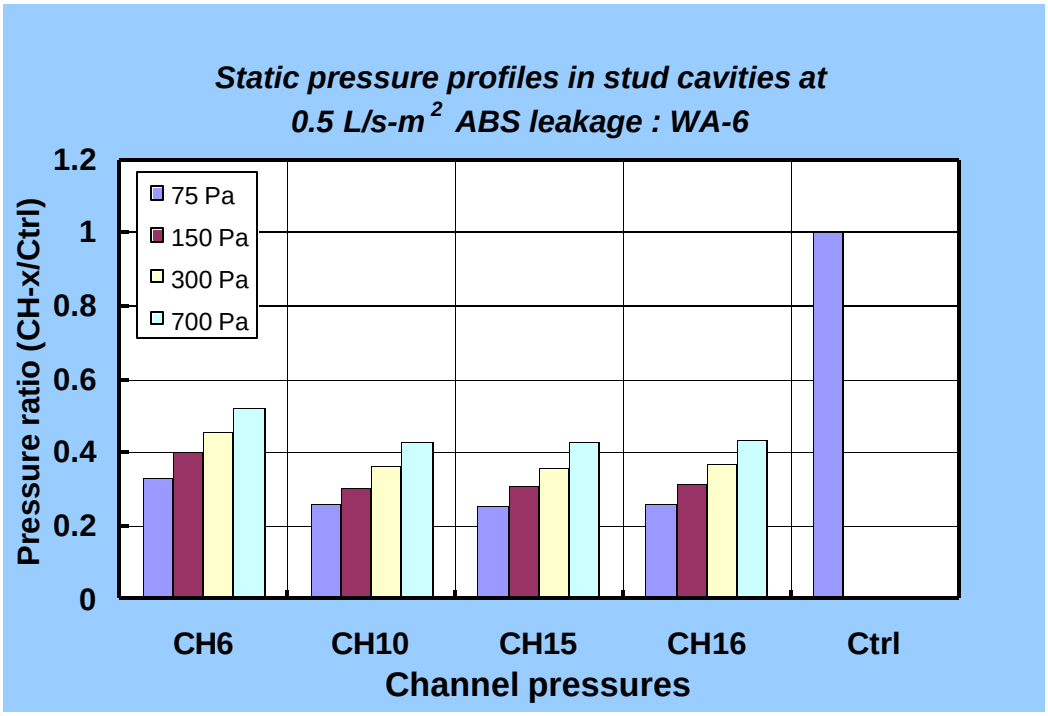

Figure B.32 – WA-6: Static pressure ratios over a range of driving pressures in stud cavities across width of wall. Nominal air barrier system leakage: 0.5 L/s-m²

2.2 DYNAMIC PRESSURE RESPONSE

2.2.1 STUCCO DYNAMIC PRESSURE RESPONSE

Results obtained from tests undertaken to evaluate the dynamic response of the wall assembly are provided in Tables B.1 to B.4 and in Figures B.53 and B.54. The results shown are limited to pressure response in wall portion No. 1 (right most cavity) in which are located pressure taps 3, 4, 6 and 7 (Figure B.53). Pressure tap 6 is located in the stud cavity whereas all other taps are located between the membrane and the stucco.

The results provided in Tables B.1 and B.2, and Figure B.53, reflect data obtained when subjecting the wall to a sinusoidal pressure fluctuation of 700 + 300sin(2pft) at 2 Hz with an air barrier system leakage (ABS) set at a nominal value of 0.5 L/s-m^2. The data in Table B.1 represent the values of mean pressure, pressure amplitude, and frequency and phase angle when fitted to the following sinusoidal function:

$$P(Pa) = Y_0 + a?sin(2pft + f)$$

Values presented in Table B.2 and B.4 and include the amplitude ratio and the phase shift derived from the regression of pressure data to the sinusoidal function. The amplitude ratio is the ratio of the pressure amplitude of a given channel to that of channel 2, the driving pressure (i.e. $a_{ch.\ x}/ a_{ch.\ 2}$). The phase shift is evaluated by finding the difference between the phase angle of a given channel to that of channel 2 (i.e. $f_{ch.\ 2} - f_{ch.\ x}$).

The data in Table B.1 indicate that all mean pressures are lower than the driving pressure (Ch. 2) and the pressure signals are attenuated as they pass deficiencies or other openings in the wall assembly, as might be expected in a non pressure-equalised wall. The pressure in the cavity (Ch. 6) is ca. 40% that of the driving pressure (Table B.1), with pressure in the interstitial spaces varying between 46 to 80%, depending on the location of the pressure tap. Figure B.53 corresponds to the pressure response curves for specific pressure taps (channels), for locations shown in the figure.

Table B.1 – Mean and amplitude pressures and phase angle at given pressure taps derived from regression of data to 700 + 300sin(2pft) at 2 Hz and ABS leakage of 0.5 L/s-m^2

P(Pa) =	***Y_0***	***+***	***a***	***Sin2p***	***f***	***t +***	***f***
Pressure Tap (Channel)	Mean pressure, Pa		Pressure amplitude, Pa		Frequency, Hz		Phase angle, radians
2*	722		312		2		4.6440
3	496		145		2		3.9860
4	509		155		2		3.9810
6	367		125		2		3.9400
7	659		250		2		4.4720

- driving pressure

Table B.2 – Amplitude ratio and phase shift at given pressure taps derived from regression data: 700 + 300sin(2pft) at 2 Hz and ABS leakage of 0.5 L/s-m²

Channel	Amplitude ratio	Phase shift (radians)
2	1	0
3	0.46	0.658
4	0.50	0.663
6	0.40	0.704
7	0.80	0.172

The results provided in Tables B.3 and B.4, and Figure B.54, reflect similar data for pressure fluctuations of 700 + 300sin(2pft) at 2 Hz but in this instance offering data obtained with an ABS leakage of 0.2 L/s-m^2.

As in the previous case, all pressures are lower than the driving pressure with phase shift for each response. Again, the lowest pressure is found in Ch. 6 (cavity ca. 51% driving pressure), with pressure in the interstitial spaces varying between ca. 59% and 84% of driving pressure. The amplitude ratios derived from the response of pressure taps in walls having an ABS of 0.2 L/s-m^2 in comparison to 0.5 L/s-m^2 are higher by ca. 28% with the exception of Ch. 7 (+5%). This reflects the higher pressure drop across the ABS, as might be expected for a tighter wall.

Table B.3 – Mean and amplitude pressures and phase angle at given pressure taps derived from regression of data to 700 + 300sin(2pft) at 2 Hz and ABS leakage of 0.2 L/s-m²

P(Pa) =	Y_0	+	*a*	*Sin2p*	*f*	*t +*	*f*
Pressure Tap (Channel)	Mean pressure, Pa		Pressure amplitude, Pa		Frequency, Hz		Phase angle, radians
2*	721		306		2		4.6338
3	612		180		2		3.9816
4	635		197		2		4.0150
6	474		157		2		3.9762
7	693		256		2		4.4445

*driving pressure

Table B.4 – Amplitude ratio and phase shift at given pressure taps derived from regression data: 700 + 300sin(2pft) at 2 Hz and ABS leakage of 0.5 L/s-m²

Channel	Amplitude ratio	Phase shift (radians)
2	1	0
3	0.59	0.6522
4	0.64	0.6188
6	0.51	0.6576
7	0.84	0.1893

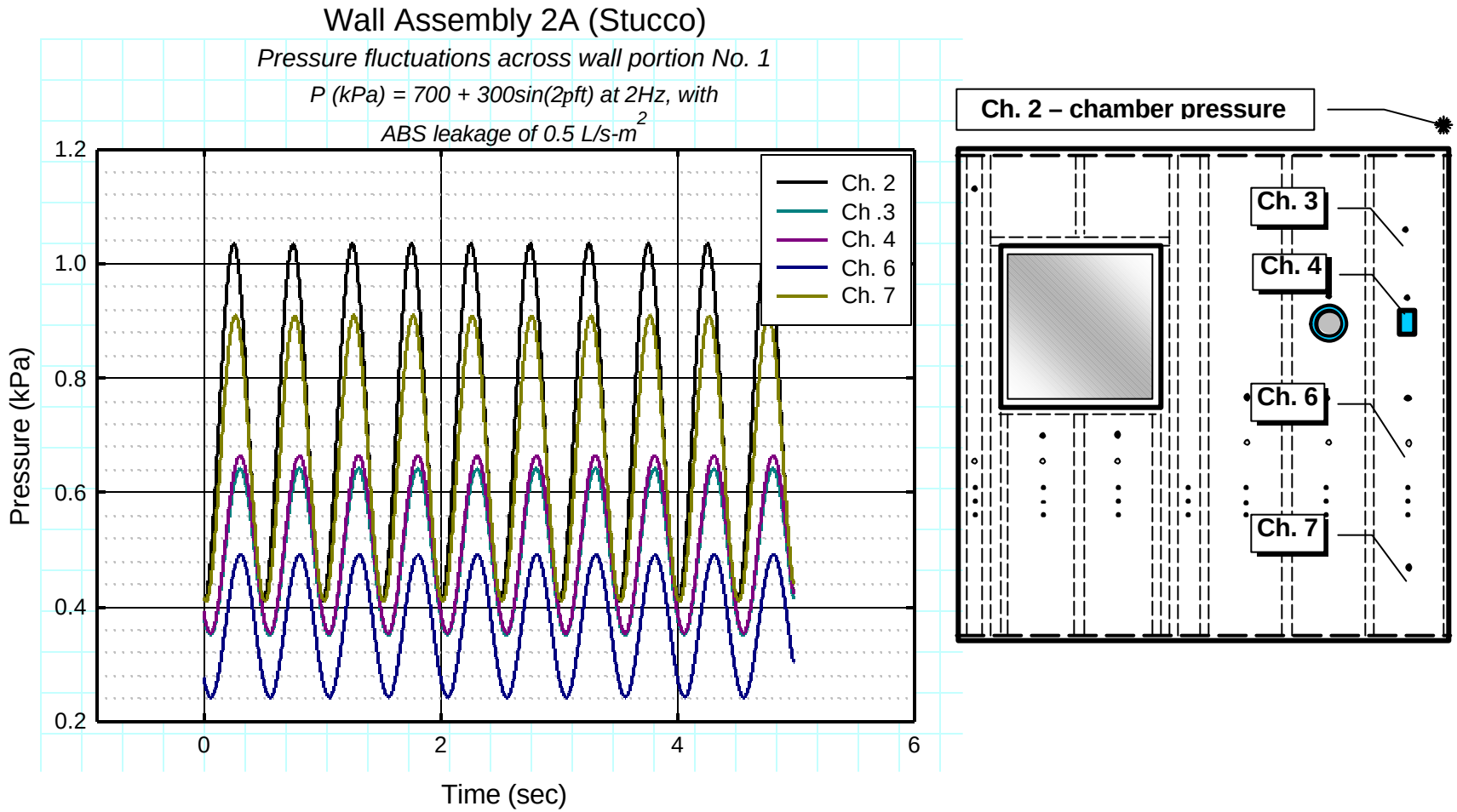

Figure B.33 – Pressure fluctuations across wall portion No. 1 for a pressure of 700 + 300sin(2pft) at 2 Hz and ABS leakage of 0.5 L/s-m^2

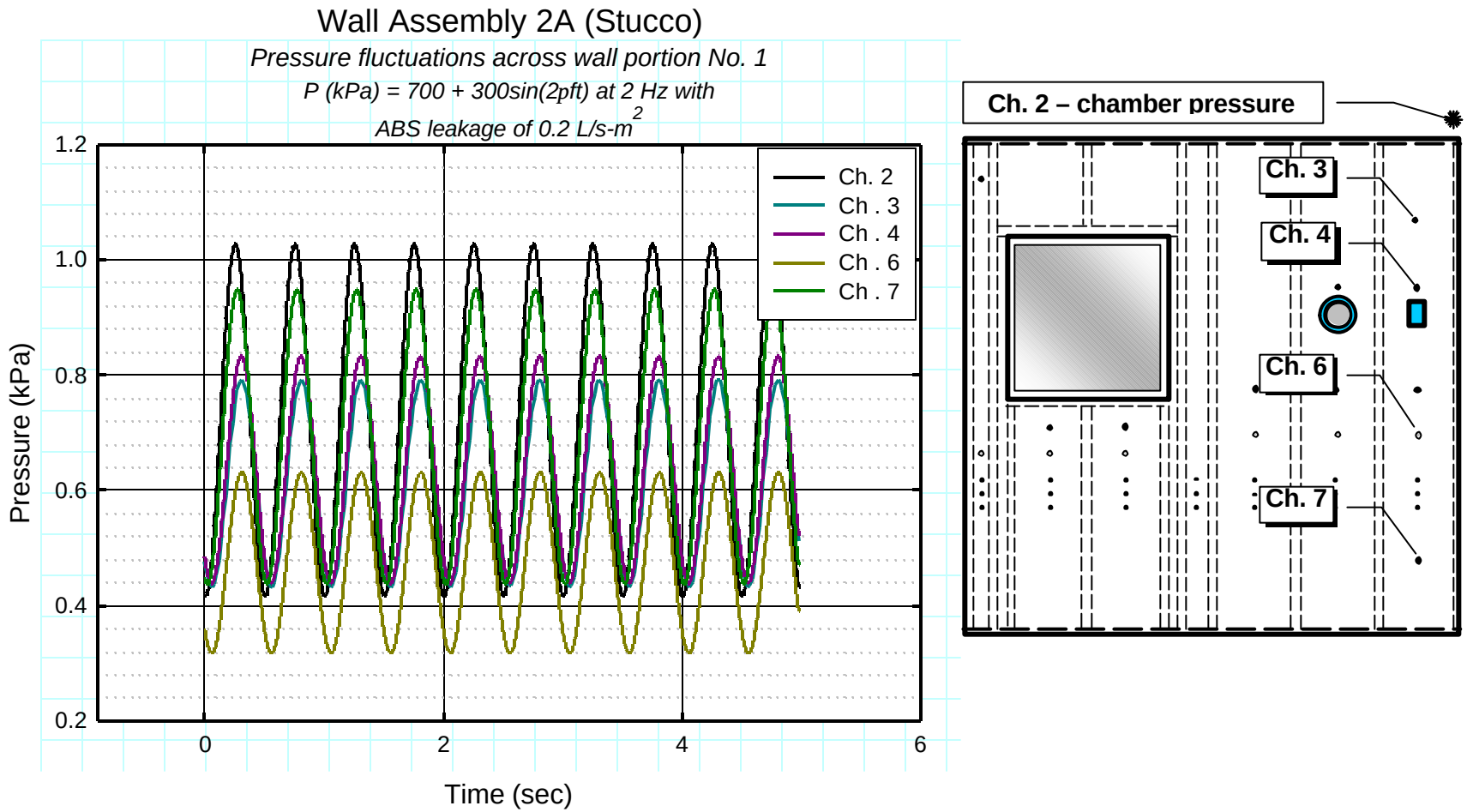

Figure B.34 – Pressure fluctuations across wall portion No. 1 for a pressure of 700 + 300sin(2pft) at 2 Hz and ABS leakage of 0.2 L/s-m²

2.2.2 DYNAMIC PRESSURE RESPONSE - ADDITIONAL INFORMATION

Dynamic Pressure response – EIFS wall assemblies

Dynamic pressure response characteristics of EIFS wall assemblies WA-6 is given in Figures B.55 and WA-8 in Figures B.56.

Dynamic Pressure response – Brick masonry wall assemblies

Dynamic pressure response characteristics of brick masonry wall assemblies WA-11 is given in Figures B.57, WA-12 in Figure B.58; WA-13 in Figures B.59 and, WA-14 in Figure B.60.

Dynamic Pressure response – Siding wall assemblies

Dynamic pressure response characteristics of siding wall assemblies WA-15 are given in Figures B.61 and; WA-16 in Figure B.62.

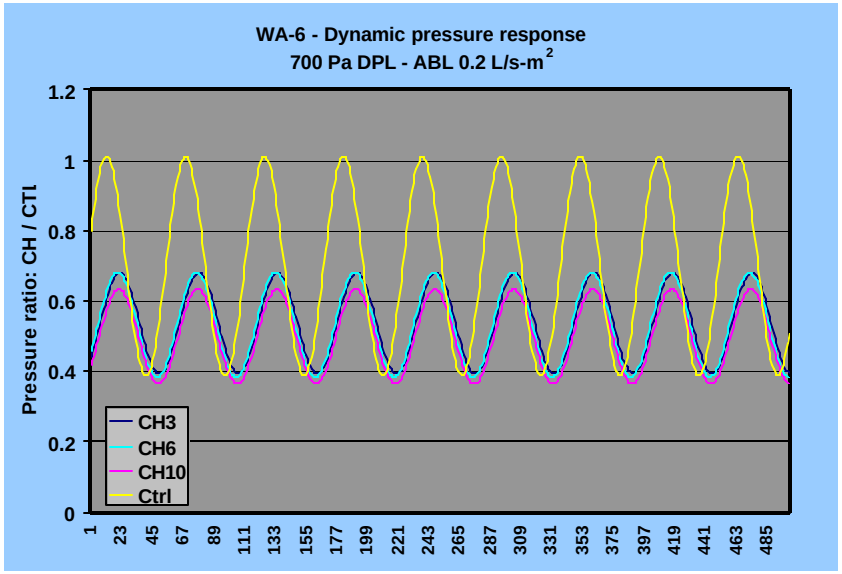

Figure B.35 – WA-6 Dynamic pressure response at 700 DPL – ABL 0.2 L/s-m²

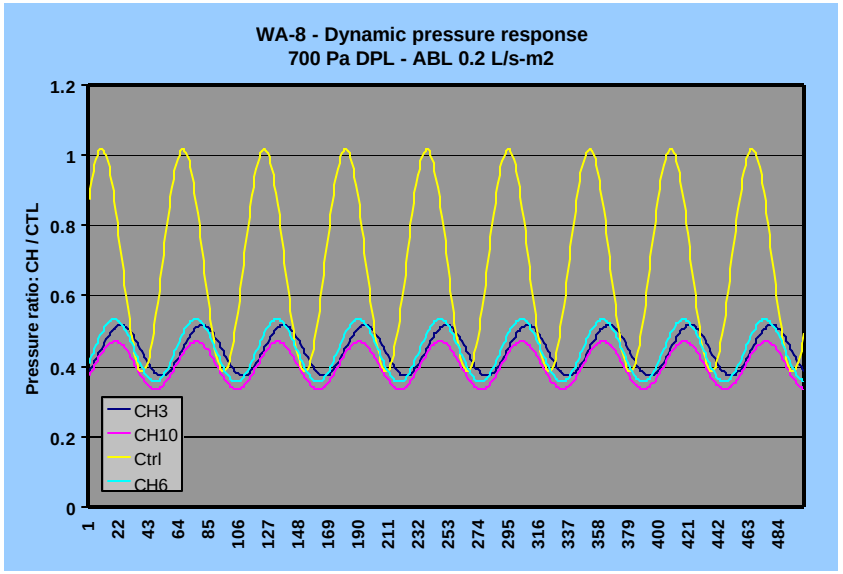

Figure B.36 - WA-8 Dynamic pressure response at 700 DPL – ABL 0.2 L/s-m²

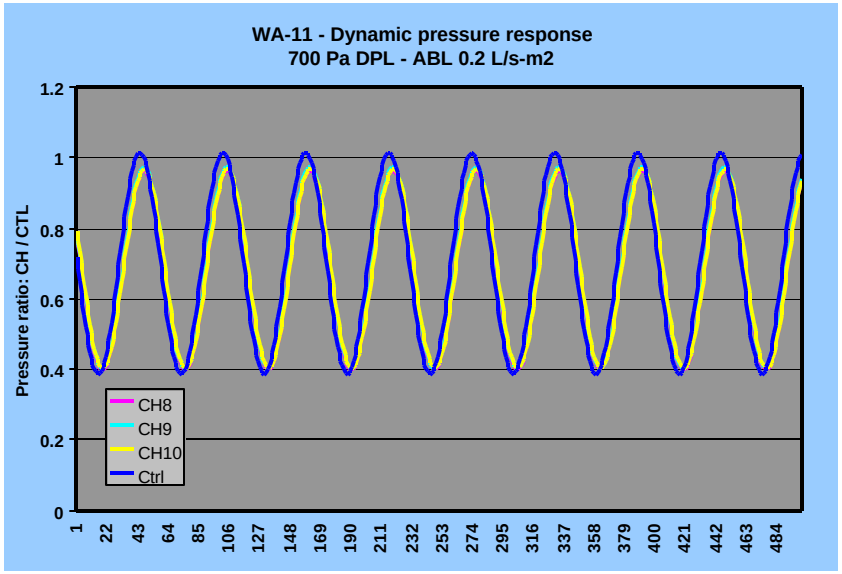

Figure B.37 - WA-11 Dynamic pressure response at 700 DPL – ABL 0.2 L/s-m²

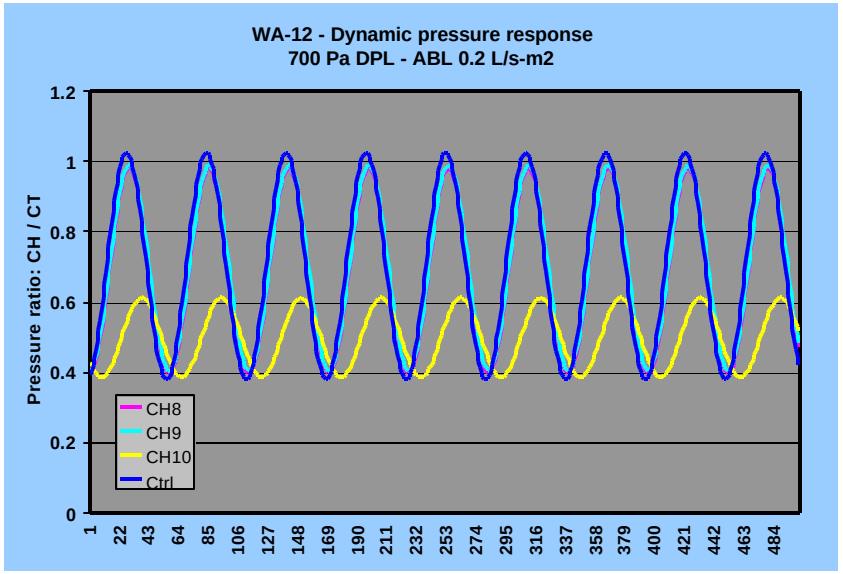

Figure B.38 - WA-12 Dynamic pressure response at 700 DPL – ABL 0.2 L/s-m²

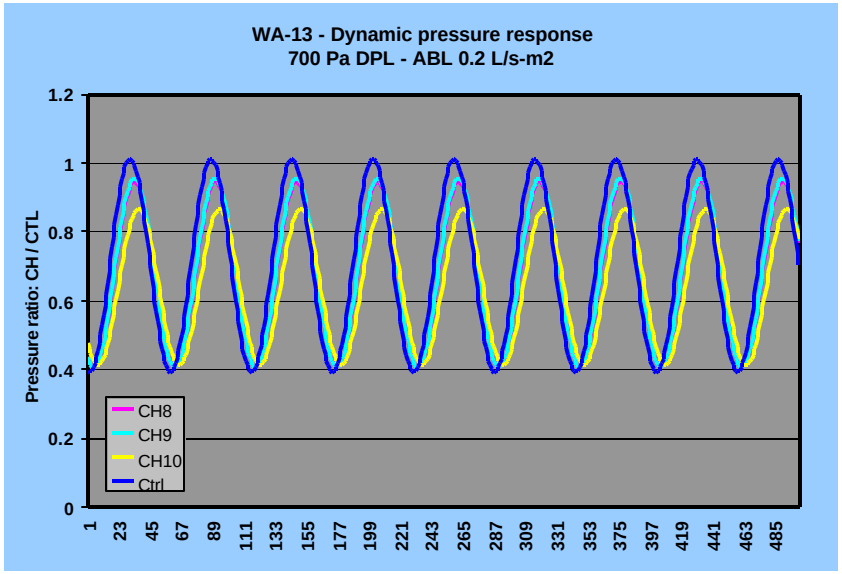

Figure B.39 - WA-13 Dynamic pressure response at 700 DPL – ABL 0.2 L/s-m²

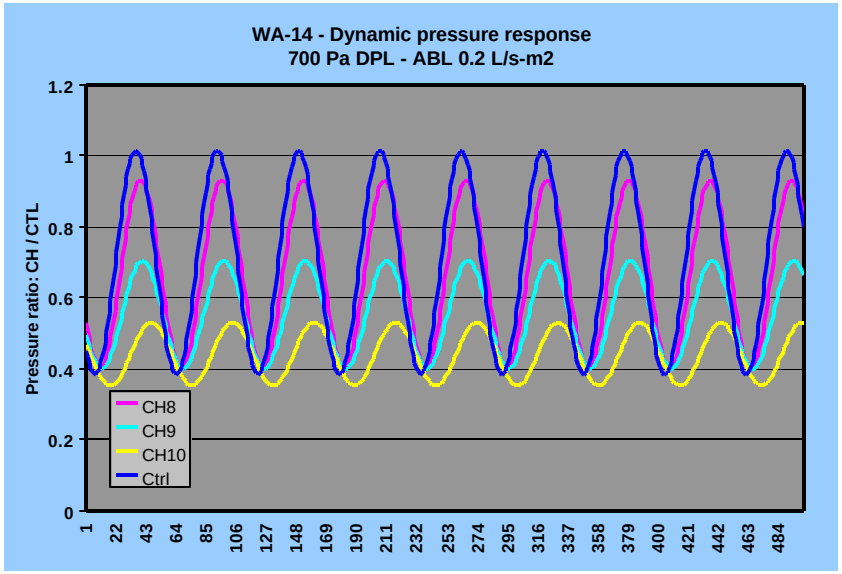

Figure B.40 - WA-14 Dynamic pressure response at 700 DPL – ABL 0.2 L/s-m²

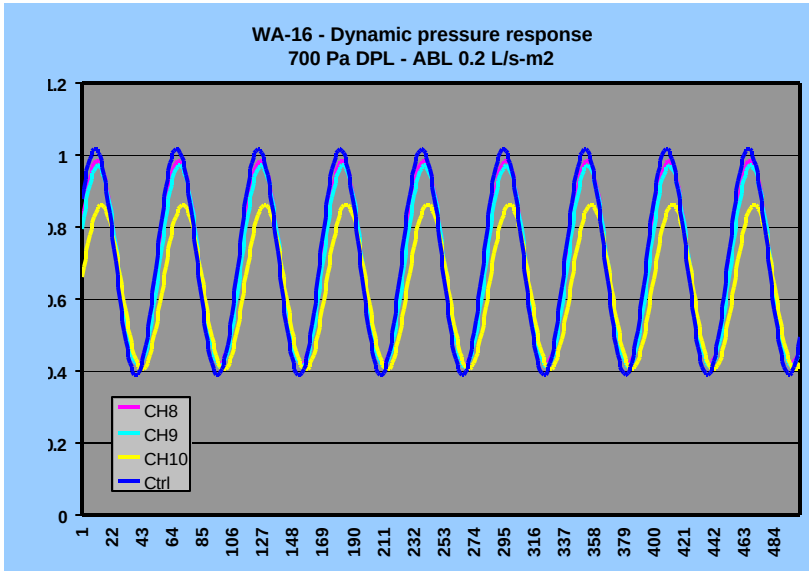

Figure B.41 - WA-15 Dynamic pressure response at 700 DPL – ABL 0.2 L/s-m²

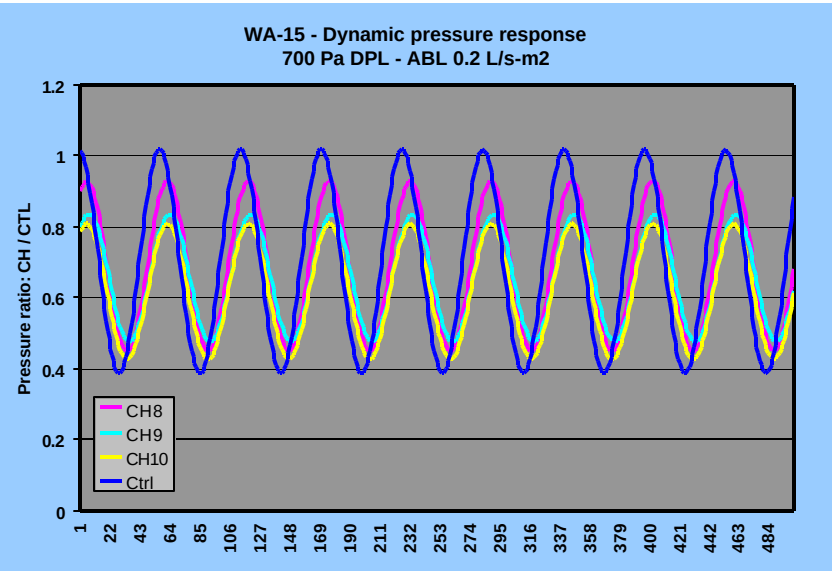

Figure B.42 - WA-16 Dynamic pressure response at 700 DPL – ABL 0.2 L/s-m²

3. MOISTURE DISTRIBUTION WITHIN THE WALL STUD CAVITY OF WATER ENTERING THROUGH INCIDENTAL OPENINGS IN THE CLADDING

3.1 INTRODUCTION

Knowledge of moisture distribution of accidental water entering inside a wall stud cavity through incidental openings in the wall cladding is of prime importance to determine the initial boundary conditions needed to undertake numerical simulations of wall assemblies using hygIRC. It has been observed in previous water entry trials on large-scale specimens that water typically comes into contact with both the wall sheathing and bottom plate as water flows down freely from the entry point towards the bottom plate along the surface of the wood sheathing. In order to obtain additional information in this regard, and a more complete understanding of the wetting phenomenon within the wall assembly, two small-scale experiments and a series of large-scale tests were carried out. These trials were aimed to determine the extent to which water is adsorbed by batt insulation placed in a stud cavity and hence, establish the proportion of water finding its way to the bottom of the cavity. Essentially, these experiments provided both qualitative and quantitative data regarding the distribution of water absorbed by fiberglass and OSB following the entry of water into the stud cavity, and also to assess the drainage time. Details regarding the nature of both of these tests, small-scale and large-scale, are provided below and results from each are provided at the end of respective section.

3.2 SMALL-SCALE EXPERIMENTS

A detailed sketch of test apparatus for the small-scale experiments is shown in Figure B.43. This apparatus can be considered as a scaled-down replica of a full-scale wall assembly. The apparatus consists of a plexiglas enclosure and the batt insulation is placed inside it, sandwiched between a front and back panel. The back panel resembles the side the wall facing the interior room climate and front panel the exterior face of the wall. Hence, the front panel represents the sheathing board encompassing the exterior side insulation cavity. In this set of two tests, plexiglas was used in the initial one, and OSB in the subsequent water entry trial as front panel. At the top of the apparatus is a water reservoir that is sufficiently high (15 mm) as to provide 150 Pa pressure at its base. Here, a series of 2 mm diameter holes allow water to enter the upper portion of the specimen (batt insulation) at a height of 457 mm from the base of the apparatus.

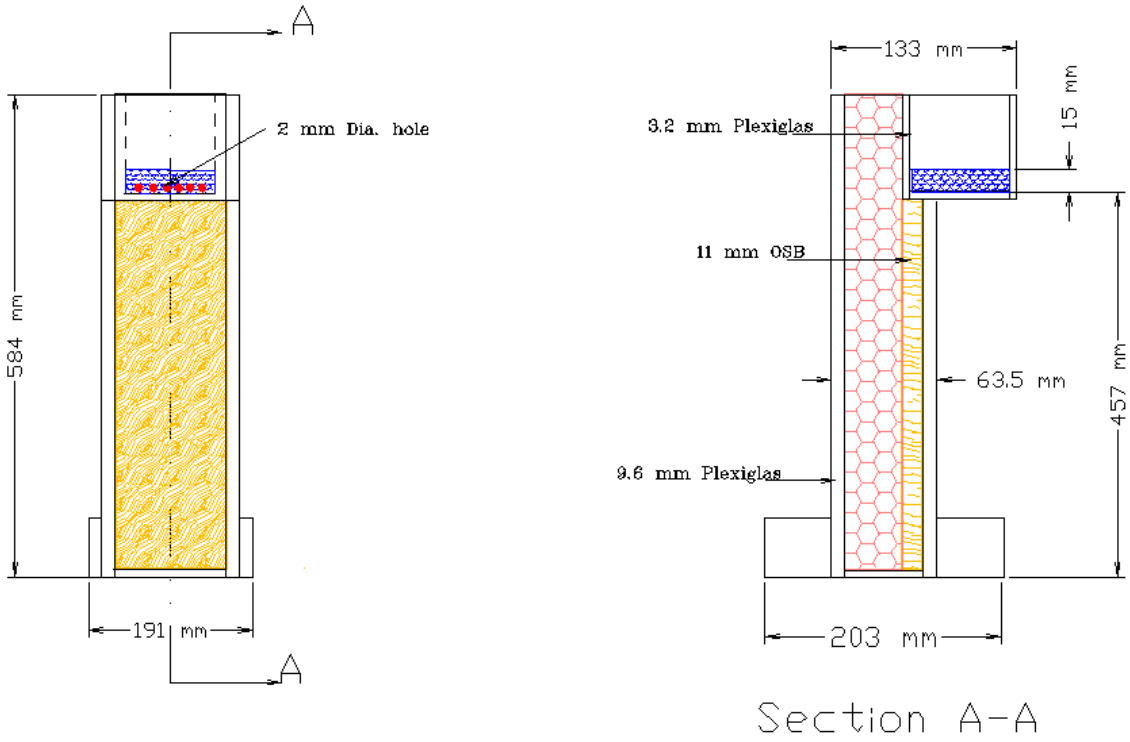

Figure B.43 - Detailed sketches of test apparatus used in small-scale experiments

In the initial experiment (Figure B.44), water flows from the reservoir to the interface between a fiberglass specimen and the plexiglas front panel. This test is taken as a base case in which water is either absorbed by the fiberglass or drains to the base of the apparatus. In the second experiment (Figure B.45) water likewise flows to the interface between the batt insulation and the front panel, however, in this case the front panel is OSB of the same type used in full-scale tests as sheathing board. The second test resembles more closely a “real” case and is intended to show the distribution of water on the OSB sheathing board and batt insulation.

3.3 RESULTS – SMALL-SCALE TESTS

It has been observed that the lateral absorption of water by either the batt insulation or OSB is virtually negligible in comparison to the action of gravity, as all the water entering the cavity runs down on the sheathing board (i.e. front panel) to the base of the cavity in a matter of minutes. This observation is true for both experiments as shown in Figure B.46 and Figure B.47. Hence, it is concluded that the amount of water retained by the batt insulation and OSB sheathing board during the flow of accidentally entered water inside the insulation cavity from the top to the bottom of the cavity is insignificant.

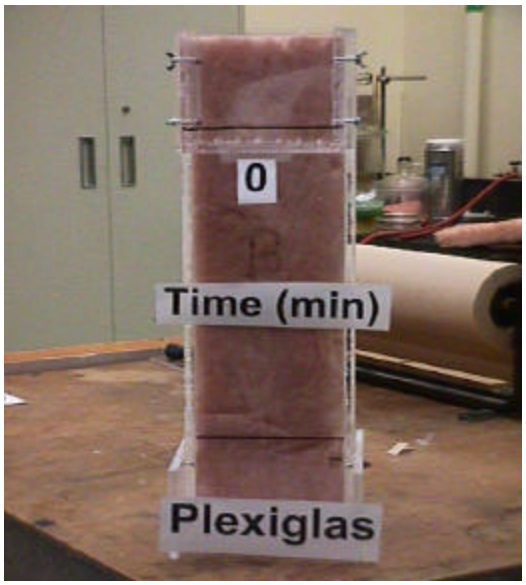

Figure B.44 - Set-up for initial test with plexiglas backing

Figure B.45 - Set-up for test case No. 2 with OSB backing

Figure B.46 - Initial test a few minutes after water entry

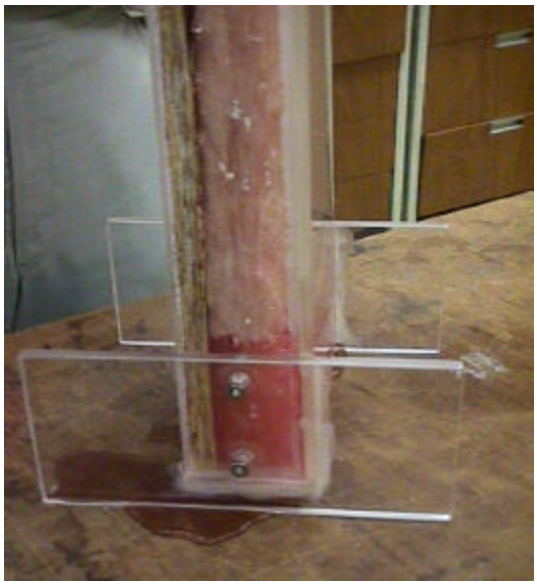

Figure B.47 - Test case No. 2 a few minutes after water entry

3.4 LARGE-SCALE EXPERIMENTS

A batt of fiber glass wool insulation (400 mm x 1550 mm) was fitted in a stud cavity of an existing stucco clad wall (WA-4) as shown in Figure B.48. The top of the batt insulation was placed half way around a ventilation duct and remaining length of batt insulation continued to within 350-mm of the bottom plate. The final length of batt reached the bottom plate. Two sections were used in such a manner that the water accumulating in the bottom half could more readily be weighed and compared to that portion of water adsorbed by the upper half of batt insulation. The depth of the batt insulation (110-mm) was such that it fitted snugly inside the stud cavity as might be expected in a typical installation. The bottom plate was fitted with a metal plate funnel to permit drainage of water accumulating at the base of the stud cavity.

Water was sprayed onto the wall assembly at a rate of 3.4-L/min-m^2 and entered inside the wall cavity through a defect (nominal 1 mm x 40 mm) located above the ventilation duct. The point of water entry into the stud cavity was located beneath the ventilation duct. The wall was also subjected to a pressure differential of 75 Pa and the air barrier system had a nominal leakage of 0.5 L/min-m^2. Water collection started immediately upon activating the water spray and continued for 20 minutes, the duration of the trial. Water accumulating at the base of the stud cavity was collected in a funnel and directed into 2-L plastic bottles. To ensure that the pressure difference in the bottle was the same as that of the cavity, the bottles were connected to the cavity by means of a plastic tube. A series of six trials were conducted in which the quantities of water collected in the bottle and the weights of the batt insulation, both dry and wet, were recorded. Results from six trials are reported below.

3.5 RESULTS OF LARGE-SCALE TESTS

Results from four trials are shown in Table 8.5. The initial trial was used to perfect the collection technique and these results are shown here to demonstrate that essentially all trials are within the same order of magnitude as that collected in the cavity without insulation in place (*ie* 4.75 L in 20 min.). As can be seen from these results, the major amount of the water was collected in the bottle with a small fraction of the total accumulating in the insulation (ca. 4%). This fraction was essentially confined to the lower portion of the insulation as can bee seen in Figure B.43 and Figure B.50. Figure B.49 shows the lower batt insulation just prior to the start of the test whereas Figure B.50 depicts the same portion but after 20 minutes of water collection.

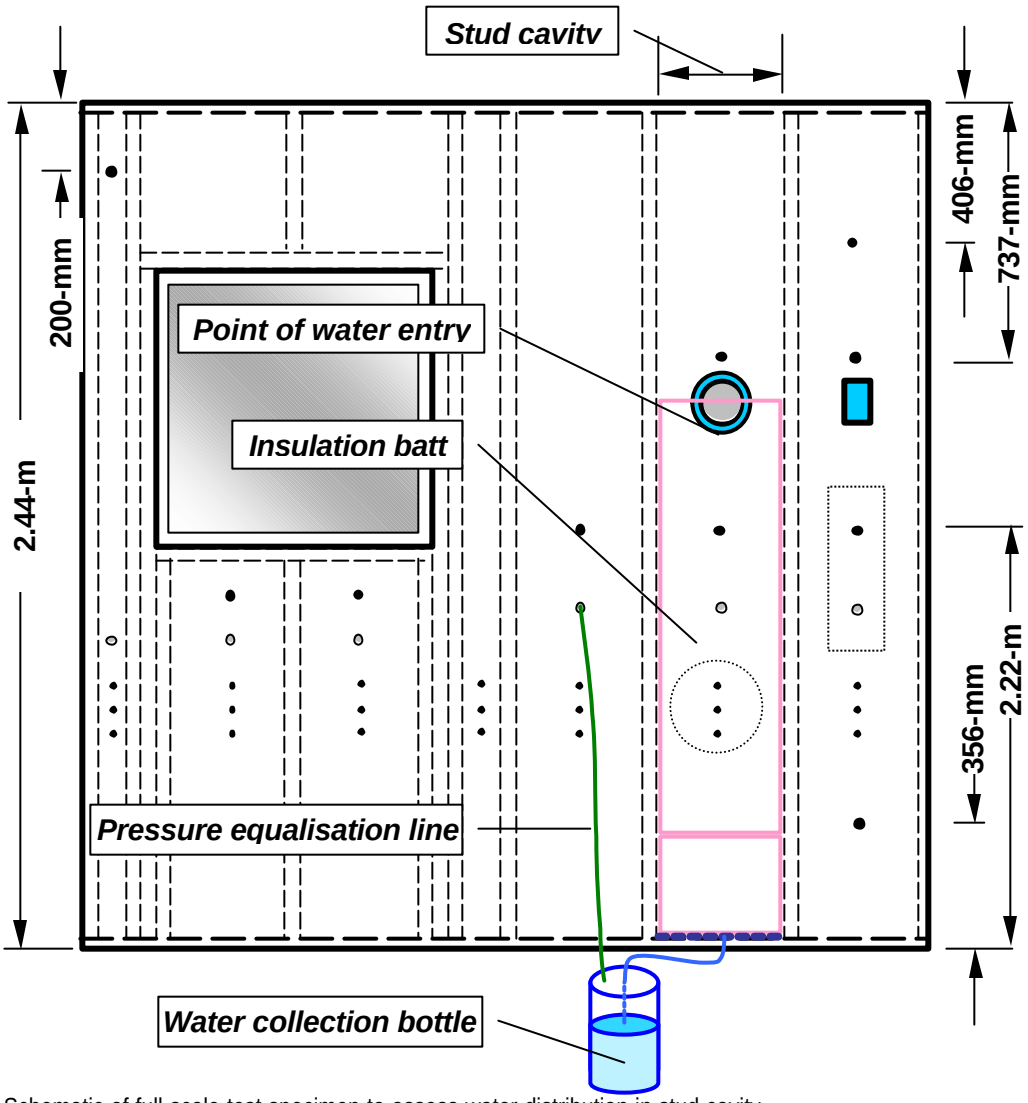

Figure B.48 - Schematic of full-scale test specimen to assess water distribution in stud cavity

Table 8.5 - Volume of water (L) collected in 20 minutes

	TEST NO.				Avg Tests 2-4
	1*	2	3	4	
Collection Bottle	5.44	3.90	4.62	5.17	4.56
Insulation	0.22	0.28	0.19	0.12	0.20
TOTAL	5.66	4.18	4.81	5.28	4.76
Previous**					4.75

*initial trial – not considered representative
**result from previous tests undertaken without batt insulation in stud cavity

The accumulation of water is highlighted in the figure. It was observed, following each test and upon removal of the insulation from the cavity, that very little water was adsorbed by the sheathing board. These results essentially confirm those observations derived from the tests conducted with small-scale specimens.

3.6 CONCLUSIONS

Based on these observations made in both small-scale and full-scale tests, it would appear that initial conditions in hygrothermal simulations should place the water entering inside the stud cavity at the bottom of the cavity.

Figure B.49 - Bottom plate of cavity showing insulation batt and collection point prior to start of test

Figure B.50 - Stud cavity at bottom plate after 20 minutes of water accumulation

4. CALIBRATION OF RESISTANCE READINGS TO MOISTURE CONTENT OF ORIENTED STRAND BOARD

The following calibration curve was used to estimate the moisture content of the oriented strand board when moisture sensors were activated over the course of the water penetration trials. Lights were activated when a threshold value of 250 MO was reached corresponding to approximately 14% moisture content. The actual moisture content in the sheathing boards incorporated in the respective wall assembly specimens would likely differ varying in amount depending on the physical properties of the board at the actual pin location. The density of the board would affect results, as would the actual depth of the pins in relation to that of pins used in the calibration.

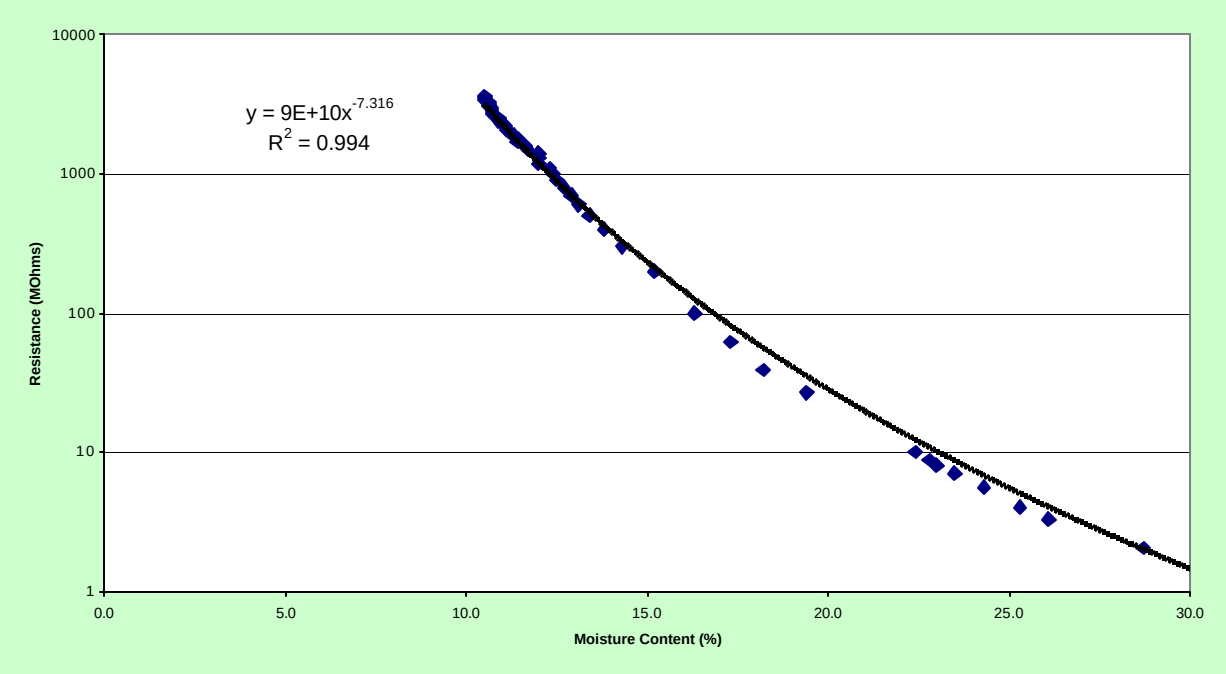

Figure B.71 – Resistance (MO) in relation to moisture content of OSB